



## Actinide speciation using synchrotron-based methods

M. A. Denecke<sup>1</sup>

<sup>1</sup>Dalton Nuclear Institute, University of Manchester, Manchester, M13 9PL, UK

*Abstract – Synchrotron-based techniques are increasingly used to characterize materials and elucidate determinant processes relevant to the nuclear fuel cycle. Most recent advances are driven by the need to characterize materials with high spatial resolution, for example localized components of heterogeneous systems or interstitial/interfacial junctions. In this presentation, examples of synchrotron-based investigations covering a wide range of wavelengths (infra-red to hard X-ray) and spatial resolution (nanometer range to bulk) will be introduced. The examples are chosen to illustrate various themes of research and development over the entire range of the nuclear fuel cycle, from power plant lifetime extension scenarios to nuclear waste disposal and future fuel/target development.*

*Keywords – Actinide speciation, X-ray techniques, synchrotron radiation*

## Radionuclides in Diagnostic Nuclear Medicine

Jun Hatazawa

Department of Nuclear Medicine and Tracer Kinetics, Osaka University Graduate School of Medicine  
WPI-Immunology Frontier Research Center, Osaka University

*Abstract – Diagnostic Nuclear Medicine (NM) is an essential procedure in modern medical practice. Recent survey reported that more than 2 million NM examinations are conducted every year in Japan. Around 75% of diagnostic NM employs single photon emission tomography (SPECT) with  $^{99m}\text{Tc}$ ,  $^{123}\text{I}$ ,  $^{133}\text{Xe}$ , or  $^{201}\text{Tl}$ -labeled compound, and 25% positron emission tomography (PET) with  $^{18}\text{F}$ -fluorodeoxy glucose,  $^{15}\text{O}$ -labeled  $\text{H}_2\text{O}$ ,  $\text{CO}$ ,  $\text{O}_2$ , or  $^{11}\text{C}$ -labeled compounds. Modern medicine is based on the intervention of molecular pathology of the diseases. Therefore, NM is expanding in number and in quality in daily medical practice including early diagnosis of Alzheimer's diseases, cancer, and cardiovascular diseases, strategy decision of treatment, evaluation of regeneration medicine. Furthermore, the NM is being utilized to facilitate new drug development. Combining molecular diagnosis with radionuclide therapy (Theranostics) is another future direction of clinical NM.*

*Keywords – Nuclear Medicine, Molecular Imaging, Theranostics*

Nuclear Medicine is now employed as a major tool of sensitively detecting molecular changes of the diseases before symptom onset. In Alzheimer's disease, amyloid deposition in brain tissue can be detected more than 10 years earlier than the onset. Abnormality in cerebral perfusion predicts a probability of ischemic stroke onset. PET examination can detect small cancer in volume before invasion and remote metastasis. Therapy response can be detected most sensitively among imaging modalities. The number of NM examination is therefore increasing dramatically recent years.

The application of NM is extending to facilitate new drug development (PET micro-dosing test). Because of high specific activity of radionuclide-labeled compound, pharmacokinetics of candidate compounds can be examined in humans. Combining molecular diagnosis of NM with radio-nuclide therapy (Theranostics) is another direction of NM. Nano particles with designed chemistry, size, surface charge, and target-specific binding ligands can extend "Nuclear Medicine Theranostics" by specifically carrying therapeutic radioisotopes and drugs to diseased tissues.

There are several problems to expand clinical NM. The shortage of  $^{99}\text{Mo}$  supply is most critical.

$^{99}\text{Mo}$  is now being produced by old nuclear reactors of specific countries.  $^{99}\text{Mo}$ - $^{99m}\text{Tc}$  generator completely depends on the import of  $^{99}\text{Mo}$ . We are now trying to produce  $^{99}\text{Mo}$  with accelerator by  $^{100}\text{Mo}(n,2n)^{99}\text{Mo}$  reaction. After improving irradiation of solid target, separation and purification of  $^{99}\text{Mo}$  in solid target, we obtained  $^{99m}\text{Tc}$  for bone scintigraphy of rats. Following steps of this project are mass production, clinical trial, approval by regulatory authority, and commercial delivery.

For the NM theranostics, we need radionuclides with specific characteristics. It should emit gamma ray with appropriate energy (100~200keV) for imaging and beta particles for therapy. Nowadays,  $^{89}\text{Sr}$  and  $^{90}\text{Y}$  are utilized to treat bone metastasis of cancers and malignant lymphoma, respectively. Since these tracers are pure beta particle emitting radionuclides, an evaluation of radio-nuclides accumulation is not possible by NM imaging.  $^{131}\text{I}$  (gamma ray of 364keV, beta particle of 606keV) is utilized for the treatment of hyperthyroidism, pheochromocytoma, and thyroid cancer. Imaging is possible by adapting heavy collimation of high energy gamma ray.

Functional nano particles are now applied to NM. Non-radioactive nano particles have been safely used in clinical trials of anti-cancer drugs (Nature 496:S58-60, 2012). The difficulty of radionuclides labeled nano particles is that the labeling process should be rapid because of physical decay of radionuclides. Long enough physical decay (13 hour of  $^{64}\text{Cu}$ , 13 hour of  $^{123}\text{I}$ , and 100 hour of  $^{124}\text{I}$ ) is required for this purpose.

Finally, the process from experimental study to clinical trial (translational medical center) has been installed in Osaka University Hospital under the support of Ministry of Health, Labor, and Welfare, Japan, which will be introduced in this presentation.

## Addressing Challenges in Preparation of $^{211}\text{At}$ -Labeled Biomolecules for Use in Targeted Alpha Therapy

D. Scott Wilbur<sup>1</sup>, Donald K. Hamlin<sup>1</sup>, Ming-Kuan Chyan<sup>1</sup>, Ethan R. Balkin<sup>1</sup>, John M. Pagel<sup>2,3</sup>,  
Oliver W. Press<sup>2,3</sup>, and Brenda M. Sandmaier<sup>2,3</sup>

<sup>1</sup>Radiation Oncology and <sup>2</sup>Medicine, University of Washington, Seattle, WA, USA

<sup>3</sup>Fred Hutchinson Cancer Research Center, Seattle, WA, USA

*Abstract* – There are significant challenges in the development of  $^{211}\text{At}$ -labeled biomolecules for application to targeted alpha therapy. Challenges that we have addressed include development of: (1) labeling methods to obtain high in vivo  $^{211}\text{At}$ -label stability, (2) approaches to consistently obtain high recovery yields of  $\text{Na}[^{211}\text{At}]\text{At}$  from irradiated bismuth targets, (3) methods to optimize biomolecule labeling yields, (4) reagents for use of  $^{211}\text{At}$  in pretargeting approach to cancer therapy, and (5)  $^{211}\text{At}$ -labeled antibodies in conditioning for hematopoietic cell transplantation.

*Keywords* – Astatine-211, antibodies, pretargeting, biotin

### I. INTRODUCTION

There are only ten  $\alpha$ -emitting radionuclides identified as having properties suitable for targeted alpha therapy [1]. Of that small group of radionuclides, astatine-211 ( $^{211}\text{At}$ ) is particularly attractive due to its reasonable half-life ( $t_{1/2} = 7.21$  h), lack of  $\alpha$ -emitting daughter radionuclides, and relative ease of preparation from an inexpensive target material (bismuth metal). However, application of  $^{211}\text{At}$  to the development of targeted alpha therapy has been difficult due to the low number of cyclotrons with (operating) alpha beams used in its production [2], and a host of problems involving the labeling chemistry and in vivo stability of  $^{211}\text{At}$ -labeled biomolecules [3]. We have investigated  $^{211}\text{At}$ -labeled biomolecules for over two decades and have had to address many challenging problems associated with  $^{211}\text{At}$  during that time.

### II. RESULTS AND DISCUSSION

One of the most impactful challenges to development of  $^{211}\text{At}$ -labeled biomolecules has been their low in vivo stability. Early studies demonstrated that the  $^{211}\text{At}$  label was stabilized on non-activated aryl compounds. However, the in vivo stability is only retained in slowly metabolized biomolecules, such as intact monoclonal antibodies (MAbs). Thus, in vivo stability has been a problem with MAb fragments, peptides or smaller biomolecules, where the aryl-At bond can be rapidly cleaved in vivo. We have investigated chelation of  $^{211}\text{At}$ , oxidation of  $^{211}\text{At}$  on aryl groups, and changing the bonding atom to boron for stabilization of the  $^{211}\text{At}$  bonding. In the latter approach, a number of boron cage molecules have been evaluated as pendant groups for attachment of  $^{211}\text{At}$  to biomolecules.

Of the different types of boron cage molecules studied, the *closo*-decaborate(2-) cage [B10 cage] has proven to provide high in vivo stability. In addition to high stability, that pendant group has made labeling of proteins much more efficient and easy to conduct. This is due to the fact

that the high electrophilic reactivity of the *closo*-decaborate(2-) moiety permits conjugation with proteins prior to astatination. This is in contrast to using a 2-step labeling procedure required with aryl-astatine reagents.

Another significant challenge became apparent when the size of the bismuth target was increased in preparation for translating  $^{211}\text{At}$ -labeled MAbs into clinical studies. Our standard method for isolation of  $^{211}\text{At}$  was “dry distillation”. However, the larger bismuth target and requisite larger quartz glassware resulted in low and inconsistent distillation yields of  $^{211}\text{At}$ . Therefore, we switched to a “wet chemistry” isolation approach. That approach has provided very consistent and high recovery yields. Another advantage of the wet chemistry approach is that it may permit automation of the isolation process.

Developing  $^{211}\text{At}$ -labeled reagents for use in pretargeting approaches to cancer therapy has been another challenge. For example, it initially appeared that preparation of an  $^{211}\text{At}$ -labeled biotin reagent might be relatively straightforward. However, many of the biotin derivatives prepared localized to kidneys or liver, or did not work in the pretargeting protocol. In some studies, biotin derivatives that did not localize in tumor bound with MAb-streptavidin conjugates. We knew the lack of binding with tumor could be due to formation of biotin-sulfone. We investigated formation of biotin-sulfone with chloramine-T (ChT) oxidant, but believed that our labeling conditions did not form the sulfone as the labeled product bound to an avidin column. Presently, we are investigating labeling biotin derivatives with other oxidants or no oxidant.

The oxidant ChT has also been found to cause problems with  $^{211}\text{At}$ -labeled MAb-B10 conjugates. Studies to decrease the amount of ChT in the radiolabeling reactions with MAb-B10 conjugates have shown that no oxidant is required in the  $^{211}\text{At}$  reactions. We now know that under acidic or neutral conditions, At is electropositive enough to undergo electrophilic reactions with *closo*-decaborate(2-) cages. In reactions without oxidant we obtain labeling yields equivalent to those with oxidant.

A further challenge is developing methods to keep  $^{211}\text{At}$ -labeled small biomolecules from localizing in kidneys. We have conducted a number of studies in that area as well. An overview of some of our research to circumvent challenges encountered when using  $^{211}\text{At}$  in development of Targeted Alpha Therapy agents will be presented.

### REFERENCES

- [1] D. S. Wilbur, *Current Radiopharm.* **4**, 214 (2011).
- [2] M. R. Zalutsky, M. Pruszyński, *Current Radiopharm.* **4**, 177 (2011)
- [3] D. S. Wilbur, *Current Radiopharm.* **1**, 144 (2008).

# Generation of nuclear data for the production of $^{97}\text{Ru}$ from $^{12}\text{C}+^{89}\text{Y}$ reaction

Moumita Maiti<sup>1</sup>, Susanta Lahiri<sup>2</sup>

<sup>1</sup>Department of Physics, Indian Institute of Technology Roorkee, Roorkee-247667, India

<sup>2</sup>Saha Institute of Nuclear Physics, 1/AF Bidhannagar, Kolkata-700064, India

**Abstract** – This article reports the measurement of cross section and yield of  $^{97}\text{Ru}$  in  $^{12}\text{C}$  induced reaction on natural yttrium target in the 40-75 MeV incident energy range. Cumulative cross section/yield of  $^{97}\text{Ru}$  was measured by stacked foil technique followed by off line  $\gamma$ -ray spectrometry. Measured data follows the trend of theoretical estimation.

**Keywords** –  $^{97}\text{Ru}$ , cross section measurement, yield, stacked foil technique,  $^{89}\text{Y}$  target,  $^{12}\text{C}$  projectile

## I. INTRODUCTION

Due to the suitable nuclear properties,  $^{97}\text{Ru}$  has been proposed for a number of applications. Besides high chemical reactivity of ruthenium helps to produce various  $^{97}\text{Ru}$ -labelled complexes concerned to the application. Investigation on the production cross section of  $^{97}\text{Ru}$  is important as it helps to optimize the production and to maintain the purity of the product.

Several attempts to produce  $^{97}\text{Ru}$  through p,  $^3\text{He}$  and  $\alpha$ -particle induced reactions on suitable targets have been reported. In a recent attempt we produced no-carrier-added (NCA)  $^{97}\text{Ru}$  through  $^{93}\text{Nb}(^7\text{Li},3n)^{97}\text{Ru}$  reaction and developed radiochemical separations[1]. This article reports the experimental measurement of production cross section and yield of  $^{97}\text{Ru}$  from  $^{12}\text{C}+^{89}\text{Y}$  reaction.

## II. EXPERIMENTAL

Production cross sections and yield of  $^{97}\text{Ru}$  produced in  $^{12}\text{C}+^{89}\text{Y}$  reactions were measured by the stacked foil technique followed by off-line  $\gamma$ -ray spectroscopy. Thin self supporting Y foils (99.9% purity) of thickness 1.9-2 mg/cm<sup>2</sup> were prepared by proper rolling. A target stack was assembled with 3 such Y foils; each Y foil was backed by an aluminum catcher foil of thickness 1.5 mg/cm<sup>2</sup>, and was irradiated with  $^{12}\text{C}^{6+}$  ions. A total of four such target stacks were irradiated independently varying the incident energy with an overlap between them. The experiment was carried out at the BARC-TIFR pelletron accelerator facility, Mumbai, India. The integrated charge was recorded in each irradiation by an electron-suppressed Faraday cup stationed at the back of the target assembly. The cross sections of  $^{97}\text{Ru}$  produced at various incident energies were calculated using the standard activation equation whose detail description is available elsewhere [2].

## III. RESULTS AND DISCUSSION

Production  $^{97}\text{Ru}$  was contributed by the direct reaction (i)  $^{nat}\text{Y}(^{12}\text{C},p3n)^{97}\text{Ru}$  and (ii) indirect reaction, through the decay of short-lived  $^{97}\text{Rh}(30.7\text{min})$ ,  $^{97m}\text{Rh}(46.2\text{min})$

produced through  $^{nat}\text{Y}(^{12}\text{C},4n)^{97}\text{Rh}(\text{EC})^{97}\text{Ru}$  &  $^{nat}\text{Y}(^{12}\text{C},4n)^{97m}\text{Rh}(\text{EC}: 94.4\%, \text{IT}: 5.6\%)^{97}\text{Ru}$  reactions. Measured cross sections of  $^{97}\text{Ru}$  at different projectile energies are therefore cumulative of all reaction channels. All possible errors are considered in the error analysis and the data presented up to the 95% confidence level. Figure 1 shows the maximum cross section of  $^{97}\text{Ru}$  is  $\sim 780$  mb at  $\sim 67$  MeV bombarding energy and the trend of the measured data nicely follows the theoretical estimation of PACE4, which essentially calculates the fusion-evaporation cross section following the Hauser-Feshbach model. Moreover, measured cross sections of  $^{97}\text{Ru}$  are comparable to the sum of cross sections of  $^{97}\text{Ru}+^{97}\text{Rh}$ . Figure 2 shows the measured yield of  $^{97}\text{Ru}$  at various bombarding energies. The maximum yield of 110 kBq/ $\mu\text{A}\cdot\text{h}$  was obtained at  $\sim 67$  MeV energy. However, a thick target yield of  $>0.5$  MBq/ $\mu\text{A}\cdot\text{h}$  can easily be achieved if the thickness of the Y foil and proper projectile window is chosen.

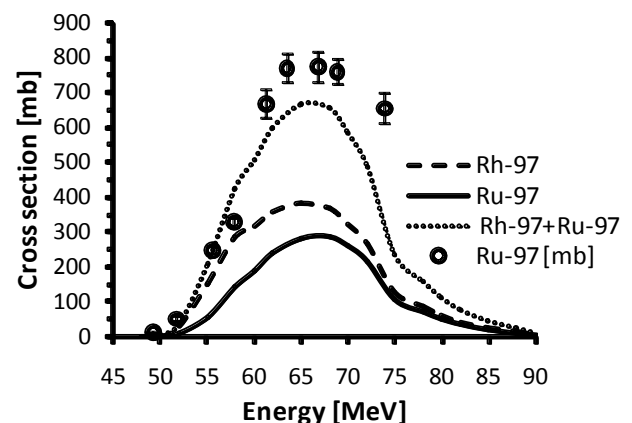


Figure 1. Comparison of cross sections of  $^{97}\text{Ru}$  (symbol) with the theoretical excitation functions of  $^{97}\text{Ru}$ ,  $^{97}\text{Rh}$  and sum of ( $^{97}\text{Rh}+^{97}\text{Ru}$ ) as obtained from PACE4

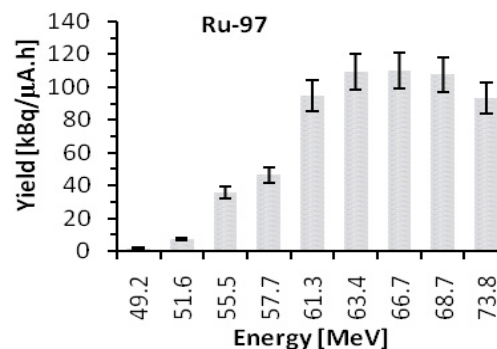


Figure 2. Measured yield of  $^{97}\text{Ru}$  at different projectile energies

- [1] M. Maiti, S. Lahiri, *Radiochim. Acta* 99, 359 (2011)  
 [2] M. Maiti, S. Lahiri, *Phys. Rev. C* 81, 024603 (2010)

## Towards an automatic procedure for the production of astatinated antibodies

Emma Aneheim<sup>1</sup>, Sture Lindegren<sup>1</sup>, Holger Jensen<sup>2</sup>

<sup>1</sup>Targeted Alpha Therapy group, Department of Radiation Physics, Sahlgrenska Academy at Gothenburg University, SE41345  
Gothenburg, Sweden

<sup>2</sup>Cyclotron and PET Unit, KF-3982, Rigshospitalet, Copenhagen, Denmark

*In recent time targeted radiotherapy of cancer tumors have been given a larger interest. For microscopic tumors, alpha therapy is especially interesting due to the high LET of the alpha particles. One promising nuclide for targeted alpha therapy is <sup>211</sup>At. <sup>211</sup>At decays with 100% alpha-emission along two different branches and does not emit any major quantities of gamma, allowing for safe handling of large activities. At Sahlgrenska Academy in Sweden, research regarding alpha therapy using astatine and monoclonal antibodies has been ongoing for over fifteen years. The research has been taken from bench to bedside including a number of preclinical studies and a phase I clinical trial on nine patients with recurrent ovarian cancer. However, to be able to move forward towards phase II/III studies the current synthesis of radiolabeled antibodies would benefit from being automated. The automation will be performed using a custom made radiopharmaceutical module from Scintomics GmbH. This procedure, however, requires both modifications of the synthesis, as well as an adaptation of the astatine distillation process. The work presented here concerns such an automation of the production of astatinated antibodies.*

*Keywords – Astatine-211, antibodies, radiopharmaceutical module*

## Production of $^{95m}\text{Tc}$ for Compton Camera Imaging

Yuichi Hatsukawa<sup>1</sup>, Kazuyuki Hashimoto<sup>1</sup>, Kazuaki Tsukada<sup>1</sup>, Tetsuya Sato<sup>1</sup>, Masato Asai<sup>1</sup>, Atsushi Toyoshima<sup>1</sup>, Yasuki Nagai<sup>1</sup>, Toru Tanimori<sup>2</sup>, Shinya Sonoda<sup>2</sup>, Shigeto Kabuki<sup>3</sup>,  
 Hideo Saji<sup>4</sup>, Hiroyuki Kimura<sup>4</sup>

<sup>1</sup>Japan Atomic Energy Agency

<sup>2</sup>Department of Physics, Kyoto University

<sup>3</sup>School of Medicine, Tokai University

<sup>4</sup>Faculty of Pharmaceutical Sciences, Kyoto University

**Abstract** – With the development of the Compton camera which can realize high position resolution, technetium isotopes emitting high energy gamma-rays are required. In this study, technetium-95m which emits some gamma rays with higher than 500 keV was produced by the  $^{95}\text{Mo}(p,n)^{95m}\text{Tc}$  reaction. Image of gamma-rays from Tc-95m was taken by a Compton gamma-ray camera

**Keywords** –Technetium-95m, Compton gamma-ray camera, MDP labeling,  $^{95}\text{Mo}(p,n)^{95m}\text{Tc}$  reaction,

### I. INTRODUCTION

Technetium-99m is used in radioactive medical diagnostic tests, for example as a radioactive tracer that medical equipment can detect in the human body. It is well suited to the role because it emits readily detectable 141 keV gamma rays, and its half-life is 6.01 hours (meaning that about 94% of it decays to technetium-99 in 24 hours). There are at least 31 commonly used radiopharmaceuticals based on technetium-99m for imaging and functional studies of the brain, myocardium, thyroid, lungs, liver, gallbladder, kidneys, skeleton, blood, and tumors. Recent years, with the development of the Compton camera which can realize high position resolution, technetium isotopes emitting high energy gamma-rays are required. In this study, technetium-95m which emits some gamma rays around 800 keV was produced by the  $^{95}\text{Mo}(p,n)^{95m}\text{Tc}$  reaction.

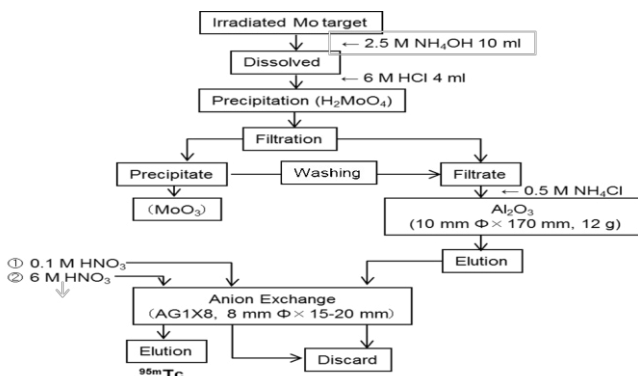


Fig.1 Chemical purification procedure of Tc-95m from MoO<sub>3</sub> target.

### II. EXPERIMENTAL and RESULTS

A 300-700 milligrams of  $^{nat}\text{MoO}_3$  targets were irradiated with 15 MeV proton beam for 7 hours at the JAEA Tandem

accelerator. Averaged beam currents were 1.2  $\mu\text{A}$ . After a few weeks cooling time, about 300-500 kBq of  $^{95m}\text{Tc}$  were extracted from the irradiated MoO<sub>3</sub> target after a chemical separation shown in Fig.1

Using purified  $^{95m}\text{Tc}$ , a labeled compound,  $^{95m}\text{Tc}$ -MDP (methylene diphosphate) was synthesized. In order to examine quality of the labeled compounds obtained in this study, thin-layer chromatography (TLC) method was carried out. A spot of solution of the labeled compound was placed at the edge of the TLC plate, and the plate stood upright in a solvent. Two kind of solvents, Methyl ethyl ketone (MEK) and physiological saline were used. After about 10 -30 min dipping time, TLC plates were dried and taken autoradiography images using imaging plates for 12 hours. The result of labeling experiment was shown in Fig. 2. According to this result, labeled compound,  $^{95m}\text{Tc}$ -MDP was synthesized well.

Then, Compton camera imaging was taken by the Electron-tracking Compton gamma-ray camera which was developed by prof. T. Tanimori's group of Kyoto university for medical usage.[2-3] The results obtained from these experiments will be discussed in the APSORC meeting.

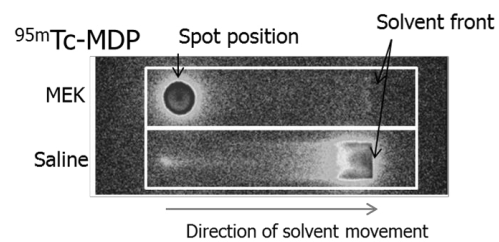


Fig.2 Autoradiography images form  $^{95m}\text{Tc}$ -MDP. MEK and physiological saline was used as solvents.

### Reference

- [1] M.Izumo, et al., Appl. Radiat. Isot. 42 297-310 (1991)
- [2] T. Tanimori et al., New Astron. Rev. 48 (2004) 236.
- [3] S.Kabuki et al., NIM,A623(2010) 606

## Relativistic Quantum Chemical Studies on Electronic Structures and Photoelectron Spectra of Actinide Complexes

Jing Su and Jun Li\*

Department of Chemistry, Tsinghua University, Beijing 100084, China

\*E-Mail: junli@tsinghua.edu.cn

*Abstract* – Investigations of the actinide spectroscopy and chemistry have been an active field of research recently. Actinide complexes are challenging for theoretical studies because of their significant relativistic effects and strong electron correlation effects. Photoelectron spectroscopy (PES) is a powerful experimental technique in providing detailed information about the electronic structures of ground states and excited states of actinide species. In this talk we will present our recent results from a series of joint relativistic quantum mechanical and photoelectron spectroscopy studies on actinyl complexes and uranium halides. Computational details on how to accurately describe excited states with spin-orbit coupling (SOC) will be given. We will focus on the electronic structures of  $\text{UO}_2\text{X}_3^-$  and  $\text{UO}_2\text{X}_4^{2-}$  ( $X = \text{F}, \text{Cl}, \text{Br}, \text{I}$ ) complexes. Theoretical simulation of their experimental photoelectron spectra will also be discussed.

*Keywords* – Actinyl, Relativistic Effects, Spin-Orbit Coupling, Photoelectron Spectrum, Ab initio Wavefunction Theory

### I. INTRODUCTION

Uranyl halides play important roles in the extraction of uranium into the aqueous phase and in serving as useful starting materials for the syntheses of a wide variety of uranium compounds. In this work, we report a joint photoelectron spectroscopy (PES) and relativistic quantum chemistry study on the bonding and stability of a series of gaseous tricoordinate uranyl halide complexes:  $\text{UO}_2\text{X}_3^-$  ( $X = \text{F}, \text{Cl}, \text{Br}, \text{I}$ ). Low temperature PES spectra were obtained at 20 K for the first time by Wang and coworkers at Brown University and these uranyl trihalides were observed to be highly stable electronically with extremely high electron binding energies. Theoretical results from *ab initio* wavefunction theory (WFT) calculations agree well with experiments (Table 1). Extensive bonding analyses for  $\text{UO}_2\text{X}_3^-$  and the doubly-charged tetracoordinate complexes ( $\text{UO}_2\text{X}_4^{2-}$ ) show that the U–X bonds are dominated by ionic interactions with weak covalency. Further theoretical calculations show that the gaseous  $\text{UO}_2\text{X}_4^{2-}$  complexes are thermodynamically unstable against dissociation to  $\text{UO}_2\text{X}_3^- + \text{X}^-$  with decreasing dynamic stability from  $X = \text{F}$  to  $\text{I}$ . The competition between the U–X bonding and the Coulomb repulsions determines the kinetic stability of  $\text{UO}_2\text{X}_4^{2-}$  (Figure 1).<sup>1-4</sup>

**Table 1.** Observed and calculated adiabatic (ADE) and vertical (VDE) detachment energies for  $\text{UO}_2\text{X}_3^-$  ( $X = \text{F}, \text{Cl}, \text{Br}, \text{I}$ ).<sup>a</sup>

		Exp <sup>b</sup>	DFT/PBE		CCSD(T)	
			SR	SO	SR	SO <sup>c</sup>
$\text{UO}_2\text{F}_3^-$	ADE	6.25 (5)	5.44	5.31	6.48	6.35
	VDE	6.53 (5)	5.62	5.52	6.81	6.71
$\text{UO}_2\text{Cl}_3^-$	ADE	6.64 (5)	5.47	5.41	6.82	6.76
	VDE	6.72 (5)	5.52	5.47	6.88	6.83
$\text{UO}_2\text{Br}_3^-$	ADE	6.27 (5)	5.24	5.18	6.45	6.39
	VDE	6.37 (5)	5.24	5.18	6.45	6.39
$\text{UO}_2\text{I}_3^-$	ADE	5.60 (5)	4.84	4.71	5.86	5.73
	VDE	5.72 (5)	4.85	4.72	5.86	5.73

<sup>a</sup> All the energies are in eV. <sup>b</sup> The numbers in parentheses represent the experimental uncertainties in the last digit. <sup>c</sup> These SO results are estimated using the SR CCSD(T) energies with the *ad hoc* SO-corrections from the DFT/PBE calculations.

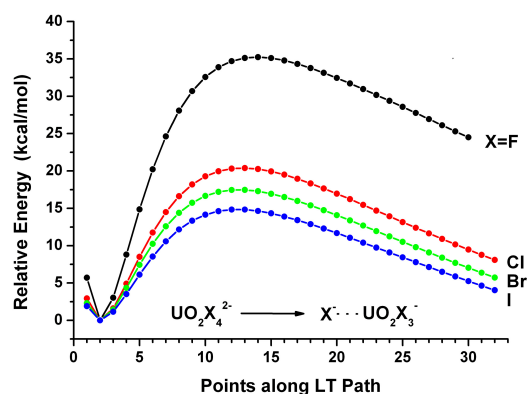


**Figure 1.** Linear transit (LT) energy curves illustrating the dissociation of  $\text{UO}_2\text{X}_4^{2-} \rightarrow \text{UO}_2\text{X}_3^- + \text{X}^-$  ( $X = \text{F}, \text{Cl}, \text{Br}, \text{I}$ ). The energies are obtained from the DFT/PBE calculations.

### REFERENCES

- [1] J. Su, P. D. Dau, Y.-H. Qiu, H.-T. Liu, C.-F. Xu, D.-L. Huang, L.-S. Wang, J. Li, "Probing the Electronic Structure and Chemical Bonding in Tricoordinate Uranyl Complexes  $\text{UO}_2\text{X}_3^-$  ( $X = \text{F}, \text{Cl}, \text{Br}, \text{I}$ ).", *Inorg. Chem.* **52**, 6617-6626 (2013).
- [2] P. D. Dau, J. Su, H.-T. Liu, J.-B. Liu, D.-L. Huang, J. Li, L.-S. Wang, "Observation and investigation of  $\text{UO}_2\text{F}_4^{2-}$  and its solvation complexes with water and acetone nitrile", *Chem. Sci.* **3**, 1137-1146 (2012).
- [3] F. Wei, G. Wu, W. H. E. Schwarz, J. Li, "Excited States and Absorption Spectra of  $\text{UF}_6$ : A RASPT2 Theoretical Study with Spin-Orbit Coupling", *J. Chem. Theory Comp.* **7**, 3223-3231 (2011).
- [4] J. Su, Y.-L. Wang, F. Wei, W. H. E. Schwarz, J. Li, "Theoretical Study of the Luminescent States and Electronic Spectra of  $\text{UO}_2\text{Cl}_2$  in an Argon Matrix", *J. Chem. Theory Comp.* **7**, 3293-3303 (2011).
- [5] J. Su, K. Zhang, W. H. E. Schwarz, J. Li, "Uranyl-glycine-water complexes in solution: comprehensive computational modeling of coordination geometries, stabilization energies, and luminescence properties." *Inorg. Chem.* **50**, 2082-2093 (2011).

## Flow electrolysis of actinide ions utilizing electrocatalysis

Yoshihiro Kitatsuji

Nuclear Science and Engineering Directorate, Japan Atomic Energy Agency

*Abstract – Flow electrolysis enables the exhaustive redox reaction rapidly even the electrochemically irreversible reaction such as reduction of actinide (V) ions. The flow electrolysis cell with platinized glassy carbon fiber working electrode which acts as electrocatalyst is effective to decrease overpotentials of reduction of  $\text{NpO}_2^+$  and  $\text{PuO}_2^+$ . A rapid and precise method for the preparation of U, Np and Pu ions of a desired oxidation state was proposed by taking advantage of the electrocatalytic reaction.*

*Keywords – platinized electrode, actinide ion, flow electrolysis, selective redox reaction*

### I. INTRODUCTION

Actinide ions (An) such as U, Np and Pu exist stably as trivalent to hexavalent ions in acidic and neutral solutions. Control of the oxidation state of these ions to a desired one and determine them are inevitable for the efficient chemical separation or the precise analyses of them, because chemical reactions such as liquid-liquid distribution and complex formation with ligands depend strongly on the oxidation state of the ions.

Electrode reactions of  $\text{An}^{4+}/\text{An}^{3+}$  and  $\text{AnO}_2^{2+}/\text{AnO}_2^+$  couples are electrochemically reversible, and they have been well studied. On the other hand, those of  $\text{An}^{4+}$  and  $\text{AnO}_2^+$  ions couples, which accompanying formation or cleavage of An-O bond, are generally electrochemically irreversible and required a large overpotential. For this reason, selective control of oxidation state of actinide ions by electrolysis is difficult.

Flow electrolysis can attain the exhaustive redox reduction even irreversible one, because electrolytes are electrolyzed repeatedly during the stay of the sample solution in the flow cell. It was reported that reduction of  $\text{AnO}_2^+$  and oxidation of  $\text{U}^{4+}$  can be carried out rapidly when flow electrolysis was applied<sup>1</sup>.

Catalytic reaction can decrease the overpotential as a result of facilitation of the charge transfer between the ion and the electrode. The author has studied redox mechanisms of actinide ions, and clarified that electrocatalytic reaction at Pt electrode can decrease overpotential of reduction of  $\text{NpO}_2^+$  ion<sup>2</sup>. Based on these studies, platinized carbon fiber electrode as a working electrode of the flow electrolysis is expected to be a rapid and precise electrolytic method for controlling oxidation state of actinide ions.

### II. EXPERIMENTAL

Flow electrolysis was performed by using the column electrode system with glassy carbon (GC) fiber working electrode. The GC fiber was packed tightly in a porous glass cylinder of 8 mm inner diameter and 50 mm long.

The platinization of GC working electrode (abbreviated as Pt/GC-WE, hereafter) was carried out by electrodeposition of platinum black onto GC fiber from an aqueous  $\text{H}_2\text{PtCl}_6$  solution.

Flow electrolysis was performed by passing a solution containing an actinide ion through narrow paths among GC fibers in the column electrode at a constant flow rate.

### III. RESULTS AND DISCUSSION

Relations between current and potential for reductions of  $\text{UO}_2^{2+}$ ,  $\text{NpO}_2^+$  and  $\text{PuO}_2^{2+}$  in 1 M  $\text{HClO}_4$  were investigated. Two-electron reduction of  $\text{NpO}_2^+$  to  $\text{Np}^{3+}$  is occurred at -0.14 V when the ordinary GC-WE were employed. This reduction is explained by the catalytic reaction where  $\text{Np}^{4+}/\text{Np}^{3+}$  couple acts as an electron transfer mediator for  $\text{NpO}_2^+$  reduction. So the potential observed for the  $\text{NpO}_2^+$  reduction is close to that of  $\text{Np}^{4+}$  reduction. On the other hand, overpotential of  $\text{NpO}_2^+$  reduction is mitigated by Pt/GC-WE electrode, and two-step reduction, i. e. the one-electron reduction of  $\text{NpO}_2^+$  to  $\text{Np}^{4+}$  followed by that of  $\text{Np}^{4+}$  to  $\text{Np}^{3+}$ , proceeded at the Pt/GC-WE. The overpotential of reduction of  $\text{PuO}_2^+$  is also decreased at Pt/GC-WE, but reduction of  $\text{UO}_2^{2+}$  to  $\text{U}^{4+}$  in 1 M  $\text{HClO}_4$  was less affected by the electrode materials.

Based on the results of the flow electrolysis with Pt/GC-WE, the selective adjustment of the oxidation states of actinide ions can utilize. For example, when a solution containing Np ions of various oxidation states is electrolyzed at the potential in the ranges more positive than +1.1 V, from +0.2 to 0 V, and more negative than -0.26 V, the oxidation state of Np is adjusted to  $\text{NpO}_2^{2+}$ ,  $\text{Np}^{4+}$  and  $\text{Np}^{3+}$ , respectively; when a solution containing U, Np and Pu ions is electrolyzed at the potential in the range between +0.20 and +0.15 V, U, Np and Pu ions of different oxidation states (i.e.,  $\text{UO}_2^{2+}$ ,  $\text{Np}^{4+}$  and  $\text{Pu}^{3+}$ ) can be prepared<sup>3</sup>.

### REFERENCES

- [1] H. Aoyagi, Y. Kitatsuji, Z. Yoshida, S. Kihara, *Anal. Chim. Acta*, 538(2005)283.
- [2] Y. Kitatsuji, T. Kimura, S. Kihara, *J. Electroanal. Chem.*, 641(2010)83.
- [3] Y. Kitatsuji, T. Kimura, S. Kihara, *Electrochim. Acta*, 74(2012)215.

## Determination of the thermodynamic quantities of U(VI) complexation with “aliphatic” and “aromatic” di-carboxylic acids by calorimetry

Akira Kirishima and Nobuaki Sato

Institute of Multidisciplinary Research for Advanced Materials, Tohoku University,  
2-1-1, Katahira, Aoba-ku, Sendai, 980-8577, Japan

The thermodynamic quantities ( $\Delta G$ ,  $\Delta H$ ,  $\Delta S$ ) of complex formation of U(VI) with four “aliphatic” di-carboxylic acids, *i.e.*, glutalic acid (GA)<sup>[1]</sup>, oxydiacetic acid (ODA), thiodiacetic acid (TDA), iminodiacetic acid (IDA), and four “aromatic” di-carboxylic acids, *i.e.*, isophthalic acid (IPA), 2,5-frandicarboxylic acid (FDA), 2,5-thiophenedicarboxylic acid (TDCA) and dipicolinic acid (DPA) were determined by the potentiometric titration and micro-calorimetric titration. So far, extensive data on stability constant have been obtained and summarized in databases for a variety of combinations of actinide ions and ligands, which plays important role as the basic parameters for the prediction of migration behavior of these elements in the geosphere, and for the development of new separation process. However, enthalpy and entropy data of actinide elements are scarce in comparison with stability constants. These data are demanded not only for the understanding of the reaction mechanism but also for the estimation of stability constants at elevated temperatures outside the range of 20 – 30 °C by the extrapolation from those at a room temperature with using thermodynamic models. Following our previous study reporting thermodynamic data ( $\Delta G$ ,  $\Delta H$ ,  $\Delta S$ ) of complexation of 8 di-carboxylates with U(VI) [1], this paper presents the thermodynamic quantities of U(VI) complexation with four “aliphatic” di-acetic acids and four “aromatic” di-acetic acids. Those ligands have a different center atom between two carboxylic groups, *i.e.*, carbon for GA and IPA, oxygen for ODA and FDA, sulfur for TDA and TDCA, and nitrogen for IDA and DPA, which may coordinate with a metal cation. The obtained thermodynamic quantities are compared with each other for the discussion of the effect of structural difference *i.e.*, aliphatic- and aromatic structure and types of central atom in the ligands on the complex formation thermodynamics.

From the obtained thermodynamic quantities, it is indicated that these reactions are mainly driven by the entropy change while the enthalpy change is not promoting the progress of the reaction. The  $\Delta G$ ,  $\Delta H$  and  $\Delta S$  of 1:1 IDA complex show remarkable difference from those of GA complex, while those of ODA and TDA complex are almost equal to those of GA complex. The  $-\Delta G$  of 1:1 IDA complex with U(VI) was 30 kJ/mol larger than that of GA complex, which is attributed to the chelate effect of the ligand. Our calorimetric measurement has revealed that this “chelate effect” should be ascribed to the “entropy effect” since  $T\Delta S$  of IDA complex was 50 kJ/mol larger than that of GA complex.

[1] A. Kirishima, Y. Onishi, N. Sato and O. Tochiyama, *Radiochim. Acta* **96** (2008) 581–589.

## Electrochemical Behavior of Americium in NaCl-2CsCl Melt

Hirokazu Hayashi<sup>1</sup>, Mitsuo Akabori<sup>1</sup>, Kazuo Minato<sup>1,2</sup>

<sup>1</sup>Nuclear Science and Engineering Directorate, Japan Atomic Energy Agency,  
2-4 Shirakata-shirane, Tokai-mura, Naka-gun, Ibaraki-ken 319-1195, Japan

<sup>2</sup>Present address: Tokai Research and Development Center, Japan Atomic Energy Agency,  
2-4 Shirakata-shirane, Tokai-mura, Naka-gun, Ibaraki-ken 319-1195, Japan

*Abstract* –The behavior of Am in NaCl-2CsCl melt was investigated by voltammetry, and potentiometry with an yttria-stabilized zirconia membrane electrode. Redox reactions of Am(III)/Am(II) and Am(II)/Am(0) were observed. Chemical reaction of Am<sup>3+</sup> ions with O<sup>2-</sup> ions in NaCl-2CsCl melt at 823K has been considered to make Am<sub>2</sub>O<sub>3</sub> precipitates.

*Keywords* – Am, molten salt, electrochemistry

### I. INTRODUCTION

For a basis of the future nuclear fuel cycle, it is very important to understand and control the behavior of TRU (Np, Pu, Am, Cm) in the nuclear fuel cycle. Experimental study of pyrochemical process of fuels containing TRU is one of the important topics. But, few data are available in literature on the behavior of TRU such as americium in NaCl-2CsCl melt which is considered to be used as one of the solvents for pyrochemical reprocessing. In the present study, the behavior of Am in NaCl-2CsCl melt was investigated by electrochemical methods.

### II. EXPERIMENTAL

Anhydrous NaCl-2CsCl mixed salts (99.99%, Anderson Physical Laboratory Engineered Materials (APL)), cadmium chloride (99.9%, APL), and silver chloride (99.9%, APL) were used as purchased in this study. AmCl<sub>3</sub> was prepared by the solid-solid reaction of americium nitride and cadmium chloride [1]; <sup>241</sup>AmO<sub>2</sub> sample prepared 35 years ago was used as a starting material. All the materials were handled in a glove box or a hot cell maintained with a purified argon gas atmosphere [2]. Typical impurities in the argon gas were H<sub>2</sub>O < 1 ppm and O<sub>2</sub> < 1 ppm.

The sample in an alumina crucible was heated under an Ar gas flow after setting a cover of the furnace having the electrodes, and a stirrer made of Mo metal. Electrochemical measurements with 3 electrodes were carried out for AmCl<sub>3</sub>-(NaCl-2CsCl) system with X(AmCl<sub>3</sub>)=4.0×10<sup>-4</sup> mainly at 823K using a PAR263A potentiostat/galvanostat with a CorrWare electrochemical software (Scribner Associates Inc.). The working electrode was a 1mmφ tungsten wire. Assembled two tungsten wires (1mmφ) were used as the counter electrode. The reference electrode was a silver wire (1mmφ) dipped in the AgCl (X(AgCl)=0.0487) - (NaCl-2CsCl) placed in a mulite tube. Potentiometric titration of Am<sup>3+</sup> ion with O<sup>2-</sup> ion using BaO (mixture of BaO and NaCl-2CsCl) was carried out at 823K. The values for pO<sup>2-</sup> were monitored with a pO<sup>2-</sup> indicator electrode made with yttria-stabilized zirconia filled with

molten NaCl-2CsCl containing oxide ion and silver ion ([O<sup>2-</sup>]=0.01mol/kg, [Ag<sup>+</sup>]=0.37mol/kg) in which a silver wire was dipped. The electromotive force (EMF) of the cell Ag|NaCl-2CsCl-AgCl-O<sup>2-</sup>|ZrO<sub>2</sub>-Y<sub>2</sub>O<sub>3</sub>|NaCl-CsCl-AmCl<sub>3</sub>-O<sup>2-</sup>|Mulite|NaCl-2CsCl-AgCl|Ag was measured with an electrometer (Keithley Model6514). Temperatures of the molten salt sample were measured with R type thermocouple set in an alumina tube.

### III. RESULTS AND DISCUSSION

A typical cyclic voltammogram shows 2 groups of signals close to the lower limit of the electrochemical window. The lower limit signals around -2.3V correspond to electrodeposition of alkaline metal. The higher limit signal around +1.0V corresponding to evolution of chlorine gas was also observed. The signals can be assigned to redox reactions of Am(III)/Am(II) and Am(II)/Am(0) comparing with those in LiCl-KCl eutectic melt [3].

The EMF values were measured during the additions of BaO from α= [O<sup>2-</sup>]/[Am<sup>3+</sup>]=0 to 2.22. α is defined as the ratio of added oxide ion over the initial Am(III) ion. The titration curve shows only one equivalent point at α = 1.5. This value corresponds to the formation of Am<sub>2</sub>O<sub>3</sub> according to the reaction, 2Am<sup>3+</sup>+3O<sup>2-</sup>=Am<sub>2</sub>O<sub>3</sub>(s). The chemical form of the precipitation of plutonium in the molten salts has been reported as Pu<sub>2</sub>O<sub>3</sub> [4, 5]. Our results indicate the similarity of the precipitation behavior of Am with that of Pu in molten salts.

### ACKNOWLEDGMENTS

Part of the present study was carried out within the collaborative research program of TRU behavior in pyrochemical processes with Tohoku Electric Power Company, Tokyo Electric Power Company and The Japan Atomic Power Company.

### REFERENCES

- [1] H. Hayashi, M. Takano, M. Akabori, K. Minato, J. Alloys Compd. 456, 243-246 (2008).
- [2] K. Minato, M. Akabori, T. Tsuboi, S. Kurobane, H. Hayashi, M. Takano, H. Otobe, M. Misumi, T. Sakamoto, I. Kato, T. Hida, JAERI-Tech 2005-059 (2005) (in Japanese).
- [3] H. Hayashi, M. Akabori, K. Minato, Nucl. Technol., 162, 129-134 (2008).
- [4] D. Lambertin, S. Ched'homme, G. Bourges, S. Sanchez, G. Picard, J. Nucl. Mater., 341, 124-130 (2005).
- [5] C. Caravaca, A. Laplace, J. Vermeulen, J. Lacquement, J. Nucl. Mater., 377, 340-347 (2008).

## **Production of High Specific Activity Radiolanthanides for Medical Purposes using the UC Irvine TRIGA Reactor**

Leila Safavi-Tehrani<sup>1</sup>, George E. Miller<sup>2</sup> and Mikael Nilsson<sup>1</sup>

University of California, Irvine

<sup>1</sup>Department of Chemical Engineering & Materials Science

<sup>2</sup>Department of Chemistry

916 Engineering Tower, Irvine, CA 92697-2575

Lsafavit@uci.edu

Radioactive lanthanides have become an important imaging, diagnostic and therapeutic tool in the medical field. For example, the neutron rich samarium isotope of <sup>153</sup>Sm has been proven to have desirable characteristics for treatment of bone cancer. However, for medical purposes, the radioactive lanthanide isotope must be produced at high specific activity, i.e. low concentration of inactive carrier, so they are both beneficial for therapy and the concentration of the metal ions does not exceed the maximum sustainable by the human body. The objective of our research is to produce radioactive lanthanides with high specific activity in a small-scale research reactor using the Szilard-Chalmers method. The Szilard-Chalmers process is a method that separates radioactive ions away from a bulk of nonradioactive ions by neutron capture. We propose an innovative experiment setup to instantaneously separate the radioactive recoil product formed during irradiation from the bulk of non-radioactive ions. The instant separation prevents the recoiled radioactive nucleus from reforming its original bonds with the target matrix and chemically separates it from the non-radioactive target matrix, resulting in a carrier free radiolanthanide with increased specific activity. We will present methods for preparation and synthesis of the material used for irradiations and the results of enrichment factors and extraction yields in radioactive lanthanide solutions. We will also investigate degradation by ionizing radiation that occurs during neutron activation to determine the stability of the target material during irradiations. The obtained results will be compared to previously published methods and their corresponding results.

## Mycoremediation: Fungus-based Soil Remediation of Radioisotope Contamination

Steven LaZar<sup>1</sup>, Eric Rasmussen, MD, MDM, FACP<sup>2</sup>, and Paul Stamets, D.Sc.<sup>3</sup>

<sup>1</sup>Managing Director and Department of Energy (DOE) Program Manager, MGI, Seattle, Washington

<sup>2</sup>Research Professor, Environmental Security and Global Medicine, San Diego State University, San Diego, California

<sup>3</sup>Chief Scientist, Fungi Perfecti Research Laboratories, Kamilche Point, Washington, USA

*Abstract – Fungal mycelia in soil can hyperaccumulate radioisotopes at up to 25,000 Bq per kg of mushrooms [1]. Mycelium Group International (MGI) here introduces mycelial radioactive decontamination techniques (mycoremediation) that can potentially restore safe soil levels on Fukushima farmland in less than ten years with high efficiency, without loss of topsoil, and less expensively than current destructive methods.*

*Keywords – cesium, farmland, Fukushima, fungi, mycelium, remediation, topsoil*

### 1. Introduction

Mycoremediation uses selected fungi to reduce contaminants in a step-function based on species and soil characteristics, weather and season parameters, harvest frequency, and contamination concentration.

The 2011 Fukushima nuclear disaster released more than 538,000 teraBecquerels (TBq) of radioactive Iodine-131, Cesium-134, and Cesium-137. As a result of that cesium deposition, the Japanese government has declared more than 1,300 square kilometers of northern Japan to be unsafe for human habitation and unsafe for food production. Conventional remediation is currently removing valuable farm topsoil at a rapid rate.

MGI has developed new capabilities for reducing radioactive Cesium-137 contamination in soil to achieve safety goals set by the IAEA, while retaining valuable topsoil and restoring safe farming decades earlier than anticipated. MGI's mycological research and industrial process designs are currently undergoing independent testing at two US Department of Energy Laboratories.

Our mycoremediation technique uses our unique strains of cultivated fungi to remove Cesium-137 by either biosorption or metabolism-dependent intracellular uptake. Our fungi start as microscopic spores that form spreading

mycelial strands similar to a spider's web in topsoil, with measurements in some species of 300 square meters per meter of plant root [2]. The mycelia in the soil then concentrate the Cesium-137 in their strands as they form into mushrooms which are then harvested as radioactive waste. Since, in some fungal biochemistry, cesium mimics potassium - a necessary element in cellular metabolism - local cesium uptake can be rapid. Also, since mycelium are only a single cell thick and yet can comprise up to 45% of soil biomass in temperate zones [3], the calculated mycelial surface area available for cesium absorption is enormous.

Some hyper-accumulating fungal species can form mushrooms from mycelial mats every 60 days. Harvesting radioactive mushrooms therefore results in the removal of significant fractions of cesium contamination from topsoil multiple times each year. Our current research is showing that we can very likely use our mycoremediation techniques on radioactive farmland around Fukushima to meet IAEA safety standards in less than ten years while preserving topsoil critical to the restarting of a productive farm economy.

### 2. Mycoremediation Processes

MGI's mycoremediation processes include in-situ remediation, post-sort hot-pile remediation, and acid-leach resin column adsorption. The processes are safe, nearly silent, rapidly implemented, have low infrastructure requirements and can, in many cases, improve the soil to better than pre-contamination condition. The result is land again available for crop production earlier than anticipated, with far less volume for radioactive waste disposal, and at a cost that is substantially less than any other remediation process.

[1]Epik and Yprack, 2003

[2]Jones, 1991

[3]Stamets, 2005

## Automatic Cs-Uptake Device for Radioactive-Cs Evaluation in Environmental Water

Kimitaka Minami<sup>1</sup>, Takayuki Funabashi<sup>2</sup>, Ryuichi Kamimura<sup>2</sup>, Tetsuo Yasutaka<sup>1</sup>, Hisashi Tanaka<sup>1</sup>,  
 Akiko Kitajima<sup>1</sup>, Hiroshi Ogawa<sup>1</sup>, and Tohru Kawamoto<sup>1</sup>

<sup>1</sup>National Institute of Advanced Industrial Science and Technology (AIST)

<sup>2</sup>Tokyo Power Technology Ltd.

**Abstract** –We developed an automatic Cs-uptake device for concentrating the dilute radioactive cesium (r-Cs) in environmental water, especially paddy fields water. The device was set onto paddy fields and the r-Cs in more than 400 L of water in 24 hours was automatically concentrated in the small columns without external power supply. With this device, 0.01 Bq/L of r-Cs concentration can be evaluated by the r-Cs measurement of the columns.

**Keywords** – Prussian blue, radioactive cesium, environmental water, monitoring

### I. INTRODUCTION

By the Fukushima Daiichi Nuclear Power Plant accident by the March 2011 Great East Japan Earthquake and subsequent tsunami, radioactive materials were released into the atmosphere and deposited over widespread agricultural, forest, and urban areas.

Now, radioactive materials, especially radioactive cesium (r-Cs), gradually migrate into environmental water and affect farm products even if these are low-level concentration. We have developed a monitoring method to investigate the low-level r-Cs concentration in environmental water by each existence form. Yasutaka et al. (2013) developed a method to adsorb 90% of dissolved r-Cs in 20 L water within 10 minutes using Prussian Blue (PB) impregnated nonwoven fabric. Tsuji et al. (2013) developed a cartridge filter which can concentrate up to 30 g of suspended solid in environmental water and more than 98% of suspended solid r-Cs in 20 L water was concentrated within 10 minutes. In this way, we can easily evaluate level of r-Cs in a short time by using germanium detector.

In this study, we developed another device for concentrating dilute r-Cs in environmental water, especially paddy fields water, as the average for a long time more than 1 day automatically without external power supply.

### II. SETUP AND RESULTS

The developed device was shown in Fig 1. It includes pump, battery, cartridge filter, cesium adsorbed column with PB nanoparticles, and flow meter. The pump and the battery were chosen so that flow rate continually became 0.3 L/min for 24 hours. Suspended solid in environmental water was filtrated and concentrated by cartridge filter with large filtration area and 1  $\mu$ m of pore-size. Dissolved Cs in the filtrate was adsorbed and concentrated onto PB. This PB

column was developed for the structure that was measured by simple operation when it was measured by germanium detector. The device was designed so that less than 5 cm sank in order to use in the paddy with the very shallow water depth.

The r-Cs concentrations in a pond and paddy in Fukushima evaluated with the device were shown in Table 1. By passing more than 400 L of water through the device, around 0.01 Bq/L of dissolved r-Cs in paddy water can be evaluated in the 1,800 seconds measurement by the germanium semiconductor detector.

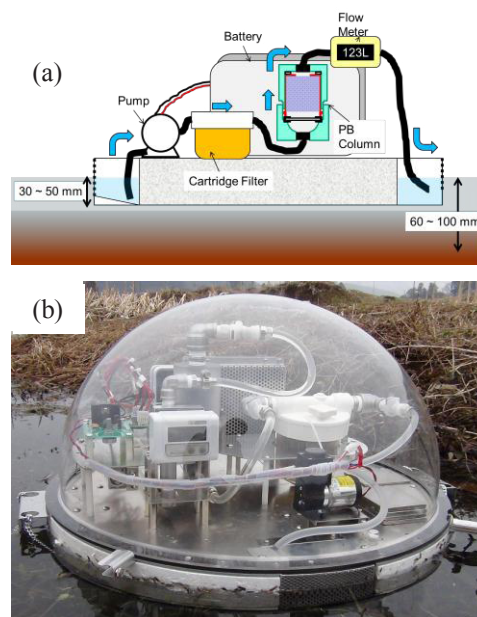


Fig 1. The automatic r-Cs uptake device (a) schematic view (b) appearance

Table 1. r-Cs Concentration in environmental water

Environmental Water	Flow Rate (L/min)	Pass Water (L)	Sample	Measuring Time of Ge 1,800 sec		
				r-Cs* Concentration (Bq/L)	Counting Error ( $\pm$ Bq/L)	Detection Limit (Bq/L)
Paddy	0.3	419	SS Cartridge	0.068	0.0034	0.0036
			PB Column	0.014	0.0020	0.0031
Pond	0.3	348	SS Cartridge	0.042	0.0031	0.0047
			PB Column	0.049	0.0038	0.0037

\*Cs<sup>134</sup>+Cs<sup>137</sup>

- [1] Yasutaka et al.(2013), Appl. Chem. (in Japanese), in press  
 [2] Tuji et al. (2013), APSORC13

## Pilot plant for volume reduction of Cs-contaminated combustible materials

Kitataka Minami<sup>1</sup>, Hiroshi Ogawa<sup>1</sup>, Hisashi Tanaka<sup>1</sup>, Akira Takahashi<sup>1</sup>, Tatsuya Uchida<sup>1</sup>, Akiko Kitajima<sup>1</sup>, Durga Parajuli<sup>1</sup>, Tohru Kawamoto<sup>1</sup>, Masaki Yamaguchi<sup>2</sup>, Mitsuo Osada<sup>2</sup>, Nobuaki Otake<sup>2</sup>, Syuichi Sato<sup>2</sup>, Ryuichi Kamimura<sup>2</sup>, and Yukiya Hakuta<sup>1</sup>

<sup>1</sup>Nanosystem Research Institute, AIST, Japan

<sup>2</sup>Tokyo Power Technology Ltd., Japan

*Abstract* – We report the pilot plant test for volume reduction of radioactive-Cs (r-Cs)-contaminated combustible materials for the volume reduction of the contaminated waste, and to reduce the r-Cs leaching from the waste. The combustible wood is incinerated by the biomass boiler. The radioactive-Cs stored in ash is extracted into the water, and finally is captured into the Prussian blue-nanoparticle adsorbents.

*Keywords* – radioactive-Cs, Prussian blue, incineration, adsorbents

### I. INTRODUCTION

Around Fukushima area, there are so much combustible materials contaminated by the radioactive Cs (r-Cs), e.g. the wood in forests, municipal waste, and waste from agriculture. Japan government showed the policy that the municipal waste with r-Cs contamination should be incinerated. In addition, the biomass power system with the incineration of the contaminated wood materials is also planned around Fukushima area.

There are problems in the management of the incineration of the combustible material. One is the large amount of the volume of ash and the other is the r-Cs leaching from the ash. In order to solve the problems, the extraction of leachable r-Cs from the ash as the pre-treatment before disposal is gathering attention. In order to confirm the method for the safety management based on the incineration and the r-Cs extraction from the ash, we carried out the plant-scale test.

### II. METHOD AND RESULTS

The firewood was incinerated in a biomass boiler shown in Fig. 1(a). To avoid the emission of the r-Cs in the exhaust, the bag filter and HEPA filter is prepared. The r-Cs is trapped in ash mainly stored in the boiler and the bottom of the bag filter. In the next step, the r-Cs is extracted from the ash into the water in the ash-decontamination unit shown in Fig.1(b)[1]. Finally the r-Cs is captured by the adsorbents with Prussian blue nanoparticles shown in Fig.2.

When 465 kg of firewood was incinerated (r-Cs concentration  $\sim 0.3$  kBq/kg), 1.35 kg of ash was obtained. The highest r-Cs concentration of was  $\sim 210$  kBq/kg at the bag filter. The r-Cs in the exhaust in the incineration was undetectable. The r-Cs extraction ratio from the ash into water was 50-90%. The r-Cs in the water after the decontamination of the adsorbent was also undetectable.

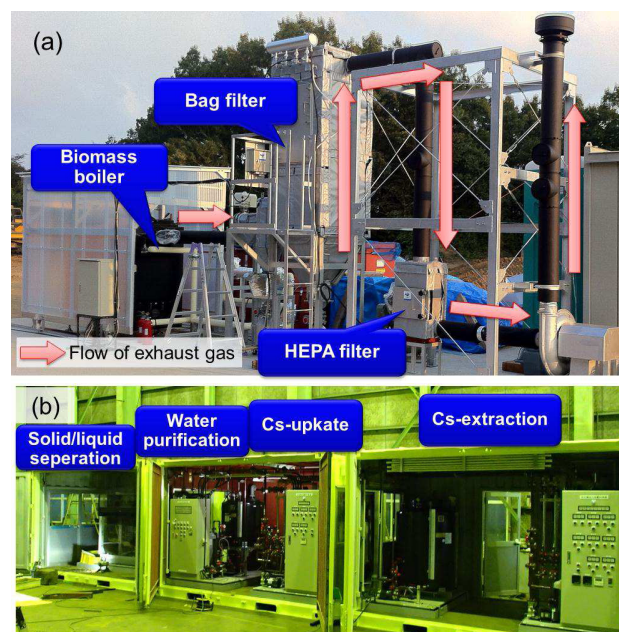


Fig. 1. for volume reduction of Cs-contaminated combustible materials. (a) biomass boiler with gas-filters for Cs-reduction from exhaust, (b) Ash-decontamination unit.



Fig. 2. Various Cs-adsorbents with Prussian blue nanoparticles

[1] D Parajuli et al., Env. Sci. Tech., *in press*.

## Decontamination of Radioactive Cesium from Ash and Soil

Durga Parajuli<sup>1</sup>, Hisashi Tanaka<sup>1</sup>, Shigeharu Fukuda<sup>2</sup>, Ryuichi Kamimura<sup>2</sup>, Tohru Kawamoto<sup>1</sup>  
<sup>1</sup>Nanosystem Research Institute, AIST, <sup>2</sup>Tokyo Power Ltd., Japan

**Abstract** – Methods for the removal of Cesium from contaminated tsunami-debris, top-soil, and forest litter was studied. Incineration of tree bark resulted over 95% volume reduction. Fly ashes from wood, municipal garbage, and sewage sludge with enriched Cesium were washed with water at varying temperatures. Cesium along with other alkali metals was easily washed from the garbage ash and wood ash. But, only acid treatment at higher temperature could release Cesium from sewage sludge ash. Also, Cesium removal from soils with acid solutions was studied from 25 to 200 °C. Though the release was higher at higher temperatures, results varied with the soil type.

**Keywords** – Radioactive Cesium, Extraction, Ash, Soil, Soil type

### I. INTRODUCTION

Now two years after the Fukushima Daiichi Nuclear Power Plant disaster, the main problem is exposure to the radioactivity due to the long living radioisotopes of Cesium, <sup>134</sup>Cs (approx.  $1.8 \times 10^{16}$  Bq) and <sup>137</sup>Cs (approx.  $1.5 \times 10^{16}$  Bq).<sup>1-3</sup> So, we are conducting elaborated study to address the issues of Cs contaminated tsunami-debris, paddy field soil, forest litter and stream water so as to control the long term entry of the radioactive Cs to the ecosystem.

### II. EXPERIMENTAL

Wood incineration ash, municipal garbage incineration ash, and sewage sludge ash were studied for Cs extraction. Also, soil samples collected from different areas in Fukushima prefecture were also tested for Cs removal. Ash samples were washed with water in flow or batch by varying ash-water ratio, temperature, etc. For comparison, dilute acid solutions were also studied. Acid solutions were tested for the extraction of Cs from clay containing substrates: sludge ash and soil.

### III. RESULTS AND DISCUSSION

#### *Incineration of contaminated waste and extraction of Cs*

Incineration is the most suitable option for volume reduction and compaction of burnable wastes like tsunami debris, forest litter, plants, and household garbage. For this, incineration experiment taking the radioactive cesium contaminated tree bark was performed. When the volume was reduced to 5% of the initial mass, its fly ash showed 137 kBq/kg Cs-activity. Because the current Japanese Government's guideline allows landfill of wastes showing

less than 8 kBq/kg, the disposal of enriched ash is problematic. Therefore, Cs-extraction study was performed taking ashes of tree-bark, household garbage, and municipal sewage sludge. Over 70% Cs-133 along with other alkali metals was easily washed with water from the garbage ash and wood ash. Figure 1 shows the change in the residual mass of the wood fly ash, Cs, and K in after washing with water in 1:10 ratio at different temperatures. The residual mass was 18-25% less, with higher drop at higher temperature. This result shows 70-80% dissolution of Cs and more than 90% K. These outcomes suggest the feasibility of compaction of the burnable waste by incineration followed by decontamination by washing with water.

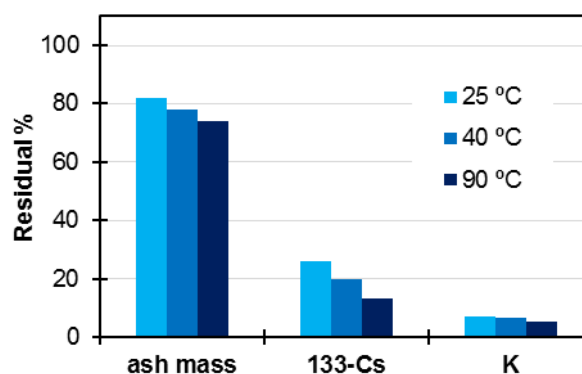


Figure 1. Change in residual mass of ash, Cs, and K with respect to the initial mass in the wood ash before and after washing with water.

#### *Extraction of Cs from Soil and Sludge ash*

Unlike the significant Cs removal observed with wood ash or garbage ash, the method was ineffective for the removal of Cs from soil and sewage sludge. So, a number of reagents were tested, and mineral acid solutions at higher temperature were found to be effective. However, the results varied widely depending upon the soil type. At 95 °C with 0.5 M nitric acid solution, Cs removal from the brown forest soil was around 50%, however only 20% release was observed for Kuroboku-soil. Results to the date showed that Cs extraction from soils other than Kuroboku type is effective with acid at higher temperature.

#### References

- [1] IAEA Radiological Assessment Report Series (2006)
- [2] Y. Masumoto, et al. *Elements*, 8, 207 (2012)
- [3] R. Stone, *Science*, 331, 1507 (2011).

## Rapid radioanalytical determination of U, Pu, and Am in radioactive wastes via extraction chromatography, alpha spectrometry, and thermal ionization mass spectrometry

Tae-Hong Park, Yong Sul Choi, Jong-Ho Park, Jong-Yun Kim, Sang-Eun Bae, Young-Hwan Cho,  
 Jei-Won Yeon, Kyuseok Song

Nuclear Chemistry Research Division, Korea Atomic Energy Research Institute, 989-111 Daedeok-daero, Yuseong-gu, Daejeon,  
 305-353, Korea

### Abstract

We optimize extraction chromatographic separation procedures to assay alpha particle emitting nuclides for disposal purpose of radioactive wastes generated from power plants and pyroprocessing laboratories. In particular, U isotopes are isolated on UTEVA resin, whereas Pu and Am/Cm isotopes are subsequently separated on TRU resin.

### Keywords

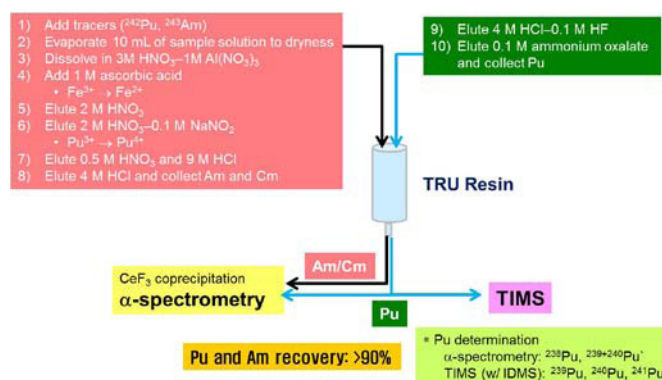
Actinides, Extraction chromatography, Radioactive wastes

### I. INTRODUCTION

Management of radioactive wastes requires sensitive and accurate radioanalytical determination procedures that include rapid and reliable chemical separation methods for a broad range of sample types, and radiometric evaluation tools [1]. Extraction chromatography has been successfully applied to separate the radionuclides of interest for a wide variety of environmental samples and thus many reliable procedures have been also developed with commercially available resin [2]. Here, we optimize rapid and reliable radiochemical determination of U, Pu, and Am/Cm isotopes via extraction chromatography, coprecipitation, alpha spectrometry, and isotope dilution-thermal ionization mass spectrometry (IDMS-TIMS) by which we estimate the alpha-emitting nuclide activities of low-level wastes generated from power plants and pyroprocessing laboratories.

### II. EXPERIMENTAL

A radiochemical determination procedure of Pu, and Am/Cm nuclides is illustrated in Scheme 1.



Scheme 1. Radiochemical determination of Pu and Am/Cm

### III. RESULTS

The method in scheme 1 typically presented recovery yields of nuclides > 90% when a cocktail of ~0.1 Bq of  $^{242}\text{Pu}$ , and  $^{243}\text{Am}$  was separated on TRU resins. We also separated out Pu, Am, and Cm isotopes from low-level waste samples, and determined the nuclide activities via alpha spectrometric measurements of  $\text{CeF}_3$  coprecipitating alpha-emitters and ID-TIMS especially for  $^{239}\text{Pu}$ ,  $^{240}\text{Pu}$ , and  $^{241}\text{Pu}$ .

### IV. CONCLUSION

The methods developed in this report have shown good separation of U, Pu, and Am/Cm nuclides from radioactive wastes with high recovery yields. Because the isolated nuclides are determined by alpha spectrometry and ID-TIMS that can effectively quantify the nano- and picogram amounts of alpha emitters, the rapid and efficient chromatographic separation procedures in this report need marginal amounts of radioactive samples leading to reduction of chemical waste and radiation exposure.

- [1] M. H. Lee, E. C. Jung, W. H. Kim, K. Y. Jee, J. Alloys Compd. 444-445 (2007) 544-549
- [2] S. L. Maxwell III, B. K. Culligan, G. W. Noyes, J. Radioanal. Nucl. Chem. 286, (2010), 273-282

## Luminescence Spectroscopy of Uranium Complexes in Non-Aqueous Media

Noboru Aoyagi<sup>1\*</sup>, Masayuki Watanabe<sup>1</sup>, Akira Kirishima<sup>2</sup>, Nobuaki Sato<sup>2</sup>, Takaumi Kimura<sup>1</sup>

<sup>1</sup>Nuclear Science and Engineering Directorate, Japan Atomic Energy Agency,  
 Shirakatashirane 2-4, Tokai-mura Naka-gun, Ibaraki, 319-1195, Japan

<sup>2</sup>Institute of Multidisciplinary Research for Advanced Materials, Tohoku University,  
 1-1 Katahira, 2-chome, Aoba-ku, Sendai, 980-8577, Japan

*Abstract* – Syntheses and optical properties of tetravalent or hexavalent uranium compounds were studied to understand photo-physics under the unexplored condition such as in non-aqueous media or the cryogenic temperature. Uranium dioxide, halides or uranium metal were used as starting materials to yield the luminescent compounds in a series of organic solvents; the luminescence-solvent structure relationship was investigated using UV-Vis absorption and time-resolved laser-induced luminescence spectroscopies.

*Keywords* – Uranium(IV), (VI) complexes, Luminescence, Time-Resolved Laser-induced Fluorescence Spectroscopy (TRLFS)

Luminescence studies on uranium compounds have been mainly related to  $U^{VI}O_2$  for the stability under ambient conditions and its high quantum yield of luminescence. In contrast, only a few studies on the luminescence properties of  $U^{4+}$  are known<sup>[1-3]</sup> due to the lack of information on the structure-spectrum relationship and its much less quantum yield. A fundamental study to further understand the optical property is indispensable and considered in two approaches; a molecular design to enhance the luminescence intensity using asymmetric complexes or ligand-to-metal energy transfer, or a spectroscopic method performed at cryogenic temperatures. Wang et al.<sup>[4]</sup> and our previous studies<sup>[5,6]</sup> report on the advantages in measuring luminescence of  $U^{VI}O_2^{2+}$  at 77 K or below 77 K, however, such studies are uncommon. And thus we demonstrate a photophysical study on a series of uranium compounds designed to make luminescence intensity enhanced in order to elaborately obtain well-defined spectra in the present work.

A series of uranium sulfides, oxides, or halides such as  $US_2$ ,  $UOS$ ,  $UF_4$ ,  $UCl_4$ ,  $UBr_4$ ,  $UI_4$  were synthesized as starting materials via the reaction of uranium metal with halogen gasses at elevated temperature, and the resulting powder was characterized by XRD. In an Ar-operated glove box the powder were added into 1,4-dioxane, ethanol, tetrahydrofuran (THF), 1-methyl-THF, etc. The solution was put into non-luminescent cell. Under the irradiation of excitation UV-lamp at 302 nm, luminescence spectra are observed (Fig. 1) in time-gated ICCD camera.

Emission spectra of  $[Li(THF)_4][UCl_5(THF)]$ , **1** which forms a crystalline solid is first characterized and investigated by Baker<sup>[3]</sup>, reporting three featureless bands observed in the UV and visible region centered at 365 nm, 421 nm, and 518 nm for the solution of **1** in THF with  $\lambda_{ex}$  = 260 to 390 nm as an excitation wavelength. While the present spectrum of  $UCl_4$  in THF, **2** also exhibits the

structureless bands with two peaks around 368 nm and 416 nm at room temperature, the third peak seen for **1** in THF was not observed. However,  $UCl_4$  in dioxane, **3** provides more intense and featured spectrum having peaks at 349 nm, 378 nm, and 459 nm. Compared to **1** in THF, the remarkable blue shifts for all peaks appeared in **3**. This still seems a structureless band of  $U^{4+}$  ion, so that the spectral shape might be almost identical to that of  $UCl_4(THF)_3$  in THF, except different peak values: 362 nm, 410 nm, and 500 nm. There was no peak of  $UCl_4$  found in ethanol in which quenching of luminescence is taken place or the higher symmetrical structure could presumably provide the less probability in the f-f transitions. Further spectroscopic data such as TRLFS and low temperature measurements are to be discussed with regard to possible structures in solutions by digging into unexplored photoluminescence.

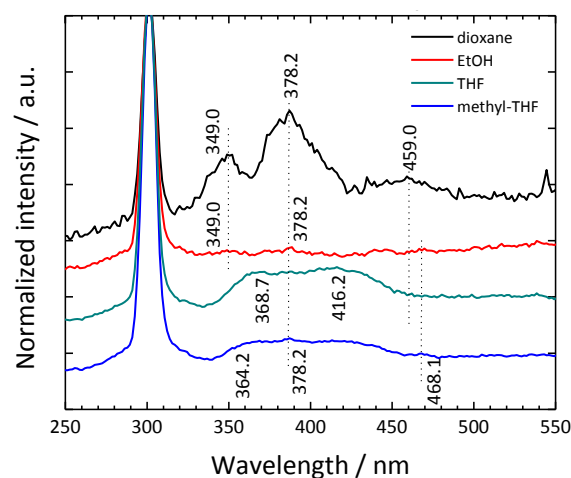


Fig. 1. Luminescence spectra of  $UCl_4$  in organic solvents:  $\lambda_{ex}$  = 302 nm.

### References

- [1] A. Kirishima, T. Kimura, O. Tochiyama, Z. Yoshida, *Chem. Commun.* **2003**, 910.
- [2] L. S. Natrajan, *Coord. Chem. Rev.* **2012**, 256, 1583-1603.
- [3] E. Hashem, A. N. Swinburne, C. Schulzke, R. C. Evans, J. A. Platts, A. Kerridge, L. S. Natrajan, R. J. Baker, *RSC Advances*, **2013**, 3, 4350-4361.
- [4] Z. Wang, J. M. Zachara, W. Yantasee, P. L. Gassman, C. Liu and A. G. Joly, *Environ. Sci. Technol.*, **2004**, 38, 5591-5597.
- [5] R. N. Collins, T. Saito, N. Aoyagi, T.E. Payne, T. Kimura and T.D. Waite, *J. Environ. Qual.* **2011**, 40, 731-741.
- [6] N. Aoyagi, K. Shimojo, N. R. Brooks, R. Nagaishi, H. Naganawa, K.V. Hecke, L.V. Meervelt, K. Binnemans and T. Kimura, *Chem. Commun.* **2011**, 47, 4490-4492.
- [7] L. S. Natrajan, *Dalton Trans.*, **2012**, 41, 13167.

## Chemical studies of Mo and W in preparation of a seaborgium (Sg) reduction experiment using MDG, FEC, and SISAK

A. Toyoshima<sup>1</sup>, S. Miyashita<sup>1</sup>, M. Asai<sup>1</sup>, T. K. Sato<sup>1</sup>, Y. Kaneya<sup>1</sup>, K. Tsukada<sup>1</sup>, Y. Kitatsuji<sup>1</sup>, Y. Nagame<sup>1</sup>, M. Schädel<sup>1</sup>, H. V. Lerum<sup>2</sup>, J. P. Omtvedt<sup>2</sup>, Y. Oshimi<sup>3</sup>, K. Ooe<sup>3</sup>, Y. Kitayama<sup>4</sup>, A. Yokoyama<sup>4</sup>, A. Wada<sup>5</sup>, Y. Oura<sup>5</sup>, H. Haba<sup>6</sup>, J. Kanaya<sup>6</sup>, M. Huang<sup>6</sup>, Y. Komori<sup>7</sup>, T. Yokokita<sup>7</sup>, Y. Kasamatsu<sup>7</sup>, A. Shinohara<sup>7</sup>, V. Pershina<sup>8</sup>, J. V. Kratz<sup>9</sup>

<sup>1</sup>Advanced Science Research Center, Japan Atomic Energy Agency, Tokai, Ibaraki 319-1195, Japan

<sup>2</sup>Department of Chemistry, University of Oslo, Oslo 0371, Norway

<sup>3</sup>Institute of Science and Technology, Niigata University, Niigata 950-2181, Japan

<sup>4</sup>College and Institute of Science and Engineering, Kanazawa University, Kanazawa 920-1192, Japan

<sup>5</sup>Graduate School of Science and Engineering, Tokyo Metropolitan University, Hachioji, Tokyo 192-0397, Japan

<sup>6</sup>Nishina Center for Accelerator-Based Science, RIKEN, Wako, Saitama 351-0198, Japan

<sup>7</sup>Graduate School of Science, Osaka University, Toyonaka, Osaka 560-0043, Japan

<sup>8</sup>GSI Helmholtzzentrum für Schwerionenforschung GmbH, D-64291 Darmstadt, Germany

<sup>9</sup>Institut für Kernchemie, Universität Mainz, 55128 Mainz, Germany

*Abstract* –We are developing a new chemistry assembly to perform continuous reduction experiments of seaborgium (element 106, Sg). In preparation for the Sg experiment, we have begun studies on the dissolution, reduction, and extraction of Mo and W isotopes. Our present status of the preparation with Mo and W will be presented.

*Keywords* – Superheavy elements, Seaborgium (Sg), Electrochemistry, Solvent extraction, Flow electrolytic column, SISAK, Membrane degasser

Seaborgium (Sg) is expected to be redox-active similarly to its lighter group-6 homologs, Mo and W. Theoretical calculation show that Sg can be reduced from the most stable hexavalent state Sg(VI) to, e.g., the tetravalent one [1]. They also predict that the Sg(VI)/Sg(IV) couple will have a more negative redox potential than those of the corresponding W ions in acidic solution [1]. In such reduction reactions, electrons occupy the vacant valence 6d orbital of the Sg(VI) ion. The redox potential of the Sg(IV)/Sg(VI) couple, therefore, provides information on the stability of the 6d orbital which is anticipated to be influenced by increasingly strong relativistic effects.

Because of low production rates of <sup>265a,b</sup>Sg (a and b stand for two different states) in the <sup>248</sup>Cm(<sup>22</sup>Ne, 5n) reaction and their short half-lives of 8.5 and 1.4 s [2], only single atoms of Sg are present. This means that standard electrochemical techniques are not applicable to its reduction study. In our previous works, we have developed a novel electrochemical method of electrolytic column chromatography available for single ions [3]. Carbon fibers modified with Nafion perfluorinated cation-exchange resin were employed as a working electrode as well as a cation-exchanger. This technique was successfully applied to the oxidation of nobelium (No) [4] and the reduction of mendelevium (Md) [5]. It is, however, technically difficult to apply this batch-wise chromatographic method to the reduction study of Sg because of its very short half-lives. We are, therefore, developing a new chemistry assembly consisting of a membrane degasser (MDG), a flow electrolytic column (FEC), the continuous liquid-liquid extraction apparatus, and the liquid scintillation counting

system (SISAK) [6] to continuously perform the dissolution, reduction, separation, and detection of Sg, respectively.

In preparation for our future experiment with Sg, we have begun studies on the dissolution, reduction, and extraction of Mo and W isotopes. On-line experiments using the newly developed MDG were carried out to examine the dissolution efficiency of nuclear reaction products transported by a gas-jet. The aqueous solution dissolving the reaction products was successfully separated from the carrier gas using the MDG after continuous mixing of the carrier gas with the aqueous solution. Electrolytic reduction of Mo and W was examined using a FEC. Redox couples of Mo(VI)/Mo(V) and W(VI)/W(V) in HCl have been so far characterized for macro amounts of Mo and W with cyclic voltammetry and UV/Vis. absorption spectrometry. Batch extractions of hexavalent <sup>93m</sup>Mo and <sup>181</sup>W were performed to search for suitable conditions in the separation between Sg(IV) and Sg(VI). Variations of extraction ratios of Mo(VI) and W(VI) between toluene containing hinokitiol (HT) and HCl were successfully observed as a function of HT and HCl concentrations. On-line extractions of short-lived <sup>91m</sup>Mo and <sup>176</sup>W were also carried out using SISAK and MDG. Extraction ratios of these elements were increased with increasing HT concentration, reflecting results of the batch experiments. In the symposium, our present status of the preparation with Mo and W will be presented.

- [1] V. Pershina *et al.*, *J. Phys. Chem. A* **103**, 8463 (1999).
- [2] H. Haba *et al.*, *Phys. Rev. C* **85**, 024611 (2012).
- [3] A. Toyoshima *et al.*, *Radiochim. Acta* **96**, 323 (2008).
- [4] A. Toyoshima *et al.*, *J. Am. Chem. Soc.* **126**, 9180 (2009).
- [5] A. Toyoshima *et al.*, to be submitted.
- [6] For example, J. P. Omtvedt *et al.*, *Eur. Phys. J. D* **45**, 91 (2007).

## Diamond Detectors for Isothermal Vacuum Chromatography

P. Steinegger<sup>1,2</sup>, R. Dressler<sup>1</sup>, R. Eichler<sup>1,2</sup>, A. Türlér<sup>1,2</sup>

<sup>1</sup> Paul Scherrer Institut, CH-5232 Villigen PSI, Switzerland

<sup>2</sup> University of Bern, CH-3012 Bern, Switzerland

*Keywords:* Superheavy elements, isothermal vacuum chromatography, diamond detectors.

### I. INTRODUCTION

On-line thermochromatography is a well established gas phase experiment for the chemical characterization of the superheavy elements. However, recent experiments with state of the art detectors such as COLD [1] and COMPACT [2] are limited in terms of the upper bound of the applied temperature gradient. Therefore, the experimental characterization of less volatile elements with stronger adsorption interaction is not feasible. Already the rather volatile mercury with  $-\Delta H_{\text{ads}}^{\text{Au}}(\text{Hg}) = 98 \text{ kJ/mol}$  [3] - corresponding to a deposition temperature of about 430 K using the experimental conditions of the COLD system - reveals the constrained range of the currently used setups. Pushing the starting temperature of the gradient above the current limit, would open up a new range of elements accessible by on-line thermochromatography, including candidates like element 113.

#### A. Diamond Detectors

The upper limit of the temperature gradient however, evolves due to the maximum operation temperature of the currently applied Si PIN-diodes or Si PIPS-detectors respectively at around 315 K. Above this threshold, thermal excitation of the low band gap material (1.1 eV) prevents any spectroscopic measurement.

In recent years the development of chemical vapor deposition (CVD) single crystal diamonds made a considerable progress concerning the available size, quantity, and most importantly the quality. Diamond, as a large band gap material (5.5 eV), can be operated under IR and UV-Vis irradiation as well as at elevated temperatures even higher than 500 K without any spectroscopic degradation [4]. In addition, diamond has the largest known thermal conductivity, which is important for a reliable reconstruction of the surface temperature at vacuum conditions.

#### B. Experimental Section

In the course of the development of an isothermal vacuum chromatography setup for application in SHE chemistry experiments, we tested the new detector material with respect to the change of the spectroscopic behavior under heating and

in first experiments with carrier-free  $^{211}\text{Pb}$ , where the detector was successfully tested in the immediate vicinity of the isothermal oven held at temperatures up to  $T_{\text{max}} = 1193 \text{ K}$  (see Fig. 1).

**Acknowledgment:** This project is supported by the Swiss National Foundation project number 200020\_144511 / 1.

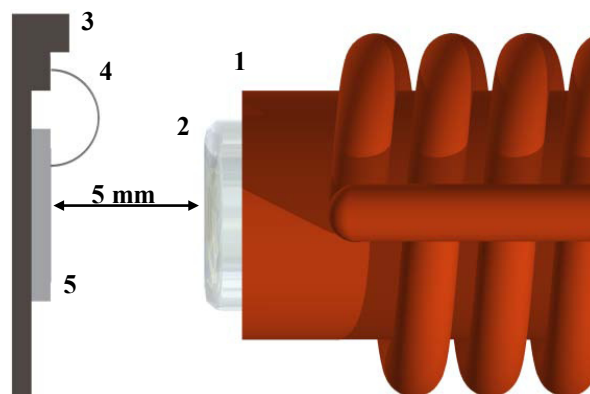


**Fig. 1:** Isothermal vacuum chromatography with carrier-free  $^{211}\text{Pb}$ ; 1 isothermal oven, 2 quartz column exit, 3 ceramic carrier, 4 wire bonds, 5 CVD diamond detector.

- [1] R. Eichler et al., *Radiochim. Acta* **98(3)** (2010) 133
- [2] J. Dvořák, *Ph.D. TU Munich* (2007)
- [3] B. Eichler et al., *Radiochim. Acta* **33** (1983), 121
- [4] J. H. Kaneko et al., *Nucl. Instr. and Meth. A* **422** (1999), 211

## Angular distribution of projectile like fragments in $^{16}\text{O}+^{89}\text{Y}$ reaction

R. Tripathi<sup>1</sup>, S. Sodaye<sup>1</sup>, K. Mahata<sup>2</sup>, P. K. Pujari<sup>1</sup>

<sup>1</sup>Radiochemistry Division, Bhabha Atomic Research Centre, Mumbai, India

<sup>2</sup>Nuclear Physics Division, Bhabha Atomic Research Centre, Mumbai, India

*Abstract – Angular distribution of projectile like fragments have been measured in  $^{16}\text{O}+^{89}\text{Y}$  reaction at  $E_{\text{lab}}=62$  and 84 MeV. A systematic change in the angular distribution of PLFs was observed with increasing mass transfer indicating the evolution of reaction mechanism from quasi-elastic transfer to massive transfer or incomplete fusion. Elastic scattering measurements have been carried out to obtain grazing angle and total reaction cross section.*

*Keywords – Incomplete fusion, angular distribution*

### I. INTRODUCTION

Reactions involving incomplete mass transfer, namely direct and quasi-elastic transfer (QET), incomplete fusion (ICF) or massive transfer and deep inelastic collisions (DIC), have been an active area of investigation. Study of these reactions at beam energies below  $\sim 10$  MeV/nucleon has been actively investigated in the recent past [1-5] as existing theories and models [6-9] explain the observations of such reactions at higher beam energies. Measurement of angular distribution and cross sections data of PLFs ( $Z=3-7$ ) in  $^{19}\text{F}+^{66}\text{Zn}$  [3],  $^{89}\text{Y}$  [4],  $^{159}\text{Tb}$  [5] showed a systematic decrease of PLF cross sections with their decreasing  $Z$ . A comparison of PLF cross sections with those of respective evaporation residues gave information about the relative magnitude of cross section for total projectile break-up and break-up followed by the capture of one of the fragments [5]. As projectile structure plays an important role in these reactions [10,11], angular distributions of projectile like fragments ( $Z=3-7$ ) have been measured in  $^{16}\text{O}+^{89}\text{Y}$  reaction at  $E_{\text{lab}}=62$  and 84 MeV corresponding to  $E_{\text{c.m.}}/V_b$  value of 1.18 and 1.58 respectively. Elastic scattering measurements have been carried out to determine the grazing angle and total reaction cross section.

### II. EXPERIMENTAL DETAILS

Experiments were carried out at BARC-TIFR pelletron accelerator facility, Mumbai. Self-supporting metallic target of  $^{89}\text{Y}$  was bombarded with  $^{16}\text{O}$  beam and projectile like fragments were measured in the forward hemi-sphere using Si detector based E- $\Delta E$  telescopes. Telescope data were normalized for the target thickness and beam current using the data from a monitor detector kept at  $20^\circ$  with respect to the beam direction to obtain absolute cross sections.

### III. RESULTS AND DISCUSSION

Lab Angular distribution of PLFs at  $E_{\text{lab}}=62$  and 84 MeV, obtained from a preliminary data analysis is shown in Fig. 1 (a) and (b) respectively. It can be seen from Fig. 1(a), that

the angular distribution of PLFs become more and more forward peaked with increasing mass transfer. This indicates the increasing overlap of the projectile and target nuclei with increasing mass transfer. This observation is

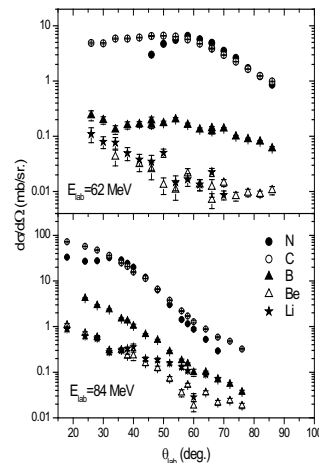


Fig. 1. Angular distribution of PLFs in  $^{16}\text{O}+^{89}\text{Y}$  reaction

consistent with our earlier measurements in  $^{19}\text{F}$  induced reactions [3-5]. However, the comparable cross sections of C and N PLFs indicate the role of alpha cluster structure, leading to a large cross section for even Z C PLF. Also,  $^{12}\text{C}$  yield was significantly larger than the other isotopes indicating the preferential break-up of the  $^{16}\text{O}$  projectile into  $^{12}\text{C}+^4\text{He}$ . At higher beam energy, angular distributions of all the

PLFs become forward peaked, suggesting the formation of even lighter PLFs in collision trajectories with deeper interpenetration. A qualitative comparison of angular distributions of PLFs at the two beam energies shows a larger decrease in the yields of lighter PLFs with decreasing beam energy. This is consistent with the picture that the formation of these PLFs involves substantial overlap of the projectile and the target nuclei, which was indicated by the sharp fall in the cross sections of lighter PLFs with decreasing beam energy [3,4].

In the further analysis, angular distributions and kinetic energy spectra of PLFs would be analyzed in more detail. Integrated cross section data for PLFs would be compared with the incomplete fusion cross section data obtained from evaporation residue measurements [12] as well as those obtained in  $^{19}\text{F}$  induced reactions.

### REFERENCES

- [1] Abhishek Yadav et al., Phys. Rev. C **85**, 064617 (2012).
- [2] Rahbar Ali et al., J. Phys. G **37**, 115101 (2010).
- [3] R. Tripathi et al., Phys. Rev. C **79**, 064604 (2009).
- [4] R. Tripathi et al., J. of Physics. G. **35**, 025101 (2008).
- [5] Amit Kumar et al., Eur. Phys. J A **49**, (2013).
- [6] K. Siwek-Wilczynska et al., Phys. Rev. Lett. **42**, 1599 (1979).
- [7] T. Udagawa and T. Tamura, Phys. Rev. Lett. **45**, 1311 (1980).
- [8] V. Zagrebaev and Yu. Penionzhkevich, Prog. Part. Nucl. Phys. **35**, 575 (1995).
- [9] B.G. Harvey, Nucl. Phys. A **444**, 498 (1985).
- [10] R. Tripathi et al., Eur. Phys. J. A **42**, 25 (2009).
- [11] Chr. V. Christov, Z. Phys. A **325**, 221 (1986).
- [12] B. S. Tomar et al., Z. Phys. A **343**, 223 (1992).

## Studies on Solution Chemistry of Actinides and Lanthanides by Time-resolved Laser-induced Fluorescence Spectroscopy

Takaumi Kimura

Nuclear Science and Engineering Directorate, Japan Atomic Energy Agency  
Shirakata-shirane 2-4, Tokai-mura Naka-gun, Ibaraki, 319-1195, Japan

*Abstract* – Several topics on solution chemistry of actinides(An) and lanthanides(Ln) studied by time-resolved laser-induced fluorescence spectroscopy(TRLFS) will be mentioned in this presentation. Those are hydration studies of An(III) and Ln(III) and its applications, speciation study of U(VI), and luminescence of U(IV) in aqueous solution.

*Keywords* – Hydration, Speciation, Actinides, Lanthanides, Time-resolved Laser-induced Fluorescence Spectroscopy(TRLFS)

As a highly sensitive and selective speciation method, time-resolved laser-induced fluorescence spectroscopy (TRLFS) is a powerful tool to study luminescent actinides(An) and lanthanides(Ln) in solution, in solid and at their interface. We have started hydration study of Cm(III)[1] and speciation study of U(VI)[2] by TRLFS in the beginning of the nineteen-nineties.

A luminescence study of Cm(III) has shown a linear correlation between the reciprocal of the excited-state lifetime  $\tau_{\text{obs}}$  and the number of water molecules  $N_{\text{H}_2\text{O}}$  in the first coordination sphere of complexes. From measurements of  $\tau_{\text{obs}}$  of  $\text{Cm}^{3+}$  in  $\text{D}_2\text{O}$ - $\text{H}_2\text{O}$  solutions and of Cm(III) doped lanthanum compounds, the following correlation for  $\tau_{\text{obs}}(\text{ms})$  vs.  $N_{\text{H}_2\text{O}}$  was established:  $N_{\text{H}_2\text{O}} = 0.65(1/\tau_{\text{obs}}) - 0.88$ [1]. This relationship was applied to study the residual hydration of Cm(III) complexes of polyaminopolycarboxylate ligands and to determine the  $N_{\text{H}_2\text{O}}$  of Cm(III) in various aqueous solutions. All of the  $N_{\text{H}_2\text{O}}$  values calculated from the lifetime were chemically reasonable[3]. For Am(III) and several Ln(III)(Ln=Nd, Sm, Eu, Tb and Dy), the similar calibration relations were also proposed and the validity was confirmed through the study of a series of polyaminopolycarboxylate complexes[4-6]. The  $N_{\text{H}_2\text{O}}$  of Ln(III) in concentrated aqueous salt solutions at room and liquid nitrogen temperatures was estimated on the basis of the correlation obtained at each temperature[7]. To understand the solvation of An(III) and Ln(III) in non-aqueous solutions, their  $\tau_{\text{obs}}$  in perprotonated and perdeuterated solvents, i.e., DMSO, DMF, MeOH and water, were measured systematically and the quenching behavior of the ions in the solvents and the preferential solvation of them in water/non-aqueous solvent mixtures were evaluated[8,9].

The determination of the  $N_{\text{H}_2\text{O}}$  by the measurement of  $\tau_{\text{obs}}$  is a simple and effective method for the speciation study of An(III) and Ln(III). This method makes it possible to study chemical species at solid-water interface. TRLFS accelerated the speciation study on sorption behavior of Eu(III) and Cm(III) at mineral-water interface in the presence or absence of humic substances[10] and on the cell surfaces of microorganisms[11]. This also makes it possible to compare directly the coordination environment

between An(III) and Ln(III) using same experimental technique. TRLFS improved the understanding of separation mechanisms of An(III) and Ln(III) using ion exchange resin[12] and solvent extraction[13].

Chemical species of U(VI) in 0.1 M  $\text{NaClO}_4$  in equilibrium with 0.03 %  $\text{CO}_2$  partial pressure were investigated by TRLFS[2]. The emission spectra of U(VI) solutions (pH = 3.8 to 7.0) in solid-liquid equilibrium with schoepite  $\text{UO}_3 \cdot 2\text{H}_2\text{O}$  were interpreted by the summation of the emission spectra of the individual components,  $\text{UO}_2^{2+}(\text{aq})$ ,  $(\text{UO}_2)_2(\text{OH})_2^{2+}(\text{aq})$ ,  $(\text{UO}_2)_3(\text{OH})_5^+(\text{aq})$  and  $\text{UO}_2\text{CO}_3(\text{aq})$ . Numerical evaluation of the species gave a satisfactory agreement with the distribution of the species calculated from the formation constants of U(VI). Furthermore, the speciation study of U(VI) by TRLFS with an optical cell system was extended to the hydrothermal conditions[14]. The results shows that TRLFS is an effective *in-situ* speciation method not only U(VI) hydrolysis but also for complexation at elevated temperatures(25-200 °C) and pressures(0.1-40 MPa).

U(IV) in aqueous solution has been considered to have no luminescence except for phosphate complex. From an analysis of transition energy level structure of U(IV), we found there was a possibility of  $\text{U}^{4+}$  exhibiting luminescence in aqueous solution and discovered the emission spectrum consisting of 12 bands in the range 280 to 560 nm[15]. Temperature dependence and isotope effect between H and D on the  $\tau_{\text{obs}}$  suggest that water molecules in a bulk solution participates considerably in quenching process of the luminescence, which is quite different from the luminescence properties of An(III) and Ln(III).

### REFERENCES

- [1] T. Kimura, G.R. Choppin, J. Alloy Compd., **213/214**, 313-317 (1994).
- [2] Y. Kato, G. Meinrath, et al., Radiochim. Acta, **64**, 107-111 (1994).
- [3] T. Kimura, G.R. Choppin, et al., Radiochim. Acta, **72**, 61-64 (1996).
- [4] T. Kimura, Y. Kato, J. Alloy Compd., **225**, 284-287 (1995).
- [5] T. Kimura, Y. Kato, J. Alloy Compd., **271-273**, 867-871 (1998).
- [6] T. Kimura, Y. Kato, J. Alloy Compd., **275-277**, 806-810 (1998).
- [7] T. Kimura, Y. Kato, J. Alloy Compd., **278**, 92-97 (1998).
- [8] T. Kimura, R. Nagaishi, et al., Radiochim. Acta, **89**, 125-130 (2001).
- [9] T. Kimura, R. Nagaishi, et al., J. Alloy Compd., **323-324**, 164-168 (2001).
- [10] Y. Takahashi, T. Kimura, et al., Geochim. Cosmochim. Acta, **66**, 1-12 (2002).
- [11] T. Ozaki, T. Kimura, et al., Radiochim. Acta, **94**, 715-721 (2006).
- [12] T. Kimura, Y. Kato, et al., J. Alloy Compd., **271-273**, 719-722 (1998).
- [13] G. Tian, T. Kimura, et al., Radiochim. Acta, **92**, 495-499 (2004).
- [14] T. Kimura, R. Nagaishi, et al., J. Nucl. Sci. Technol., **Suppl. 3**, 233-239 (2002).
- [15] A. Kirishima, T. Kimura, et al., Radiochim. Acta, **92**, 705-710 (2004).

## Poster Session 3

Wednesday, 25 September 2013

18:50 ~ 20:00

### Scientific Topics (Abbrev.)

1. Fukushima issues (FK)
2. Education in nuclear and radiochemistry (ED)
3. Nuclear forensics (NF)
4. Nuclear energy chemistry (NE)
5. Nuclear chemistry (NC)
6. Actinide chemistry (AC)
7. Environmental radiochemistry (EN)
8. Radiopharmaceutical chemistry and Nuclear medicine (RP)
9. Nuclear probes for materials science (NP)
10. Activation analysis (AA)
11. Application of nuclear and radiochemical techniques (AP)

**$^{235}\text{U}/^{238}\text{U}$  Isotopic Ratio in Environmental Samples at the Fukushima Area**

Y. Shibahara<sup>1</sup>, T. Fujii<sup>1</sup>, S. Fukutani<sup>1</sup>, T. Kubota<sup>1</sup>, R. Okumura<sup>1</sup>, T. Ohta<sup>2</sup>, K. Takamiya<sup>1</sup>, N. Sato<sup>1</sup>,  
M. Tanigaki<sup>1</sup>, Y. Kobayashi<sup>1</sup>, H. Yoshinaga<sup>1</sup>, H. Yoshino<sup>1</sup>, A. Uehara<sup>1</sup>,  
S. Mizuno<sup>3</sup>, T. Takahashi<sup>1</sup>, and H. Yamana<sup>1</sup>

<sup>1</sup>Research Reactor Institute, Kyoto University

<sup>2</sup>Faculty of Engineering, Hokkaido University

<sup>3</sup>Nuclear Power Safety Division, Fukushima Prefectural Government

*Abstract* –  $^{235}\text{U}/^{238}\text{U}$  isotopic ratio of environmental samples in Fukushima prefecture was analyzed by thermal ionization mass spectrometry and inductively coupled plasma mass spectrometry. A possibility of atmospheric release of uranium during the accident of Fukushima Daiichi nuclear power plant was discussed.

*Keywords*– uranium isotope ratio, thermal ionization mass spectrometry, inductivity coupled plasma mass spectrometry

Uranium has three major isotopes ( $^{234}\text{U}$ ,  $^{235}\text{U}$ , and  $^{238}\text{U}$ ) and is widely distributed in the environment. The relative isotopic abundances are 0.0054% ( $^{234}\text{U}$ ), 0.7200% ( $^{235}\text{U}$ ), and 99.2745% ( $^{238}\text{U}$ ), respectively [1]. The range of natural variations of uranium isotopes [1] are shown in Table 1. Fukushima Daiichi nuclear power plant used  $\text{UO}_2$  and mixed oxide (MOX) fuels, in which the averaged  $^{235}\text{U}$  concentrations are 3.4-3.7 wt% and 1.2 wt%, respectively.

Table 1. Isotopic composition of uranium[1]

Isotope	Range of natural variations [%]
$^{234}\text{U}$	0.0050-0.0059
$^{235}\text{U}$	0.7918-0.7207
$^{238}\text{U}$	99.2739-99.2752

On the accident of Fukushima Daiichi nuclear power plant, huge amount of fission products were widely released. Since uranium is a heavy element, if it was released, the fallout may have been distributed at the near site of nuclear power plant.

The purpose of the present study is, from the viewpoint of safety assessment, to check that the  $^{235}\text{U}/^{238}\text{U}$  ratio in environmental samples at the Fukushima area falls within the range of natural variations. The spent nuclear fuel includes  $^{236}\text{U}$  generated via the neutron capture of  $^{235}\text{U}$ . The  $^{236}\text{U}/^{238}\text{U}$  ratio in the river and ocean close to the Fukushima area has been investigated with accelerator mass spectrometer [2]. In the present study, we analyzed  $^{235}\text{U}/^{238}\text{U}$  in environmental samples (soils, plants, and so on) at the Fukushima area with thermal ionization mass spectrometer (TIMS) and inductively coupled plasma mass spectrometer (ICP-MS).

Samples were immersed in concentrated  $\text{HNO}_3$  and heated at 413 K. After evaporation of  $\text{HNO}_3$ , diluted  $\text{HNO}_3$  was added, and then, uranium was recovered from the samples by ion-exchange chromatography with ion-exchange resin and extraction chromatography with UTEVA-resin. The concentration of uranium recovered was analyzed with

quadrupole ICP mass spectrometer (ICP-QMS) or ICP atomic emission spectrometer (ICP-AES).

Uranium isotopic ratios were analyzed with a TIMS (Triton-T1, Thermo Fisher Scientific) with a rhenium double filament system and/or an ICP-MS (Element 2, Thermo Fisher Scientific). As the reference material of mass spectrometry, standard material CRMU010, in which the atomic percent of  $^{235}\text{U}$  is certified to be  $1.0037 \pm 0.0010\%$  [3], was used.

The sample solution of 1 ppm uranium in 1 M  $\text{HNO}_3$  was prepared for TIMS. Each solution of 1  $\mu\text{L}$  (1 ng of U) was loaded onto a rhenium evaporation filament. The mass spectrum was obtained with a secondary electron multiplier detector. The sample solution of 10 ppb uranium in 0.1%  $\text{HNO}_3$  was also prepared for ICP-MS. Our analytical result of CRMU010 agreed with the certified value within  $2\sigma$  analytical error. Based on the validity of isotopic analysis, the  $^{235}\text{U}/^{238}\text{U}$  ratio in the environmental samples inside the 3 km range from the Fukushima Daiichi nuclear power plant was analyzed. A possibility of atmospheric release of nuclear fuel matrix during the accident of Fukushima Daiichi nuclear power plant is discussed.

[1] J. K. Böhlke *et al.*, *J. Phys. Chem. Ref. Data*, **34**, 57 (2005).

[2] A. Sakaguchi *et al.*, *Geochemical J.*, **46**, 355 (2012).

[3] E. L. Garner *et al.*, *Nat. Bur. Stand. (U.S.)*, Spec. Publ. 267-27 (1971).

## Particulates of Ag and Pu radioisotopes released from Fukushima Daiichi nuclear power plants

H. Kimura<sup>1</sup>, M. Uesugi<sup>2</sup>, A. Muneda<sup>2</sup>, R. Watanabe<sup>1</sup>, A. Yokoyama<sup>3</sup>,  
T. Nakanishi<sup>4</sup>

<sup>1</sup>Grad. School Nat. Sci. Tech., Kanazawa Univ., <sup>2</sup>Col. Sci. Eng., Kanazawa Univ., <sup>3</sup>Inst. Sci. Eng., Kanazawa Univ.,  
<sup>4</sup>Adv. Sci. Res. Cent., Kanazawa Univ.

**Abstract** –Due to Fukushima Daiichi nuclear power plants accident, a large amount of radionuclides were released into environment. The radioactivities of <sup>134</sup>Cs, <sup>137</sup>Cs, <sup>110m</sup>Ag, <sup>238</sup>Pu, and <sup>239+240</sup>Pu in a soil sample collected in Futaba, Fukushima were determined by a spectrometry or  $\gamma$  spectrometry. We searched for the dispersion of these radioactivities in a soil sample, which suggests the existence of hot particles for Pu contamination.

**Keywords** –<sup>238</sup>Pu, <sup>110m</sup>Ag, <sup>137</sup>Cs, hot particle,

### I. INTRODUCTION

Massive radionuclides were released into environment due to the Fukushima Daiichi nuclear power plant (FDNPP) accident. The volatile fission products, such as <sup>137</sup>Cs, <sup>134</sup>Cs were considered to be deposited as several chemical forms through dry deposition and wet deposition. On the other hand, the deposition procedures of non-volatile nuclides such as Pu isotopes and <sup>110m</sup>Ag were not clear, and it is predicted that these radionuclides were deposited as hot particles. The existence of hot particles may cause their radioactivity concentrations to vary over a wide range even if soil samples are collected in a place. In this work, we researched for the dispersion of radioactivities in a homogenized soil sample collected in Futaba, Fukushima.

### II. EXPERIMENTS

#### Sample collection

A soil sample was collected in Futaba located at 4km north-west of Fukushima DNPP.

#### Preparation

Firstly, the sample was agitated by hand hundred times, and it was dried at 105°C overnight. Secondly, it was crushed in a mortar, and sieved through at 2mm sieve. Finally, it was heated at 450°C for 4 hours to decompose organics.

#### 1 Measurement of Pu

After addition of a tracer of <sup>242</sup>Pu, six aliquots of 10g soil were leached with 10 M HNO<sub>3</sub>-0.01M HF. And then, after isolation of Pu atoms through an ion exchange procedure the atoms were electrodeposited on a steel plate and subjected to  $\alpha$  spectrometry.

#### 2 Measurement of <sup>110m</sup>Ag

Some aliquots of 1.0g soil sample were prepared, and they were subjected to  $\gamma$  spectrometry.

### III. RESULTS

Figure 1 shows correlation between <sup>238</sup>Pu and <sup>137</sup>Cs for six aliquots. The radioactivity of <sup>238</sup>Pu in one aliquot is clearly higher than the others, and the ratio of <sup>238</sup>Pu/<sup>239,240</sup>Pu of the former is also higher. This result suggests the existence of hot particle of Pu in that aliquot. Figure 2 shows the good correlation between <sup>137</sup>Cs and <sup>110m</sup>Ag. Therefore it was suggested that hot particles of <sup>110m</sup>Ag did not exist in the soil sample. These results suggest the difference of the release processes of <sup>110m</sup>Ag and <sup>238</sup>Pu although both of them are non-volatile nuclides.

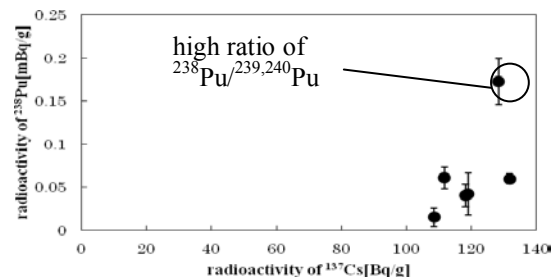


Fig.1 Correlation between <sup>238</sup>Pu and <sup>137</sup>Cs

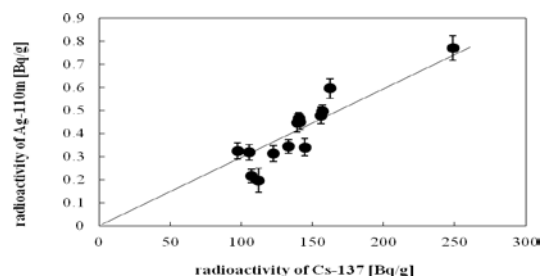


Fig.2 Correlation between <sup>110m</sup>Ag and <sup>137</sup>Cs

# The measurement of $^{14}\text{C}/^{12}\text{C}$ ratios in Japanese plant samples affected by anthropogenic sources

Risa Hashimoto<sup>1</sup>, Aki Inoue<sup>1</sup>, Yasuyuki Muramatsu<sup>1</sup>, Hiroyuki Matsuzaki<sup>2</sup>

<sup>1</sup>Department of Chemistry, Gakushuin University

<sup>2</sup>School of Engineering, the University of Tokyo

*In relation to anthropogenic influences of  $^{14}\text{C}$  in the atmosphere, we have carried out the following two different studies;*

- (1) secular variation of  $^{14}\text{C}/^{12}\text{C}$  ratio in rice harvested in Japan,*
- (2) influence of the Fukushima nuclear accident on  $^{14}\text{C}/^{12}\text{C}$  ratio in plant leaves in the region.*

*Analytical results by AMS for rice collected from 1951 to 2012 showed that  $^{14}\text{C}/^{12}\text{C}$  ratios decreased exponentially after the Partial Test Ban Treaty in 1963. The residence time of  $^{14}\text{C}$  in the atmosphere is estimated to be about 10 years.*

*Plant leaves collected about 9km from the reactor showed a weak increase of  $^{14}\text{C}/^{12}\text{C}$  ratios. This suggests that  $^{14}\text{C}$  was released by the accident and influenced the  $^{14}\text{C}/^{12}\text{C}$  ratios in plant leaves collected near the reactor.*

**Keywords** –  $^{14}\text{C}$ ; anthropogenic sources; plant samples; secular variation; Fukushima; AMS

## I. INTRODUCTION

$^{14}\text{C}$  is produced in nature by cosmic ray reactions in the upper atmosphere, and its production changes by the flux of cosmic rays. The produced  $^{14}\text{C}$  immediately reacts with an oxygen molecule, resulted in the production of  $^{14}\text{CO}_2$  and it is absorbed by plants through photosynthesis. Therefore plants are reflected atmospheric  $^{14}\text{C}/^{12}\text{C}$  ratios at that time.

$^{14}\text{C}$  is also released into the atmosphere by anthropogenic sources such as nuclear weapons tests and nuclear accidents. In this study, we focus on  $^{14}\text{C}$  released from anthropogenic sources and carried out the following two studies using AMS. We determined  $^{14}\text{C}/^{12}\text{C}$  ratios in rice harvested in Japan to study recent influence of the past nuclear weapons tests. We also studied whether there were influences on  $^{12}\text{C}/^{14}\text{C}$  ratios in the plants due to the accident at the Fukushima Daiichi Nuclear Power Plant (FDNPP) occurred in March, 2011. Although there are many papers reporting the release of several nuclides, there are almost no data for  $^{14}\text{C}$ . In the last year, we have determined  $^{14}\text{C}/^{12}\text{C}$  ratios in Japanese cedars and pine needles collected in Fukushima prefecture. Some enhancements of  $^{14}\text{C}$  levels were observed. However, we still have lack of  $^{14}\text{C}$  data. Therefore, we analyzed additional samples collected near the FDNPP and studied whether the  $^{14}\text{C}/^{12}\text{C}$  ratios in the plants were affected by the accident.

## II. EXPERIMENT

Rice samples harvested from 1951 to 2012 were used for the analysis. They were homogenized in a blender and oxidized to produce  $\text{CO}_2$ . Then, the  $\text{CO}_2$  was purified in a vacuum line and reduced to prepare graphite target for AMS.  $^{14}\text{C}/^{12}\text{C}$  ratio in the graphite was measured by AMS

at the University of Tokyo and Japan Atomic Energy Agency.

In order to examine the possible influences of  $^{14}\text{C}$  for plants, we have collected leaves of Japanese cedar in Okuma, 9km far from FDNPP, in September, 2011. Since cedars are evergreen, leaves were contaminated at the time of the accident. We analyzed old leaves, which were grown before the accident, and new leaves, which were grown after the accident. Cedar leaves were washed with pure water in order to remove particulate matters deposited on the plant surface. For comparison with background samples collected far from FDNPP, we analyzed pine needles in Chiba prefecture and rice samples collected in Niigata prefecture. The samples were also homogenized in a blender, and prepared graphite targets for AMS.

## III. RESULTS

Results obtained for rice showed that  $^{14}\text{C}/^{12}\text{C}$  ratios decreased exponentially with time after the Partial Test Ban Treaty in 1963. The residence time of  $^{14}\text{C}$  in the atmosphere is estimated to be about 10 years.

For the cedar samples collected in Okuma,  $^{14}\text{C}/^{12}\text{C}$  ratios in the old leaves (grown before the FDNPP accident) were found to be higher than the new leaves (see Fig.1). Since  $^{14}\text{C}/^{12}\text{C}$  ratios in new leaves were almost the same as the ratios in the other samples collected from outside of Fukushima. From the above-mentioned results,  $^{14}\text{C}$  in the old leaves was increased because of the influence of  $^{14}\text{C}$  released by the FDNPP accident.  $^{14}\text{C}/^{12}\text{C}$  ratios did not change so much, even the samples were washed. Therefore, we assume that most of  $^{14}\text{C}$  were taken as gaseous forms and associated with plant tissues in the leaves. Contribution of  $^{14}\text{C}$  associated with particulate matters deposited on the leaves seems to be small.

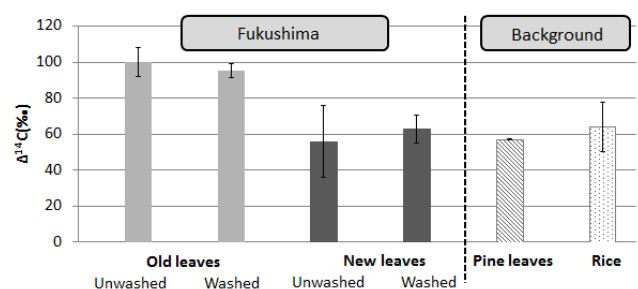


Fig 1.  $^{14}\text{C}/^{12}\text{C}$  ratios in Japanese cedar leaves collected from Fukushima and those in other samples from background areas

## Radiocesium and stable cesium in edible wild plants (Sansai) collected from forests in Fukushima Prefecture

SUGIYAMA, M.<sup>1</sup>, MURAMATSU, Y.<sup>1</sup>, OHNO, T.<sup>1</sup>, SATO, M.<sup>2</sup>

<sup>1</sup>Gakushuin University

<sup>2</sup>Fukushima Agricultural Technology Center

### Abstract –

High concentrations of radiocesium were observed in edible wild plants and bamboo shoots collected from forests in Fukushima Prefecture following the nuclear accident. We have analyzed radiocesium and stable cesium in a variety of plant samples. The highest concentrations of radiocesium and stable cesium were found in leaves of *Acanthopanax sciadophylloides*. The Cs/Rb ratios and the Cs/K ratios were also high in this species. These results suggest that leaves of *Acanthopanax sciadophylloides* absorb Cs selectively from surface forest soil.

Keywords – radiocesium, stable cesium, edible wild plants, transfer to plants

### I. INTRODUCTION

An accident occurred at the Fukushima Dai-ichi Nuclear Power Plant in March 2011, consequently large quantities of radioactive materials were released into the environment. Farmlands and forests in Fukushima Prefecture were widely contaminated and their products were affected by the released radionuclides. The most important radionuclides related to vegetation are Cs-134 (half-life: 2y) and Cs-137 (half-life: 30y), which have relatively long half-lives. Concentrations of radiocesium in vegetables and rice decreased with time. However, radiocesium concentrations in edible wild plants and mushrooms often exceeded the guideline (100 Bq/kg) for foods stuffs. Therefore, it is important to identify plants which accumulate cesium and to clarify the transfer mechanism of radiocesium. In this study, we analyzed both radiocesium and stable cesium and considered the mechanism of high radiocesium transfer into the plants. We also compared the transfer of stable cesium with other stable elements to examine the availability of cesium to plants.

### II. MATERIALS AND METHODS

Four different edible wild plants, *Acanthopanax sciadophylloides* (Koshiabura), *Kalopanax septemlobus* (Harigiri), *Aralia elata* (Taranoki), bamboo shoots (Takenoko), were collected from forests in Iitate-mura, Fukushima, and they were measured with a Ge-detector. Then the samples were freeze-dried and milled with a mixer. Powdered samples (0.1 g) were digested in teflon vessels with an acid mixture (HNO<sub>3</sub>, HF and HClO<sub>4</sub>) on a hot plate. After digestion, the samples were evaporated to dryness. Then, the residues were dissolved in 2% HNO<sub>3</sub>. Concentrations of stable elements (Li, Na, Mg, K, Ca, Mn, Co, Cu, Zn, Rb, Sr, Cs and Ba) were determined by ICP-MS. To have a better precision in the analysis, triplicate samples were prepared and determined for these elements.

### III. RESULTS AND DISCUSSION

Radiocesium concentrations differed by the plant species. We first expected that the concentrations of radiocesium should be similar within a same group (*Araliaceae*) collected from the same area. However, leaves of *Acanthopanax sciadophylloides* showed very high concentrations up to about 20,000 Bq/kg. Therefore, transfer mechanism of cesium for *Acanthopanax sciadophylloides* seems to be different from the other two species of *Araliaceae*. For stable cesium, we also found the highest concentration in this species. This suggests that the transfer through roots should be a dominant pathway to explain high radiocesium concentrations in *Acanthopanax sciadophylloides*. The high uptake of stable cesium in this species suggests that the contribution of translocation pathways from barks and leaves might be low, because stable cesium exists mainly in soils and not in barks of the trees. In addition, we also compared stable Cs with K and Rb which are also one of the alkali elements. The Cs/Rb ratios and the Cs/K ratios in leaves of *Acanthopanax sciadophylloides* were higher than those in the other species of *Araliaceae* and bamboo shoots. These findings indicate that *Acanthopanax sciadophylloides* absorbs cesium selectively than the other alkaline elements. In forests, radiocesium is accumulated in surface soil layers (including litter layer) in which contents of organic matters are high. Since radiocesium is more mobile in organic layers compared to mineral soil, it was more readily taken up by the plant.

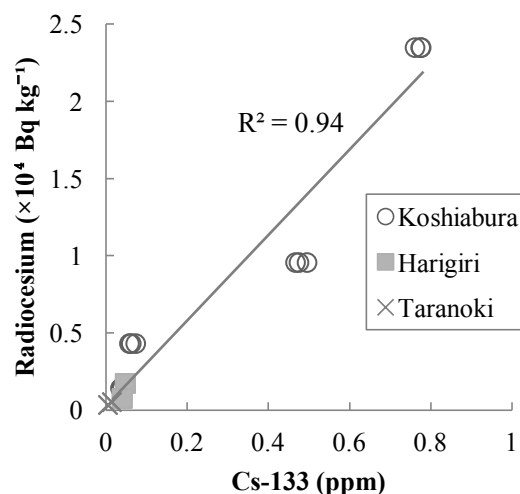


Fig. 1. Relationship between radiocesium and stable cesium in plant leaves of *Araliaceae* collected from Iitate-mura, Fukushima.

## Annual Variation of Radioactivity in Marine Biota in the Pacific off Fukushima after TEPCO's Fukushima Daiichi Nuclear Power Station Accident

Tatsuo Aono<sup>1</sup>, Satoshi Yoshida<sup>1</sup>, Tadahiro Saotome<sup>2</sup>, Takuji Mizuno<sup>2</sup>,  
Yukari Ito<sup>3</sup>, Jota Kanda<sup>3</sup>, Takashi Ishimaru<sup>3</sup>

<sup>1</sup> National Institute of Radiological Sciences

<sup>2</sup> Fukushima prefecture fisheries experimental station

<sup>3</sup> Tokyo University of Marine Science and Technology

*Abstract – Many kinds of marine biota could be observed in the coastal area around off Fukushima after this accident, and it is suggested that the changes of activity are caused by the feeding and sediment effects in biota.*

*Keywords – Marine organisms, <sup>134</sup>Cs, <sup>137</sup>Cs, <sup>110m</sup>Ag*

### I. Introduction

The pollution in marine environment spread by radioactive substances widely after the accident of TEPCO's Fukushima Daiichi Nuclear Power Station (F1NPP) with the 2011 Great East Japan Earthquake and Tsunami. It's been 2.5 years since this accident. The activities of Cs-134 and Cs-137 decreased exponentially in seawater. When the activities of radionuclides had decreased in seawater, it was thought that these gradually decreased in marine biota and sediment before this accident. However, the high activities of radio cesium have been monitored in fish in the coast area around off Fukushima. Little notice of the benthos was taken, because there are not edible as foodstuff. Marine biota were collected around off Fukushima due to investigate the activities of radionuclides. The aims of the present study were to examine the temporal changes in radioactivity and to clarify the variation factor in marine biota.

### II. Method

Marine biota samples were collected with plankton net, dredge sampler, and trawl during the cruise of T/S Umitaka, T/S Shinyo, and some research and fishing vessels. After being classified into species (Polychaete, Sea Urchin, Starfish, Sea Slug and Crab etc.) and packed into a plastic container. The radioactivity was determined by gamma ray spectrometry using a HPGe detector (Canberra, GX-2019). The activities of radionuclides of biota in the sampling date were calculated with the correction of the decay and the coincidence - summing of <sup>134</sup>Cs. Detection limits of <sup>134</sup>Cs, <sup>137</sup>Cs, and <sup>110m</sup>Ag were estimated within 1 and 0.5 Bq/kg (wet wt), respectively.

### III. Results and Discussion

The radioactivities of <sup>137</sup>Cs and <sup>110m</sup>Ag in marine biota were from 1 to 400 Bq/kg (wet wt) and from less than 1 to 55 Bq/kg (wet wt), respectively. The high correlation between the activities in biota and densities in dry samples were observed in the benthos. It is suggested that it is caused by the feeding and sediments effects in biota.

## Migration behavior of $^{134}\text{Cs}$ and $^{137}\text{Cs}$ in the Niida River water in Fukushima Prefecture, Japan during 2011-2012

Seiya Nagao<sup>1</sup>, Masaki Kanamori<sup>2</sup>, Shinya Ochiai<sup>1</sup>, Masayoshi Yamamoto<sup>1</sup>

<sup>1</sup>Low Level Radioactivity Laboratory, Kanazawa University

<sup>2</sup>Graduate School of Natural Science and Technology, Kanazawa University

**Abstract** – The radioactivity of  $^{134}\text{Cs}$  and  $^{137}\text{Cs}$  in the water samples from the Niida River, which flows through high contaminated area, was measured with gamma-spectrometry using ammonium molybdophosphate (AMP)/Cs compound method. Total radioactivity of  $^{134}\text{Cs}$  and  $^{137}\text{Cs}$  ranged from 0.254 to 4.18 Bq/L during May 2011-August 2012 and decreases with increasing time except for the rain events. The radioactivity was 1.20 Bq/L for  $^{134}\text{Cs}$  and 1.83 Bq/L for  $^{137}\text{Cs}$  after the rain event due to the typhoon No.4 in June 2012. The particulate phase of  $^{134}\text{Cs}$  and  $^{137}\text{Cs}$  was 47-93% in normal flow condition and 86-91% in high flow condition by rain events. These results indicate that suspended solids are major carrier of  $^{134}\text{Cs}$  and  $^{137}\text{Cs}$  in the Niida River.

**Keywords** – radiocesium, radioactivity, heavy rain, suspended solids

### I. INTRODUCTION

A nuclear accident at the Fukushima Daiichi Nuclear Power Plant (NPP) occurred after the 2011 Tohoku earthquake and tsunami. About 15 PBq of both  $^{134}\text{Cs}$  and  $^{137}\text{Cs}$  was released from the NPP as a result of venting operations and hydrogen explosions. Surface deposition of  $^{134}\text{Cs}$  and  $^{137}\text{Cs}$  reveals considerable external radioactivity above 3000k Bq/m<sup>2</sup> in a zone extending northwest from the NPP. Therefore, it is important to elucidate the short-term to long-term impacts of the Fukushima Daiichi NPP accident on ecosystems of river watershed environments. This study investigated the transport of  $^{134}\text{Cs}$  and  $^{137}\text{Cs}$  in a small river, Niida River running through Iidate, in Fukushima Prefecture, Japan at normal and high flow conditions during 2011-2012.

### II. MATERIALS AND METHODS

Niida River is located in Fukushima Prefecture, Japan and flows through Iidate with higher contaminated area of radiocesium and Minami-Souma with medium to low accumulation area. It has a watershed area of 585 km<sup>2</sup> and 78 km in length.

Field experiments were conducted at a fixed station in the lower Niida River during the period of May 2011-November 2012. The 20 L of surface river water samples were collected at the station using buckets. In normal flow condition, dissolved and particulate phase of radiocesium was separated using cartridge filters with pore sizes of 10  $\mu\text{m}$ , 1  $\mu\text{m}$ , and 0.45  $\mu\text{m}$ . The radioactivity of  $^{134}\text{Cs}$  and  $^{137}\text{Cs}$  in the river waters before and after the filtration was measured with gamma-ray spectrometry using ammonium molybdophosphate (AMP)/Cs compound method. In heavy rain events with typhoon, particles were separated using centrifugation and filtration with No. 5A (approximate pore

size of 7  $\mu\text{m}$ ) filters and a pore size of 0.45  $\mu\text{m}$  membrane filters. Filtration was conducted using No. 5A filters and then filtered with membrane filters.

The  $^{134}\text{Cs}$  and  $^{137}\text{Cs}$  were measured using gamma-ray spectrometry with a low background Ge detector at the Low Level Radioactivity Laboratory and the Ogoya Underground Laboratory of Kanazawa University.

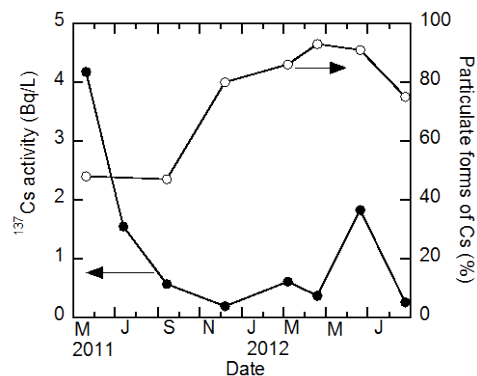
### III. RESULTS AND DISCUSSION

Radioactivity of  $^{134}\text{Cs}$  and  $^{137}\text{Cs}$  in the river waters ranged from 0.15 Bq/l to 3.83 Bq/l, and from 0.19 Bq/l to 4.18 Bq/L, respectively during May 2011-August 2012 (Fig. 1). Highest value was found in May 2011. The radiocesium concentration indicates decreasing trend with increasing time after the Fukushima Daiichi NPP accident. However, the higher radioactivity was observed in March and June 2012 after rain events.

Percentage of  $^{134}\text{Cs}$  and  $^{137}\text{Cs}$  associated with riverine suspended solids was 47-48% at normal flow condition in July and September 2011, but after December 2011 ranged from 75 to 93% at normal flow condition and 86-91% at high flow condition due to rain events. It appears to be differences in the radioactivity and existence forms between early period of July-September and after December 2011.

These results indicate that the transport processes of  $^{134}\text{Cs}$  and  $^{137}\text{Cs}$  from watershed to river vary with river watershed condition and water discharge condition.

Figure 1. Radioactivity and percentage of particulate phase of  $^{137}\text{Cs}$  in waters from the Niida River.



## Migration Behavior of Radiocesium Released from Fukushima Daiichi Nuclear Power Plant Accident

Toshihiko Ohnuki<sup>1</sup>, Naofumi Kozai<sup>1</sup>, Fuminori Sakamoto  
<sup>1</sup>Japan Atomic Energy Agency, Tokai, Ibaraki, 319-1195 Japan

**Abstract** – The migration behavior of radiocesium in plants and soil collected in Fukushima, Japan have been studied by the analyses of contaminated plants and soil using autoradiography, sequential desorption, size fractionation, XRD, and SEM analysis. Autoradiography analysis of tree samples collected after 2 and 8 months after the accident showed that radiocesium was mainly distributed as like spots on the branches and leaves of the trees emerged before the accident, and was little detected in new branch and leaves emerged after the accident. On the contrary, radiocesium was detected at the outermost tip of branches in the trees collected after 20 months of the accident. More than 65% of radiocesium were remained in the residual fraction of the soil samples after the sequential desorption. Approximately 70% of radiocesium in the residual fraction were associated with the size fractions larger than the elutriated one, even though mica like minerals were contained in the elutriated one. Therefore, plants and soil act as retardation barrier in the migration of radiocesium.

**Keywords** – Radiocesium, migration, autoradiography, desorption

### I. INTRODUCTION

The nuclear accident at the Fukushima Daiichi Nuclear Power Plant (FDNPP) occurred as a consequence of the massive earthquake and associated tsunami that struck the Tohoku and north Kanto regions of Japan on 11 March 2011. A series of hydrogen explosion was occurred from 13 March to 15 March at the units 1, 2, and 3. The release rate of <sup>137</sup>Cs on 15 March is estimated between 10<sup>12</sup> and 10<sup>15</sup> Bq/h. This fallout radioactive Cs were dispersed from FDNPP to ocean and land. Some of the released radioactive Cs was deposited on the ground of the area located north-west direction from FDNPP. Many scientists have studied migration of radiocesium to estimate dose rate and to estimate the fate in the terrestrial environment. However, the migration behavior of radiocesium is not fully understood.

In the present study, migration behavior of radiocesium has studied by the analyses of contaminated plants and soil using autoradiography, sequential desorption, size fractionation, XRD, and SEM analysis.

### II. EXPERIMENTAL

The samples of plants were collected on the places located between 4 and 55 km from FDNPP at approximately 2, 8, 20, and 22 months after the accident. The spatial distribution of radiocesium on the plants was analyzed by autoradiography analyses.

Soil was sampled in Iitate, Fukushima on 1 month after

the accident. For the analyses of soil spatial distribution was measured by autoradiography, and mobility was examined by sequential desorption using appropriate desorption reagent solutions. Size distribution of residual radiocesium after the sequential desorption was analyzed by size fractionation using sieve and the elutriation. The mineralogical components of soil were analyzed by XRD and SEM-EDS analyses.

### III. RESULTS AND DISCUSSION

The autoradiography analyses of *Cryptomeria japonica*, *Torreya nucifera*, and *Thujaopsis dolabrata* var. *hondae* collected on approximately 2 and 8 months after the accident showed that radiocesium was mainly distributed as like spots on the branches and leaves of the trees emerged before the accident, and was little detected in new branch and leaves emerged after the accident. On the contrary, radiocesium was detected at the outermost tip of branches in the trees collected after 20 months of the accident. *Morus alba* collected after 22 months contained radiocesium in and outside of the stem, even though no radiocesium was detected in the root, strongly suggesting that some radiocesium was translocated from the outside stem to inside. These results indicate that distribution of radiocesium deposited on/in the trees has been gradually changed with time in the scale of the year.

Autoradiography analysis of the thin section of soil showed that radiocesium in soil was distributed as like spots on the soil particles. More than 65% of radiocesium were remained in the residual fraction of the soil samples after treatment of a 1 mole L<sup>-1</sup> NH<sub>4</sub>Cl solution and a 1 mole L<sup>-1</sup> CH<sub>3</sub>COOH solution. Approximately 70% and 10% of radiocesium in the residual fraction were associated with the size fractions larger than the elutriated one and with elutriated one, respectively. XRD and SEM-EDS analyses showed that a variety of minerals were present in the soil involving mica like minerals. XRD spectrum of elutriated soil fraction showed the presence of mica like minerals. These results strongly suggest that radiocesium was irreversibly associated with soil components other than mica like minerals in the contaminated soil.

Therefore, plants and soil function as barrier to retard the migration of radiocesium deposited by the accident of FDNPP.

## Research on Atmospheric Radionuclides from the Fukushima Nuclear Accident at the MRI, Japan

Yasuhito Igarashi<sup>1</sup>, Koji Adachi<sup>1</sup>, Taichu Tanaka<sup>1</sup>, Mizuo Kajino<sup>1</sup>, Tsuyoshi Sekiyama<sup>1</sup>,  
Takashi Maki<sup>1</sup>, Yuji Zaizen<sup>1</sup>, Masao Mikami<sup>1</sup>

<sup>1</sup>Meteorological Research Institute, Japan

*Abstract* – By the Fukushima nuclear accident, atmospheric environments over Japan, especially the eastern part, were seriously polluted by a massive amount of the anthropogenic radionuclides. The Meteorological Research Institute, Japan (MRI) has devoted into the clarification of these earlier environmental impact not only by the observations but also by model simulation endeavors. Major research activities at the MRI are briefly introduced in this presentation.

*Keywords* – Fukushima nuclear accident, radio-Sr, radio-Cs, Radioactive aerosol, Numerical transport and deposition modeling

### I. INTRODUCTION

The Meteorological Research Institute, Tsukuba, Japan (MRI) has carried out observations on the atmospheric radionuclides for more than 50 years. In order to clarify the impacts of the Fukushima nuclear accident in the atmospheric environment and its control factors, the observations have continued after the disaster in March 2011. Also, the model simulations were conducted to reconstruct radioactive plume transport and depositions of the radioactive contaminants over the regional as well as the global environment.

### II. OBSERVATION ENDEVOURS

The MRI locates ca.170 km southwest of the accidental site. The monthly total deposition of <sup>137</sup>Cs at the MRI was 23±0.9 kBq/m<sup>2</sup> in March, 2011. This amount is 6-7 digits higher than the level prior to the disaster. The total <sup>137</sup>Cs deposition was 25.5 kBq/m<sup>2</sup> for the year 2011. Simple sum of the monthly <sup>137</sup>Cs deposition flux due to the global weapon tests since 1954 gives about 7 kBq/m<sup>2</sup>. Considering the physical decay for the global fallout <sup>137</sup>Cs, the Fukushima <sup>137</sup>Cs contamination could be about 20 times larger than the global fallout. Almost the same extent of <sup>134</sup>Cs deposited, thus the surface radio-Cs contamination extended about 50 kBq/m<sup>2</sup>. This value almost corresponds to that around Tsukuba obtained by the air-borne survey conducted by the Ministry of Education, Culture, Sports, Science and Technology, Japan (MEXT).

On the contrary, the monthly <sup>90</sup>Sr deposition at the MRI was 4.4±0.1 Bq/m<sup>2</sup> in March, 2011, which was about 1/5000 of that of <sup>137</sup>Cs during the same month. Referring to the level before the disaster, this deposition exhibits 2-3 digits of enhancement; the environmental and health impacts were not as enormous as radio-Cs. The total <sup>90</sup>Sr deposition was about 11 Bq/m<sup>2</sup> for the year 2011 and it was about 1/2500 of <sup>137</sup>Cs. Until the middle of 2012, the <sup>90</sup>Sr/<sup>137</sup>Cs activity ratio varied about 400~5000 and after all

the degree of the pollution by the radio-Sr can confirm trivial compared with Cs over the metropolitan region.

As further trials an imaging plate (IP) analysis, which visualizes the radioactivity distributions in air filter samples, and particle analysis using a scanning electron microscope (SEM) with energy-dispersive X-ray spectrometer (EDS), have been carried out. The purpose of these analyses is to identify the host particles which carry the radionuclides.

### III. SIMULATION ENDEVOURS

In order to improve our understanding of the temporal and spatial distributions of transport and depositions of the radionuclides due to the Fukushima accident, both global and regional atmospheric transport models have been employed. For the global transport MASINGAR (Model of Aerosol Species IN the Global Atmosphere), with horizontal model grid of about 0.56° and 40 vertical layers (from surface to 0.4hPa), was used. The horizontal wind components were nudged by global analysis of Japan Meteorological Agency (GANAL) dataset. The model deals with <sup>137</sup>Cs, <sup>133</sup>Xe, and <sup>131</sup>I. Emission flux estimates by Chino et al. (2011) and Stohl et al. (2011) were used for <sup>137</sup>Cs and <sup>131</sup>I, and <sup>133</sup>Xe, respectively. The model simulated advective transport, eddy diffusion, convective transport, dry and wet depositions, and radioactive decay.

More detailed distribution and processes for the Fukushima radioactivity, a regional transport model MRI-PM/r (Passive-tracers Model for Radioactivity) has been developed. This model classifies the aerosol particles into 6 categories, and considers condensation, evaporation, cohesion, activation of cloud condensation nuclei and ice nuclei, dissolution, collision (washout), cloud microphysical processes (conversion processes among rainout, cloud water, ice clouds, raindrops, snow, hail) and dry deposition. The model also incorporated physical and chemical processes of radionuclides and the interaction with the environment aerosol.

In addition to these, emission analysis from the accident by inverse modeling approach, and advanced approach of ensemble simulation of atmospheric dispersion of radionuclides during the accident have been performed.

The overview of the current status and challenges of these observations as well as simulation studies are given.

- [1] Igarashi et al., 2013EGU
- [2] Adachi et al., 2013EGU
- [3] Maki et al., 2013EGU
- [4] Sekiyama et al., 2013EGU
- [5] Tanaka et al., 2013AMS
- [6] Kajino et al., 2011JMSJ Fall Meeting

## Presuming techniques of radioactive cesium concentration in muscle for beef cattle

T. Ohtsuki<sup>1</sup>, F. Koga<sup>2</sup>, M. Uchida<sup>2</sup>, Y. Ishikawa<sup>2</sup>, T. Takase<sup>3</sup>, K. Kawatsu<sup>3</sup>, M. Mogi<sup>4</sup>, S. Murayama<sup>4</sup>,  
Y. Izumi<sup>4</sup>, H. Kikunaga<sup>1</sup>, T. Tachiya<sup>5</sup>, Y. Shiraishi<sup>2</sup>, K. Endo<sup>2</sup>

<sup>1</sup>Research Center for Electron Photon Science, Tohoku University

<sup>2</sup>Fukushima Agricultural Technology Center Livestock Industry Research Center, Fukushima Prefecture

<sup>3</sup>Faculty of Symbiotic System Science, Fukushima University

<sup>4</sup>Japan Environment Research Co., LTD,

<sup>5</sup>Comtec Eng. Co., LTD, Fukushima

*Abstract* – The contamination of livestock products by the radioactive cesium ( $Cs134$  and  $Cs137$ ) is a serious problem in Tohoku area after the accident of the Fukushima No.1 nuclear power plant. The presuming techniques of the radioactive cesium concentration in muscle and blood for these beef cattle were developed in this study. We found that the measurements of the radioactive cesium from outside of body are really possible by using several inches(“) NaI scintillation detectors.

*Keywords* – radioactive cesium, beef cattle, measurement from outside of body, NaI scintillation detector

### I. INTRODUCTION

The contamination to the livestock products, by radioactive cesium is becoming a serious problem in Tohoku area after the accident of the No.1 nuclear power plant of Fukushima. Especially, beef cattle which fed excessively contaminated stock food should be still continuously monitored. Since Ge-detectors are restricted and if we use them, so much time is needed for presuming of the cesium contamination by taking blood sample[1], then, another technique for the concentration check inside body(muscle) for the living cattle should be considered. Here we demonstrate the monitoring system by using NaI scintillation detectors from outside of cattle body.

### II. MONITORING SYSTEM AND MEASUREMENTS

The monitoring system is consist of 2”, 2.5” and 5” NaI scintillation detectors for measuring the  $Cs134$  and  $Cs137$  concentrations in the cattle body, collimators (Pb material), phantoms (plastic tank: the specific liquid like inside materials are contaminated by several concentrations of  $Cs134$  and  $Cs137$ ), special frame for keeping the cattle body on the inside and its radiation shielding materials consist of several sheets of Pb curtains. We use a portable MCA system for data acquisition. The 5” NaI detector and its collimator are shown in Fig. 1(a) and the special frame for keeping the cattle body and the portable MCA system are also shown in Fig. 1(b). Firstly, we took calibration curves between the Ge and NaI detectors by using phantoms by which the cesium concentration is known. The practical measurements were performed by comparison of contamination-free cattle and contaminated them. The measurement time and position were set to 600 sec at the thigh and haunches (further shorter time like 300 sec. is needed for the measurements). The data are analyzed by the code Fukushima by provided Niki Grass Co. Ltd. for doing better deconvolution.

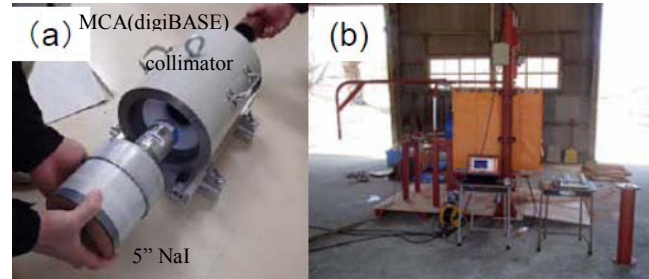


Fig. 1(a) 5” NaI detector and its collimator: setting inside the collimator, (b) Measurement system of cattle from outside of the body (special frame for keeping the cattle body).

### III. RESULTS

Results of the measurements are shown in Fig. 2. From the figure it is clearly seen the cesium peaks, namely, the cesium contaminated cattle has much higher count rates of  $Cs134$  and  $Cs137$  than those of the contamination-free cattle even though the similar count rates of K40 between them. Small peaks of  $Cs134$  and  $Cs137$  for contamination-free cattle are due to the back ground from atmosphere. Detail of the results will be shown and discussed in the conference.

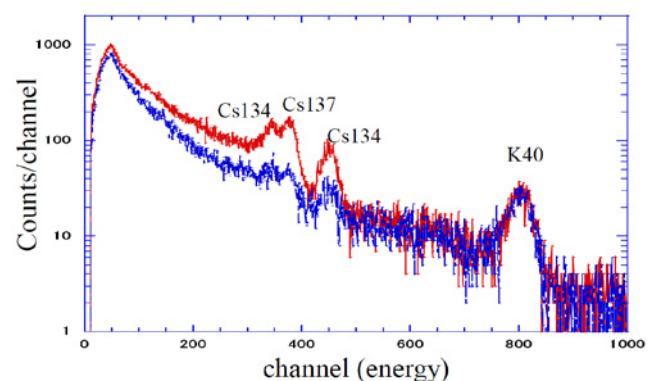


Fig. 2 Two spectra with 5” NaI scintillation detector are shown, the results of contaminated cattle fed by the contaminated stock food (higher count rate) and the contamination-free cattle (lower count rate).

[1] T. Takase et. al., Radioisotopes 62 (2013), in press.

# Spatio-temporal distribution of atmospheric radiocesium at monitoring stations for Suspended Particulate Matter in Fukushima area released from the TEPCO Fukushima Daiichi Nuclear Power Plant accident

Haruo Tsuruta<sup>1</sup>, Yasuji Oura<sup>2</sup>, Mitsuru Ebihara<sup>2</sup>, Mitsunori Ishimoto<sup>3</sup>, Yosuke Katsumura<sup>3</sup>,  
Toshimasa Ohara<sup>4</sup>, Teruyuki Nakajima<sup>1</sup>

<sup>1</sup> Atmosphere and Ocean Research Institute, The University of Tokyo, Japan

<sup>2</sup> Department of Chemistry, Tokyo Metropolitan University, Japan

<sup>3</sup> Center for Regional Environmental Research, National Institute for Environmental Studies

<sup>4</sup> Nuclear Professional School, The University of Tokyo, Japan

*Keywords* Spatio-temporal distribution, atmospheric <sup>137</sup>Cs, Fukushima, filter tapes of SPM monitor

## I. INTRODUCTION

No data has been found of continuous monitoring of radioactive materials in the atmosphere in Fukushima area after the Fukushima Daiichi Nuclear Power Plant (FD1NPP) accident on March 11, 2011, although it greatly contributes to accurate evaluation of the internal exposure dose, to reconstruction of emission time series of released radionuclides, and to validation of numerical simulations by atmospheric transport models. Then, we have challenged to retrieve the radioactivity in atmospheric aerosols collected every hour on a filter tape which was installed in Suspended Particulate Matter (SPM) monitor with beta-ray attenuation method used at air pollution monitoring networks in Japan. In the previous paper [1], the concentration of <sup>134</sup>Cs and <sup>137</sup>Cs collected on the filter tapes has been successfully measured by a Ge detector, and time series of hourly atmospheric concentrations of <sup>134</sup>Cs and <sup>137</sup>Cs was also made at many monitoring stations for SPM in Fukushima prefecture and the adjacent areas. The purpose of this paper is that, by using these data, spatio-temporal distribution of <sup>137</sup>Cs will be shown in Fukushima area, and the transport of radioactive materials from the FD1NPP will be discussed by analyzing meteorological data and radiation dose rate.

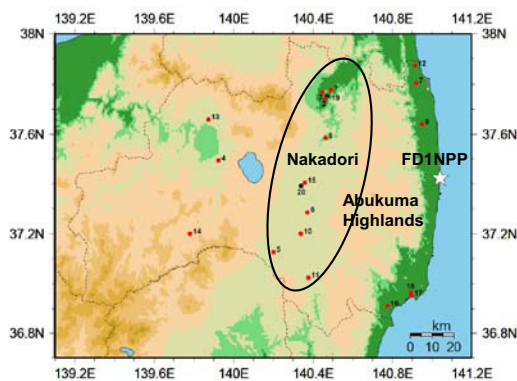


Fig. 1 SPM monitoring stations in Fukushima prefecture

## II. DATA FOR ANALYSIS

Hourly atmospheric concentrations of <sup>134</sup>Cs and <sup>137</sup>Cs in several monitoring stations in Nakadori of Fukushima

prefecture (Fig. 1) during March 15-16 and 20-23, 2011, was used for a detailed analysis. Meteorological data of AMeDAS stations, GPV (Grid Point Value) and Radar-AMeDAS precipitation by Japan Meteorological Agency was also used. Regional deposition rate for <sup>137</sup>Cs on the earth's surface with airborne measurements by MEXT was used in comparison with spatial distribution of the polluted air masses.

## III. RESULTS AND DISCUSSION

High concentrations of <sup>137</sup>Cs (>10 Bq m<sup>-3</sup>) were measured in Nakadori twice, the first period from 9:00 (JST) Mar. 15 to 3:00 Mar. 16, and the second period from 13:00 Mar. 20 to 06:00 Mar. 21. In the first period, the polluted air masses transported from the FD1NPP over Abukuma Highlands, were found in the afternoon of Mar. 15. The time of the maximum concentration changed from the early afternoon in the south to the night in the north, and the maximum concentration was much higher in the south than in the north. According to the deposition rate of <sup>137</sup>Cs on the soil surface in regional scale measured by MEXT [2], higher deposition rate was measured in the northern part than in the southern part, possibly due to more precipitation in the northern part. In the second period, however, higher <sup>137</sup>Cs concentrations began to be measured in the northern part in the early afternoon of Mar. 20. In the night, the time of the maximum <sup>137</sup>Cs was found early in the north and late in the south. During the second period, radiation dose rate in Nakadori did not show any increase due to no precipitation. Thus, the radiocesium dataset by measuring filter tapes installed in the SPM monitor is very useful to retrieve the spatio-temporal distribution of <sup>137</sup>Cs in an area which has no continual data of radionuclides in the atmosphere.

[1] Oura, Y. et al.: a paper in this Symposium, 2013

[2] MEXT: Intensive field study on the measurements of radionuclides deposited on the soil surface in east Fukushima, HP of MEXT, 2011.

## Education of Nuclear and Radiochemistry in Hallym University, Korea

Y. H. Chung

Department of Chemistry, Hallym University, 1 Hallymdaehak-gil, Chuncheon 200-702, Korea  
[yhchung@hallym.ac.kr](mailto:yhchung@hallym.ac.kr)

Nuclear and radiochemistry course has been provided by Department of Chemistry in Hallym University (HU) for more than ten years. It is designed mainly for undergraduates who want to pursue their career in the pertinent fields such as chemistry of spent fuel of nuclear reactors, radiopharmaceutical chemistry, radiation chemistry and nuclear chemistry. There are twenty-two reactors currently operating in Korea and a few research facilities are treating cancer patients using an accelerator. A heavy-ion accelerator, RAON, will be commissioned in 2017 and provide various rare isotopes produced by IF (in-flight fragment) and ISOL (Isotope Separation On-Line) methods [1]. RAON's superconducting linear accelerator will accelerate uranium beam up to 200 MeV/u with 400 kW beam power. In addition to RAON, a KHIMA (Korea Heavy Ion Medical Accelerator) project for cancer therapy was initiated in 2010 by KIRAMS (the Korea Institute of Radiological & Medical Sciences) and will include a superconducting cyclotron to be completed at the end of 2016 [2]. The cyclotron will provide heavy ions whose maximum energy and beam intensity are 430 MeV/u and  $1.7 \times 10^{10}$  pps, respectively. Nuclear and radiochemistry program in Hallym University is going to embrace the ongoing progress in Korea.

[1] S. K. Kim, *RAON: Heavy Ion Accelerator for Rare Isotope Science in Korea*, The 16<sup>th</sup> Inter. Conf. on Accelerators and Beam Utilizations, November 8-9, 2012, Gyeongju, Korea.

[2] G. B. Kim, *Current Status of KHIMA Project*, The 16<sup>th</sup> Inter. Conf. on Accelerators and Beam Utilizations, November 8-9, 2012, Gyeongju, Korea.

## Use of Small $^{68}\text{Ge}/^{68}\text{Ga}$ Generators in Experiments for the Education of Radioisotope-related Fields as well as of Natural and Social Sciences in General

Tadashi Nozaki,<sup>1</sup> Koji Ogawa<sup>2</sup>

<sup>1</sup>School of Sciences, Kitasato University

<sup>2</sup>School of Allied Health Sciences, Kitasato University

Experiments undertaken in schools usually give more vivid and unforgettable impression to the students than lectures. Several characteristics of radioisotopes can be used efficiently in the education of radioisotope-related fields as well as of natural and social sciences in general. Many radioisotopes useful for education are given from isotope generators, of which  $^{68}\text{Ge}/^{68}\text{Ga}$  generator has proved to be of the widest use, as understood from the decay properties of both nuclides shown here and from chemical properties of the daughter,  $^{68}\text{Ga}$ .

$^{68}\text{Ge}$ : 271 d, EC, no  $\gamma$  ---- Black matter for many detections  
 $^{68}\text{Ga}$ : 67.7 m;  $\beta^+$ , 90 % 1.9 MeV; EC, 10 %  
 $\gamma$ , 1.07 MeV 1.0 %, etc.

Although large scale  $^{68}\text{Ge}/^{68}\text{Ga}$  generators for PET use are commercially available, we were unable to find any stable supply of small types. For full use of this generator, thus we should become able to make it by ourselves. First we examined the method of preparing the adsorbent for parent-daughter separation, and have proved the following procedure to be highly useful: (1) prepare gelatinous precipitate of hydrated  $\text{SnO}_2$  from  $\text{SnCl}_4$  and  $\text{NaOH}$  solutions and wash it by repeated centrifugation and re-suspension in water; (2) collect and warm gently the centrifuged mass with occasional turn-over with a non-metallic spatula to give moist particles; (3) push gently the particles on a sieve of 200  $\mu\text{m}$  mesh size to crash them into smaller sizes, and leave them over potassium acetate ( $\text{CH}_3\text{CO}_2\text{K}$ ) at room temperature for drying; (4) after 1 week, treat the particles just as in Step 3 but with a sieve of about 100  $\mu\text{m}$  mesh size; (5) collect by sieving particles of about 50 to 100  $\mu\text{m}$  size, and keep them over  $\text{CH}_3\text{CO}_2\text{K}$ ; (6) after more than 2 weeks, dip the particles in refluxing 0.1 M  $\text{HNO}_3$  for 3 hours, and (7) after being left to cool, replace the  $\text{HNO}_3$  with 1 M  $\text{HCl}$ . After 2 days, the particles, hydrated  $\text{SnO}_2$ , is ready for use.

Usually 1 mL disposable plastic syringe is used for the generator column, to which the adsorbent (apparent volume of 0.3 - 0.4 mL) suspended in  $\text{HCl}$  is added. Then 1 M  $\text{HCl}$  solution of  $^{68}\text{Ge}$  (1 to 100 kBq) with daughter  $^{68}\text{Ga}$  is added to the column. The column is further washed with 100 mL of 1 M  $\text{HCl}$  flowing slowly through it for wash away some fine suspensions. In Japan, the generator with  $^{68}\text{Ge}$  activity under 100 kBq can be used free from law regulation.

The  $^{68}\text{Ga}$  is eluted into 1/3 mL of 1 M  $\text{HCl}$  in about 30 sec with 65-70 % yield. Since quantitative separation is possible for  $^{68}\text{Ge}$  and  $^{68}\text{Ga}$  in 1 M  $\text{HCl}$ , some hot-atom effect is thought to make  $^{68}\text{Ga}$  formed in the column partly non-elutable. Under frequent milking, the breakthrough of  $^{68}\text{Ge}$  is a few tens ppm. No change was observed in these characteristics in 9 months, the half-life of  $^{68}\text{Ge}$ .

Self-making of the generator is thought to be a common experimental theme, and can be guessed to give joy and satisfaction to the participants in handling samples prepared by their self-made devices, even when ready-made adsorbent was supplied them in the generator making. Comparison of the growth curve of  $^{68}\text{Ga}$  observed after milking with the curve obtained by calculation from the differential equation is expected to be highly effective in the study of how to treat some observed phenomena by mathematical means. The eluted  $^{68}\text{Ga}$  is highly suitable for the following chemical experiments: adsorption on cellulose under various pH; solvent extraction and ion exchange separation; and isotopic exchange between  $\text{Ga}^{3+}$  and  $\text{Ga-EDTA}$  complex.

We have almost completed a guide book for the experiments given above, and now are working further for the following themes: (1) utilizing the generator as the source of annihilation radiation,  $\gamma$ -ray absorption by various substances, and coincidence measurement for localization and for low background counting; and (2) utilizing  $^{68}\text{Ga}$  as tracer, studies on contamination and decontamination, leak hunting, synthesis of radiopharmaceuticals, and measurement of uptake by plants.

Since a vast variety exists in the principal aim, experiences and scientific levels of possible candidates to the experimental study, at least three courses should be prepared. Also, the guide book should be so made as the teachers and instructors are able to select adequately the themes for each course. As for usual high school curriculums, only a few to several days are allotted to the education related with nuclear phenomena. Hence, it is of prime importance, we believe, to set up a rental system, in which generators, radiation detectors, etc., are sent to individual high schools from regional centers according to predetermined schedules, preferably together with instructor(s).

## Application of alpha spectrometry to the measurement of a single plutonium particle for nuclear safeguards

Kenichiro Yasuda, Daisuke Suzuki, Fumitaka Esaka and Masaaki Magara  
Research group for analytical chemistry, Japan Atomic Energy Agency

*Abstract* – For rough estimation of isotopic composition in a single plutonium particle before precise measurement by thermal ionization mass spectrometry (TIMS), alpha spectrometry was demonstrated using 10 particles in a standard reference material NBS947. The particles with diameters of around one micrometer were picked up and put onto TIMS filaments by a micromanipulator attached to a scanning electron microscope (SEM). The particle on the filament was transferred to an alpha spectrometer chamber. And then, the activity ratio of ( $^{238}\text{Pu}+^{241}\text{Am}$ )/( $^{239}\text{Pu}+^{240}\text{Pu}$ ) was measured for each particle. Finally, precise Pu isotope ratios of  $^{240}\text{Pu}/^{239}\text{Pu}$  and  $^{241}\text{Pu}/^{239}\text{Pu}$  were determined with TIMS. The measured activity ratios and isotope ratios were in good agreement with the reference data within the measurement uncertainty.

*Keywords* – alpha spectrometry, plutonium particle, nuclear safeguards

### I. INTRODUCTION

The International atomic energy agency (IAEA) has adopted environmental sampling as a new method for the strengthened safeguards system [1-2]. The objectives of this method are to detect undeclared nuclear materials and activities. One of the analytical methods for environmental sampling is particle analysis, which is a powerful tool for nuclear safeguards to detect undeclared nuclear activities.

In this method, isotope ratios of nuclear materials in individual particles were measured by secondary ion mass spectrometry (SIMS) [3-5] or thermal ionization mass spectrometry (TIMS) [6-8]. Prior to the analysis with TIMS, the particle containing nuclear materials should be put onto a filament. However, there is no conclusive proof that nuclear materials exist in the particle on the filament. The purpose of this study is to check if the particle on the filament contains nuclear materials before measuring the isotope ratios by TIMS, and to compare the activity ratios and the isotope ratios of the particle.

- [1] D.L. Donohue, J. Alloys Compd., 11, 271-273 (1998).
- [2] D.L. Donohue, Anal. Chem., 74, 28A-35A (2002).
- [3] G. Tamborini, M. Betti, V. Forcina, T. Hiernaut, B. Giovannone, L. Koch, Spectrochim. Acta B53, 1289-1302 (1998).
- [4] M. Betti, G. Tamborini, L. Koch, Anal. Chem., 71, 2616-2622 (1999).
- [5] F. Esaka, K.T. Esaka, C.G. Lee, M. Magara, S. Sakurai, S. Usuda, K. Watanabe, Talanta, 71, 1011-1015 (2007).
- [6] C.G. Lee, L. Iguchi, F. Esaka, M. Magara, S. Sakurai, K. Watanabe, S. Usuda, Jpn. J. Appl. Phys., 45, L294-L296 (2006).
- [7] C.G. Lee, D. Suzuki, F. Esaka, M. Magara, N. Shinohara, S. Usuda, J. Nucl. Sci. Technol., 46, 809-813 (2009).
- [8] O. Stetzer, M. Betti, J. van Geel, N. Erdmann, J.V. Kratz, R. Schenkei, N. Trautmann, Nucl. Instrum. Meth. Phys. Res. A525, 582-292 (2004).

## High LET Radiolytic Degradation Studies of Separation Processes for Spent Nuclear Fuel

Jeremy Pearson and Mikael Nilsson

University of California – Irvine, USA

Department of Chemical Engineering and Materials Science, 916 Engineering Tower, Irvine, CA, 92697

E-mail: nilssonm@uci.edu

Treatment of used nuclear fuel through solvent extraction separation processes is hindered by radiolytic damage from radioactive isotopes present in used fuel. The nature of the damage caused by the radiation may depend on the radiation type, whether it be low linear energy transfer (LET) such as gamma radiation or high LET such as alpha radiation. Used nuclear fuel contains beta/gamma emitting isotopes but also a significant amount of transuranics which are generally alpha emitters. The effects of gamma radiation on solvent extraction ligands have been more extensively studied than the effects of alpha radiation. This is due to the inherent difficulty in producing a sufficient and confluent dose of alpha particles within a sample without leaving the sample contaminated with long lived radioactive isotopes. Helium ion beam and radioactive isotope sources have been studied in the literature. We have developed a method for studying the effects of high LET radiation *in situ* via  $^{10}\text{B}$  activation and the high LET particles that result from the  $^{10}\text{B}(n,\alpha)^7\text{Li}$  reaction which follows. This method has been applied to organic solutions of TBP and CMPO, two ligands common in TRU solvent extraction treatment processes. Rates of degradation of TBP and CMPO and their respective degradation products in the presence of high LET radiation are presented and discussed. These results are also compared to gamma studies performed in our lab and other gamma and alpha studies found in the literature. The possible application of this method to a variety of other solvent extraction ligands to study the effects of high LET radiation is also considered.

## Effects of helium retention and lithium depletion on tritium behaviors in $\text{Li}_2\text{TiO}_3$

Makoto Kobayashi<sup>1</sup>, Hiromichi Uchimura<sup>1</sup>, Kensuke Toda<sup>1</sup>, Misaki Sato<sup>1</sup>,  
Katsuyoshi Tatanuma<sup>2</sup>, Yasuhisa Oya<sup>1</sup> and Kenji Okuno<sup>1</sup>

<sup>1</sup>Radioscience Research Laboratory, Faculty of Science, Shizuoka University, Shizuoka, Japan

<sup>2</sup>Kaken Co. Ltd., 1044, Hori, Mito-city, Ibaraki, 310-0903, Japan

**Abstract** – The effects of helium retention on tritium behaviors in lithium-titanate ( $\text{Li}_2\text{TiO}_3$ ) were investigated. The synergetic effect of helium retention and lithium-depletion was also examined with using lithium-depleted  $\text{Li}_{1.8}\text{TiO}_{2.9}$ . Deuterium introduced into  $\text{Li}_2\text{TiO}_3$  by ion implantation was desorbed as three peaks at 400, 490 and 620 K. Deuterium retention at 400 K for  $\text{Li}_{1.8}\text{TiO}_{2.9}$  was larger than that for  $\text{Li}_2\text{TiO}_3$  due to the existence of larger amount of lithium vacancies. Deuterium retention by lithium vacancies was decreased by He implantation because of the occupation of vacancies by He.

**Keywords** – Tritium,  $\text{Li}_2\text{TiO}_3$ , Helium, TDS

### I. INTRODUCTION

For the establishment of D-T fusion reactors, a comprehensive model of tritium migration processes in solid tritium breeder materials must be developed. Tritium migration behavior in lithium-titanate ( $\text{Li}_2\text{TiO}_3$ ), which is one of candidates for tritium breeder materials, has been studied by out-of-pile annealing experiments. However, the effects of helium generated by  $\text{Li}(n,\alpha)\text{T}$  reaction on tritium migration in  $\text{Li}_2\text{TiO}_3$  have not been focused in detail. It is generally known that helium can retain in the materials by forming bubbles, which will exist in  $\text{Li}_2\text{TiO}_3$  after long-term operation, and affect on tritium migration process by acting as diffusion passes and/or trapping sites. These predictions motivated us to investigate the contributions of helium retention on trapping and release of hydrogen isotopes in  $\text{Li}_2\text{TiO}_3$ . The pre-irradiation of  $\text{He}^+$  was performed into sintered  $\text{Li}_2\text{TiO}_3$  pellet. Thereafter,  $\text{D}_2^+$  irradiation was carried out. Thermal desorption spectroscopy (TDS) measurements were adopted for the elucidation of deuterium retention and release behaviors. The same experimental procedure was also done for lithium-depleted  $\text{Li}_2\text{TiO}_3$  ( $\text{Li}_{1.8}\text{TiO}_{2.9}$ ) to understand the effects of helium retention with lithium burn-up, which are simultaneously occurred in actual environment.

### II. EXPERIMENTAL

The powders of  $\text{Li}_2\text{TiO}_3$  and  $\text{Li}_{1.8}\text{TiO}_{2.9}$  were pressed into a disc shape with the size of  $10\text{ mm}^\phi \times 0.5\text{ mm}^t$ , and sintered at 1173 K for 3 h. These samples were installed into a vacuum system and heated at 1173 K for 3 h to remove impurities. The  $\text{He}^+$  implantations were done with the implantation energy of 3 keV  $\text{He}^+$ , ion flux of  $1.0 \times 10^{18}\text{ He}^+\text{ m}^{-2}\text{ s}^{-1}$  and ion fluence of  $1.0 \times 10^{22}\text{ He}^+\text{ m}^{-2}$ . Thereafter, 3.0 keV  $\text{D}_2^+$  implantations were carried out with the ion flux and ion fluence of  $2.0 \times 10^{18}\text{ D}^+\text{ m}^{-2}\text{ s}^{-1}$  and  $2.0 \times 10^{22}\text{ D}^+\text{ m}^{-2}$ , respectively. The deuterium

desorption behaviors were examined by TDS using a high resolution mass spectrometer to separate  $\text{He}^+$  and  $\text{D}_2^+$  from room temperature to 1173 K with the heating rate of  $5\text{ K min}^{-1}$ .

### III. RESULTS AND DISCUSSION

D-TDS spectra for  $\text{Li}_2\text{TiO}_3$  and  $\text{Li}_{1.8}\text{TiO}_{2.9}$  are shown in the figure. D-TDS spectrum for only  $\text{D}_2^+$  irradiated  $\text{Li}_2\text{TiO}_3$  showed that D release was distributed in the temperature of 350- 750 K. The D release spectrum was consisted of three release peaks at around 400, 490 and 620 K. The TDS spectrum for the  $\text{D}_2^+$ -irradiated  $\text{Li}_{1.8}\text{TiO}_{2.9}$  also showed the same D release peaks. However, the deuterium retention in the peak at 400 K was increased compared to that for  $\text{Li}_2\text{TiO}_3$ . This fact indicates that deuterium released at 400 K was weakly trapped by lithium vacancies.  $\text{He}^+$  pre-irradiated  $\text{Li}_2\text{TiO}_3$  showed the decrease of deuterium retention in the release peaks at 400 and 490 K. The deuterium trapping sites for the release peaks at 490 K and 620 K would be the irradiation defects such as oxygen vacancies and the dangling oxygen atoms, respectively. Therefore, helium retention would only reduce the deuterium retention in irradiation defects. These results suggest that helium would disturb deuterium to retain at irradiation defects by substituting them, however, hardly affects for chemical binding due to the little chemical affinity of helium.

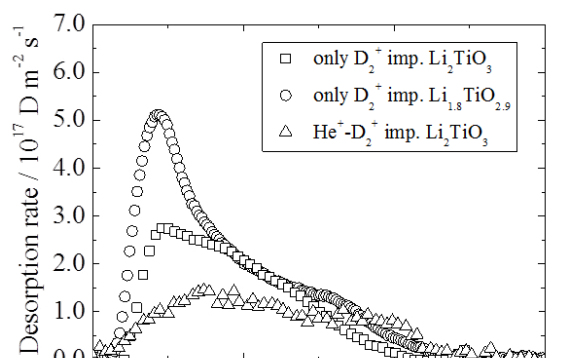


Fig. D-TDS spectra for  $\text{Li}_2\text{TiO}_3$  and  $\text{Li}_{1.8}\text{TiO}_{2.9}$  900 with  $\text{D}_2^+$  and  $\text{He}^+$  implantations

## Adsorptivity of Various Metal Ions onto Benzo-18-crown-6 and Dibenzo-18-crown-6 Resins

Masanobu Nogami<sup>1</sup>, Tomohiro Haratani<sup>1</sup>, Yu Tachibana<sup>2</sup>, Toshitaka Kaneshiki<sup>3</sup>,  
 Masao Nomura<sup>3</sup>, Tatsuya Suzuki<sup>2</sup>

<sup>1</sup>Department of Electric and Electronic Engineering, Kinki University

<sup>2</sup>Department of Nuclear System Safety Engineering, Nagaoka University of Technology

<sup>3</sup>Research Laboratories for Nuclear Reactors, Tokyo Institute of Technology

*Abstract* – Adsorptivity of various metal ions onto silica-supported resins consisting of benzo-18-crown-6 (B18C6) and dibenzo-18-crown-6 (DB18C6), respectively, was investigated in hydrochloric acid and nitric acid media. Pd(II) and Ag(I) for HNO<sub>3</sub> and Fe(III) and Ba(II) for HCl were found to be adsorbed by both resins, respectively. It was also found that Sr(II) for HCl and Ca(II) for HNO<sub>3</sub> were adsorbed by B18C6 and DB18C6 resins, respectively. These facts indicate that the two resins which have almost the same ring size adsorbed metal ions with smaller cationic diameters except Ba(II) with different selectivity.

*Keywords* – benzo-18-crown-6, dibenzo-18-crown-6, resin, nuclide separation

### I. INTRODUCTION

It is well known that macrocyclic compounds such as crown ethers selectively form complexes with metal ions, and their applications to the treatment of radioactive liquid wastes by liquid-liquid extraction have widely been investigated. Recently we have synthesized silica-supported resins where crown ethers are chemically bonded to the polymer network[1,2]. The chemical structure of dibenzo-18-crown-6 (DB18C6) resin, for example, is shown Figure 1. So far the resins have mainly been studied for the purpose of isotope separation, e.g. zinc and calcium, and little information on adsorptivity of various metal ions by these resins is available. In the present study, adsorptivity of various metal ions onto benzo-18-crown-6 (B18C6) and DB18C6 resins was investigated in hydrochloric acid and nitric acid media.

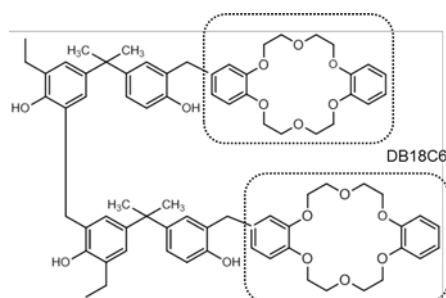


Figure 1 Chemical structure of DB18C6 resin

### II. EXPERIMENTAL

B18C6 and DB18C6 resins were synthesized by following the earlier paper[2]. Adsorptivity of metal ions by the resins to at equilibrium was examined by a batch method at 25°C using solutions of HNO<sub>3</sub> or HCl up to 9 mol/dm<sup>3</sup> (= M) containing each metal ion (1 mM).

### III. RESULTS AND DISCUSSION

Pd(II) and Ag(I) for HNO<sub>3</sub> and Fe(III) and Ba(II) for HCl were found to be adsorbed by both resins, respectively. It was also found that Sr(II) for HCl and Ca(II) for HNO<sub>3</sub> were adsorbed by B18C6 and DB18C6 resins, respectively. In general, the distribution ratios increased with increasing concentrations of HCl. On the other hand, dependence of HNO<sub>3</sub> concentrations on the distribution ratios was found much smaller for HNO<sub>3</sub> system. No or very little adsorptions were observed for the other examined metal ions. These facts indicate that the two resins which have almost the same ring size adsorbed metal ions with smaller cationic diameters except Ba(II) with different selectivity. Extraction experiments using DB18C6 and dichloromethane as the diluent showed different selectivity, *i.e.*, Zn(II) and Zr(IV) were extracted from HNO<sub>3</sub> of higher concentrations and Fe(III) was extracted from HCl of higher concentrations, respectively. No or very little extractions were observed for the other examined metal ions. Such a difference may result from the structure except the part of DB18C6, e.g. oxygen atoms of the hydroxyl group. Investigation of detailed adsorption mechanisms is the task in the future.

### ACKNOWLEDGMENT

This work was partially supported by the Grant-in-Aid for Scientific Research (B) (KAKENHI No. 23360423).

- [1] Ding X, Suzuki T, Nomura M, Kim HJ, Sugiyama Y, Fujii Y (2007) J Radioanal Nucl Chem 273:79-84
- [2] Hayasaka K, Kaneshiki T, Nomura M, Suzuki T, Fujii Y (2008) Prog Nucl Energy 50:510-513

## Cesium adsorption ability and stability of metal hexacyanoferrate irradiated with gamma-rays

Makoto Arisaka<sup>1</sup>, Masayuki Watanabe<sup>1</sup>, Manabu Ishizaki<sup>2</sup>, Masato Kurihara<sup>2</sup>, Rongzhi Chen<sup>3</sup>, Hisashi Tanaka<sup>3</sup>

<sup>1</sup>Research Group for Radiochemistry, Nuclear Science and Engineering Directorate, Japan Atomic Energy Agency

<sup>2</sup>Department of Material and Biological Chemistry, Faculty of Science, Yamagata University

<sup>3</sup>Nanosystem Research Institute, National Institute of Advanced Industrial Science and Technology

**Abstract** – The influence of irradiation with gamma-rays to metal hexacyanoferrate (MHCF: M = Fe, Cu or Ni), which is known as an adsorbent for selective adsorption of cesium (Cs) ion in solution, on Cs adsorption ability and stability was investigated in HNO<sub>3</sub> solutions. Under the adsorbed dose conditions (50 - 300 kGy), it was found that the MHCF is fully stable although the radiolytic decomposition of MHCF was slightly observed with an increase of the total adsorbed dose, which was confirmed by an increment of Fe, Cu or Ni concentration in HNO<sub>3</sub> solution after the irradiation. The weight percent of the metal in the solution to initial weight of MHCF was less than unity. Moreover, no change in composition of carbon, hydrogen and nitrogen in MHCF was observed. On the other hand, the distribution coefficients of Cs to the irradiated MHCF were independent of the total adsorbed dose. This indicates that the Cs adsorption ability was maintained under gamma-ray irradiation.

**Keywords** – cesium, metal hexacyanoferrate, gamma-irradiation, adsorption ability, stability

### I. INTRODUCTION

Metal hexacyanoferrate, MHCF, is known as an adsorbent for selective adsorption of cesium (Cs) ion in solutions. In nuclear industry, an application of MHCF (M = Fe, Cu or Ni) to recovery of Cs from high level radioactive waste has been studied. Recently, we reported an electrochemical application of MHCF for Cs recovery [1, 2].

It has been commonly accepted that the selectivity of MHCF to Cs ions are caused by regular lattice spaces surrounded by cyanide-bridged metals. However, the intrinsic mechanism of Cs ion adsorption still has not been made clear. So far, we have revealed that synthesized FeHCF, obtained as a charge-compensated salt (Fe<sup>III</sup><sub>4</sub>[Fe<sup>II</sup>(CN)<sub>6</sub>]<sub>3</sub>), has much higher Cs adsorption ability than that of commercially purchased FeHCF, i.e., prussian blue having ideal perfect lattice. The higher ability is attributed to the presence of lattice defect sites [3].

In this study, the influence of irradiation with gamma-rays to MHCF having lattice defect sites on Cs adsorption ability and stability in HNO<sub>3</sub> solutions was investigated for application of MHCF to practical Cs separation process.

### II. EXPERIMENTAL

Irradiated sample is a mixture of MHCF and HNO<sub>3</sub> solution. MHCF used in this study is as follows; Fe<sup>III</sup><sub>4</sub>[Fe<sup>II</sup>(CN)<sub>6</sub>]<sub>3</sub> (FeHCF), Cu<sup>II</sup><sub>3</sub>[Fe<sup>III</sup>(CN)<sub>6</sub>]<sub>2</sub> (CuHCF), Ni<sup>II</sup><sub>3</sub>[Fe<sup>III</sup>(CN)<sub>6</sub>]<sub>2</sub> (NiHCF).

Irradiation with gamma-rays was done at the Co-60 gamma ray irradiation facilities in Takasaki Advanced Radiation Research Institute of Japan Atomic Energy Agency. Samples in glass tubes were intermittently irradiated with gamma-rays from 1.0 × 10<sup>16</sup> Bq <sup>60</sup>Co source at an absorbed dose rate of 10 kGy h<sup>-1</sup> in air at room temperature for a maximum of 27 hours. A dose absorbed by each sample was corrected for an electron density. Absorbed doses were calibrated by a cellulose triacetate film dosimeter.

### III. RESULTS AND DISCUSSION

After gamma-ray irradiation, the HNO<sub>3</sub> solutions were separated from the sample by filtration. To evaluate the radiolytic degradation of MHCF, the amount of M (= Fe, Cu or Ni) in HNO<sub>3</sub> solution was determined by ICP-AES. The result for CuHCF was shown in Fig.1 as an example. It was found that the amounts of Fe and Cu increased slightly with an increase of the total adsorbed dose. The increase was attributed to radiolytic decomposition of CuHCF. Under the adsorbed dose conditions (50 - 300 kGy), the weight percent of Fe and Cu in the solutions to initial weight of CuHCF was less than 0.05%. From the viewpoint of usage for a long period, it suggests that the CuHCF is fully stable. Moreover, the composition of carbon, nitrogen and hydrogen in CuHCF is independent of the total adsorbed dose.

The Cs adsorption experiment was performed using the irradiated MHCF as adsorbent. The distribution coefficients of Cs into MHCF were independent of the total adsorbed dose. This indicates that the Cs adsorption ability was maintained under gamma-ray irradiation.

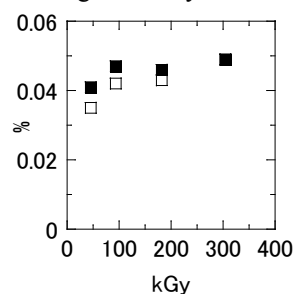


Fig.1 Weight percent of Fe (■) and Cu (□) to initial weight of CuHCF in HNO<sub>3</sub> solutions after the irradiation.

- [1] R. Chen et al., *Electrochem. Commun.*, **25**, 23-25 (2012).
- [2] R. Chen et al., *Electrochim. Acta*, **87**, 119-125 (2013).
- [3] M. Ishizaki et al., *Phys. Chem. Chem. Phys.*, submitted.

## Residual Actinides Separation from the DIAMEX/SANEX Secondary Waste and Decontamination of the Spent DIAMEX Solvent from the “Difficult-to-Strip” Elements

Jan John, Ferdinand Šebesta, Kamil V. Mareš, František Klimek, Martin Vlk

Czech Technical University in Prague, Department of Nuclear Chemistry, Brehova 7, 115 19 Prague, Czech Republic

### Abstract

One of the contemporary issues connected with the spent nuclear fuel is its reprocessing. The presence of long-lived radionuclides in the spent nuclear fuel is responsible for its long-term radiotoxicity. A decrease of the long-term radiotoxicity may be achieved by partitioning of minor actinoids with their subsequent transmutation. The main goals of the Partitioning and Transmutation are decreasing the time and the volume needed to store high radioactive waste, and a reduction of the hazard associated with the spent fuel and radioactive waste.

Among the processes under development for the Partitioning, the families of DIAMEX and SANEX processes studied by the broad international collaborations in Europe should be mentioned. This paper summarizes the results of the studies of two process-relevant issues of these processes – development of materials and processes for the residual actinides separation from the secondary waste, and decontamination of the spent organic solvent from the “difficult-to-strip” elements.

During the study of *materials and processes for residual actinides separation*, the behaviour of TODGA–PAN solid extractant in applications involving processing of large volumes of solutions was tested. In an experiment with  $5 \cdot 10^{-3}$  M  $\text{Eu}(\text{NO}_3)_3$  sorption from 3 M  $\text{HNO}_3$ , it was confirmed that no significant washing of TODGA from the solid extractant occurs even during the processing of more than 300 BV of the simulated waste. In another experiment, it was shown that the repeated sorption / elution cycles do not significantly influence the practical sorption capacity of the solid extractant.

For the mutual separation of An and Ln, pre-concentrated from the secondary waste streams, two novel solid extractants (SEXs) – the E5-C<sub>5</sub>BTBP[nitrobenzene] and E5-CyMe<sub>4</sub>BTBP(cyclohexanone) – were proposed and developed. With the E5-C<sub>5</sub>BTBP[nitrobenzene] SEX, very good separation of americium and europium was achieved. From a loaded column, 98.6 % of europium was washed in 8.7 BV of the eluant; the europium fraction contained only 0.3 % of the total amount of americium sorbed on the column. Then, americium was efficiently eluted with 0.5 M glycolic acid with pH ~ 4. In the total volume of the eluant used (3.1 BV), 99.7 % of americium was recovered; the americium fraction contained 1.4 % of the amount of europium originally sorbed on the column.

The E5-CyMe<sub>4</sub>BTBP(cyclohexanone) SEX was tested for the selective separation of An from Ln and other components of the simulant of a model secondary waste stream – PUREX raffinate without both the major and minor actinides. In batch experiments, the Am  $D_g$  was found to display a pronounced maximum at 1 M  $\text{HNO}_3$ . As

expected on the basis of the liquid-liquid extraction experiments, the kinetic studies revealed that the uptake of Am by the new SEX is much faster than for the similar materials with 1-octanol or nitrobenzene diluents.

Two dynamic experiments were performed with a column loaded by the new E5-CyMe<sub>4</sub>BTBP(cyclohexanone) SEX. The experiments revealed that the maximum achievable flow-rate for a negligible Am break-through is ~ 5 BV/hr for the given experimental set-up. An almost quantitative uptake of Am from a mixed carrier free Am – Eu solution in 1 M  $\text{HNO}_3$  was achieved during the treatment of all the ~ 60 BV of the feed; Am could be easily eluted from the column by 0.5 M HGlyc at pH = 4. The cumulative data for the experiment were: americium: recovery > 98 %, < 1 % of Eu in Am fraction; europium fraction: recovery > 99 %, contaminated by < 2 % of Am.

A serious obstacle in industrialization of the DIAMEX process is accumulation of “difficult-to-strip” elements (e.g. Ru, Y, Mo, Pd, Zr, Sr etc.) in the spent solvents. The aim of the study performed was to verify the possibility to decontaminate such spent solvents by solid sorbents. A problem in the pre-selection of potentially suitable sorbents turned out to be the fact that for the case of spent solvents and the metals like Ru or Pd, their speciation in organic phase is hardly predictable and may well be of non-ionic nature (colloids or pseudo-colloids containing reduced species etc.).

For the experimental part of this work, the DIAMEX solvent based on TODGA in kerosene / 1-octanol (5 vol.%) mixture was used as a reference system. An attempt to characterize speciation of the elements of interest in the simulant of the spent solvent was done by FTIR, ESI-MS, APCI-MS, and thin layer chromatography.

More than 50 solid sorbents of various nature, identified as potentially prospective, were obtained and their efficiency for the removal of Ru and Y from the simulated spent solvent was screened in batch contact experiments. The results obtained revealed that relatively high weight distribution ratios  $D_g$ , sufficient for the design of a process for quantitative separation of the contaminants from the solvent, can be achieved for some of the solid sorbents, e.g. Amberlyst A26 or Fe-EDA-SAMMS. For the prospective materials, sorption kinetics and sorption isotherms were determined. The materials with the highest sorption capacity were tested in dynamic column experiments. The results obtained in these tests will be presented in detail.

## Thorium based Molten Salt Fuel Cycle

Qing-nuan Li\*, Lan Zhang, Wen-xin Li, Guo-zhong Wu

*Shanghai Institute of applied physics, Chinese Academy of Sciences, Shanghai, China*

\*Corresponding author. Tel: +86 21 39194059. Email: liqingnuan@sinap.ac.cn

*Abstract –In 2011, Chinese Academy of Sciences (CAS), after discontinuing the research and development activity in nuclear energy for decades, started to implement Strategic Priority Research Program "Future Advanced Fission Nuclear Energy (FANE)". To perform this program, two sub-bases, the north and the south, were deployed in CAS. Shanghai Institute of applied physics (SINAP), as the south sub-base, is taking in charge of research and development of "Thorium-based Molten Salt Reactor Nuclear Energy System (TMSR)". According to this research plan, two kinds of molten salt nuclear reactors, i.e. 2MW uranium-thorium fluoride molten salt reactor (TMSR-LF1) and 2MW pebble bed fluoride salt-cooled high temperature reactor (TMSR-SF), will be designed and developed. Three fuel cycle models will also be implemented orderly, one-through fuel cycle on TMSR-SF, modified open fuel cycle on TMSR-SF and TMSR-LF, and closed fuel cycle on TMSR-LF.*

*Pyrochemical processing methods are judged to be the only*

*technologies for the fuel of MSRs with integrated reprocessing technologies. Because the liquid fuel for MSR is a mixture of molten fluorides, the fuel processing and reprocessing technologies planned are pyrochemical or pyrometallurgical techniques, which are based on separation of  $^{233}\text{U}$  and fission products in molten fluoride salt. Considering the special advantages of fluoride volatility and electrometallurgical techniques, a preliminary protocol based on closed fuel cycle has been proposed for the treatment of fuel from TMSR. The recycling techniques of fuels proposed in this protocol include fluoride volatilization, distillation of molten salt carriers, electrochemical deposition. The simple experimental devices for above techniques have been established, and the feasibility studies are ongoing in SINAP.*

*Keywords –TMSR; fuel cycle; reprocessing; pyrochemical techniques*

## Study on electrochemical behaviors of rare earth elements in FLINAK eutectic salt

Li-fang Tian, Wei Huang, Feng Jiang, Chang-feng She, Hai-yang Zheng, De-wu Long\*, Qing-nuan Li  
*Shanghai Institute of applied physics, Chinese Academy of Sciences, Shanghai, China*

\*Corresponding author. Tel: +86 21 39194677. Email: longdewu@sinap.ac.cn

*Abstract* –The reliable data on the electrochemical behaviors of key elements, such as lanthanides and actinides, is the foundation to assess the feasibility of application of the electrometallurgical method in recovery of the valuable actinides from fission products. For this purpose, the electrochemical behaviors of some rare earth elements (REs) in FLINAK eutectic salt (46.5 LiF - 11.5 NaF - 42.0 KF, mol %) at 550°C were studied, including samarium ( $\text{Sm}^{3+}$ ), europium ( $\text{Eu}^{3+}$ ), yttrium ( $\text{Y}^{3+}$ ), neodymium ( $\text{Nd}^{3+}$ ), and gadolinium ( $\text{Gd}^{3+}$ ) ions. The redox potentials, the number of exchanged electrons and the diffusion coefficients were determined by electrochemical transient techniques, such as cyclic voltammetry, square wave

voltammetry and chronopotentiometry. For  $\text{Y}^{3+}$ ,  $\text{Gd}^{3+}$  and  $\text{Nd}^{3+}$ , the results showed a three-electron reduction from the trivalent ions to metals near the potential of -1.95 V (or more negative) vs  $\text{Ni}/\text{NiF}_2$  reference electrode. However, no metallic Sm and Eu could be formed because only the reduction of their trivalent ions to divalent ions occurred in the electrochemical window of FLINAK eutectic salt. Further work on the electrochemical extraction of REs from FLINAK is ongoing.

*Keywords* –FLINAK eutectic salt; Electrochemical behavior; Rare earth elements;  $\text{Sm}^{3+}$ ,  $\text{Eu}^{3+}$ ,  $\text{Y}^{3+}$ ,  $\text{Nd}^{3+}$  and  $\text{Gd}^{3+}$

## Measurement of cosmogenic nuclides in meteorites by well-type Ge detector in Ogoya Underground Laboratory

### - Correction of coincidence sum effect for Al-26, Co-56, Na-22, and Co-60 -

Yasunori Hamajima  
Kanazawa Univ. LLRL.

**Abstract** – Two carbonaceous chondrite samples of about 3 ~ 5g, which have fallen in California on April 22, 2012, were measured by well-type Ge detector in Ogoya Underground Laboratory from May 21, 2012 for 30 days. Cosmogenic Co57, Cr51, Be7, Co58, Mn54, Co56, Co60, Na22, and Al26 were detected within the error of 20% or less. (That of Al26 is about 33%). The correction of coincidence sum effect would require for Al26, Co56, Na22 and Co60. The correction factors of these nuclides have been estimated from total efficiency as a function of gamma-ray energy.

**Keywords** – chondrite cosmogenic nuclides, well-type Ge detector, sum coincidence effect, total efficiency

#### I. INTRODUCTION

Measurement of cosmogenic nuclides in meteorite, usually several tens of g, has been carried out by using a coaxial Ge detector. In case of small samples, a well-type Ge detector will be advantageously, because of high counting efficiency. And also, the efficiency does not depend much on the sample shape and its height up to about 40 mm in the well. On the other hand, coincidence sum effect is not negligible small, for annihilation and cascade gamma-ray.

In this experiment, two carbonaceous chondrites were measured by a well-type Ge detector in Ogoya Underground Laboratory. The correction of coincidence sum effect would require for Al26, Co56, Na22 and Co60. The correction factors of these nuclides have not been estimated from peak to total ratio, but from total efficiency as a function of gamma-ray energy. In this paper, I will discuss the method of the correction that will be required for all Ge detectors.

#### II. EXPERIMENTAL

Two carbonaceous chondrite samples of about 3.15 g and 5.16 g, which have fallen in Sutter's Mill, California on April 22, 2012, were measured by well-type Ge detector in Ogoya Underground Laboratory from May 21, 2012 for 30 days. Counting efficiency was determined by JRIA mixing standard volume source (Cd109, Co57, Ce139, Cr51, Sr85, Cs137, Mn54, Y88, and Co60), Na22 source and natural Lu176.

#### III. RESULTS AND DISCUSSION

Cosmogenic Co57, Cr51, Be7, Co58, Mn54, Co56, Co60, Na22, and Al26 were detected within the error of 20% or less, (That of Al26 is about 33%). The corrections of coincidence sum effect with annihilation gamma-ray for Na22 and Al26, and with cascade gamma-ray for Co56 and Co60 have been required. Those of Na22 and Co60 are corrected by standard.

Total efficiency as a function of energy was estimated as following equation;

$$\varepsilon_1^* = \varepsilon_1(1-T_2), \quad (1)$$

here,  $\varepsilon_1^*$ ,  $\varepsilon_1$  and  $T_2$  are apparent peak and single peak, and total efficiency, respectively. Figure 1 shows the results of efficiency. The lower cross marks are apparent efficiencies, triangles and diamonds are single peak efficiencies, and upper line shows the total efficiency. The total efficiency curve as a function of energy leads to correction of coincidence sum effect of all of nuclides including those with extremely complicate decay scheme, such as Co56.

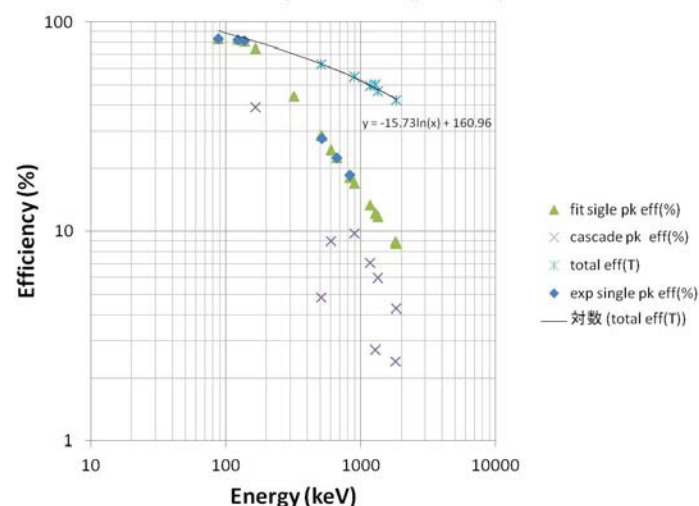


Figure 1. Efficiency of well Ge detector

I have estimated the apparent efficiency of 1809 keV of Al26 from the total efficiency of 511 keV of Na22. This estimated apparent efficiency (2.62%) was consistent with the result of Al26 standard AMS source (2.69%).

Correction of coincidence sum effect by total efficiency is practical.

## Development of Multipurpose Neutron Irradiation Apparatus at KUR

K. Takamiya<sup>1</sup>, Y. Yoshida<sup>2</sup>, H. Tanaka<sup>1</sup>, T. Fujii<sup>1</sup>, S. Fukutani<sup>1</sup>, T. Sano<sup>1</sup>, H. Yoshino<sup>1</sup>, Y. Inuma<sup>1</sup>,  
 R. Okumura<sup>1</sup>, S. Shibata<sup>1</sup>

<sup>1</sup>Research Reactor Institute, Kyoto University

<sup>2</sup>Graduate School of Engineering, Kyoto University

*Abstract – A new apparatus for various neutron irradiation experiments has been developed at Kyoto University Reactor. The apparatus can transport a larger space gently to a neutron irradiation field adjacent to the reactor core. Therefore, various samples, for examples, large and liquid samples can be irradiated with neutrons. And also samples can be joined to experimental instruments with tubes that realize online measurements and cyclic irradiation experiments. Since setting samples at different range from the reactor core can change irradiated neutron flux, various experiments by wide range neutron flux can be performed. Neutron activation analysis for large samples and liquid samples becomes enabled by these characteristics. In order to apply the apparatus effectively, the neutron flux and gamma-ray dose rate has been measured at various irradiation position. And changing spectrum of irradiating neutrons has been tried using polyethylene blocks as a moderator. The characteristics of the apparatus and the future plan are reported in this paper.*

*Keywords – Neutron Irradiation, Neutron Activation Analysis, Online Measurement*

### I. INTRODUCTION

Neutron irradiation experiments, such as neutron activation analysis and isotope production, have been performed using various apparatuses at research reactors. One of the most general apparatus is a pneumatic system, which transport small capsules enclosing samples from a laboratory to a neutron irradiation field near a reactor core. However, sizes and weights of samples are limited by the transporting capacity of capsules, and irradiating liquid samples is difficult for reactor safety in the pneumatic system. A new neutron irradiation apparatus has been developed at Kyoto University Reactor (KUR, 5 MW thermal power) to overcome such limitations.

### II. APPARATUS

The developed neutron irradiation apparatus transport samples loaded on a carrier from an experimental room adjacent to the reactor to nearby the reactor core through a horizontal beam hole (B-2) of KUR. The sample carrier has a capacity of about 6 cm × 6 cm × 30 cm and materials of up to 10 kg can be loaded. The carrier can be connected with plastic tubes to monitors and instruments placed at the experimental room at a distance of about 4 m from the reactor wall. Circulating liquid samples can be irradiated using pumps and the tube.

### III. MEASUREMENT OF NEUTRON FLUX AND GAMMA-RAY DOSE RATE

The neutron flux and gamma-ray dose rate at various position of irradiation field of the apparatus have been measured. The neutron flux was measured by activation method using gold wires. The gamma-ray dose rate was measured by thermo luminescence dosimeters. Both measurements were performed at the positions of 100 to 300 cm at intervals of 50 cm, and only neutron flux measurements were carried out additionally at 0 and 50 cm from the reactor-side edge. The results of the measurements are shown in Fig. 1. The wide range of neutron flux that is from 10<sup>8</sup> to 10<sup>12</sup> n/cm<sup>2</sup>/s was observed, which realizes various kinds of neutron irradiation experiments. The neutron flux and gamma-ray dose rate decrease as the range from the edge increases. The decreasing trend of neutron flux changes around the range at 100 cm because the sectional shape of the beam hole changes here. The uniformity of neutron flux was also measured by activation method using PET films<sup>1)</sup> at every 100 cm from the reactor-side edge, and it was found the neutron flux at a section is uniform.

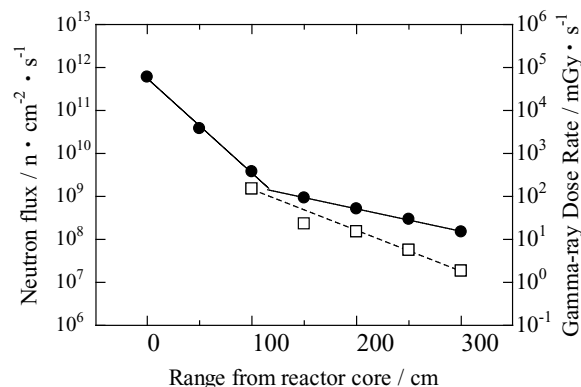


Fig. 1 Variation of neutron flux and gamma-ray dose rate at various positions in the B-2 beam hole.

[1] K. Takamiya, et al, Proc. Radiochim. Act 1 (2011) 63-66.

## Development of a new continuous dissolution apparatus with a hydrophobic membrane for superheavy element chemistry

K. Ooe<sup>1,2</sup>, K. Tsukada<sup>2</sup>, M. Asai<sup>2</sup>, T. K. Sato<sup>2</sup>, A. Toyoshima<sup>2</sup>, S. Miyashita<sup>2</sup>, Y. Nagame<sup>2</sup>, M. Schädel<sup>2</sup>, Y. Kaneya<sup>3</sup>, H. V. Lerum<sup>4</sup>, J. P. Omtvedt<sup>4</sup>, J. V. Kratz<sup>5</sup>, H. Haba<sup>6</sup>, A. Wada<sup>7</sup>, Y. Kitayama<sup>8</sup>

<sup>1</sup>Institute of Science and Technology, Niigata University

<sup>2</sup>Japan Atomic Energy Agency

<sup>3</sup>Graduate School of Science and Engineering, Ibaraki University

<sup>4</sup>Department of Chemistry, University of Oslo

<sup>5</sup>Institut für Kernchemie, Universität Mainz

<sup>6</sup>Nishina Center for Accelerator-Based Science, RIKEN

<sup>7</sup>Department of Chemistry, Tokyo Metropolitan University

<sup>8</sup>Graduate School of Natural Science and Technology, Kanazawa University

*Abstract* – A new continuous dissolution apparatus of gas-jet transported products was developed for superheavy element chemistry. The new apparatus has a hydrophobic membrane for separation of aqueous solution from the gas. We investigated the dissolution efficiencies with the apparatus for short-lived nuclides. In the conference, the dependence of the efficiencies on the aqueous- and gas-flow rates will be reported.

*Keywords* – Molybdenum, Tungsten, Continuous dissolution, Hydrophobic membrane

### I. INTRODUCTION

For investigation of the redox potentials of element 106, seaborgium (Sg), we plan to combine a flow electrolytic column (FEC) [1] with the rapid liquid-liquid extraction apparatus SISAK [2]. There is a technical problem in connection with these two apparatuses; a typical liquid flow rate for SISAK of ~24 mL/min is quite higher than that for FEC of ~1 mL/min. To successfully work with these two apparatuses, it is required to reduce the liquid flow rate of the SISAK system. However, the dissolution efficiency with the SISAK centrifuging degasser, which continuously dissolves gas-jet transported nuclear reaction products into an aqueous solution, drops with decreasing liquid flow rate. In the present study, therefore, we fabricated a completely new continuous dissolution apparatus which successfully works with a lower liquid flow rate.

### II. NEW CONTINUOUS DISSOLUTION APPARATUS WITH A HYDROPHOBIC MEMBRANE

Our new degasser utilizes a hydrophobic Teflon membrane to separate aqueous solution from gas (hereafter called membrane degasser, MDG). It continuously dissolves transported products by a gas-jet as follows. The mixture of gas and aqueous solution enters the MDG. Then, only the gas is sucked through the membrane with a vacuum pump. On the other hand, the aqueous solution does not pass through the hydrophobic membrane and elutes from an outlet.

### III. PERFORMANCE TEST

Dissolution efficiencies of gas-jet transported products were measured using the MDG. Short-lived isotopes, <sup>91m</sup>Mo ( $T_{1/2} = 65$  s), <sup>93m</sup>Mo ( $T_{1/2} = 6.9$  h), and <sup>176</sup>W ( $T_{1/2} = 2.5$  h), which are lighter homologues of Sg, were produced simultaneously in the <sup>89</sup>Y(<sup>7</sup>Li, 5n)<sup>91m</sup>Mo, <sup>89</sup>Y(<sup>7</sup>Li, 3n)<sup>93m</sup>Mo, and <sup>175</sup>Lu(<sup>7</sup>Li, 6n)<sup>176</sup>W reactions, respectively, at the JAEA tandem accelerator. Reaction products recoiling out of the targets were transported to the chemistry laboratory by a He/KCl gas-jet. The pressure in the target chamber was 130–140 kPa. The transported products were mixed with 1 M HCl/10<sup>-4</sup> M HF solution before entering the MDG. The carrier gas was then sucked through the membrane in the MDG, while the aqueous solution was eluted from the MDG. The aqueous sample was collected in a plastic bottle and was then measured with a Ge detector.

### IV. RESULTS AND DISCUSSION

The dissolution efficiencies for Mo and W at a He gas flow rate of 1.5 L/min were investigated as a function of aqueous flow rate. In the result, a dependence of the dissolution efficiencies on the half-life was observed; the efficiency for <sup>93m</sup>Mo ( $T_{1/2} = 6.9$  h) was higher than that for <sup>91m</sup>Mo ( $T_{1/2} = 65$  s) at aqueous flow rate of 0.6–6 mL/min. The dissolution efficiency for <sup>176</sup>W ( $T_{1/2} = 2.5$  h) was almost the same as that for <sup>93m</sup>Mo. Nevertheless, a dissolution efficiency of more than 80% was obtained for short-lived <sup>91m</sup>Mo at aqueous flow rates of 6–24 mL/min. A high yield of around 70% was also observed at flow rates of 1.8–3 mL/min. These results show that the MDG works with a lower aqueous flow rate than the previous SISAK degasser.

In the conference, the dependence of dissolution efficiency on the He gas flow rate will be also reported.

[1] A. Toyoshima et al., *Radiochim. Acta* **96**, 323-326 (2008).

[2] J. P. Omtvedt et al., *Eur. Phys. J. D* **45**, 91-97 (2007).

## Cross-section Measurements of High Energy Neutron-induced Reactions for Cu and Nb

K. Ninomiya<sup>1</sup>, T. Omoto<sup>1</sup>, R. Nakagaki<sup>1</sup>, N. Takahashi<sup>1</sup>, Y. Kasamatsu<sup>1</sup>, A. Shinohara<sup>1</sup>, S. Sekimoto<sup>2</sup>,  
 H. Yashima<sup>2</sup>, S. Shibata<sup>2</sup>, T. Shima<sup>3</sup>, H. Matsumura<sup>4</sup>, M. Hagiwara<sup>4</sup>, Y. Iwamoto<sup>5</sup>, D. Satoh<sup>5</sup>,

M. W. Caffee<sup>6</sup> and K. Nishiizumi<sup>7</sup>

<sup>1</sup> Graduate School of Science, Osaka University

<sup>2</sup> Research Reactor Institute, Kyoto University

<sup>3</sup> Research Center of Nuclear Physics, Osaka University

<sup>4</sup> Radiation Research Center, High Energy Accelerator Organization

<sup>5</sup> Nuclear Science and Engineering Directorate, Japan Atomic Energy Agency

<sup>6</sup> Department of Physics, Purdue University

<sup>7</sup> Space Sciences Laboratory, University of California

*Abstract* – High-energy monoenergetic neutron-induced reactions above 100 MeV have been studied for Cu and Nb targets. Excitation functions of short-lived radionuclides were determined by gamma-ray spectrometry. We also measured cross-sections by proton-induced reactions with the same energy range and compared with each other. The cross-sections of neutron-rich nuclides by neutron-induced reaction were systematically larger than these by proton-induced reactions.

*Keywords* – cross-section, neutron-induced reaction, monoenergetic neutron

The determination of cross-sections by neutron-induced nuclear reaction is very important in the view point of space and planetary sciences to investigate the history of cosmic ray exposure. These data are also required for estimation of residual radioactivities in accelerator facilities. However, cross section measurements in the energy region > 100 MeV have scarcely been undertaken because of the difficulty in obtaining high energy monoenergetic neutrons. So neutron-induced cross-sections are estimated by a proton-induced cross-section with the same energy or calculated using theoretical models.

Our group has developed a method for determination of high energy monoenergetic neutron cross-sections at the Research Center for Nuclear Physics (RCNP), Osaka University [1]. This method is based on two neutron irradiation experiments produced by <sup>7</sup>Li (p, n) <sup>7</sup>Be reaction with two different angles for the axis of the primary proton beam to correct the contribution of the low energy neutron reaction [2]. In this study, we performed cross-section measurements with 197, 287 and 386 MeV neutrons for Cu and Nb.

All neutron irradiation experiments were performed at N0 beam line in RCNP. We obtained quasi monoenergetic neutron fluence with 197, 287 and 386 MeV from 200, 300 and 392 MeV incident proton beam, respectively. The details of the experimental methods were written in elsewhere [1]. Produced short-lived radionuclides were identified by high-purity germanium detectors, and neutron cross-sections were determined. We also performed proton irradiation experiments at the same beam line to obtain proton cross sections with the same incident energies.

The excitation function of <sup>60</sup>Co for Cu target by proton- and neutron-induced reactions are shown in Figure 1 with the related literature values [2-5]. We found the cross-sections of neutron-rich nuclides such as <sup>60</sup>Co by neutron bombardment reactions have a tendency larger than these by proton reactions, and proton-rich nuclides such as <sup>58</sup>Co have an opposite trend. In the presentation, we will report the detail experimental cross-section data and discuss such cross-section difference by projectile using empirical models for nuclear spallation reactions.

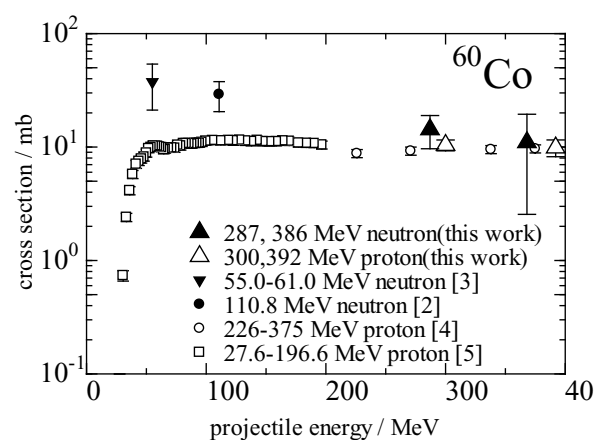


Figure 1. Excitation function for <sup>nat</sup>Cu (n, x) <sup>60</sup>Co and <sup>nat</sup>Cu (p, x) <sup>60</sup>Co reactions.

- [1] K. Ninomiya et. al., *Proc. Radiochim. Acta.*, **1**, 123 (2011)
- [2] J. M. Sisterson et. al., *Nucl. Instrum. Meth.*, **B240**, 617 (2005)
- [3] E. J. Kim et. al., *Nucl. Sci. Technol.*, **36**, 29 (1999)
- [4] Th. Shiekkel et. al., *Nucl. Instrum. Meth.*, **B114**, 91 (1996)
- [5] S. J. Mills et. al., *Appl. Radiat. Isot.*, **43**, 1019 (1992)

## Development of a rapid solvent extraction technique with flow injection analysis for superheavy element chemistry

T. Koyama<sup>1</sup>, N. Goto<sup>1</sup>, M. Murakami<sup>1,2</sup>, K. Ooe<sup>1</sup>, H. Haba<sup>2</sup>, J. Kaneya<sup>2</sup>, S. Goto<sup>1</sup>, and H. Kudo<sup>1</sup>,  
<sup>1</sup>Department of Chemistry, Faculty of Science, Niigata University, Niigata 950-2181, Japan  
<sup>2</sup>Nishina Center for Accelerator-Based Science, RIKEN, Saitama 351-0198, Japan

**Abstract** – A rapid solvent extraction system with flow injection analysis based on microchip chemistry was developed to study chemical properties of superheavy elements. Using this system, solvent extraction experiments of <sup>95g</sup>Nb were performed as model experiments of element 105, dubnium. The extraction equilibrium of Nb was reached in approximately 2 s. For on-line liquid-liquid phase separation, a phase separator was also developed by use of a membrane filter.

**Keywords** – microchip, flow injection analysis, liquid-liquid extraction, niobium, phase separation

### I. INTRODUCTION

For the chemical investigation of superheavy elements with atomic numbers  $\geq 104$ , a rapid chemical separation apparatus is needed because of their extremely short half-lives. As a rapid chemistry apparatus, we developed a solvent extraction system with flow injection analysis (FIA) based on microchip chemistry. This FIA system consists of solvent extraction and phase separation parts. In the solvent extraction part, aqueous and organic phases are mixed in a tube with a very small inner diameter of 100-200  $\mu\text{m}$ . Because of a large specific interfacial area and a short diffusion length in the tube, chemical equilibrium is rapidly reached. In the phase separation part, on-line liquid-liquid phase separation is achieved with a hydrophobic Teflon membrane. In this work, solvent extraction of 35-d <sup>95g</sup>Nb with this system was investigated as a model experiment of element 105, dubnium. The performance of the membrane phase separator was also investigated separately.

### II. EXPERIMENTAL

The <sup>95g</sup>Nb tracer was produced in the bombardment of a <sup>nat</sup>Zr target foil with a 14-MeV proton beam supplied by the RIKEN AVF cyclotron. The carrier-free <sup>95g</sup>Nb tracer was prepared by the chemical separation from the target using anion-exchange technique[1].

A schematic view of the FIA system is shown in Figure 1. Aqueous and organic solutions introduced in each reservoir coils were pumped with double-plunger pumps, and mixed in T-connector. As aqueous and organic solutions, 5 M HCl solution containing <sup>95g</sup>Nb tracer and 0.1 M Aliquat 336 in 1,2-dichloroethane solution were used, respectively. The mixture was fed into the extraction coil of poly(tetrafluoroethylene) (PTFE) tube of 0.17 mm i.d..

In order to examine the time needed for the extraction equilibrium, a flow rate and an extraction coil length were independently varied. After extraction, both solutions were collected in a polypropylene tube and two phases were separated by centrifugation. The separated two phases were then subjected to  $\gamma$ -ray spectrometry using a Ge detector. A batch extraction experiment of <sup>95g</sup>Nb using the same solutions was also performed to compare with these using FIA system.

Two phase separation experiment with the membrane phase separator was performed without radiotracers. The flow rate was 0.5 mL/min, and the length of extraction coil was 1 m. The phase separation was checked by weighing the separated solutions varying backpressure coil length in the aqueous outlet (0.17 mm i.d.). The length of outlet tube for organic phase was 10 cm.

### III. RESULTS AND DISCUSSION

In the batch experiment, shaking time of 40 min was needed to attain the extraction equilibrium. On the other hand, the equilibrium was reached within the contact time of 2 s using the FIA system.

In the two phase separation experiment, a clear phase separation was observed with back pressure coil length of about 5-15 cm. And the separator withstood 6 h continuous operation without replaining a membrane.

Therefore, this FIA system can be used for the solvent extraction experiments of superheavy elements with half-lives of several tens of seconds.

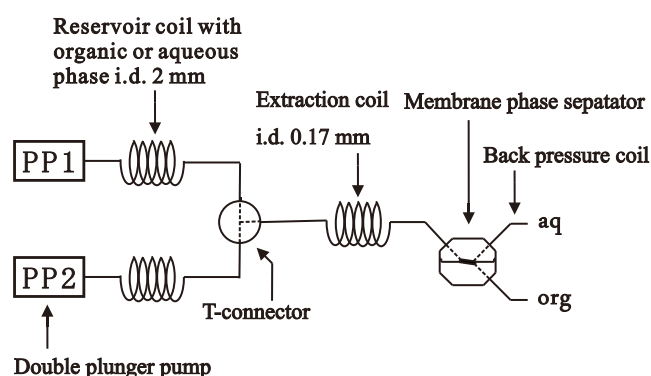


Figure 1. Schematic view of the FIA system

[1] Y.Kasamatsu et al, J. Nucl. Radiochem. Sci. 8, 69 (2007).

## Solid-liquid extraction of Mo and W by Aliquat 336 from HF and HCl solutions towards extraction chromatography experiments of Sg

Y. Komori<sup>1</sup>, T. Yokokita<sup>1</sup>, K. Toyomura<sup>1</sup>, K. Nakamura<sup>1</sup>, Y. Kasamatsu<sup>1</sup>, H. Haba<sup>2</sup>, J. Kanaya<sup>2</sup>,  
M. Huang<sup>2</sup>, Y. Kudou<sup>2</sup>, A. Toyoshima<sup>3</sup>, N. Takahashi<sup>1</sup>, A. Shinohara<sup>1</sup>

<sup>1</sup>Graduate School of Science, Osaka University

<sup>2</sup>Nishina Center for Accelerator-Based Science, RIKEN

<sup>3</sup>Advanced Science Research Center, Japan Atomic Energy Agency

*Abstract* – We are aiming to investigate complex formation properties of Sg with fluoride and chloride ions by extraction chromatography from HF and HCl solutions. We have selected Aliquat 336 as an extractant for anionic species in aqueous solution. In this study, solid-liquid extraction behaviors of carrier-free radiotracers Mo and W on Aliquat 336-loaded resin from 1–10 M HF and 0.1–10 M HCl solutions were investigated.

*Keywords* – Superheavy elements, Seaborgium (Sg), Molybdenum, Tungsten, Solid-liquid extraction

Element 106, seaborgium (Sg) is a group-6 element and the most stable oxidation state of Sg in aqueous solution is expected to be 6+ as with its lighter homologues, molybdenum (Mo) and tungsten (W). The pioneering aqueous chemical studies on complex formation and hydrolysis of Sg were carried out by Schädel et al. with cation-exchange chromatography in  $5 \times 10^{-4}$  M HF/0.1 M HNO<sub>3</sub> [1] and in HNO<sub>3</sub> [2] using a liquid chromatography apparatus, ARCA [3]. However, there are no reports on aqueous chemical studies of Sg following these works. It is extremely difficult to perform chemical experiments of Sg due to its low production rates and short half-lives of the isotope <sup>265</sup>Sg<sup>a,b</sup> ( $T_{1/2} = 8.5$  s/14.4 s [4]). To progress chemical studies of Sg, it is important to search for experimental systems and conditions applicable to the Sg experiment.

We are aiming to investigate complex formation properties of Sg with fluoride and chloride ions by extraction chromatography from HF and HCl solutions using ARCA. We have selected Aliquat 336 as an extractant for anionic species in aqueous solution. In this study, we have investigated solid-liquid extraction behaviors of carrier-free radiotracers Mo and W on Aliquat 336-loaded resin (Aliquat 336/CHP20Y resin) from 1–10 M HF and 0.1–10 M HCl solutions by a batch method. Extraction reaction kinetics was investigated and distribution coefficients ( $K_d$ ) of Mo and W were obtained as functions of HF and HCl concentrations. Extraction chromatography with ARCA was also performed in 2–8 M HCl solutions.

The short-lived isotopes <sup>90</sup>Mo ( $T_{1/2} = 5.7$  h) and <sup>173</sup>W ( $T_{1/2} = 7.6$  min) were produced using the RIKEN K70 AVF cyclotron. The  $K_d$  values of <sup>90</sup>Mo and <sup>173</sup>W were obtained as functions of HF and HCl concentrations by a batch method. Reaction products transported by the He/KCl gas-jet system were deposited on a Naflon sheet for 1 or 5 min. The collected reaction products were dissolved in 240  $\mu$ L of 0.1–10 M HCl (or 1–10 M HF) solutions. A 10–20 mg of

51.9-wt.% Aliquat 336/CHP20Y resin, 100  $\mu$ L of the HCl (or HF) solution containing <sup>90</sup>Mo and <sup>173</sup>W, 400  $\mu$ L of a certain concentration of HCl (or HF) solution were mixed in a PP tube. These samples were shaken for 5 min at 25 °C. Standard samples of <sup>90</sup>Mo and <sup>173</sup>W which contained no resin were also prepared and were shaken together with the resin-containing samples. After centrifugation, the aqueous phase was pipetted into another PP tube which was subjected to  $\gamma$ -ray spectrometry using a Ge detector to determine radioactivities of <sup>90</sup>Mo and <sup>173</sup>W. Reaction kinetics was also investigated at 25 °C by varying the shaking time to be 10 s, 5 min, and 10 min in each 4 M HF and 2, 6, and 10 M HCl solution. These batch solid-liquid extractions were also performed using the isotopes <sup>93m</sup>Mo ( $T_{1/2} = 6.9$  h) and <sup>181</sup>W ( $T_{1/2} = 121$  d).

The on-line extraction chromatography of Mo and W was performed with ARCA. The 51.9-wt.% Aliquat 336/CHP20Y resin was filled into the 1.0 mm i.d.  $\times$  3.5 mm microcolumn of ARCA. The reaction products transported by the gas-jet system were deposited on the collection site of ARCA for 5 min. After the collection, the reaction products attached to the KCl aerosols were dissolved with 2, 4, 6, and 8 M HCl solutions and were subsequently fed onto the column at a flow rate of 1 mL/min for 30 s. The effluents were collected in PP tubes for every 50 or 80  $\mu$ L. Then, the remaining <sup>90</sup>Mo and <sup>173</sup>W in the column were eluted with 400–500  $\mu$ L of 6 M HNO<sub>3</sub>/0.01 M HF solution and were collected in another PP tube. These fractions of the effluents were assayed by  $\gamma$ -ray spectrometry with a Ge detector.

It was found that extraction reaction kinetics in 4 M HF and 6 and 10 M HCl solutions is fast enough to reach the equilibrium state within approximately 10 s. In the extraction chromatography of Mo and W in 2–8 M HCl solutions with ARCA, the order of extractability was Mo > W, which is consistent with the order of the  $K_d$  values obtained in the batch experiment.

[1] M. Schädel et al., *Radiochim. Acta* **77**, 149 (1997).

[2] M. Schädel et al., *Radiochim. Acta* **83**, 163 (1998).

[3] M. Schädel et al., *Radiochim. Acta* **48**, 171 (1989).

[4] H. Haba et al., *Phys. Rev. C* **85**, 024611 (2012).

## Off-line isothermal gas chromatography of Zr and Hf compounds

Y. Oshimi, S. Goto, T. Taguchi, T. Tomitsuka, K. Ooe, H. Kudo

Department of Chemistry, Faculty of Science, Niigata University, Niigata 950-2181, Japan

**Abstract** – We obtained isothermal chromatographic data of Zr and Hf chlorides in a macro-scale (about  $10^{18}$  molecules). The adsorption enthalpies ( $\Delta H_a$ ) of the Zr and Hf chlorides on a quartz surface were determined to be about  $-78$  kJ/mol and  $-73$  kJ/mol, respectively, with analyzing these retention curves. The present  $\Delta H_a$  values are very different from the earlier work[1] in micro-scale, but agree with the volatility deduced from the vapor pressure in macro-scale.

**Keywords** – isothermal gas chromatography, zirconium and hafnium, adsorption enthalpy

### I. INTRODUCTION

Gas-phase chemical separation is one of the most utilized method to study chemical properties of superheavy elements. Using this method, adsorption enthalpies ( $\Delta H_a$ ) of volatile compounds of these elements can be determined based on their adsorption-desorption processes on a column surface. To clarify chemical property of element 104, Rf, gas chromatographic behavior of chlorides of Rf and its homologs, Zr and Hf, has been studied in the single-atom scale[1]. The reported sequence of volatility was  $Zr \geq Rf > Hf$ . But this volatile relation between Zr and Hf chlorides differ from volatile sequence requested from the macro-scale these vapor pressure curves[2]. Appropriate explanation about this difference has not been given until now.

In this study, we investigated gas chromatographic behavior of volatile compounds which were formed with thermal decomposition of oxychlorides of Zr and Hf.

### II. EXPERIMENTAL

In this work, stable isotopes of Zr and Hf were used to confirm whether the experimental technique is suitable before the experiments under tracer scale. Schematic view of the experimental equipment is shown Fig. 1. Quartz wool was impregnated with  $80 \mu\text{L}$  of  $ZrOCl_2$  or  $HfOCl_2$  water solution containing about  $2240 \mu\text{g}$  of Zr or Hf, and dried at  $200^\circ\text{C}$ . After drying, the wool was mounted in the reaction part which is composed of a quartz tube. Because the deposited oxychloride may be hydrate, the reaction part was heated at  $210^\circ\text{C}$  to remove hydration water completely. Then, heating the reaction part at above  $400^\circ\text{C}$ , the oxychlorides decomposed into nonvolatile dioxide and volatile tetrachloride, for example,



The produced tetrachloride was fed into an isothermal chromatographic quartz column with He gas ( $1.0$  L/min, purity  $\geq 99.999\%$ ). The tetrachloride compounds of Zr and

Hf through the column were collected in quartz wool plugged in a quartz tube connected just behind the column. An absorption photometry using arsenazo III was applied to determine the quantity of collected Zr and Hf.

### III. RESULT AND DISCUSSION

The passed-through yields for Zr and Hf were obtained as a function of the temperature of the isothermal column. Adsorption enthalpies were calculated using a simulation which is generally used in gas phase chemistry[3] and taken into account the fact that thermal decomposition reaction of the oxychlorides takes time. Adsorption enthalpies ( $\Delta H_a$ ) on a quartz surface for the Zr and Hf chlorides were obtained about  $-78$  kJ/mol and  $-73$  kJ/mol, respectively. The present  $\Delta H_a$  values for Hf are very different from the previously reported values. This result is consistent with the fact that  $\text{HfCl}_4$  is more volatile than  $\text{ZrCl}_4$ . Our results agree with the volatility deduced from the vapor pressure. Hence, there is some possibility that the Hf compound observed in the previous work was not pure tetrachloride.

In the symposium, the experiments and the results will be presented in more detail.

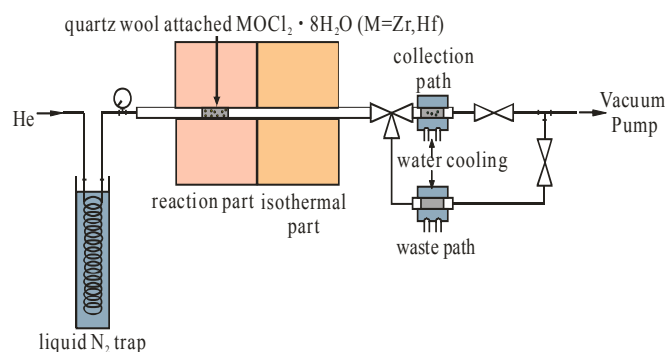


Fig. 1. schematic views of the experimental equipment

- [1] B. Kadkhodayan *et al.*, *Radiochim. Acta* **72**, 169 (1996)  
 [2] A. Türler *et al.*, *J. Alloys Comp* **271**, 287 (1998)  
 [3] I. Zvara, *Radiochim. Acta* **38**, 95 (1985).

## Chemical studies of Rf and Db in liquid-phases using automated rapid chemical separation apparatuses at JAEA

K. Tsukada<sup>1</sup>, A. Toyoshima<sup>1</sup>, M. Asai<sup>1</sup>, Y. Kasamatsu<sup>2</sup>, Z. J. Li<sup>3</sup>, Y. Ishii<sup>1</sup>, H. Haba<sup>4</sup>,  
T. K. Sato<sup>1</sup>, Y. Nagame<sup>1</sup>, M. Schädel<sup>1</sup>

<sup>1</sup> Japan Atomic Energy Agency, Tokai, Ibaraki 319-1195, Japan

<sup>2</sup> Graduate School of Science, Osaka University, Toyonaka, Osaka 560-0043, Japan

<sup>3</sup> Institute of High Energy Physics, Chinese Academy of Science, China

<sup>4</sup> Nishina Center for Accelerator Based Science, RIKEN, Wako, Saitama 351-0198, Japan

*Abstract* – We present chemical studies of element 104, rutherfordium (Rf), and element 105, dubnium (Db), in liquid-phases at JAEA. The experiments based on an atom-at-a-time scale have been performed using an automated rapid ion-exchange separation apparatuses, AIDA and AIDA-II. We have found interesting information for the complex formations of Rf with chloride, nitrate, sulfate, and fluoride ions and Db with fluoride ions in aqueous solutions.

*Keywords* – Superheavy elements, Rutherfordium, Dubnium, Ion-exchange separation, Complex formation with chloride, nitrate, sulfate and fluoride, Automated apparatus

### I. INTRODUCTION

Chemical studies of the superheavy elements are extremely challenging subjects in the fields of nuclear and radiochemistry [1]. An interesting aspect is to clarify basic chemical properties of these elements, such as ionic radii, complex formation and so on, and to elucidate the influence of relativistic effects on valence electrons of the superheavy elements [2]. The superheavy elements produced in heavy-ion-induced nuclear reactions at accelerators with low production rates. As the available isotopes are short-lived, they are usually available in quantities of only a few atoms at a time. Chemical characterization of the superheavy elements in liquid-phase experiments is performed by a partition method with single atoms. In order to have statistically significant results, it needs to repeat same experimental procedures over several hundred times within a cyclic time of a life-time of objective nuclides. In JAEA we have developed automated rapid chemical separation apparatuses to study chemical properties of Rf and Db in liquid-phases.

### II. EXPERIMENTAL

The nuclides <sup>261</sup>Rf ( $T_{1/2} = 78$  s) and <sup>262</sup>Db ( $T_{1/2} = 34$  s) were produced in the reactions <sup>248</sup>Cm(<sup>18</sup>O, 5n) and <sup>248</sup>Cm(<sup>19</sup>F, 5n), respectively, at the JAEA tandem accelerator. For characterization of Rf, we conducted cyclic discontinuous column chromatographic separations of short-lived nuclides in aqueous solutions and automated detection of  $\alpha$ -particles within a typical cycle of 1 min using the automated rapid ion-exchange separation apparatus AIDA (Automated Ion-exchange separation apparatus coupled with the Detection system for Alpha spectroscopy) [3] that consists of a modified computer-controlled liquid chromatography system ARCA

(Automated Rapid Chemistry Apparatus) [4] and an automated on-line  $\alpha$ -particle detection system. The experimental approach involves comparative studies on the chemical properties of the superheavy elements with those of respective lighter homologues and a pseudo-homologue. Thus, the experiments should be conducted together with the lighter homologues under identical conditions. To shorten the time for the sample preparation, the newly developed rapid ion-exchange apparatus AIDA-II was introduced. The apparatus is based on continuous sample collection and evaporation of effluents, and successive  $\alpha$ -particle measurement. The ion-exchange part is the same as that of AIDA. The AIDA-II was successfully applied for the chemical experiments with Db.

### III. RESULTS

We have investigated the ion-exchange chromatographic behaviors of Rf in HCl, HNO<sub>3</sub>, H<sub>2</sub>SO<sub>4</sub>/HNO<sub>3</sub>, HF/HNO<sub>3</sub> and HF solutions [3,5-10]. It has been found that the chemical properties of Rf are quite similar to those of the group-4 homologues, Zr and Hf, in the formation of chloride, nitrate, and sulfate complexes, although there are some differences in complexation strength between Rf and the lighter homologues [3,5,6]. In contrast, fluoride complex formation of Rf was found to be remarkably weaker than those of Zr and Hf studied over a wide range of fluoride ion concentrations [7,8]. The formation constant of [RfF<sub>6</sub>]<sup>2-</sup> was observed to be at least one order of magnitude smaller than those of [ZrF<sub>6</sub>]<sup>2-</sup> and [HfF<sub>6</sub>]<sup>2-</sup> [5]. This result on the fluoride complexation is in agreement with theoretical calculations including relativistic effects.

Anionic fluoride complexation of Db has also been studied [9,10]. The result demonstrates that the fluoride complex formation of Db is considerably different from that of the group-5 homologue Ta, while the behavior of Db is similar to that of the lighter homologue Nb [10].

- [1] M. Schädel (ed), The Chemistry of Superheavy Elements, Kluwer Academic Publishers, Dordrecht (2003).
- [2] Pyykkö P, Chem. Rev. 88, 563 (1988).
- [3] Y. Nagame *et al.*, J. Nucl. Radiochem. Sci. 3, 85 (2002).
- [4] M. Schädel *et al.*, Radiochim. Acta 48, 171(1989).
- [5] Y. Ishii *et al.*, Chem. Lett. 37, 288-289 (2008).
- [6] Z. J. Li *et al.*, Radiochim. Acta 100, 157 (2012).
- [7] H. Haba *et al.*, J. Am. Chem. Soc. 126, 5219 (2004).
- [8] A. Toyoshima *et al.*, Radiochim. Acta 96, 125-134 (2008).
- [9] K. Tsukada *et al.*, Radiochim. Acta 97, 83 (2009).
- [10] Y. Kasamatsu *et al.*, Chem. Lett. 38, 1084 (2009)

## Solvent extraction of hexavalent Mo and W using 4-isopropyltropolone (Hinokitiol) for Seaborgium (Sg) reduction experiment

S. Miyashita<sup>1</sup>, A. Toyoshima<sup>1</sup>, K. Ooe<sup>2</sup>, M. Asai<sup>1</sup>, T. K. Sato<sup>1</sup>, K. Tsukada<sup>1</sup>, Y. Nagame<sup>1</sup>, M. Schädel<sup>1</sup>, Y. Kaneya<sup>3</sup>, H. Haba<sup>4</sup>, J. Kanaya<sup>4</sup>, M. Huang<sup>4</sup>, Y. Kitayama<sup>5</sup>, A. Yokoyama<sup>5</sup>, A. Wada<sup>6</sup>, Y. Oura<sup>6</sup>, J. V. Kratz<sup>7</sup>, H. V. Lerum<sup>8</sup> and J. P. Omtvedt<sup>8</sup>

<sup>1</sup> Advanced Science Research Center, Japan Atomic Energy Agency, Tokai, Ibaraki 319-1195, Japan

<sup>2</sup> Institute of Science and Technology, Niigata University, Niigata 950-2181, Japan

<sup>3</sup> Graduate School of Science and Engineering, Ibaraki University, Mito, Ibaraki 310-8512, Japan

<sup>4</sup> Nishina Center for Accelerator-Based Science, RIKEN, Wako, Saitama 351-0198, Japan

<sup>5</sup> College and Institute of Science and Engineering, Kanazawa University, Kanazawa 920-1192, Japan

<sup>6</sup> Graduate School of Science and Engineering, Tokyo Metropolitan University, Hachioji, Tokyo 192-0397, Japan

<sup>7</sup> Institut für Kernchemie, Universität Mainz, 55128 Mainz, Germany

<sup>8</sup> Department of Chemistry, University of Oslo, P.O. Box 1033 - Blindern, NO-0315, Oslo, Norway

*Abstract* – Solvent extraction of <sup>93m</sup>Mo and <sup>176</sup>W using 4-isopropyltropolone (Hinokitiol, HT) was investigated. Extraction mechanism of Mo and W with HT was examined by slope analysis. The slope of the distribution ratio of Mo and W vs. [HT] in logarithmic scale are 1.88 and 1.54, respectively.

*Keywords* – Superheavy elements, Solvent extraction, Hinokitiol, Molybdenum, Tungsten, Seaborgium

### I. INTRODUCTION

For the determination of the reduction potentials of Seaborgium (Sg), we plan to carry out reduction experiments using a rapid and continuous system consisting of a flow electrolytic column (FEC) [1] combined with the liquid-liquid extraction apparatus SISAK [2]. The oxidation states of Sg will be chemically characterized its extraction behavior, and thus, rapid extraction enabling separation of Sg with different oxidation states is required. From our results of extraction-kinetics studies of <sup>181</sup>W as lighter homologue of Sg into toluene containing several extractants from 0.1 M HCl, we found that 4-isopropyltropolone (Hinokitiol, HT) has fast kinetics enough to be used together with SISAK. In the work presented here, we examined the extraction with HT of <sup>93m</sup>Mo ( $T_{1/2} = 6.9$  h) and <sup>176</sup>W ( $T_{1/2} = 2.5$  h) from a mixed solution 1.0 M HCl and 1.0 M LiCl solution.

### II. EXPERIMENTAL

<sup>93m</sup>Mo and <sup>176</sup>W were produced in the <sup>89</sup>Y(<sup>7</sup>Li, 3n)<sup>93m</sup>Mo and <sup>175</sup>Lu(<sup>7</sup>Li, 6n)<sup>176</sup>W reactions, respectively. <sup>89</sup>Y metallic foil and <sup>nat</sup>Lu<sub>2</sub>O<sub>3</sub> on Be foil were irradiated by a 62 MeV <sup>7</sup>Li beam from a tandem accelerator in JAEA. Reaction products recoiling out of the target foils were transported with a He/KCl gas-jet to the chemistry laboratory. Transported products were collected on a PTFE sheet, and dissolved by a mixed solution of 1.0 M HCl and 1.0 M LiCl. Then, a hydrogen ion concentration of solution was adjusted to desired ones. An organic phase was toluene containing a certain concentration of HT. 700  $\mu$ L of each aqueous and

organic phase was mixed in a vial and shaken for 600 s using a mechanical shaker. After shaking, two phases were separated by centrifugation for 30 s. 500  $\mu$ L of each aqueous and organic phase was taken into the vials. Radioactivity of both phases, 263 keV  $\gamma$ -rays of <sup>93m</sup>Mo and 102 keV  $\gamma$ -rays of <sup>176</sup>W, was detected by a Ge-detector. The distribution ratio ( $D$ ) was calculated by the ratio of radioactivity of <sup>93m</sup>Mo and <sup>176</sup>W in the two phases.

### III. RESULT AND DISCUSSION

Figure 1 show that the variation of the  $D$  value of Mo and W with respect to the concentration of HT in the organic phase ([HT]) when the concentration of hydrogen ion in the aqueous phase was 0.1 M. The  $D$  value of Mo and W increased by increasing of [HT]. The slopes of the  $D$  value of Mo and W vs. [HT] in logarithmic scale are 1.88 and 1.54, respectively. Those results indicated that Mo is formed an extractable complex with two HT molecules and W is one and/or two molecules.

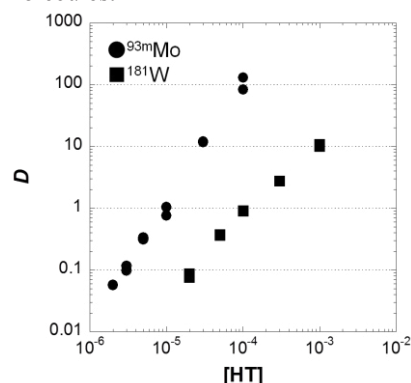


Figure 1. Variation of the distribution ratio of Mo and W vs. the concentration of HT in the organic phase when aqueous phase was 0.1 M HCl / 0.9 M LiCl. Closed cycles and squares represent Mo and W, respectively.

[1] A. Toyoshima et al., *Radiochim. Acta*, **2008**, 96, 323

[2] J. P. Omtvedt et al., *Eur. Phys. J. D*, **2007**, 45, 91

## Development of Surface Ionization Ion-source for Determination of the First Ionization Potentials of Heavy Actinides

Y. Kaneya<sup>1,2</sup>, T. K. Sato<sup>2</sup>, M. Asai<sup>2</sup>, K. Tsukada<sup>2</sup>, A. Toyoshima<sup>2</sup>, S. Miyashita<sup>2</sup>,  
Y. Nagame<sup>1,2</sup>, M. Schädel<sup>2</sup>, N. Sato<sup>3</sup>, K. Ooe<sup>4</sup>, A. Osa<sup>5</sup>, S. Ichikawa<sup>2,6</sup>, T. Stora<sup>7</sup>, J. V. Kratz<sup>8</sup>

<sup>1</sup>Graduate School of Science and Engineering, Ibaraki University, Mito, Ibaraki 310-8512, Japan

<sup>2</sup>Advanced Science Research Center, Japan Atomic Energy Agency, Tokai, Ibaraki 319-1195, Japan

<sup>3</sup>Nuclear Science and Engineering Directorate, Japan Atomic Energy Agency, Tokai, Ibaraki 319-1195, Japan

<sup>4</sup>Institute of Science and Technology, Niigata University, Niigata 950-2181, Japan

<sup>5</sup>Department of Research Reactor and Tandem Accelerator, Japan Atomic Energy Agency, Tokai, Ibaraki 319-1195, Japan

<sup>6</sup>Nishina Center for Accelerator Based Science, RIKEN, Wako, Saitama 351-0198, Japan

<sup>7</sup>ISOLDE, CERN, CH-1211 Geneva 23, Switzerland

<sup>8</sup>Institut für Kernchemie, Universität Mainz, 55128 Mainz, Germany

*Abstract* – We have developed a surface ionization ion-source as part of the JAEA-ISOL that is coupled to a He/CdI<sub>2</sub> gas-jet transport system to determine the first ionization potential (IP) of heavy actinides. Separation efficiencies of various short-lived lanthanide isotopes as homologs of actinides that were produced in nuclear reactions were measured with the present system. Obtained results demonstrate that the developed ion-source would be applicable to a measurement of the IP of heavy actinides.

*Keywords* – ionization potential ; lanthanide ; surface ionization ; ISOL

### I. INTRODUCTION

The first ionization potential (IP) directly reflects an atomic valence state influenced by relativistic effects which are significantly noticeable for heavy elements. Therefore information on the IP of heavy elements give us a better understanding of relativistic effects. IPs of the heavy actinides, however, have not been measured because of their short half-lives and low reaction cross-sections. In order to measure the IP of the heavy actinides, we need an apparatus which has higher separation efficiency.

In our previous work, we utilized a surface ionization ion-source coupled to a gas-jet transport system to study nuclear decay properties and spectroscopy of short-lived lanthanides and actinides [1]. Then, have improved the ion-source to measure the IP of lawrencium (Lr,  $Z = 103$ ) and other heavy actinides [2]. In this work, to evaluate a performance of the developed ion-source, we measured separation efficiencies of various short-lived lanthanide isotopes as homologs of actinides.

### II. EXPERIMENTAL

Short-lived lanthanide isotopes, <sup>140m</sup>Pm, <sup>142m</sup>Eu, <sup>143</sup>Eu, <sup>143m</sup>Sm, <sup>148m</sup>Tb, <sup>154</sup>Ho, <sup>157</sup>Er, and <sup>165</sup>Yb, were produced in the irradiation of a 67.9 MeV <sup>11</sup>B<sup>4+</sup> beam from the JAEA tandem accelerator on <sup>136</sup>Ce / <sup>141</sup>Pr / <sup>159</sup>Tb and <sup>142</sup>Nd / <sup>147</sup>Sm / <sup>nat</sup>Eu

targets. Short-lived <sup>168</sup>Lu was also produced in the reaction of <sup>162</sup>Dy with a <sup>11</sup>B<sup>4+</sup> beam. Nuclear reaction products recoiling from the targets were transported to

the ion-source by a He/CdI<sub>2</sub> gas-jet transport system. The products were ionized in the ion-source, accelerated with 30 kV, mass-separated at mass-separator in ISOL, and collected on the aluminized Mylar tape. The amounts of ions were determined by  $\gamma$ -ray measurement with a HP-Ge detector. To calculate separation efficiencies, nuclear reaction products transported from a target recoil chamber were directly collected on a separate catcher system.

### III. RESULTS AND DISCUSSION

Separation efficiencies of various short-lived lanthanide isotopes were measured. We compared the efficiencies obtained by the developed ion-source with those the previous ion-source. It is clearly found that the yields of all the isotopes with the developed ion-source are larger than those with the previous one. The separation efficiency of Sm, for example, was 12% with the developed ion-source while that with the previous ion-source was 3%. Furthermore, separation efficiency of Lu whose volatility would be similar to that of Lr was about 4.2%.

From this result, the present system has sufficient separation efficiencies to apply to measurement of the IP of the heavy actinides.

[1] S. Ichikawa, et al. Nucl. Instr. and Meth. A **374** (1996) 330.

[2] T. K. Sato, et al. Rev. Sci. Instrum. **84** (2013) 023304

## Comparison of the decay constants of $^{51}\text{Cr}$ with various valence states

H. Kikunaga<sup>1</sup>, K. Takamiya<sup>2</sup>, K. Hirose<sup>1\*</sup>, and T. Otsuki<sup>1</sup>

<sup>1</sup>Research Center for Electron Photon Science, Tohoku University

<sup>2</sup>Research Reactor Institute, Kyoto University

\*Present address: Advanced Science Research Center, Japan Atomic Energy Agency

*Abstract* – We have precisely measured the decay constants of  $^{51}\text{Cr}$  with 0, +3, and +6 valence states to investigate the effects of chemical states on the decay constants of  $^{51}\text{Cr}$ . The value of  $\{\lambda(\text{Cr}^{6+})-\lambda(\text{Cr}^0)\}/\lambda(\text{Cr}^0)$  was determined to be  $(5.3\pm 2.2)\times 10^{-4}$ , whereas the difference less than  $1.4\times 10^{-4}$  was observed for  $\{\lambda(\text{Cr}^{3+})-\lambda(\text{Cr}^0)\}/\lambda(\text{Cr}^0)$ . The results are compared with theoretical estimated values calculated with a simple model.

*Keywords* – half-life, decay constant, chemical effect

### I. INTRODUCTION

The decay constants of more than ten nuclides from  $^7\text{Be}$  to  $^{235}\text{U}^m$  were changed with changing environmental factors such as its chemical state [1]. Kakiuchi and Mukoyama reported the change in the decay constant of an electron capture decay nuclide  $^{51}\text{Cr}$  was observed between two chemical forms of  $\text{CrCl}_3$  and  $\text{Na}_2\text{CrO}_4$  [2]. They also estimated the value for the relative change in the decay constant among 0, +3, and +6 valence states with a simple theoretical model. The estimation shows that the relative change in the decay constant between 0 and +3 state is in the same degree as that between +3 and +6 state. In this study, the decay constants of  $^{51}\text{Cr}$  have been precisely measured with 0, +3, and +6 valence states to investigate the effects of chemical states on the decay constants of  $^{51}\text{Cr}$ .

### II. EXPERIMENTAL

The decay constants of  $^{51}\text{Cr}$  were measured for three chemical forms: chromium metal ( $\text{Cr}^0$ ), chromium (III) oxide  $\text{Cr}_2\text{O}_3$  ( $\text{Cr}^{3+}$ ), and potassium chromate  $\text{K}_2\text{CrO}_4$  ( $\text{Cr}^{6+}$ ). The isotopes  $^{51}\text{Cr}$  was produced in the  $^{nat}\text{Cr}(\gamma, xn)^{51}\text{Cr}$  reactions. Target materials were about 100 mg of Cr metal,  $\text{Cr}_2\text{O}_3$ , and potassium dichromate  $\text{K}_2\text{Cr}_2\text{O}_7$ . Each target material was sealed in a quartz tube and irradiated with bremsstrahlung photons. The irradiation was carried out with the electron linear accelerator at Tohoku University. The accelerator was operated at an electron energy of 30 MeV with a mean current of around 0.12 mA during the 8 h irradiation.

After the irradiation, the metal target and the  $\text{Cr}_2\text{O}_3$  target was maintained at  $800^\circ\text{C}$  for 5 h in argon and atmosphere, respectively, with an electric furnace. The  $\text{K}_2\text{Cr}_2\text{O}_7$  target irradiated was mixed into 250 mg of a non-radioactive  $\text{K}_2\text{Cr}_2\text{O}_7$  reagent and then dissolved in 3 mL of distilled water. The solution was heated on a hot-plate and alkalinized with potassium carbonate to produce  $\text{CrO}_4^{2-}$ . The solution was filtered and the filtrate was evaporated to less than 1 mL on a hot-plate. Finally, a  $\text{K}_2\text{CrO}_4$  sample was prepared by recrystallization from the solution. The metal,  $\text{Cr}_2\text{O}_3$ , and  $\text{K}_2\text{CrO}_4$  samples were placed in

aluminum cups separately and sealed with an epoxy resin adhesive.

These samples were measured in pairs of  $\text{Cr}_2\text{O}_3$ -metal and  $\text{K}_2\text{CrO}_4$ -metal to reduce the influence caused by the difference of detectors. The sample pairs were set in an automated sample changer [3] and alternately placed in front of a high-purity Ge detector at intervals of 7200 s. The procedures were repeated over at least 95 d. A  $^{137}\text{Cs}$  source was attached to near the Ge detector as a reference source to correct for influential factors for determination of half-life such as pile-up effect.

### III. RESULTS AND DISCUSSION

The decay constant of  $^{51}\text{Cr}$  was determined based on a reference source method [4]. The ratio  $R(t)$  is given by the following equation:

$$R(t) = C_{\text{sample}}^0(t) / C_{\text{ref}}^0(t), \quad (1)$$

where  $C_{\text{sample}}^0(t)$  and  $C_{\text{ref}}^0(t)$  are count rates of a sample and a reference source at the beginning of each data acquisition, respectively. The decay constant of the radionuclide in the sample  $\lambda_{\text{sample}}$  is described in the following equation:

$$\lambda_{\text{sample}} = \lambda_{\text{ref}} - a_{\text{slope}}, \quad (2)$$

where  $a_{\text{slope}}$  is the slope of the graph of  $\ln R(t)$  against time.  $\lambda_{\text{ref}}$  is the decay constant of the reference source, here that of  $^{137}\text{Cs}$ .

In the present work, the relative difference in the decay constant of  $^{51}\text{Cr}$ ,  $\{\lambda(\text{Cr}^{6+})-\lambda(\text{Cr}^0)\}/\lambda(\text{Cr}^0)$  was determined to be  $(5.3\pm 2.2)\times 10^{-4}$ . On the other hand, the difference less than  $1.4\times 10^{-4}$  at a 68% confidence level was observed for  $\{\lambda(\text{Cr}^{3+})-\lambda(\text{Cr}^0)\}/\lambda(\text{Cr}^0)$ . Kakiuchi and Mukoyama reported the value of  $(5.3\pm 2.1)\times 10^{-4}$  for  $\{\lambda(\text{Cr}^{6+})-\lambda(\text{Cr}^{3+})\}/\lambda(\text{Cr}^{3+})$  [2], which is in good agreement with the our value of  $\{\lambda(\text{Cr}^{6+})-\lambda(\text{Cr}^0)\}/\lambda(\text{Cr}^0)$ . In the presentation, we will discuss the comparison between the results obtained and the theoretical estimation with a simple model calculation [2].

- [1] G. T. Emery: Ann. Rev. Nucl. Sci. **22**, 165 (1972)
- [2] S. Kakiuchi and T. Mukoyama: Bull. Inst. Chem. Res., Kyoto Univ. **59**, 27 (1981)
- [3] T. Ohtsuki et al.: Phys. Rev. Lett. **93**, 112501 (2004)
- [4] H. Kikunaga et al.: Proc. Radiochim. Acta **1**, 113 (2011)

## Selective Separation of Strontium (II) from Nitric Acid Solution by a Macroporous Silica-based DtBuCH18C6 Adsorbent Modified with Surfactants

WU Yan, CHEN Zi, WEI Yuezhou\*

School of Nuclear Science and Engineering, Shanghai Jiao Tong University, China

\* Corresponding author. Tel.: +86-21-34207654. E-mail address: yzwei@sjtu.edu.cn.

*Keywords – Sr(II); silica-based support; crown ether; dodecyl benzenesulfonic acid; adsorption*

4',4'(5'')-di(*tert*-butylcyclohexano)-18-crown-6 (DtBuCH18C6), a macrocyclic crown ether, has the ability to extract Sr(II) due to the effective complexation of Sr(II) with hydrophilic crown ether, and a good match between the cavity of crown ether and ionic radius of Sr(II) ion. The SiO<sub>2</sub>-P support is a kind of inorganic material, which is prepared by synthesizing the SDB-copolymer inside the macroporous SiO<sub>2</sub> substrate. In this study, DtBuCH18C6 modified with dodecanol and dodecyl benzenesulfonic acid (DBS) was impregnated onto SiO<sub>2</sub>-P ((DtBuCH18C6+dodecanol + DBS)/SiO<sub>2</sub>-P). The equilibrium and kinetics of (DtBuCH18C6 + dodecanol + DBS)/SiO<sub>2</sub>-P for adsorption of Sr(II) were investigated under the conditions: varying the shaking times, HNO<sub>3</sub> concentration, and initial concentration of metal ions. The chemical stability of adsorbent in HNO<sub>3</sub> medium was examined by measuring the leakage of total organic carbon (TOC) in liquid phase. In order to confirm the effect of surfactant (DBS) on adsorption of Sr(II), the (DtBuCH18C6+dodecanol)/SiO<sub>2</sub>-P are synthesized for comparison. Compared to (DtBuCH18C6 + dodecanol)/SiO<sub>2</sub>-P, much higher distribution coefficient ( $K_d$ ) for (DtBuCH18C6+dodecanol + DBS)/SiO<sub>2</sub>-P was obtained in the range of 0.5 to 4 M nitric acid. The uptake rate of Sr(II) on (DtBuCH18C6+dodecanol + DBS)/SiO<sub>2</sub>-P in the presence of 0.5 M HNO<sub>3</sub> was attained equilibrium within 1 h, and the relatively large  $K_d$  value around  $4 \times 10^2$  cm<sup>3</sup>/g was obtained, which was improved 428 times compared with (DtBuCH18C6+dodecanol)/SiO<sub>2</sub>-P. The adsorbent had almost no uptake for other tested metals such as Cs(I), Na(I), K(I), Pd(II), Ru(III), Y(III), La(III), Nd(III) and Gd(III). The uptake of Sr(II) for (DtBuCH18C6+dodecanol + DBS)/SiO<sub>2</sub>-P was explained by Langmuir adsorption equation and the saturated amount of adsorption was estimated to be 0.24 mmol/g in 0.5 M HNO<sub>3</sub>. The leakage of TOC from the (DtBuCH18C6+dodecanol + DBS)/SiO<sub>2</sub>-P into aqueous phase were below 95 ppm even in 4 M HNO<sub>3</sub>. These findings suggest that the (DtBuCH18C6+dodecanol + DBS)/SiO<sub>2</sub>-P are stable in HNO<sub>3</sub> solution and would be effective for the selective separation of Sr(II) from radioactive liquid waste.

## Exploring the Synthesis and Characterization of Binary Technetium Chlorides and Bromides

Erik Johnstone<sup>1</sup>, Frederic Poineau<sup>1</sup>, Paul M. Forster<sup>1</sup>, Phillippe Weck,<sup>2</sup> Christos D. Malliakas<sup>3</sup>, Eunja Kim<sup>4</sup>, Mercouri G. Kanatzidis<sup>3</sup>, Brian L. Scott<sup>5</sup>, Alfred P. Sattelberger<sup>6</sup>, and Kenneth R. Czerwinski<sup>1</sup>

<sup>1</sup> Department of Chemistry, University of Nevada Las Vegas, Las Vegas, NV, USA.

<sup>2</sup> Sandia National Laboratories, Albuquerque, NM, USA.

<sup>3</sup> Department of Chemistry, Northwestern University, Evanston, IL, USA

<sup>4</sup> Department of Physics and Astronomy, University of Nevada Las Vegas, Las Vegas, NV, USA

<sup>5</sup> Materials Physics and Applications Division, Los Alamos National Laboratory, Los Alamos, NM, USA

<sup>6</sup> Energy Engineering and Systems Analysis Directorate, Argonne National Laboratory, Lemont, IL, USA.

**Keywords** –Technetium, solid-state synthesis, binary transition metal halides

Technetium ( $Z = 43$ ) is the lightest element on the periodic table with no stable isotopes. The most common isotope, <sup>99</sup>Tc ( $t_{1/2} = 2.1 \times 10^5$  a), is produced in nuclear fuels as a primary fission product in ~6% yield. In comparison to the surrounding stable transition metals, the fundamental chemistry of technetium has been poorly studied. An example of this is the binary halide system, which prior to 2008 consisted of 3 known compounds for technetium (TcF<sub>6</sub>, TcF<sub>5</sub>, and TcCl<sub>4</sub>), whereas for rhenium there have been 12 identified.[1] In this work low-valent binary technetium chlorides and bromides were synthesized in the solid state and analyzed using various physicochemical characterization methods including single-crystal and powder X-ray diffraction (XRD), IR spectroscopy, X-ray absorption fine structure (XAFS), and elemental analysis.

### A. Binary Technetium Chlorides

Technetium dichloride was synthesized from the stoichiometric reaction of the elements as a novel compound with a new structure-type containing a Tc-Tc triple bond. The  $\alpha$ -phase of technetium trichloride was prepared from the reaction of Tc<sub>2</sub>(O<sub>2</sub>CCH<sub>3</sub>)<sub>4</sub>Cl<sub>2</sub> with passing HCl(g) at elevated temperatures.[3] It is isostructural to ReCl<sub>3</sub> with a triangular Tc<sub>3</sub><sup>9+</sup> core structure containing Tc=Tc bonds. The  $\beta$ -phase of the trichloride was synthesized from the stoichiometric reaction of Tc metal with Cl<sub>2</sub>(g) and it exhibits structural characteristics comparable to the trichlorides of ruthenium and molybdenum.[4] Technetium tetrachloride was synthesized from the metal and excess chlorine gas in sealed Pyrex tubes and used as a starting material for decomposition to TcCl<sub>2</sub> and TcCl<sub>3</sub>. [5]

- [1] Schwochau, K. Technetium: Chemistry and Radiopharmaceutical Applications; Wiley-VCH: Weinheim, Germany, 2000.  
 [2] Poineau, F., et al., *J. Am. Chem. Soc.*, **2010**, *132*, 15864-15865.  
 [3] Poineau, F., et al. *J. Am. Chem. Soc.*, **2011**, *133*, 8814-8817.  
 [4] Poineau, F., et al. *Inorg. Chem.*, **2012**, *51*, 4915-4917.

### B. Binary Technetium Bromides

TcBr<sub>3</sub> has been prepared via two different methods: the stoichiometric reaction of the elements in sealed Pyrex tubes or by passing HBr(g) over Tc<sub>2</sub>(O<sub>2</sub>CCH<sub>3</sub>)<sub>4</sub>Cl<sub>2</sub> at elevated temperatures. Both synthetic methods yield the infinite-chain structure of distorted TcBr<sub>6</sub> face-sharing octahedra. Technetium tetrabromide was synthesized from the reaction of Tc metal with excess Br<sub>2</sub>(l).[6] It is isostructural to technetium tetrachloride, and similarly decomposes to lower-valent technetium bromides. When performed in Pyrex tubes the decomposition of the tetrabromide yields a novel trigonal prismatic Tc(II) bromide cluster, Na{[Tc<sub>6</sub>Br<sub>12</sub>]<sub>2</sub>Br}. [7]

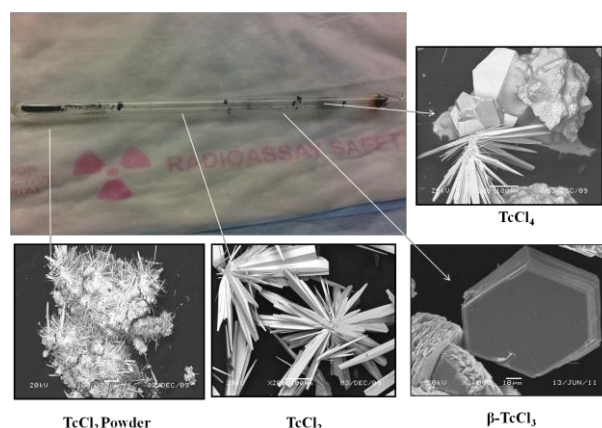


Figure 1. Binary Tc chlorides synthesized from the stoichiometric reaction of Tc metal and elemental chlorine in sealed tubes at elevated temperatures.

The low-valent technetium chlorides and bromides synthesized exhibit interesting chemical and physical properties, and may serve as potential synthetic inorganic and radiopharmaceutical precursors, as well as potential waste form-type material in the nuclear fuel cycle.

- [5] Johnstone, E. V., et al. *Inorg. Chem.* **2012**, *51*, 8462-8467.  
 [6] Poineau, F., et al. *J. Am. Chem. Soc.* **2009**, *131*, 910-911.  
 [7] Johnstone, E. V., et al., *Inorg. Chem.*, **2013**, *52*(10), 5660-5662.

## Solvent Extraction of Americium(III) and Europium(III) Using Hydroxyoctanoic Acid and N-heteroaromatic Compound

Moe Seike<sup>1</sup>, Mai Eguchi<sup>1</sup>, Atsushi Shinohara<sup>1</sup>, Takashi Yoshimura<sup>2</sup>

<sup>1</sup>Graduate School of Science, Osaka University

<sup>2</sup>Radioisotope Research Center, Osaka University

*Abstract* – Solvent extraction of Am(III) and Eu(III) was investigated using two hydroxyoctanoic acids including a new 2-hydroxy-2-trifluoromethyl-octanoic acid (**L1-CF<sub>3</sub>**) and two bidentate N-heteroaromatic compounds as extractants. The new lanthanide(III) complexes with bidentate N-heteroaromatic ligands were synthesized and the structures were characterized to eight- or nine-coordinate. Solvent extraction of Am(III) and Eu(III) in 1-octanol/acetic acid buffer solution was performed. The separation factor using **L1-CF<sub>3</sub>** was about 2.

*Keywords* – lanthanides, actinides, extraction, complex

### I. INTRODUCTION

It is recognized that separation of trivalent lanthanides and actinides is difficult because of their similar chemical properties. To date, various methods such as chromatography, extraction, and electrophoresis have been investigated. In the present study, we report on solvent extraction using hydroxyoctanoic acids and bidentate N-heterocyclic compounds that have  $\pi$  electron-accepting ability. We synthesized four extractants: two hydroxyoctanoic acids and two bidentate N-heteroaromatic ligands. The crystal structures of lanthanides(III) with bidentate N-heteroaromatic ligands were determined. The solvent extraction of <sup>152</sup>Eu and <sup>241</sup>Am was performed using hydroxyoctanoic acids and N-heteroaromatic compounds in 1-octanol/acetic acid.

### II. EXPERIMENTAL

Figure 1 shows the new 2-hydroxy-2-trifluoromethyl-octanoic acid (**L1-CF<sub>3</sub>**) and three known compounds, 2-hydroxy-2-methyl-octanoic acid (**L1-CH<sub>3</sub>**), 3-(2-pyrazinyl)-pyrazole (**L2-pz**), and 2-(1H-pyrazole-3-yl)-pyridine (**L2-py**)<sup>[1][2]</sup>. **L1-CF<sub>3</sub>** was synthesized by referring to the literature to prepare a hydroxycarboxylic acid with a long alkyl chain<sup>[3]</sup>.

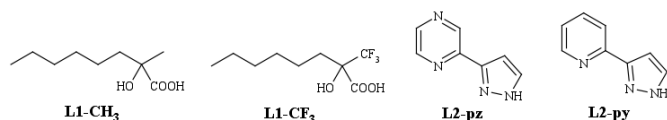


Figure 1. Extractants in this study.

Nineteen new lanthanide(III) complexes with **L2-pz** or **L2-py** were synthesized by the reactions of [Ln(H<sub>2</sub>O)<sub>9</sub>]

(CF<sub>3</sub>SO<sub>3</sub>)<sub>3</sub> (Ln = La, Nd, Sm, Eu, Gd, Tb, Dy, Ho, Er, Tm, Yb) with bidentate N-heteroaromatic ligands.

The solvent extraction experiment was performed in the acetic acid buffer solution or nitric acid solution as the aqueous phase and 1-octanol containing the extractant as the organic phase. The tube containing the same volume of two phases were shaken for 24 h in a thermostatic bath at 20 °C. The distribution ratios (*D*) of <sup>152</sup>Eu and <sup>241</sup>Am were determined by gamma-ray measurement of each phase by means of a germanium semi-conductor detector.

### III. RESULTS AND DISCUSSION

In the case of **L2-pz**, the three types of structures with eight- or nine-coordinate were obtained by changing the central lanthanide ions. The change of coordination number from nine to eight occurred between Gd and Ho. The eight-coordinate complexes exhibited intramolecular hydrogen bonds between triflate and **L2-pz**. In the case of **L2-py**, the eight-coordinated dinuclear complexes (Ln = Tb – Yb) were afforded.

The *D* value of 0.60 for Eu and that of 0.50 for Am were obtained at pH 4.8, when **L1-CH<sub>3</sub>** was used as the extractant. The *D* values were about 200 times larger than the values without extractant:  $D = 3.0 \times 10^{-3}$  for Eu and  $D = 2.2 \times 10^{-3}$  for Am. When **L1-CH<sub>3</sub>** and **L2-pz/L2-py** were added to the organic phase, the *D* values were not changed from the values using **L1-CH<sub>3</sub>** in the pH region of 4 - 5.5. This indicates that synergetic extraction of **L2-pz** and **L2-py** is not shown to be effective in this condition. This may cause that 1-octanol coordinates to Eu and Am to inhibit coordination of bidentate N-heteroaromatic ligands. In the case using only **L1-CF<sub>3</sub>**, the *D* value of 2.83 for Eu and that of 1.29 for Am were obtained at pH 5.0. The values are several times larger compared with those using **L1-CH<sub>3</sub>** under the similar condition. This would be due to decrease of *pK<sub>a</sub>* of extractant by substituting from CH<sub>3</sub> to CF<sub>3</sub> group. Namely, carboxylate proton in **L1-CF<sub>3</sub>** easily dissociates by the existence of electron-withdrawing CF<sub>3</sub> group. The value of separation factor of Eu and Am was about 2. In the case using **L1-CH<sub>3</sub>** or **L1-CF<sub>3</sub>** as the extractant, the log*D* values were increased with increasing pH. The slope values suggest that two **L1-CH<sub>3</sub>/L1-CF<sub>3</sub>** coordinate to the metal ions.

[1] T. Yabuuchi, *et al.*, *Chem. Pharm. Bull.*, **1999**, *47*, 684-686.

[2] K. L. V. Mann, *et al.*, *Polyhedron*, **1999**, *18*, 721-727.

[3] Blay, *et al.*, *Tetrahedron*, **2002**, *58*, 8565-8571.

## Stability of uranyl peroxy-carbonato complex ions in the presence of metal oxide in carbonate media

Dong-Yong Chung<sup>1</sup>, Min-Sung Park<sup>1</sup>, Keun-Young Lee<sup>1</sup>, Han-Beom Yang<sup>1</sup>, Eil-Hee Lee<sup>1</sup>, Kwang-Wook Kim<sup>1</sup>, Jei-Kwon Moon<sup>1</sup>

<sup>1</sup>Korea Atomic Energy Research Institute, Daedeok-daero 989-111, Yuseong-gu, Daejeon, 305-353, Republic of Korea

**Abstract** – This work studied the stability of uranyl peroxy carbonato complex ions in a carbonate solution with hydrogen peroxide in the presence of various metal oxides using absorption spectroscopy. The uranyl peroxy carbonato complex ions self-decomposed into uranyl triscarbonato complex ion in the presence of various metal oxides.

**Keywords** – Uranyl peroxy-carbonato complex, Hydrogen peroxide, Metal oxides, Absorption spectra

### I. INTRODUCTION

Uranium is selectively dissolved to form uranyl peroxy-carbonato complex ions,  $\text{UO}_2(\text{O}_2)_x(\text{CO}_3)_y^{2-2x-2y}$ , with a high solubility in carbonate solutions that contain hydrogen peroxide,  $\text{H}_2\text{O}_2$ . Recently, several carbonate-based processes have been studied and suggested to treat uranium-bearing waste and scraps generated during uranium fuel fabrication, uranium sludge and spent nuclear fuel [1–2]. Hydrogen peroxide is easily decomposed into water and oxygen in aqueous solutions. Additionally, uranyl peroxy-carbonato complex solution can self-decompose into uranyl triscarbonato complex ions,  $\text{UO}_2(\text{CO}_3)_3^{4-}$ , which are stable in a carbonate solution. When a carbonate-based uranium leaching process using hydrogen peroxide is applied to treat uranium-bearing compounds, the stability of the uranium peroxy-carbonato complex ions must be known to ensure that the concentration does not change during prolonged storage [3]. In this study, the decomposition of hydrogen peroxide and the stability characteristics of a uranium peroxy-carbonato complex in a carbonate solution were investigated in the presence of various metal oxides using absorption spectroscopy.

### II. RESULTS AND DISCUSSION

#### A. Decomposition of hydrogen peroxide in the presence of the metal oxides in a carbonate solution

The decomposition of  $\text{H}_2\text{O}_2$  in the presence of metal oxide follows first-order kinetics. The rate constants for  $\text{RuO}_2$ ,  $\text{PdO}$  and  $\text{MoO}_2$  are 115.1, 15.97 and 0.561  $\text{hr}^{-1}$ , respectively. Rate constants of other metal oxides are similar to the value, 0.292  $\text{hr}^{-1}$  of rate constant in a 0.5 M carbonate solution (Fig. 1). The decomposition rate of hydrogen peroxide in the presence of metal oxide powders was almost not affected with metal oxides except  $\text{RuO}_2$ ,  $\text{PdO}$  and  $\text{MoO}_2$ .

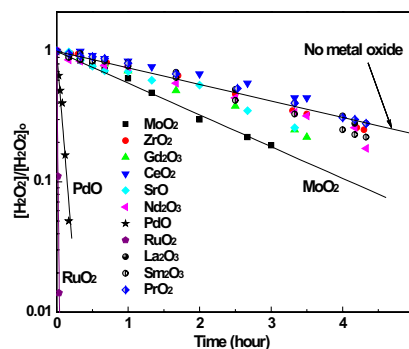


Fig. 1. Change of hydrogen peroxide concentration with time in the presence of each metal oxide at  $[\text{Na}_2\text{CO}_3]=0.5\text{M}$ ,  $[\text{H}_2\text{O}_2]=1.0\text{M}$ , amount of metal oxide = 0.5 g/L.

#### B. Stability of uranyl peroxy-carbonato complex ions in the presence of the metal oxides

When the absorbance of the uranyl peroxy-carbonato complex ion solutions were measured in the presence of  $\text{Ru}$  oxide powder. The features of the absorption spectrum of the uranyl peroxy-carbonato complex solution gradually disappeared with time. The peaks of uranyl triscarbonato complex appeared at 435, 448, and 462 nm (Fig. 2).

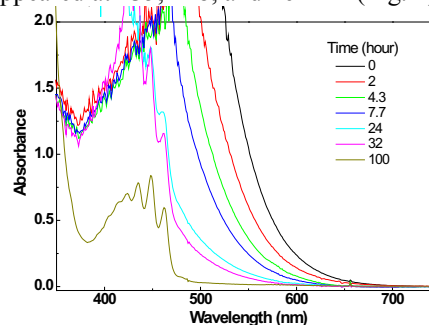


Fig. 2. Variation of absorption spectra of uranium dissolved solution ( $[\text{U}]=3.25 \times 10^{-2} \text{M}$ ) in the presence of  $\text{Ru}$  oxide powder in 0.5M  $\text{Na}_2\text{CO}_3$  solution (0.02g powder/30ml  $\text{Na}_2\text{CO}_3$  solution).

### ACKNOWLEDGMENT

This work was supported by the National Research Foundation of Korea grant funded by the Korea government (MSIP).

- [1] Kim, K.W.; Chung, D.Y.; Yang, H.B.; Lim, J.K.; Lee, E.H.; Song, K.C.; Song, K.S. *Nucl. Technol.*, **2009**, 166, 170–179.
- [2] Chung, D.Y.; Seo, H.S.; Lee, J.W.; Yang, H.B.; Lee, E.H.; Kim, K.W. *J. Radioanal. Nucl. Chem.*, **2010**, 284, 123–129.
- [3] Kim, K.W.; Lee, K.Y.; Chung, D.Y.; Lee, E.H.; Moon, J.K.; Shin, D.W. *J. Hazardous materials*, **2012**, 233–234, 213–218.

## Raman Spectroscopic Study on Uranyl and Neptunyl Complexes in Highly Concentrated Calcium Chloride

Toshiyuki Fujii<sup>1</sup>, Akihiro Uehara<sup>1</sup>, Yoshihiro Kitatsuji<sup>2</sup>, and Hajimu Yamana<sup>1</sup>

<sup>1</sup>Division of Nuclear Engineering Science, Research Reactor Institute, Kyoto University

<sup>2</sup>Nuclear Science and Engineering Directorate, Japan Atomic Energy Agency

**Abstract** – In order to understand the coordination circumstance of actinyl ions in concentrated inorganic electrolytes, U and Np species in concentrated CaCl<sub>2</sub> were analyzed by Raman spectrometry. The  $\nu_1$  symmetric vibrational frequency of actinyl ions was found to decrease with the increase of [CaCl<sub>2</sub>]. This may be attributable that hydration water molecules at the equatorial plane of actinyl were substituted by Cl<sup>-</sup> ions.

**Keywords** – Raman spectrometry, uranyl, neptunyl, calcium chloride, hydrate melt

Calcium chloride hexahydrate, CaCl<sub>2</sub>·6H<sub>2</sub>O, possesses a low melting point, 303 K. The melt is identical with 6.9 mol dm<sup>-3</sup> (M) CaCl<sub>2</sub> aqueous solution. The chemical properties of the hydrate melt are considered to be intermediate between aqueous solutions and anhydrous molten salts. A structural study on UO<sub>2</sub><sup>2+</sup> in 6.9 M CaCl<sub>2</sub> by X-ray absorption fine structure (EXAFS) analysis showed that the possible structure is UO<sub>2</sub>Cl<sub>2</sub>(H<sub>2</sub>O)<sub>2</sub> [1]. This is distinctly different from the hydrated UO<sub>2</sub><sup>2+</sup> in diluted acidic solutions, that is, UO<sub>2</sub>(H<sub>2</sub>O)<sub>5</sub><sup>2+</sup>. The coordination and redox behavior of UO<sub>2</sub><sup>2+</sup> in 6.9 M CaCl<sub>2</sub> has been studied by Raman spectrometry and by using electrochemical methods [2]. A change in the vibrational frequency of symmetrical stretching ( $\nu_1$ ) of UO<sub>2</sub><sup>2+</sup> suggested that the complexation between U(VI) and Cl<sup>-</sup> at the equatorial plane of UO<sub>2</sub><sup>2+</sup> depresses the bonding strength of U=O.

In the present study, we investigated the  $\nu_1$  frequencies of uranyl and neptunyl in highly concentrated calcium chlorides by Raman spectrometry. The  $\nu_1$  frequency was also estimated by using *ab initio* methods. The ligand exchange reaction between hydrated water and Cl<sup>-</sup> at the equatorial plane is discussed.

Calcium chloride dihydrate, CaCl<sub>2</sub>·2H<sub>2</sub>O, of analytical grade (Wako Pure Chemical Industries, Ltd.) was used without purification. Weighed amounts of CaCl<sub>2</sub>·2H<sub>2</sub>O and water were mixed for preparing various concentrations of CaCl<sub>2</sub>. As a starting material, U<sub>3</sub>O<sub>8</sub> was dissolved in 6 M HCl. A nitric acid solution containing Np was also used. A portion of these solutions was once dried by heating and then the CaCl<sub>2</sub> solution prepared was added. The concentration of U or Np was 0.01 M. The sample was taken in a quartz cell and the cell was sealed. Electronic absorption spectra of the samples were measured in the wavelength range from 340 to 1350 nm at 0.5 nm intervals by using an UV/Vis/NIR spectrophotometer (Shimadzu, UV-3100PC).

Raman spectra were measured by using a Raman spectrophotometer (NRS-3100, JASCO). A green laser with the wavelength of 531.9 nm was used at the output power of 57.6 mW. The measurement interval of a charge-coupled device (CCD) detector was set to be every 0.3 cm<sup>-1</sup>.

The operations of each 3-seconds measurement were accumulated by 25 times. The experimental temperature was 298 K.

The  $\nu_1$  frequency of UO<sub>2</sub><sup>2+</sup> in 6.8 M CaCl<sub>2</sub> was found at ~855 cm<sup>-1</sup>. This agreed with the literature value [2]. With the decrease of water content in the CaCl<sub>2</sub> system, the  $\nu_1$  frequency decreased to the extent of ~7 cm<sup>-1</sup>. This suggests that hydration water molecules at the equatorial plane of uranyl were substituted by Cl<sup>-</sup> ions, which depressed the bonding strength of U=O.

The CaCl<sub>2</sub> system containing Np showed a specific Raman spectrum. Figure 1 shows the Raman spectrum of 0.01 M Np in 6.8 M CaCl<sub>2</sub>. From electronic absorption spectrum obtained, it was suggested that Np(VI) and Np(V) coexist in the system. The Raman peaks shown in Fig. 1 are hence attributable to  $\nu_1$  vibrational modes of NpO<sub>2</sub><sup>2+</sup> and NpO<sub>2</sub><sup>+</sup> complexes. Similar to the case of U, the Raman peak at ~835 cm<sup>-1</sup> shifted by changing water content of the system. This may also suggest that the ligand exchange between hydrated water and Cl<sup>-</sup> at the equatorial plane of neptunyl occurs.

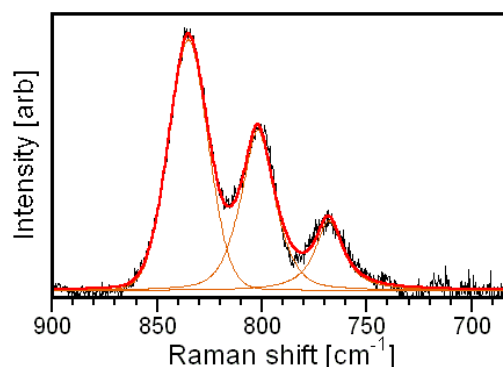


Fig. 1. Raman spectrum of 0.01 M Np in 6.8 M CaCl<sub>2</sub>. The spectrum was decomposed into three Raman peaks by Gaussian/Lorentzian sum function.

[1] A. Uehara et al., NEA/NSC/DOC (2009) 15.

[2] A. Uehara et al., J. Appl. Electrochem., 42, 455 (2012).

## Electrode Reaction of Actinide Ions in a Weak Acidic Solution

Yoshihiro Kitatsuji<sup>1</sup>, Haruyoshi Otobe<sup>1</sup>, Takaumi Kimura<sup>1</sup>  
<sup>1</sup>Nuclear Science and Engineering Directorate, Japan Atomic Energy Agency

*Abstract* – Electrode reactions of U(VI) in weak acid solution are different from those in acid solution. Electrolysis of U(VI) can produce UO<sub>2</sub> fine crystal, not hydrolyzed U(IV). The formed UO<sub>2</sub> is easily deposited on an electrode and is electrode active.

*Keywords* – actinide ions, redox, weak acidic solution, aggregate

### I. INTRODUCTION

Actinide (An) ions such as uranium, neptunium and plutonium exist as ionic species of trivalent to hexavalent in an aqueous solution. Most of studies concerning redox of actinide ions by electrochemical method have focused on acidic solution in which An ions are dissolving stably. However, redox behaviors of actinide ions in weak acid or neutral solution are expected to be different from that in an acid solution, because redox of AnO<sub>2</sub><sup>+</sup>/An<sup>4+</sup> is affected by H<sup>+</sup>. Also hydrolysis has a great influence on the redox. In this paper, the authors report unique electrode reaction of actinide ions concerning an aggregation in a weak acidic solution.

### II. EXPERIMENTAL

Voltammetry was carried out by using a microelectrode of Au of 25 μm in diameter. Controlled potential difference electrolysis was performed with an Au gauze electrode (80 mesh, 60 × 20 mm) as working electrode to bulk electrolysis. A Pt wire and a silver-silver chloride electrode with 1 M LiCl was employed as a counter electrode and a reference electrode, respectively.

Oxidation states of actinide ions in sample solutions after electrolysis were identified based on UV/VIS adsorption spectrometry. The aggregate produced in the electrolysis sample solution was analyzed by X-ray diffraction after filtration.

### III. RESULTS AND DISCUSSION

Reduction of U(VI) ion in a solution of pH 2 to 5 was investigated by cyclic voltammetry (CV) with an Au microelectrode. Reduction currents of U(VI) to U(V) were observed at ca. -0.2 V clearly (see, Fig. 1, curve a). When CV measurements were repeated, oxidation peak current was observed at +0.2 V in a first cycle of CV for a solution of pH 4. In order to investigate this oxidation current, stripping voltammetry was applied. Clear adsorption current for oxidation of species produced by preelectrolysis at -0.3 V was observed. Similar adsorption behavior at carbon electrode had been reported by Duber previously [1], and they concluded that oxidation current was attributable to oxidation of U(V) adsorbed on the electrode.

U(V) ion was prepared from U(VI) by bulk electrolysis at -0.35 V. U(V) solution showed the peak of absorbance at 260 nm on UV/VIS spectrum. U(V) in a solution of pH 2.9 was stable for about 30 min. Then the peak at 260 nm became smaller, and the absorbance at all range of measurement was increased gradually. These results suggest the formation of aggregate. Only oxidation current of U(V) to U(VI) at -0.2 V was observed (curve b) by CV measurement immediately after preparation of U(V), but CV curve was changed after aggregation (curve c): large oxidation current peak was observed at +0.15 V and +0.3 V in a first cycle of CV measurement; oxidation current of U(V) was negligible; reduction current of U(VI) is about half amount of the initial solution (cf. curves a and c). The aggregate was prepared by electrolysis at -0.35 V in a solution of pH 2.9, and fluorite structure of UO<sub>2</sub> was determined by XRD analysis.

The authors conclude that U(IV) produced via disproportionation of U(V) aggregates to form UO<sub>2</sub>. This fine UO<sub>2</sub> is easily deposited on electrode surface and is electrode active to oxidize.

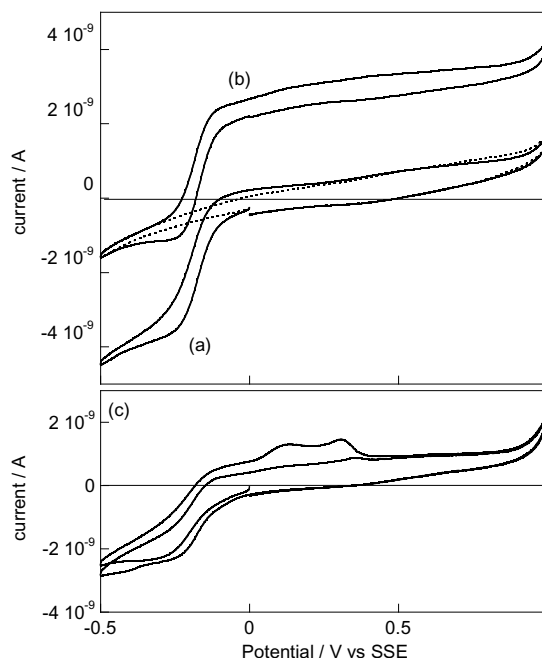


Fig 1. Cyclic voltammograms of 1mM U in a weak acid solution. (a) U(VI), (b) U(V) immediately after preparation, (c) U(V) solution after 60 min. broken line are background current.

### REFERENCE

- [1] R. E. Dueber, A. M. Bond, P. G. Dickens, J. Electrochem. Soc., 141(1994)311.

## Biominingalization of uraninite and uranyl phosphate controlled by organic acids

Yoshinori Suzuki<sup>1</sup>, Naofumi Kozai<sup>2</sup>, Toshihiko Ohnuki<sup>2</sup>

<sup>1</sup> Graduate School of Bionics, Tokyo University of Technology, 1404-1 Katakura-cho, Hachioji, Tokyo 192-0982, Japan

<sup>2</sup> Advanced Research Center, Japan Atomic Energy Agency, Tokai, Ibaraki 319-1195, Japan

**Abstract** – Biominingalization of uraninite ( $UO_2$ ) and uranyl phosphate minerals are both able to decrease the mobility of uranium in the environment. We examined biominingalization of  $UO_2$  and uranyl phosphate by *Shewanella putrefaciens* in the basic medium containing lactate as an electron donor,  $\beta$ -glycerolphosphate as a phosphorous source, and uranyl nitrate in the absence and presence of weak or strong complexing organic acids (WCOA or SCOA) under an anaerobic condition. In the basic medium, only biominingalization of  $UO_2$  was observed because of rapid reduction of U(VI). Biominingalization of  $UO_2$  and uranyl phosphate occurred in the media with WCOA, however the no biominingalization was occurred in the presence of SCOA. It is thought that formation of stable U(VI)-, and U(IV)-organic complexes prevents the biominingalization. These finding suggest that coexisting organic acids control the biominingalization of  $UO_2$  and uranyl phosphate minerals by microorganisms.

**Keywords** – biominingalization, U-organic complexes, *Shewanella putrefaciens*, effects of organic acids

### I. INTRODUCTION

Uranium is a radionuclide found in high- and low-level radioactive wastes. Its safe geological disposal requires an understanding of the migration behavior of uranium in the environment. Biominingalization of uranium is one of the immobilization mechanisms. The formation of uraninite ( $UO_2$ ) through bioreduction of U(VI) and of uranyl phosphate minerals by microbial phosphate release are well known biominingalization. These two mechanisms have been investigated individually. However, there is the possibility that the two types of biominingalization compete each other in the environment. In this study, we examined the biominingalization of  $UO_2$  and uranyl phosphate by *Shewanella putrefaciens* under the conditions they compete. It has been reported that the presence of organic acids, which form complexes with uranium, affects the reductive mineralization of  $UO_2$  [1]. Therefore we focused on the effects of weak and strong complexing organic acids (WCOA and SCOA) on the biominingalization of uranium.

### II. EXPERIMENTAL

*Shewanella putrefaciens*, an iron-reducing bacterium, was incubated in the basic medium (pH 7.0), which contained 50 mM sodium lactate as an electron donor, 1 mM uranyl nitrate as an electron acceptor, and 0.44 mM  $\beta$ -glycerolphosphate as a phosphorous source, and mineral salts under an anaerobic condition at 30°C. To evaluate the effects of organic acids, 100 mM WCOA (acetic, or adipic acid), or SCOA (oxalic, tartaric, citric acid or EDTA) were added to the basic media and the cells were incubated in the same way. Aliquots of medium were periodically

withdrawn. The uranium concentrations and UV-vis spectra of the aqueous phases were measured. The new solid phases formed in the media were analyzed by SEM-EDS.

### III. RESULTS AND DISCUSSION

The time courses of the total aqueous uranium during the incubation are shown in Fig. 1. In the basic medium, uranium in the aqueous phases decreased rapidly and new solid phases were observed. In the basic media with WCOA, the decreasing rates of aqueous uranium were slower than that in the basic medium with no WCOA. New solid phases also formed in these media. No decrease of uranium in solution was observed the media with SOCA. The UV-Vis spectra of the medium with SOCA showed that U(VI) was reduced to U(IV) and formed aqueous complexes with SOCA. This indicates that the stable complex formation inhibits the precipitation of uranium. SEM-EDS and UV-Vis analyses of the new solid phases indicated the solid phases in the basic medium were mainly  $UO_2$ , and those in the media with WCOA were mixture of  $UO_2$  and uranyl phosphate. It was thought that the addition of WCOA decreased the reduction rate of U(VI), and allowed U(VI) to react with inorganic phosphate released by biodegradation of  $\beta$ -glycerolphosphate. Uranyl phosphate was not formed in the absence of  $\beta$ -glycerolphosphate. These findings suggest that the biominingalization behavior of uranium is highly affected by organic acids and their complexing abilities with uranium.

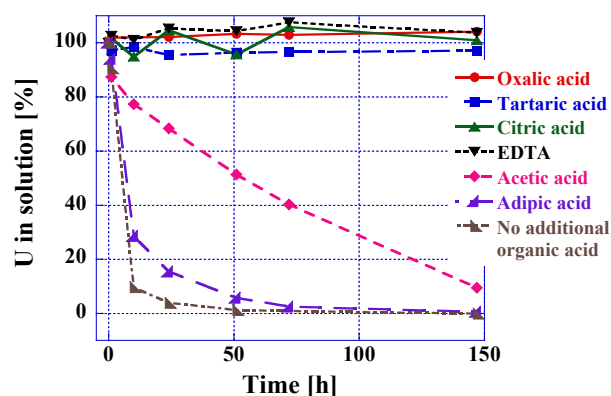


Fig. 1. Time course of aqueous uranium in the media with various organic acids during incubation with *S. putrefaciens*.

### REFERENCES

- [1] Y. Suzuki, K. Tanaka, N. Kozai, T. Ohnuki, Geomicrobiol. J., 2008, 27(3), 245-250.

## Comparison of the spectroscopic characteristics of uranium species when U(III) in a LiCl-KCl molten salt is leached out with water and ionic liquid

Hee-Jung Im, Kyuseok Song

Nuclear Chemistry Research Division, Korea Atomic Energy Research Institute,  
150 Deokjin-dong, Yuseong-gu, Deajeon 305-353, Republic of Korea

*Abstract* – U(III) in a LiCl-KCl molten salt was first dissolved into an appropriate ionic liquid and water, and identification and determination of the uranium (U) in the LiCl-KCl molten salt were performed using spectroscopic methods. The U(III) in LiCl-KCl molten salt showed the tendency of stable status in ionic liquid and unstable status in water. Based on the experimental data, a predictive theory of the factors involved in the process is discussed.

*Keywords* – Uranium species, LiCl-KCl eutectic, Molten salt, Ionic liquid, Spectroscopy

### I. INTRODUCTION

As a type of spent nuclear fuel treatment, the pyrochemical process is well known for its non-proliferation of nuclear fuel cycles, separation of long-term radioactive nuclides during processing, the recovery of uranium for re-use as a nuclear fuel, and a significant volume-reduction of high-level wastes. After the complete pyrochemical processing is finished, a remaining small amount of salt waste, apart from the salt for recycling purposes, will be stored for the long term and is composed of some actinides and lanthanide species (mainly existing as 3+ ions) dissolved in molten salt. In this study, we investigate the behavior of U(III) dissolved in LiCl-KCl molten salt, especially when U(III) is leached out with ionic liquid compared to water, to obtain better understandable information for long-term waste salt storage. An ionic liquid system, which is similar to the environment of a slushy micelle system in a ground water migration, was considered as a medium for a convenient bench-scale experiment, and the results were compared to those from the water medium for U(III) behavior in different media.

### II. EXPERIMENTAL

A U(III) in LiCl-KCl molten salt was prepared from the reaction of uranium metal with cadmium chloride in a LiCl-KCl mixture (44 wt.% LiCl) at 450 °C in an Ar-atmosphere glove box.

### III. RESULTS AND DISCUSSION

Absorption spectra of the LiCl-KCl molten salt in an ionic liquid and UCl<sub>3</sub> in the LiCl-KCl molten salt in the ionic liquid are compared. The peaks at 460 nm and 553 nm are from U(III).

However, the absorption spectrum of UCl<sub>3</sub> in the LiCl-KCl molten salt with water was very different to the spectrum of UCl<sub>3</sub> in the LiCl-KCl molten salt in the ionic liquid. As it is well known that U(III) is easily oxidized into

U(VI) during procedures, a characteristic peak of U(VI) was observed at 411 nm, and the color of the solution was changed from pale purple to yellow immediately after the solid was dissolved in water. Although at the preparation of samples, the U(III) was solidified on the LiCl-KCl molten salt from 450°C to room temperature, the solidified U(III) was oxidized immediately in the presence of water.

The excitation spectrum of UCl<sub>3</sub> in a LiCl-KCl molten salt is shown in an ionic liquid by emission at 641 nm, and the spectrum was compared to an excitation spectrum of an ionic liquid only. There were specific peaks at 515 nm and 534 nm. The emission spectrum of UCl<sub>3</sub> in a LiCl-KCl molten salt in ionic liquid was also obtained at a 515 nm excitation, which was one of the positions obtained in the absorption spectra. Peaks were observed at 588 nm, 610 nm, and 640 nm.

Many experiments were undertaken to confirm luminescence peaks and to elucidate the exact phenomenon and mechanism.

### IV. CONCLUSION

U(III) is unstable (oxidized) in an alkali fluoride molten salt or under general conditions, but is stable in LiCl-KCl molten salt. Moreover, the ionic liquid (1-hexyl-3-methylimidazolium chloride) used in this research did not cause an oxidation or reduction of U(III) as 1-ethyl-3-methylimidazolium chloride or water does. The behavior of U(III) in LiCl-KCl is dependent on the contact solvent (ionic liquid or water), and the results, including the actual assignment of each peak of the spectroscopic spectra, were conclusive.

## Distribution of Neptunium in PUREX streams

Neetika Rawat, Aishwarya Kar, M.A. Mahajan, N.B. Khedekar, R.M. Sawant,  
 B. S. Tomar and K. L. Ramakumar

Radioanalytical Chemistry Division, Bhabha Atomic Research Centre, Trombay, Mumbai 400085

**Abstract:**  $^{237}\text{Np}$ , is formed in abundance in nuclear reactors, however, the separation of neptunium from spent uranium fuel is difficult owing to the existence of its varied oxidation states in the dissolver solution. With a view to identify the stage in the PUREX plant, which can be used to tap neptunium, an exercise was undertaken to determine the distribution of neptunium in the different stages of the PUREX plant.

**Keywords:**  $^{237}\text{Np}$ , PUREX Streams,

### INTRODUCTION

$^{237}\text{Np}$ , the long lived isotope of neptunium is the target isotope for production of  $^{238}\text{Pu}$  by the neutron capture reaction. It is formed in abundance in nuclear reactors[1]. However, the separation of neptunium from spent uranium fuel is a difficult task owing to the existence of the element in varied oxidation states in the dissolver solution. With a view to identify the stage in the PUREX plant, which can be used to tap neptunium, an exercise was undertaken to determine the distribution of neptunium in the different stages of the PUREX plant.

$^{237}\text{Np}$  is a pure alpha emitter with no gamma lines and hence its analysis requires careful radiochemical separation from bulk uranium, plutonium and fission products before its estimation by alpha spectrometry. The alpha energies of plutonium isotopes are higher than that of  $^{237}\text{Np}$  and hence traces of Pu in the separated neptunium fractions would have contribution at the alpha peak of  $^{237}\text{Np}$  (Figure 1). Therefore, it was decided to measure the distribution ratios of Np in various streams of PUREX process using  $^{239}\text{Np}$  tracer ( $\beta, \gamma$  emitter) from irradiated uranium target. The actual column conditions of different streams were simulated performing solvent extraction in lab scale for the distribution of Np.

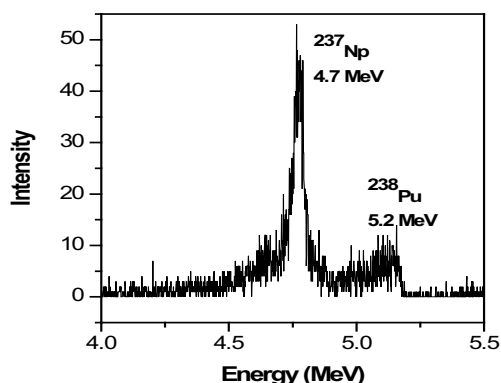


Figure 1. Alpha spectrum of sample CD1 after plutonium separation

### EXPERIMENTAL

The  $^{239}\text{Np}$  tracer was obtained by irradiating natural Uranium (10 mg) in reactor. The irradiated U was dissolved in conc  $\text{HNO}_3$  and then evaporated to dryness and made up to 20 ml using 3 M  $\text{HNO}_3$ . Aqueous feed solution was prepared by adding  $^{237}\text{Np}$ ,  $^{239}\text{Np}$  tracer and U so as to maintain U and Np concentration 380 g/L and 10 mg/L

respectively (acidity 3 M  $\text{HNO}_3$ ). Distribution of Np ( $D_{\text{Np}}$ ) in different streams was followed by counting the 278 keV gamma line in the gamma spectra using a HPGe detector. 4 ml of feed was equilibrated for 15 min with 19.6 ml of 30 % TBP in NPH (O/A = 4.9). Phases were separated by centrifugation. Suitable aliquots from the aqueous (HAW) and organic phase (HAP) were taken for assay of  $^{239}\text{Np}$ . 16.4 ml from HAP was equilibrated with 4 ml of U(IV) (28 g/l) in  $\text{N}_2\text{H}_4$  (0.2 M) at 0.6 M acidity (O/A = 4.1). After phase separation, the organic and aqueous phases, labeled as 1BXU and 1BXP, respectively, were assayed for the activity of  $^{239}\text{Np}$ . Subsequently 14 ml from 1BXU was equilibrated with 15.45 ml of 0.01 M  $\text{HNO}_3$  (O/A = 0.906), and the aqueous and organic fractions, labeled as 1CP and 1CW, respectively, were counted. 14 ml of 1CP was concentrated to 2.5 ml termed as 1CPCON. To 2.0 ml of 1CPCON, U(IV) was added such that U(IV) concentration in final solution is 4.8 g/l and  $\text{N}_2\text{H}_4$  is 0.2 M at 1.0 M acidity. 1CPCON was diluted to 3.58 mL, and was labeled as 2DCD. 1 ml of 2DCD was equilibrated with 2.3 ml of 30 % TBP (O/A = 2.3). The aqueous phase was labeled as 2DW. All the fractions were assayed for the activity of  $^{239}\text{Np}$ .

### RESULTS AND DISCUSSION

The complete experiment following the above procedure was carried out twice (Cycle 1 and Cycle 2). The  $D_{\text{Np}}$  values and percentage of Np in different steps, for both the cycle are given in table 1.  $D_{\text{Np}}$  values obtained for solvent extraction steps in both the cycles are in good agreement except for the step corresponding to HA column.  $D_{\text{Np}}$  in first cycle was found to decrease from 0.205 to 0.043 in the second cycle, which could be due to slow kinetics of change in oxidation state of neptunium. The decrease in  $D_{\text{Np}}$  values of Np from dissolver solution into TBP with the passage of time, indicates the reduction of Np(VI) to Np(V).

Table 1. D values and percentage of Np in different steps

Sample name	Cycle 1		Cycle 2	
	Distribution Coefficient, D	% Np	Distribution Coefficient, D	% Np
CD1		100		100
HAW	0.205	53	0.043	91
HAP		54		19
1BXP	0.266	26	0.26	9
1BXU		28		10
1CP	0.05	27	0.053	9.6
1CW		1.25		.4
1CPCON		27		9.6
2DCD		27		9.6
2DW	0.219	18	0.184	6.4
2DP		9		3.2

### Reference

- G.A. Burney and R.M. Harbour, Radiochemistry of neptunium, Nuclear Science Series NS-3060 (1974).



## Retardation and Release Study of U(VI) on Phlogopite at Conditions Relevant to Uranium Contamination in Environment

Pan Duoqiang<sup>1,2</sup>, Wang Zheming<sup>2</sup>, Wu Wangsuo<sup>1</sup>

<sup>1</sup> Radiochemistry Laboratory, Lanzhou University, Lanzhou 730000, China

<sup>2</sup> Pacific Northwest National Laboratory, Richland, Washington 99352, United State

Hexavalent Uranium, which is fertile in mining tailings and wastewater from nuclear production activities, is a prominent radioactive contaminant and has dispersed into both sediments and water around the related uranium processing sites, posing a potential health and environmental risk to the biosphere [1]. The mobility of U(VI) in natural medium is significantly controlled by the sorption/desorption behavior which is influenced by U(VI) speciation, sorbent properties and coexisted organic/inorganic ligands [2,3]. Desorption of adsorbed U(VI) from solid phase is actually considered to be potential secondary release sources to hydrosphere and the extent of desorption reversibility largely depends on the mechanisms involved in the sorption process [4]. As the sorption mechanism can vary by due to changes in sorption conditions, such as ligand complexation and change of pH or temperature, the uranium retardation and release rate in environmental media can be perturbed. Understanding the sorption mechanism and sorption reversibility of U(VI) is imperative to predict the future retention/migration behavior of U(VI) and to remediate contaminated soils and subsurface sediments. Many spectroscopic technologies that are capable of providing molecular-level information (FTIR, XPS, EXAFS, TRLIFS) have been employed to identify U(VI) species and local atomic structures of the surface complexes. Time resolved laser induced fluorescence (TRLIF) spectroscopy, particularly when performed at cryogenic temperatures, is one technique that offers high sensitivity and spectral resolution for the identification of U(VI) speciation in complex media at low U(VI) concentrations [5,6].

Here we applied a combination of batch sorption experiment and liquid helium temperature (LHeT) TRLIF spectroscopy to investigate sorption/desorption of U(VI) to phlogopite, which is a typical rock forming mineral in

granite terrains. Effects of pH, humic acid (HA), background electrolyte and temperature were studied in detail by batch method. The sorption isotherms at different temperatures were simulated and analyzed by using Langmuir and Freundlich models. Roles of HA and temperature on sorption reversibility were investigated by sorption-desorption isotherms. The speciation of adsorbed U(VI) at low concentration were monitored and the sorption/desorption mechanism were explored with the aid of TRLIF spectroscopy. The results shows that the sorption of U(VI) on phlogopite is influenced obviously by pH while only slightly by ionic strength. Inner-sphere surface complexation and/or precipitation rather than ion exchange and outer-sphere complexation are the primary sorption mechanisms. HA makes little difference at low pH, while inhibits U(VI) sorption at high pH mainly because of formation of soluble binary complexes and repulsive interaction between both negative charged HA and solid surface. High temperature is advantageous for U(VI) sorption, Langmuir model fits the sorption data better than Freundlich model. The presence of HA switches U(VI) sorption reversibility by forming HA-bridge ternary complex.

*Keywords: Uranium, Sorption/Desorption, Phlogopite, TRLIFS*

[1] Chakraborty S., et al., *Environ. Sci.Technol.*, 2010, 44(10): 3779-3785.

[2] Chang H.S., et al., *Environ. Sci.Technol.*, 2006, 40(4): 1244-1249.

[3] Chisholm-Brause C.J., et al., *J. Colloid Interf. Sci.*, 2001, 233(1): 38-49.

[4] Um W., et al., *Environ. Sci.Technol.*, 2009, 43(12): 4280-4286.

[5] Wang Z., et al., *Geochim. Cosmochim. Acta*, 2005, 69(6): 1391-1403.

[6] Wang Z., et al., *Geochim. Cosmochim. Acta*, 2011, 75(10): 2965-2979.

## Application of Simplified Desorption Method to Sorption Study: (2) Sorption of Neptunium (V) on Montmorillonite-based Mixtures

Naofumi Kozai<sup>1</sup>, Toshihiko Ohnuki<sup>1</sup>

<sup>1</sup>Japan Atomic Energy Agency, Tokai, Ibaraki, 319-1195 Japan

**Abstract** – To elucidate the sorption behaviors of radionuclides in multi-mineral systems and the mutual effects of minerals on the sorption, this paper carried out the sorption and desorption experiments of neptunium(V) on montmorillonite-based two-mineral mixtures. The Np sorbed on montmorillonite at pH from 4 to 8 was desorbed with 1M KCl solutions, indicating that the sorption was cation exchange. The Np sorbed on apatite and calcite was nondesorbable with 1M KCl solutions, which is in harmony with the knowledge that Np forms strong complexes with the phosphate groups of apatite and the carbonate groups of calcite. This study utilized these clear distinguishes of the desorption behaviors for examining the two-mineral systems. In montmorillonite-apatite mixtures, the sorption on the montmorillonite was decreased and Np was accumulated on the apatite. In montmorillonite-calcite mixtures, the sorption on the montmorillonite was decreased due to the interference by the calcium and carbonate ions dissolved from calcite while no accumulation of Np to calcite was observed.

**Keywords** – Neptunium, sorption, desorption, pH, montmorillonite, apatite, calcite

### I. INTRODUCTION

Sorption is one of the key mechanisms to control the subsurface environmental behavior of the radionuclides. In most of the relevant experimental studies, the sorption experiments of radionuclides have been performed in a single mineral system, while most of the subsurface environment is a multi-component system. The knowledge on the mutual influence of minerals to understand the sorption in multi-component systems is limited. This paper investigated the sorption of neptunium(V) in two-mineral systems. Montmorillonite clay used as a major component mineral is found ubiquitously in the soil environment. As minor soil component minerals, apatite ( $\text{Ca}_5(\text{PO}_4)_3\text{OH}$ ) and calcite ( $\text{CaCO}_3$ ) were used. This paper applies a simplified desorption method to the sorption study and discuss the distribution of Np between minerals.

### II. EXPERIMENTAL

This study used the same Na-montmorillonite as the one used in the former study [1]. The apatite used is fine powder of commercial calcium-phosphate having hydroxyapatite ( $\text{Ca}_5(\text{PO}_4)_3\text{OH}$ ) like structure (Wako Pure Chemical Industries Co. Ltd.). Natural calcite ( $\text{CaCO}_3$ ) was used after ground to particle sizes below 74  $\mu\text{m}$ . These minerals were used singly or used as montmorillonite-based mixtures (montmorillonite 95-99 w%). A Np (V) nitrate stock solution

was diluted with 0.01 M  $\text{NaClO}_4$  to yield a working solution having a Np concentration of about  $6 \times 10^{-7}$  M.

The sorption and the desorption experiments were conducted in the same way as the method described elsewhere [1] except that a part of the sorption experiments were carried out for up to 60 d.

### III. RESULTS AND DISCUSSION

When Na-montmorillonite was used alone, the fraction of the sorbed Np was roughly constant in the equilibrium pH range from 4 and 8. Most of the sorbed Np was desorbed by twice treatment with 1M KCl solutions. These results indicate that the sorption is electrostatic one between  $\text{NpO}_2^+$  and the constant negative surface charge of the montmorillonite [2].

On the apatite and the calcite, all of the Np was sorbed in the examined equilibrium pH ranges that were limited from neutral to weak alkaline due to their partial dissolution. The Np sorbed on these two minerals was hardly desorbed by twice treatment with 1M KCl solutions. These results are consistent with the knowledge that Np forms strong complexes with the phosphate groups of apatite and carbonate groups of calcite [3, 4]. The subsequent experiments for the montmorillonite-based mixtures utilized these clear differences; that is, the Np desorbed with 1M KCl solutions was regarded as the Np sorbed on the montmorillonite fraction and the Np not desorbed with 1M KCl solutions was the one sorbed on the apatite and calcite.

The montmorillonite-apatite mixtures sorbed several times greater amount of Np than Na-montmorillonite itself, while that on the montmorillonite fraction in the mixture decreased. Above pH 7 almost all of the Np was sorbed on the mixture within 10 d and most of the Np was sorbed on the apatite fraction. Below pH 7 the sorption on the mixtures increased with time and needed a longer time (20 d) to reach equilibrium. This slow kinetics of the sorption did not occur when those minerals were used singly and suggests a possible Np sorption involving the phosphate ligands once dissolved at low pH. The sorption on the montmorillonite-calcite mixtures was less than that on Na-montmorillonite itself and no evidence of accumulation of Np to calcite was observed, suggesting that the calcium and carbonate ions dissolved from the calcite interfered with the sorption.

[1] Kozai N and Ohnuki T., APSORC13 Abstract.

[2] Kozai N et al., *Radiochimica Acta*, 75, 149-158 (1996).

[3] Moor R. C., *Radiochim. Acta*, ().

[4] Zavarin M. et al., *Radiochim. Acta*, 93, 9-102 (2005).

## Continuous measurement of radon exhalation rate of soil in Beijing

Lei Zhang<sup>1, 2</sup>, Ke Sun<sup>2</sup>, Qiuju Guo<sup>2</sup>

<sup>1</sup>Solid Dosimetric Detector and Method Laboratory, Beijing, 102205, China

<sup>2</sup>State Key Laboratory of Nuclear Physics and Technology, School of Physics, Peking University, Beijing 100871, China

*Abstract – The continuous measurement of radon exhalation rate of soil is quite important for local radon level estimation. A continuous measurement system was developed and was applied to the measurement of the radon exhalation rate of soil in Beijing. The measurement results show that the average value of soil radon exhalation rate is  $42.5 \text{ mBq}\cdot\text{m}^{-2}\cdot\text{s}^{-1}$  in spring with a variation of  $13.1\sim 110 \text{ mBq}\cdot\text{m}^{-2}\cdot\text{s}^{-1}$  and  $20.8 \text{ mBq}\cdot\text{m}^{-2}\cdot\text{s}^{-1}$  in summer with a variation of  $1.1\sim 112 \text{ mBq}\cdot\text{m}^{-2}\cdot\text{s}^{-1}$ , which is quite constant with former surveys. The precipitation has an important influence on radon exhalation rate, normally the radon exhalation rate increases after a small rainfall, but it decreases to nearly zero shortly after a huge rainfall (with a precipitation rate of  $238.5 \text{ mm}\cdot\text{h}^{-1}$ ). In May, the radon exhalation rate of soil in Beijing shows a clear periodic variation, higher around noon and lower around midnight.*

*Keywords – Radon; Soil; Exhalation Rate; Continuous Measurement; precipitation*

## Dosimetric Evaluation of Thoron Exposure in Three Typical Rural Indoor Environments in China

Lei Zhang<sup>1</sup>, Qiuju Guo<sup>2</sup>, Shanqiang Wang<sup>1</sup>

<sup>1</sup>Solid Dosimetric Detector and Method Laboratory, Beijing, 102205, China

<sup>2</sup>State Key Laboratory of Nuclear Physics and Technology, School of Physics, Peking University, Beijing 100871, China

*Abstract – The brick houses, the mud houses and the cave houses are the three typical rural residential houses in China, usually with naked surface from where thoron gas easily comes out. In order to evaluate the thoron exposure of those indoor environments, a series of field measurements was carried out by using portable measurement devices of both thoron progeny concentration and the size distribution of them. The dose conversion factors and annual effective doses of thoron exposure in those environments are calculated using dosimetric methods. Comparing with the results in urban indoor environment, it shows that the thoron progeny size distributions of rural indoor environments (AMAD: 76.5nm; GSD: 2.7) are much smaller than those of urban (AMAD: 115nm; GSD: 2.0), which make the dose conversion factors of thoron in rural environments (307.4 nSv/(Bq·m<sup>-3</sup>·h<sup>-1</sup>)) are much higher than those in urban indoor environments (113.4 nSv/(Bq·m<sup>-3</sup>·h<sup>-1</sup>)). The annual average effective dose of thoron is influenced by dose conversion factor as well as thoron equilibrium equivalent concentration, and a quite high value of 10.12 mSv·a<sup>-1</sup> in mud house in Yangjiang area is calculated by our survey.*

*Keywords – Thoron Progeny, Size Distribution, Dose Conversion Factor, Dose Evaluation*

## Binary Technetium Phosphide Synthesis at Low Temperature Conditions

Bradley C. Childs<sup>1</sup>, William M. Kerlin<sup>1</sup>, Ken R. Czerwinski<sup>1</sup>

<sup>1</sup>University of Nevada Las Vegas, Las Vegas, Nevada 89154, USA

*Abstract – Binary technetium phosphide exists through high temperature reactions that exceed 900 °C [1]. Recent phosphide studies have indicated that transition metal phosphide species such as molybdenum, ruthenium, and rhenium can be synthesized at temperatures that do not exceed 300 °C, and will provide a more reasonable synthesis technique. This process could allow for a technetium waste form application due to the high melting point and low solubility's that many transition metal phosphide species exhibit. Experimental methods include bench-top reactions that begin with a precursor produced from a transition metal chloride combined with either sodium hypophosphite (NaH<sub>2</sub>PO<sub>2</sub>) or ammonium hypophosphite (NH<sub>4</sub>H<sub>2</sub>PO<sub>2</sub>). The second experimental method involves using hydrothermal and solvothermal experiments with phosphorus and various metal chloride species.*

*Keywords – Technetium, Phosphide, Synthesis*

### I. INTRODUCTION

Nearly 2 tons of <sup>99</sup>Tc (T<sub>1/2</sub> = 2.13x10<sup>5</sup> years, β<sup>-</sup> = 280 keV) are produced in the United States each year. As spent fuel is being reprocessed, some of the technetium is present in the intermetallic epsilon phase (Mo, Tc, Ru, Rh, Pd), but majority of the technetium can be found in the high activity waste of reprocessing plants as pertechnetate (TcO<sub>4</sub><sup>-</sup>) [2]. This becomes problematic due to the fact that TcO<sub>4</sub><sup>-</sup> has a high mobility in the environment combined with its long half-life. Waste-form consideration must be given to those compounds that exhibit low solubility's that also allow for the waste to be stored for long periods of time without degrading. Technetium phosphide compounds that can be synthesized at low temperatures may provide a method and compound that will allow such a goal to be achieved.

#### A. Synthesis with NaH<sub>2</sub>PO<sub>2</sub> or NH<sub>4</sub>H<sub>2</sub>PO<sub>2</sub>

Hypophosphite (H<sub>2</sub>PO<sub>2</sub><sup>-</sup>) is a reducing agent that can also provide phosphorus when reacting with a metal chloride [3]. This compound is also thermodynamically unstable at temperatures above 200 °C. This provides the basis for a reaction between RuCl<sub>3</sub>, ReCl<sub>3</sub>, and MoCl<sub>3</sub> to react with the hypophosphite anion. A precursor will be made by dissolving one of the metal chlorides with NaH<sub>2</sub>PO<sub>2</sub> or NH<sub>4</sub>H<sub>2</sub>PO<sub>2</sub> in distilled water [9] [10]. This mixture will then be heated to 60 – 80 °C. The resulting precursor would then be heated in static argon conditions at temperatures ranging between 200 °C and 300 °C. Based on results from the previous reactions, technetium chloride (TcCl<sub>4</sub>, TcCl<sub>3</sub>, and TcCl<sub>2</sub>) will be used in place of other metal chlorides.

#### B. Phosphorus hydro-solvothermal synthesis

A 23 mL Teflon lined Parr 4749 autoclave was used to house reactions that involved reacting phosphorus with RuCl<sub>3</sub>, ReCl<sub>3</sub>, and MoCl<sub>3</sub> while using ethylenediamine as the solvent to create a reducing environment. The area for concern in this reaction involves over reducing the metal species before it gets a chance to react with the phosphorus. Therefore, water was also used as a solvent in separate experiments to avoid too much reduction. Afterwards, TcCl<sub>4</sub>, TcCl<sub>3</sub>, and TcCl<sub>2</sub> will be considered for the same reaction depending on the phosphorus chlorine products produced in comparison to the binary phosphide product.

*Acknowledgement: Funding for this research was provided by a SISGR Grant from the U.S. Department of Energy, Office of Science, Office of Basic Energy Sciences, under Contract No. 47824B*

### REFERENCES

- [1] K. Schwochau, *Technetium: Chemistry and Radiopharmaceutical Applications*, Wiley-VCH: Weinheim, Germany, 2000.
- [2] M.C.A. Sandino and E. Östhols, eds., *Chemical Thermodynamics of Technetium*, Chemical Thermodynamics, 1999, **3**
- [3] Greenwood, Norman N.; Earnshaw, Alan (1997). *Chemistry of the Elements* (2nd ed.). Butterworth–Heinemann.
- [4] Q. Guan and W. Li, *Journal of Catalysis*, **271**, (2010), 413-415.
- [5] Q. Guan et al., *Catalysis Communications*, **14**, (2011) 114-117.
- [6] Y. Xie et al., *Journal of Solid State Chemistry*, **149**, (2000), 88-91.

## Dissolution behavior of $^{137}\text{Cs}$ absorbed on the green tea leaves

Yasuhisa Oya<sup>1</sup>, Hiromichi Uchimura<sup>1</sup>, Kensuke Toda<sup>1</sup>, Takashi Ikka<sup>2</sup>, Akio Morita<sup>2</sup>, Kenji Okuno<sup>1</sup>

<sup>1</sup>Graduate School of Science, Shizuoka University  
<sup>2</sup>Graduate School of Agriculture, Shizuoka University

*Abstract* – The green tea leaves was dipped in the  $^{137}\text{CsCl}$  solution to elucidate the dissolution behavior of  $^{137}\text{Cs}$  contaminated on the green tea leaves. It was found that the amount of  $^{137}\text{Cs}$  dissolved into tea water was controlled by the temperature of water, and the activation energy of  $^{137}\text{Cs}$  dissolution was estimated to be 0.045 eV, indicating that most of  $^{137}\text{Cs}$  would exist as the adsorbed state. In addition, the dissolution behavior was controlled by the concentration of stable Cs dissolved in water, although no large correlation with pH was observed.

*Keywords* –  $^{137}\text{Cs}$ , dissolution behavior, green tea leaves

### I. INTRODUCTION

Shizuoka is the most common tea production region in Japan and more than 40% of tea leaves are produced in Shizuoka prefecture, Japan. In the accident of 2011 Fukushima Daiichi Nuclear Power Plant (FNPP), radiocesium species was felled in Shizuoka prefecture, Japan, which leads the shipping restriction of tea products. Recently, some of studies related to the distribution of fall-out radiocesium in Shizuoka were reported [1]. In addition, the dynamics of radiocesium in tea plant is also studied. It was reported that the higher radiocesium activity was found along Warashina area and southern slope of Udo Hills, where the most tasteful tea plant is produced. This distribution is controlled by the wind condition in the afternoon on March 15, 2011. Therefore, the weather is one of key parameter for the determination of radiocesium distribution profiles. But, tea plant is grown in the unique area for radiocesium deposition and it is quite difficult to get rid of fall out of radiocesium, when the nuclear power plant accident is happened. Most of tea leaves are not eaten with raw condition and, are processed and dried to brew green tea. So the extrability of radiocesium from tea leaves harvested after FNPP accident has been reported [2]. However, more detailed elucidation of dissolution behavior of radiocesium adsorbed on the green tea leaves under well-controlled condition is the next step to elucidate the fundamental behavior of radiocesium. In this study, the dissolution behaviors of  $^{137}\text{Cs}$  to water from green tea leaves were studied as a function of water temperature, pH and cesium ion concentration in water.

### II. EXPERIMENTAL

The 6.0 g fresh green tea leaves were purchased and dipped in 39 ml of  $^{137}\text{CsCl}$  solution with the  $^{137}\text{Cs}$  concentration of 0.5 kBq/ml. These tea leaves were dried by infrared lamp for one night. Thereafter, the tea was brewed by 200 ml water. The activity of  $^{137}\text{Cs}$  dissolved into water was measured by NaI (TI) scintillation counter for 60 minutes.

### III. RESULTS

It was found that the temperature dependence on  $^{137}\text{Cs}$  dissolution rate was almost proportional to the water temperature. Fig. 1 shows the brewing time dependence on  $^{137}\text{Cs}$  dissolution rate. Large dissolution rate was derived for the higher temperature sample. The dissolution behavior was assumed to be governed by the Arrhenius correlation and the activation energy was estimated to be 0.045 eV, indicating that most of  $^{137}\text{Cs}$  would exist as the adsorbed state and no chemical interaction with tea leaves. To elucidate the key parameters to control the dissolution behavior, pH dependence on  $^{137}\text{Cs}$  dissolution rate was also evaluated from the pH = 1 to 13 and showing that no large contributions of hydrogen ion and hydroxyl ion concentrations on  $^{137}\text{Cs}$  dissolution. In addition, dependences for concentrations of  $\text{K}^+$  and  $\text{Cs}^+$  on  $^{137}\text{Cs}$  dissolution were also evaluated. It was confirmed that the dissolution rate of  $^{137}\text{Cs}$  in water was reduced almost half by the addition of the 1000 ppm  $\text{Cs}^+$ .

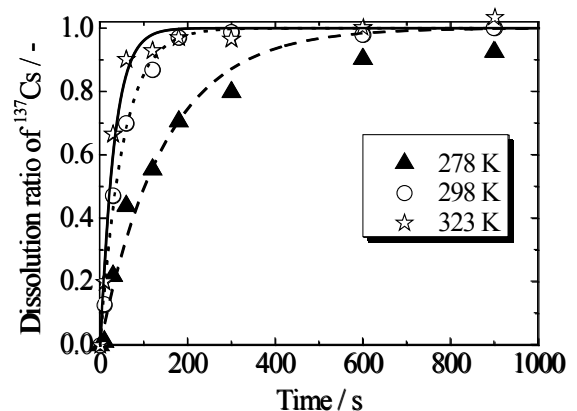


Fig. 1 Brewing time dependence on  $^{137}\text{Cs}$  dissolution rate

### REFERENCES

- [1] T. Tsuboi, H. Wada, M. Yanaga, Radiat. Safety Manag. 11 (2012) 11-18.
- [2] K. Tagami, S. Uchida, N. Ishii, J. Radioanal Nucl. Chem. 292 (2012) 243-247.

## Characterization on the Radioactive Aerosols Dispersed during Plasma Arc Cutting of Radioactive Metal Piping

T. Shimada<sup>1</sup> and T. Tanaka<sup>1</sup>

<sup>1</sup> Nuclear Safety Research Center, Japan Atomic Energy Agency, Tokai-mura, Naka-gun, Ibaraki 319-1195, Japan

### Abstract

In order to plan and execute the decommissioning of nuclear facilities safely and properly, it is necessary to understand the production and dispersion behaviors of radioactive aerosols which are dispersed during the cutting of components activated and/or contaminated. It will cause not only internal exposures of workers but public exposure resulting from discharge of those radioactive aerosols to the environment. It is also important for radiological safety assessment to figure out their behaviors. Therefore plasma arc cutting experiments were carried out to obtain particle size distribution and radionuclides concentrations.

Neutron induced-activated piping and surface contaminated piping were segmented along the outer surface by well-trained workers using air plasma arc cutting, of which current power was 100A, in the contamination control enclosure (4m length, 4m width, 4m height). The former was the stainless steel piping of primary reactor cooling system situated around the reactor pressure vessel of Japan Power Demonstration Reactor. It was 0.5m long, 318mm outer diameter, 17mm thickness. Values of specific radioactivity of <sup>60</sup>Co and <sup>63</sup>Ni in the base material were 64.4Bq/g to 170.9 Bq/g and 378.5Bq/g to 797.8Bq/g respectively. The tendency depended on the distance from the reactor core. The inner surface of the piping was grinded just in case even though its surface had been decontaminated by a chemical method after dismantling. The latter was the carbon steel piping of liquid waste treatment system of the advanced thermal reactor, FUGEN. It was 6.9m long, 60mm outer diameter, 5.5mm thickness. There was a great variability among the values of radioactive surface contamination density of inner surface of the piping, from 552.1Bq/cm<sup>2</sup> to 55,336Bq/cm<sup>2</sup> of <sup>60</sup>Co.

Air including aerosols was exhausted from the enclosure to the local ventilation system. Particle size distribution of the aerosols was obtained by sampling air through the nozzle at the center of the ventilation piping using ELPI (Electrical Low Pressure Impactor, Dekati Inc.) which could classify particles into 12 stages of 50% cutoff aerodynamic diameter, D50% ranging from 0.007 to 9.9μm. This instrument enables to measure particle size distribution and concentration of the aerosols in real-time by corona charger and electro-meters at each impactor stage. The radioactive quantity of <sup>60</sup>Co of aerosols collected on the impactor stage was measured by Ge semiconductor detector. That of <sup>63</sup>Ni was measured by liquid scintillation counter after dissolved by hydrochloric acid and separated by ion-exchange column.

Figure 1 shows the particle size distribution of specific radioactivity of <sup>60</sup>Co and <sup>63</sup>Ni of aerosols during cutting of activated piping. Those values were calculated by dividing the quantity of radionuclide at the each stage by the weight

of aerosols collected at the stage. Specific radioactivity of both <sup>60</sup>Co and <sup>63</sup>Ni of 0.09μm indicated the highest value. Those of both <sup>60</sup>Co and <sup>63</sup>Ni of 0.15μm and 0.26μm indicated the similar values to those of base material of the piping. That of <sup>60</sup>Co larger than 0.26μm indicated the half value of the base material.

Figure 2 shows the particle size distribution of <sup>60</sup>Co specific radioactivity of aerosols during cutting of surface contaminated piping. Specific radioactivity of aerodynamic diameter of 0.05μm indicated the maximum value of approximately 2.7E+4 Bq/g which was fifty times as much as the average value of the aerosols. That of 9.9μm was approximately 100Bq/g which was the eighth part of the average value. Compared with the activated piping, the difference of specific radioactivity between maximum and minimum values were larger in contaminated piping. It is considered that contaminants on the inner surface were directly melted and vaporized by plasma arc and then concentrated into smaller particles

Those results indicated that the management for dispersion behavior of smaller particles is important for the radiation protection during dismantling activities.

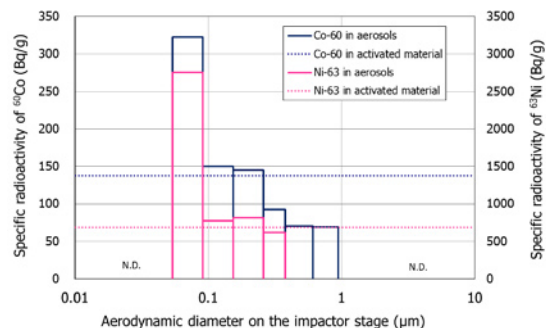


Figure 1 size distribution of specific radioactivity of activated piping

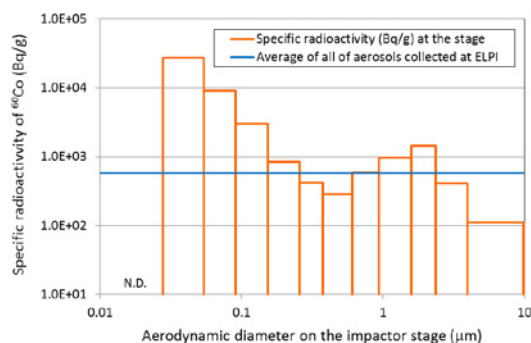


Figure 2 size distribution of specific radioactivity of surface contaminated piping

This work is a part of study funded by Japan Nuclear Energy Safety Organization.

## A passive collection method for whole size fractions of suspended river materials

Takeshi Matsunaga<sup>1</sup>, Takahiro Nakanishi<sup>1</sup>, Mariko Atarashi-Andoh<sup>1</sup>, Erina Takeuchi<sup>1</sup>, Katsunori Tsuduki<sup>1</sup>, Syusaku Nishimura<sup>1</sup>, Jun Koarashi<sup>1</sup>, Shigeyoshi Ootosaka<sup>1</sup>, Tsutomu Sato<sup>2</sup>, Seiya Nagao<sup>3</sup>

<sup>1</sup> Nuclear Science and Engineering Directorate, Japan Atomic Energy Agency, Tokai-mura, Ibaraki 319-1195, Japan

<sup>2</sup> Division of Sustainable Resources Engineering, Graduate School of Engineering, Hokkaido University, Sapporo 060-8628, Japan

<sup>3</sup> Low Level Radioactivity Laboratory, Institute of Nature and Environmental Technology, Kanazawa University, Ishikawa 923-1224, Japan

*Abstract – An innovative, yet simple method for the passive collection of radioactive materials in river water has been developed and validated. This method makes long-term, unmanned monitoring possible. In addition to regular radioactivity analyses, this method provides an opportunity for the characterization of suspended materials based on its ample collection quantities (more than several tens of grams). This method may also be applicable to sediment-bound chemicals.*

*Keywords – River, Radionuclides, Chemicals, Passive collection, Long-term monitoring, Suspended materials, Dissolved materials*

### I. INTRODUCTION

The migration behavior of atmospherically derived radionuclides and chemicals onto river catchments has been extensively studied thus far. Transport of these materials through rivers can be the most influential export process to downstream regions. These investigations, however, have often encountered essential difficulties; one of which is in sampling frequency. Rainfall events play an important role in fluvial transport of contaminants. However, it is difficult to carry out frequent manned observations for these stochastic events. Another difficulty is the ability to collect enough suspended material for characterization purposes such as chemical extractions and mineralogical analyses. The aforementioned analyses generally require several grams of suspended material. The concentration of such materials in river water typically ranges from a few mg l<sup>-1</sup> to about 100 mg l<sup>-1</sup>, meaning that ten to a thousand liters of water are required. Accordingly, handling such large amounts of water can be distressing. Here, we report an innovative, yet simple collection method for suspended and dissolved components in river water.

### II. METHODS

#### A. Collection of suspended components

Two filter vessels (957 mm height, 350 mm width, 6SL-2S, Advantec Toyo Kaisha, Ltd.) were used sequentially with different nominal pore-sized filters, 100 μm and 0.5 μm. Each vessel contained six cartridge filters of wound type polypropylene (750 mm length). River water was led to the system naturally using a drop of the riverbed by hose from upstream. After an appropriate number of days of operation, the filters and the mud deposits on the bottom of the vessels were recovered. In the laboratory, the suspended material that was collected on the wound fibers

was washed out with water in a bucket. The wash-water samples and the mud samples were concentrated via centrifugation. A composite of the mud sample was obtained and subjected to wet sieving, such that components of four sizes were obtained: 1) <2000 μm, 2) 500-2000 μm, 3) 75-500 μm, and 4) <75 μm, in principle. The first and second components were air-dried. The third and fourth components were freeze-dried to obtain final samples of suspended material.

#### B. Collection of dissolved components

The dissolved component, radiocesium in this study, was collected from part of the outlet water from the filter vessels. Namely, the outlet water was put through a series of two PVC columns (4 cm inner diameter, 20cm length), which contain Cs-specific adsorbent material (Anfezh).

### III. RESULTS AND DISCUSSION

The effectiveness of this method was validated over a period of 15 months of field operation time since December 2011. The test site was a hilly, forested catchment of 0.62 km<sup>2</sup> containing a stream, located in the Northern area of Central Japan (Ibaraki Prefecture). The site was affected by fallout from the Fukushima nuclear accident. In this validation study, the aim was to obtain samples for radiocesium analyses. During the test period, ten sets of suspended material samples were successfully recovered. Intervals were changed from two to six weeks depending on the hydrological situation. Approximately 50-350 g of suspended material was recovered per collection period; variance depended on the length of the period and precipitation conditions. Adsorbent columns for dissolved radiocesium were added after November 2012. The collection efficiency of dissolved radiocesium was as high as 95 %. A consistent working method for collection of dissolved components and suspended components has therefore been established.

### IV. CONCLUSION

A passive, yet simple collection method for radioactive materials in river water has been developed and validated. The method is advantageous as it: i) allows efficient recovery of whole size fractions of suspended material, ii) can be used in remote locations without electricity, iii) is suitable for unmanned operations over long periods of time.

## Study of factors controlling organic pollution in Lake Kiba

Yuriko Kawano<sup>1</sup>, Seiya Nagao<sup>1</sup>, Shinya Ochiai<sup>1</sup>, Masayoshi Yamamoto<sup>1</sup>

<sup>1</sup>Low Level Radioactivity Laboratory, Kanazawa Univ., Wake, Nomi, Ishikawa 923-1224, Japan

### Abstract –

Lake Kiba is located in Ishikawa Prefecture and has been facing to high COD value, a simple indicator of organic pollution, of lake water. This study analyzed organic matter content in a sediment core with time scale and discussed factors controlling COD value. Sedimentation rate estimated from depth profile of <sup>210</sup>Pb<sub>ex</sub> is divided into three periods such as present-1989, 1989-1959 and 1959-past. TOC flux at the present is five times higher than that of 1959. The TOC/TN molar ratio decreased from 15.7 to 12.8. These results suggest that accumulation of total organic matter increases but the contribution of terrestrial organic matter and phytoplankton relatively varies with time.

Keywords – <sup>210</sup>Pb, TOC,  $\delta^{13}\text{C}$

### I. INTRODUCTION

Lake as closed water area is likely to deposit pollutant because of its hydraulic characteristics. Therefore, it is not easy to improve water quality deteriorated. Chemical oxygen demand (COD) is used as a simple indicator of organic pollution in lake. The organic pollution is related to the direct load of organic matter from lake basin and the indirect load of organic matter produced by phytoplankton in lake. In order to facilitate water quality conservation, we evaluate concentration and characteristics of organic matter and its origin in lake.

This study was intended for Lake Kiba, because the lake ranked in the worst two of COD in Japanese lakes in 1990 and remains still high concentration level of COD (ca. 6 mg/l). The purpose of this study is to understand factors controlling variations in COD concentration of lake waters. We collected a sediment core sample and measured total organic carbon (TOC), total nitrogen (TN), carbon and nitrogen isotopic ratio ( $\delta^{13}\text{C}$  and  $\delta^{15}\text{N}$ ) to investigate variation of organic matter accumulation at the lake sediments because sedimentary organic matter recorded lake water environment during the period of past to present.

### II. STUDY SITE AND METHODS

Lake Kiba is located in Ishikawa Prefecture and has surface area of 1.44 km<sup>2</sup> with an average water depth of 2.2 m. Major inflow rivers are Hiyou River, Bou River and Yamashiro River. There are a number of drainage channels from paddy field. Outflow water from the lake is only Mae River.

A sediment core was collected in June 2012 with a HR-type corer at the center of lake. The collected core sample was cut into 1 cm interval at 0-10 cm depth in core and 2 cm interval below 10 cm depth. After the samples were freeze-dried, <sup>210</sup>Pb<sub>ex</sub> was measured by gamma spectrometry. Sedimentation rate was estimated using constant rate of supply (CRS) model for the <sup>210</sup>Pb<sub>ex</sub> profile. Total organic carbon (TOC) and total nitrogen (TN) were measured with an elemental analyzer after HCl treatment of sediment

samples. <sup>13</sup>C/<sup>12</sup>C and <sup>15</sup>N/<sup>14</sup>N ratios were measured using mass spectrometer and expressed as  $\delta^{13}\text{C}$  and  $\delta^{15}\text{N}$ , respectively.

### III. RESULTS AND DISCUSSIONS

<sup>210</sup>Pb<sub>ex</sub> activity in the sediment core gradually decreased from 0 to 8 cm depth in core, and was nearly constant from 8 to 14 cm, but rapidly decreased from 14 to 26.7 cm (Fig. 1a). The sedimentation rate is 0.15 g/cm<sup>2</sup>/y at 0-8 cm depth and 0.05 g/cm<sup>2</sup>/y at 14-26.7 cm depth. The changes of sedimentation rate occurred in 1959 and 1989. The sedimentation rate in recent years has been three times faster than in the past. This indicates that environmental change in the basin has occurred.

TOC flux ranges from 4.3 to 7.5 in the depth interval of 0-8 cm, 2.0 to 3.9 at 8-14 cm and 0.7 to 1.8 at 14-20 cm (Fig. 1b). This result shows increases in the accumulation of organic matter in the lake. The C/N molar ratio decreased from 15.7 to 12.8 towards the current, and  $\delta^{13}\text{C}$  showed some variation (Fig. 1c). This result suggests contribution of phytoplankton relatively increased rather an terrestrial organic matter during 1959-present.

These results suggest that organic matter supply from the lake basin and primary production in the lake increased since 1959. This may be related to the changes in lake basin environment and the increases of COD value in Lake Kiba.

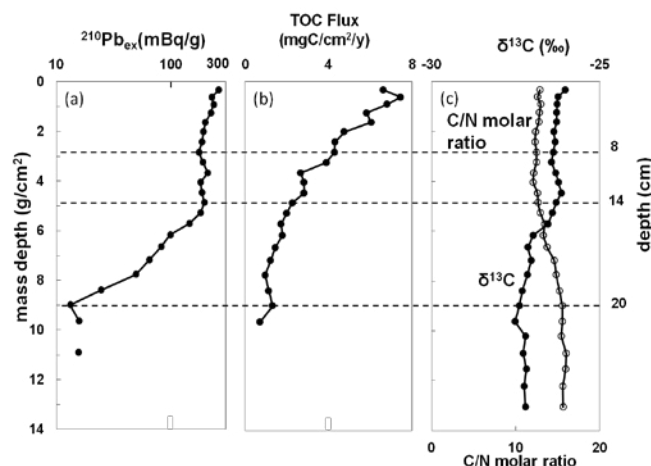


Figure 1 The depth profile of <sup>210</sup>Pb<sub>ex</sub> content (a), TOC flux (b) and C/N molar ratio and  $\delta^{13}\text{C}$  (c).

## Rapid monitoring particulate Radiocesium with nonwoven fabric cartridge filter and application to field monitoring

Hideki TSUJI<sup>1</sup>, Yoshihiko KONDO<sup>2</sup>, Shoji KAWASHIMA<sup>2</sup>, Tetsuo YASUTAKA<sup>1</sup>

<sup>1</sup> National Institute of Advanced Industrial Science and Technology

<sup>2</sup> Japan Vilene Company. Ltd.

### Abstract

A method for rapid monitoring particulate radiocesium using a nonwoven fabric cartridge filter was developed, which needs no further preprocessing before served to a detector. By a performance test, more than 98% of suspended solid (SS) was collected. This method showed the same radioactivity measurement accuracy as filtration by membrane filter and more rapid extraction capability of SS.

Keywords – radiocesium, nonwoven fabric filter, suspended solid

### I. INTRODUCTION

The monitoring of dissolved and particulate radiocesium in environmental waters became important after the accident of TEPCO Fukushima Daiichi Nuclear Power Plant. Our research group has developed a monitoring method to investigate the radiocesium concentration in water by each existence form. Yasutaka et al. (2013) developed a method to absorb 90% of dissolved <sup>137</sup>Cs in 20 L water within 10 minutes using Prussian blue impregnated nonwoven fabric. Minami et al. (2013) set monitoring device onto paddy fields and more than 99% of dissolved <sup>137</sup>Cs in 400 L water was absorbed within 24 hours. In this study, a method for monitoring particulate radiocesium using nonwoven fabric cartridge filter was developed. The measurement accuracy and pre-concentration time was compared with a traditional method. Furthermore, environmental water in Fukushima Prefecture was monitored by this method.

### II. MATERIALS AND METHODS

The radiocesium on SS was collected by the plain nonwoven fabric in the cartridge (SS-cartridge). This filter was made of polypropylene fibers with a pore size of 1 μm. The performance of the cartridges was examined using the simulated river water, which contains <sup>137</sup>Cs (4,340 Bq/kg-SS). The SS in water was set at 10 and 100 mg/L. Water samples were pumped through SS-cartridge at a rate of 2.5 L/min. The SS weight collected in the cartridge was calculated by the weight gain of SS-cartridge. The concentration of <sup>137</sup>Cs in SS-cartridge was measured by a Ge semiconductor detector. The geometric efficiency of SS-cartridge was calculated by dividing the detected <sup>137</sup>Cs radioactivity by the actual <sup>137</sup>Cs radioactivity in the cartridge, which is determined from the collected SS weight and the concentration of particulate <sup>137</sup>Cs. In addition, the maximum amount of SS weight in the SS-cartridge was determined by passing water with 1,000 mg/L of SS.

Next, this method was also applied to measure particulate <sup>137</sup>Cs concentration of environmental water in Fukushima Prefecture for testing field applicability. The river water of 20-

100 L was pumped through the SS-cartridge. The detected SS concentrations and <sup>137</sup>Cs concentrations in SS-cartridge were compared with those filtrated with a 0.45 μm membrane filter in laboratory.

### III. RESULTS

In the result of performance test, all SS in the water was collected in the cartridge for all experiments. The geometric efficiency of the cartridge was 0.71 on average (the S.D. was 0.07) and the recovery rates of <sup>137</sup>Cs, determined by dividing the detected <sup>137</sup>Cs by the geometric efficiency was calculated as Fig.1

This cartridge could hold 30 g SS under 0.2 MPa flow pressure. For the field performance test, concentrations of both SS and <sup>137</sup>Cs filtrated by two methods showed almost the same results in the samples from all locations except point E (Fig.2). In contrast to almost one day by the membrane filtration, only 10 min is needed for 20 L water filtration by this SS-cartridge method.

This study was supported by the budget (the development of systems and technology for advanced measurement and analysis) from Japan Science and Technology Agency.

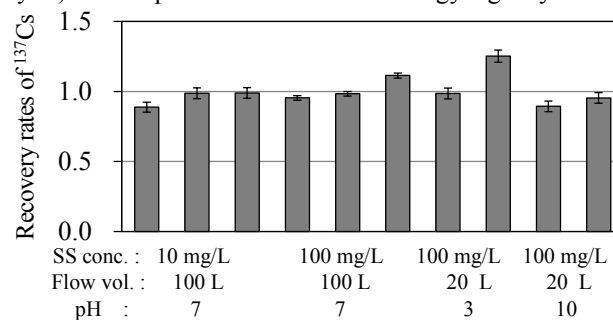


Fig.1 Recovery rates of <sup>137</sup>Cs. Error bars indicate counting error.

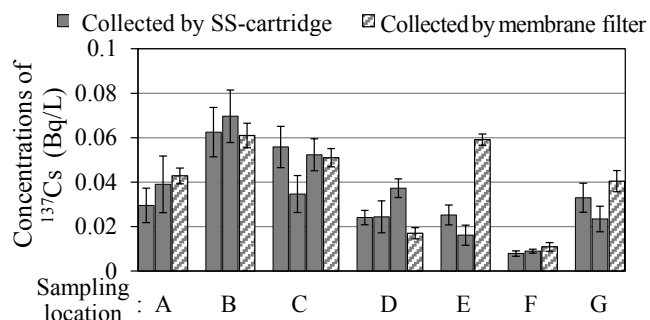


Fig.2 The concentrations of <sup>137</sup>Cs in Abukuma River water. Error bars indicate counting error.

[1] Yasutaka et al.(2013), *Appl. Chem.* (in Japanese), in press

[2] Minami et al.(2013), *Abstract of APSORC13*

# In-situ measurement of $^{134}\text{Cs}$ and $^{137}\text{Cs}$ in seabed by underwater $\gamma$ -spectrometry systems and application for the survey to the Fukushima Dai-ichi NPP accident

Hisaki KOFUJI

Japan Marine Science Foundation, Minato-Machi, Mutsu, Aomori, 035-0064 Japan

## Abstract –

Underwater  $\gamma$ -spectrometry systems (Mooring and Towing system) with NaI(Tl) detector were applied to in-situ measurement of radiocesium in seabed derived from the Fukushima Dai-ichi Nuclear Power Plant (FDNPP) accident. Radiocesium concentration was calculated from towing system data with short integrated time (2–5 min) by the separating method of the  $\gamma$ -ray counts to 4 contributions ( $^{134}\text{Cs}+^{137}\text{Cs}$ ,  $^{40}\text{K}$ , U series and Th series nuclides) using  $4 \times 4$  matrix. Concentration of  $^{134}\text{Cs}+^{137}\text{Cs}$  in sediments located about 80 km north from the FDNPP was calculated to be 150–200 at muddy site and 5–25 Bq/kg-dry at sandy site, respectively.

Keywords – In-situ  $\gamma$ -ray measurement, Sea Sediment,  $^{134}\text{Cs}$ ,  $^{137}\text{Cs}$ , Fukushima Dai-ichi NPP accident

## I. INTRODUCTION

Large amount of radionuclide were released to environment by the FDNPP accident on March 11, 2011. In contrary to the gradual decrease of radiocesium concentrations in seawater after the FDNPP accident, high levels of radiocesium have remained in sea sediments around the FDNPP. We applied underwater  $\gamma$ -spectrometry systems to measurement of radiocesium in seabed derived from the FDNPP accident.

## II. SYSTEM AND METHOD

Two underwater  $\gamma$ -spectrometry systems with  $3'' \phi$  spherical NaI(Tl) detector were applied to in-situ measurement on seabed. Mooring system: log the temporal variation of radiation on seabed. Towing system: monitor the spatial distribution of radiation on seabed with underwater movie, depth, temperature, salinity in real time from a boat. Both of the systems are small (15–20 kg), it can be lifted and retrieved by human hand from a boat (Fig. 1).

These systems were operated at 2 sites in coastal area (37–38 m depth) located about 80 km north from the FDNPP on September 6–7, 2012. The sediments are muddy at St. A and sandy at St. B, respectively. For mooring system, it was taking down to the seabed and recover after 2 hours. For towing system, it was towed slowly (1 knot) during about 15 minutes on seabed, and next measured during 1–2 hours at one position. Surface sediments were also collected in each site and analyzed the density and water content.

$\gamma$ -ray spectrum data were separated to 4 contributions ( $^{134}\text{Cs}+^{137}\text{Cs}$ ,  $^{40}\text{K}$ , U series and Th series nuclides) by  $4 \times 4$  matrix. Parameters of the matrix were obtained from calculated  $\gamma$ -ray spectrum for radionuclides in sediment and seawater by Monte Carlo simulation with EGS5 code [1].

## III. RESULTS AND DISCUSSIONS

Radiocesium derived from the FDNPP accident was detected in sediment by both systems (Fig. 2) and the posture of towing system on seabed was stable during towing. These underwater  $\gamma$ -spectrometry systems were confirmed to be available to survey radiocesium contamination in seabed.

Radiocesium concentration could be calculated from short integrated time data (2–5 min) with small  $\gamma$ -ray counts by using  $4 \times 4$  matrix. Assuming homogeneous distributions of  $^{134}\text{Cs}$  and  $^{137}\text{Cs}$  in 0–10 cm depth of sediment, the  $^{134}\text{Cs}+^{137}\text{Cs}$  concentrations in sediment were calculated from data by towing system to be 150–200 Bq/kg-dry at muddy site (St. A) and 5–25 Bq/kg-dry at sandy site (St. B), respectively.

This work was performed with grant-in-aid from Watanabe Memorial Foundation for The Advancement of New Technology.

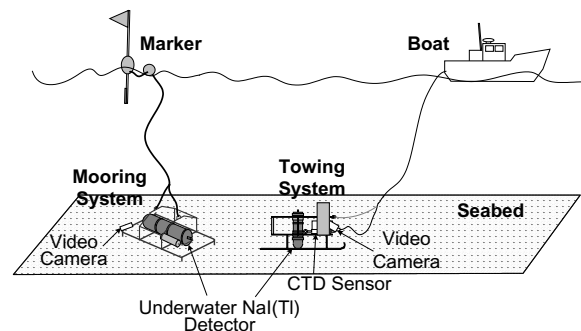


Fig. 1 Illustration of field operation of underwater gamma-ray spectrometry systems (mooring and towing system).

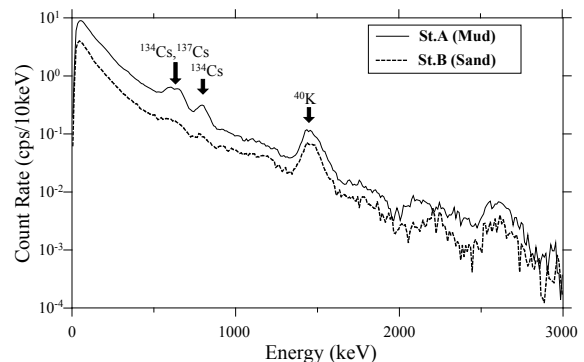


Fig. 2  $\gamma$ -ray spectrum measured on seabed by towing system. (1h integrated data)

[1] Hirayama, H., et. al, 2005, The EGS5 Code System, SLAC-R-730 and KEK Report 2005-8

## Radiocarbon dating of molluscan shells and its application

Yoshiki MIYATA<sup>1,2,3</sup>, Hiroyuki Matsuzaki<sup>2</sup>

<sup>1</sup> The Low Level Radioactivity Laboratory (LLRL), Institute of Nature and Environmental Technology, Kanazawa University, Ishikawa 923-1224, Japan

<sup>2</sup> The College of Liberal Arts, International Christian University, 181-8585, Tokyo, Japan

<sup>3</sup> National Museum of Japanese History, 285-8502, Chiba, Japan

<sup>4</sup> Department of Nuclear Engineering and Management, School of Engineering (MALT), The University of Tokyo, 113-0032, Tokyo, Japan

**Keywords** – Radiocarbon dating; Marine reservoir effect; Molluscan shell; Marine reservoir correction value ( $\Delta R$ ); Sea Current

We investigated radiocarbon age differences among marine shells, terrestrial animal and marine fish bones, charred wood fragments and charred seeds from layer IV, at the Higashi michi no ue (3) archaeological site, Japan, which was occupied during the first half of the early Jomon period (3900-3750 cal BC) as shown in Table 1.

We attributed the differences to marine reservoir effects, which differed among these organisms because of differences in their habitats and diets. The ages of *Corbicula japonica*, *Crassostrea gigas* and *Ruditapes philippinarum* (molluscan shells) show 180 yrs, 270 yrs and 450 yrs older than the radiocarbon age of the charred wood fragments, which corresponded to the actual age of the excavated archaeological site, respectively (Fig.1). This shows the habitats of these molluscan shells change from fresh to oceanic water, so that the salinity of the habitats of these molluscan shells gradually increases into the level of the sea water.

According to the age of *Ruditapes philippinarum*, the marine reservoir correction value ( $\Delta R$ ) for the Tsugaru Warm Current, which flows around Shimokita peninsula, is  $80 \pm 41$  <sup>14</sup>C years (N = 2). The radiocarbon ages were, in an increasing order, charred wood fragments, charred seeds ~ terrestrial animal bones (deer) < marine molluscan shells ~ marine fish bones < charred materials on potsherds. The different reservoir effects thus reflect difference in the diets or habitats of the shellfish, marine fish, and charred materials on potsherds found at the site.

This work was partly supported by a Grant-in-Aid for Young Scientists (B) No. 18700679 (Y.M.), Creative Scientific Research No.16GS0118 (T.N.) and Scientific Research (B) No.25282072 (Y.M.) of the Japan Society for the Promotion of Science.

Table 1. Radiocarbon ages of marine shells, charred seeds, charred woods, animal bones, marinefishes and carbonized materials adhering to pottery excavated from the Higashi michi no ue (3) archaeological site.

Sample #	Lab code	Sample name (Binomial name)	<sup>14</sup> C age ( $\pm\sigma$ ) BP	R ( $\pm\sigma$ ) <sup>1</sup> <sup>14</sup> C yr	$\Delta R$ ( $\pm\sigma$ ) <sup>2</sup> <sup>14</sup> C yr
AOKH S8	MTC-7412	Japanese walnut ( <i>Juglans mandshurica</i> var. <i>sieboldiana</i> )	4910 $\pm$ 30	-	-
AOKH C6	MTC-7410	Charred wood	5005 $\pm$ 35	-	-
AOKH B11	PLD-6043	(wild) boar ( <i>Sus scrofa</i> )	4920 $\pm$ 30	-30 $\pm$ 38	-409 $\pm$ 36
AOKH K17	MTC-7444	<i>Corbicula japonica</i> <sup>3</sup> ( <i>Ruditapes philippinarum</i> )	5210 $\pm$ 150	260 $\pm$ 152	-119 $\pm$ 151
AOKH K17	MTC-7565	<i>Corbicula japonica</i> <sup>3</sup> ( <i>Ruditapes philippinarum</i> )	5140 $\pm$ 60	190 $\pm$ 64	-189 $\pm$ 63
AOKH K16	MTC-7443	Oyster ( <i>Crassostrea gigas</i> )	5230 $\pm$ 60	280 $\pm$ 64	-99 $\pm$ 63
AOKH K15	MTC-7442	Japanese little neck <sup>3</sup> ( <i>Ruditapes philippinarum</i> )	5380 $\pm$ 60	430 $\pm$ 64	51 $\pm$ 63
AOKH K15	MTC-7562	Japanese little neck <sup>3</sup> ( <i>Ruditapes philippinarum</i> )	5430 $\pm$ 50	480 $\pm$ 55	101 $\pm$ 54
AOKH B13	PLD-6045	Japanese seabass ( <i>Lateolabrax japonicus</i> )	5425 $\pm$ 25	475 $\pm$ 34	96 $\pm$ 32
AOKH 3	MTC-7408	Charred material from inner surface of potsherd	5505 $\pm$ 35	555 $\pm$ 42	176 $\pm$ 40

Measurement error is 1 $\sigma$ .

<sup>1</sup>  $\Delta R$  was subtracted from the average age of Japanese walnut and charred wood (4950  $\pm$  23 BP), excavated from the Higashi michi no ue (3) site.

<sup>2</sup>  $\Delta R$  was subtracted from the marine model <sup>14</sup>C age (5329  $\pm$  20 BP), which corresponded to the age of the charred wood (4950  $\pm$  23 BP, 3766-3696 cal BC (68.2%).

<sup>3</sup> Each same individuals of *Corbicula japonica* and Japanese little neck were measured twice.

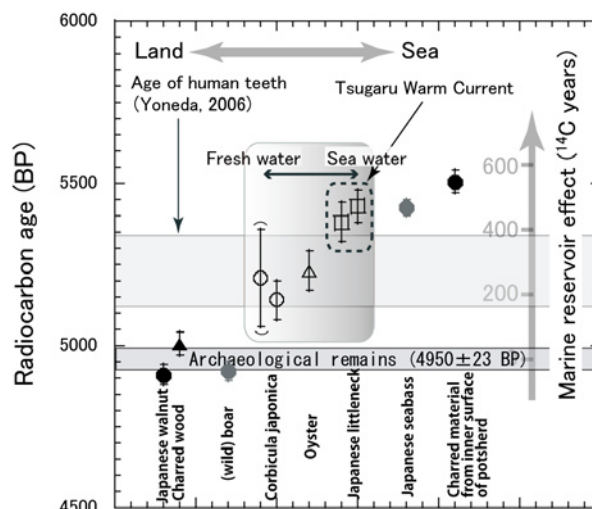


Fig. 1. Radiocarbon ages of archaeological remains from Higashi michi no ue (3) archaeological site.

## Concentration of Uranium on TiO-PAN and NaTiO-PAN Composite Absorbers

Alois Motl, Ferdinand Šebesta, Jan John, Irena Špendlíková, Mojmir Němec

Czech Technical University in Prague, Department of Nuclear Chemistry, Brehova 7, 115 19 Prague, Czech Republic

### Abstract

Inorganic ion exchangers have been extensively tested for use in separation and concentration of uranium from surface water. Except for separation of uranium from uranium-contaminated waste water (e.g. waste water from mining and milling of uranium, waste from nuclear fuel reprocessing) their main area of application has been foreseen to be their use for extraction of uranium from sea water which could partially cover future needs of uranium. Another perspective area of application is pre-concentration of uranium from natural waters followed by uranium determination via various specialized techniques such as TRLFS or AMS.

Possibilities of uranium extraction from sea water have been subject of several international conferences (e.g. Topical meetings on the Recovery of Uranium from Seawater in 1980's, ACS National Meetings 2012 etc.) and are critically evaluated in a review by Bitte [1] or recently by Kim [2]. In the Czech Republic uranium-selective inorganic ion exchangers might be applied for treatment of various wastes from uranium industry, namely underground water, uranium milling over-balance water, or acid waste water from underground uranium leaching and also like in other countries for determination of uranium isotopic composition focusing on anthropogenic and natural  $^{236}\text{U}$  content.

Among the best performing inorganic ion exchangers for the above listed purposes hydrated titanium dioxide (abbreviated as TiO) and sodium titanate (abbreviated as NaTiO) can be listed. Properties of TiO and NaTiO were reviewed by Lehto [3]. From the point of view of ion-exchange, properties of hydrated titanium oxide and sodium titanate are very similar. The main disadvantage of these ion exchangers for industrial-scale application is their insufficient mechanical stability [1]. To improve this property, the sorption materials can be embedded into a binding matrix.

Modified polyacrylonitrile (PAN) has been proposed at the Czech Technical University in Prague as a universal binding matrix for finely divided inorganic absorbers. The general procedure for the preparation of the resulting inorganic-organic composite absorbers enables preparation of suitably grained composite absorbers [4]. The contents of active component may reach up to 90 % (w/w) in dry residue.

The aim of this study was to verify possibility of extraction of uranium with TiO-PAN and NaTiO-PAN composite absorbers, to compare properties of these two absorbers and to conclude whether they are prospective for uranium collection from surface and/or waste waters.

Hydrated titanium oxide (TiO) and sodium titanate (NaTiO) - the active components of the composite materials - were prepared from industrial intermediate from

production of titanium white. Standard procedure was used to prepare the TiO-PAN and NaTiO-PAN composite absorbers [4]. In the experiments, distilled and tap water were used to compare the influence of the water hardness. pH of the effluent was also measured during the process.

The results showed that practical sorption capacity (10% break-through) from tap water containing  $2.3 \mu\text{g U.mL}^{-1}$  measured at flow rate of  $100 \text{ BV.h}^{-1}$  was  $\sim 4.6 \text{ mg}$  and  $\sim 1.5 \text{ mg}$  of uranium per ml of swollen TiO-PAN and NaTiO-PAN absorber, respectively. The maximum flow rates are  $60 \text{ BV.h}^{-1}$  and  $60\text{-}100 \text{ BV.h}^{-1}$  for TiO-PAN and NaTiO-PAN absorbers, respectively, depending on the concentration of uranium ( $2.3 - 230 \text{ mg U.L}^{-1}$ ). Elution of uranium and regeneration of the absorber may be accomplished by  $0.1 \text{ mol.L}^{-1}$  or stronger solutions of hydrochloric acid for both the absorbers.

Hence, TiO-PAN and NaTiO-PAN composite absorbers were proved to be applicable for extraction of uranium from aqueous solutions. With respect to the measured practical sorption capacity, TiO-PAN composite absorber is more suitable for the uranium collection from surface and/or waste water.

### Keywords

Uranium extraction, TiO-PAN, NaTiO-PAN, composite absorber, fresh water

- [1] Bitte J (1985) *Advances in Uranium Ore Processing and Recovery from Non-Conventional Resources*. IAEA-TC-491/18. IAEA, Vienna, 299
- [2] Kim J, Tsouris C, Mayes RT, Oyola Y, Saito T, Janke CJ, Dai S, Schneider E, Sachde D (2013) *Separ Sci Technol* 48: 367-387
- [3] Lehto J (1987) *Sodium Titanate for Solidification of Radioactive Wastes - Preparation, Structure and Ion Properties*. Academic Dissertation, University of Helsinki. Report Series in Radiochemistry 5/1987
- [4] Šebesta F (1997) *J Radioanal Nucl Chem* 220: 77-88

## USE OF RADON TO CHARACTERISE SURFACE WATER RECHARGE TO GROUNDWATER

N Hermanspahn,<sup>1</sup> M Close,<sup>1</sup> M Matthews,<sup>1</sup> L Burberry,<sup>1</sup> P Abraham,<sup>1</sup>

<sup>1</sup> Institute of Environmental Science and Research (ESR), Christchurch

### Aims

Many groundwater systems in Canterbury and other parts of New Zealand gain a significant amount of recharge from rivers. This recharge provides significant storage of water within the groundwater system and it is used for many purposes, including domestic and stock water supply, irrigation and industrial use. There is significant uncertainty in the amounts of recharge from rivers, particularly large braided systems, as river flow gauging can only be carried out under low flow conditions and measurement errors are large.

Radon-222 is present in a dissolved state in groundwater from alluvial greywacke gravel aquifers in sufficient concentration to be easily detectable (10 – 50 Bq/L) while, in contrast, concentrations in surface water are close to zero (Gregory, 1980). This difference provides a means of distinguishing surface recharge water from groundwater. Surface water infiltrating into groundwater should initially contain negligible radon, but would start accumulating radon as it flows through the aquifer, reaching equilibrium in approximately 6 half-lives ( $T_{1/2} = 3.82\text{d}$ ). In addition to providing a tracer for surface water, this radon ingrowth also allows flow-rate estimation as the radon concentration increases with time at a known rate. The use of radon to estimate recharge of surface water into a groundwater system has been applied at a site in Switzerland (Hoehn & von Gunten, 1989).

The investigation of radon to estimate recharge from rivers to groundwater systems is presented using a relatively well-characterised reach of the Waimakariri River in Canterbury to assess the potential for this method.

### Methods

A reach from the Waimakariri River near McLeans Island just north of Christchurch, was selected as the study site. The river is known to lose water from this reach and there are a number of shallow wells close to the river that are suitable for sampling in this area. Two groups of wells were selected for sampling. The first group of wells was near the river and located at increasing distances from the river. Environment Canterbury had installed 22 wells in 2 arrays at Halketts and Crossbank to study river recharge to groundwater. These wells were sampled on 2-3 occasions. The second group of wells that were sampled were located remote from recent recharge from the river but screened in a similar groundwater environment. This group of wells provide an estimate of equilibrium radon concentrations

and the likely variability within an alluvial gravel groundwater system.

### Results

The results indicate that radon levels in the river are very low and concentrations increased with increasing distance from the river. These results are consistent with radon ingrowth processes and the site hydrology.

The eleven wells from the Crossbank array and eleven wells from the Halketts array were sampled, along with water from the Waimakariri River, at both high and low flows to determine any variation of radon concentrations with flow. There was no significant variation in radon concentration with flow in the Waimakariri River ranging from 50 to 250  $\text{m}^3/\text{s}$ . The data were modelled using the “ingrowth equation” for radon to determine values for the equilibrium radon value and groundwater velocity. The groundwater velocities were 350 and 390 m/day for the Halketts and Crossbank sites, respectively. These velocities are very high but possible near a large braided river.

Estimates of recharge to groundwater over a 20km reach using this information were similar to estimates derived from a water balance approach with the largest source of error being estimates of the effective porosity of the groundwater system.

### References

- Gregory, L.P. 1980. Radioactivity of potable waters: Country-wide survey in New Zealand. NRL report 1980/4. 19 p.
- Hoehn, E.; von Gunten, H.R. 1989. Radon in Groundwater: A tool to assess infiltration from surface waters to aquifers. Water Resources Research 25: 1795-1803.

## Production and Utilization of Radioactive Astatine Isotopes in the ${}^7\text{Li}+{}^{\text{nat}}\text{Pb}$ Reaction

I. Nishinaka<sup>1</sup>, A. Yokoyama<sup>2</sup>, K. Washiyama<sup>2</sup>, R. Amano<sup>2</sup>, E. Maeda<sup>2</sup>, N. Yamada<sup>2</sup>, H. Makii<sup>1</sup>, A. Toyoshima<sup>1</sup>, S. Watanabe<sup>1</sup>, N. S. Ishioka<sup>1</sup>, K. Hashimoto<sup>1</sup>  
<sup>1</sup>Japan Atomic Energy Agency (JAEA)  
<sup>2</sup>Kanazawa University

*Abstract* – Production cross sections of astatine isotopes in 29-57 MeV  ${}^7\text{Li}+{}^{\text{nat}}\text{Pb}$  reaction have been measured by  $\alpha$ - and  $\gamma$ -ray spectrometry. Excitation functions of production cross sections have been compared with a statistical model calculation to study the reaction mechanism of the  ${}^7\text{Li}+{}^{\text{nat}}\text{Pb}$  reaction. A chemical separation of astatine from an irradiated lead target has been studied with a dry-distillation method.

*Keywords* – Astatine, Cross section, Excitation function, Chemical separation, Dry-distillation

### I. INTRODUCTION

An  $\alpha$  radioactive nuclide  ${}^{211}\text{At}$  with a half-life of 7.2 h is a prospective candidate for utilization in targeted alpha radiotherapy. In general,  ${}^{211}\text{At}$  is produced through bombardment of a bismuth target with 28 MeV helium ions in the  ${}^{209}\text{Bi}(\alpha,2n){}^{211}\text{At}$  reaction [1]. However, the nuclear reactions using lithium ion beams,  ${}^{6,7}\text{Li}+\text{Pb}$ , Bi, provide the possible production routes of  ${}^{211}\text{At}$ . Excitation functions have been extensively measured for the  ${}^{6,7}\text{Li}+{}^{209}\text{Bi}$  to study the reaction mechanism involving complete fusion and breakup reaction for weakly bound nuclei  ${}^{6,7}\text{Li}$  [2-4]. For  ${}^7\text{Li}+{}^{\text{nat}}\text{Pb}$ , however, only reports on production of astatine isotopes  ${}^{207-210}\text{At}$  have been available [5]. Therefore, we have measured excitation functions of  ${}^{207-211}\text{At}$  isotopes in the reaction of 29-57 MeV  ${}^7\text{Li}+{}^{\text{nat}}\text{Pb}$ . Besides, a chemical separation of carrier-free radioactive astatine isotopes from an irradiated lead target has been studied with a dry-distillation method.

### II. EXPERIMENT

Lead targets with thickness of 0.78-1.47 mg/cm<sup>2</sup> were prepared with vacuum evaporation onto a backing sheet of aluminum. Each target was sandwiched between the backing and a cover sheet of 2.7 or 5.4 mg/cm<sup>2</sup> of aluminum. Six sets of the bismuth target, the backing and the cover sheet were irradiated with  ${}^7\text{Li}^{3+}$  beams of 50 and 60 MeV from the 20 MV tandem accelerator at JAEA-Tokai. Activities of  ${}^{207-210}\text{At}$  were determined by  $\gamma$ -ray spectrometry to obtain production cross sections of  ${}^{207-210}\text{At}$ . Details of irradiation and  $\gamma$ -ray spectrometry are described in [6].

The sample used for  $\gamma$ -ray spectrometry which consists of the lead target on the backing and the cover sheet was placed in a test tube with length of 18 cm. After sealing the test tube, a third of the portion from the bottom of the test tube was inserted into a furnace. Astatine was distilled at 650°C for 15-40 min. After cooling and opening the test tube and taking the

sample from it, the test tube was rinsed with 1.8 ml ethanol, water, or diisopropyl ether. The solution is used for the preparation of a sample for  $\alpha$ - and  $\gamma$ -ray spectrometry. The activities of astatine in the solution were measured to obtain production cross sections of  ${}^{211}\text{At}$  and chemical yields in the dry-distillation method.

### III. RESULTS

The obtained excitation functions of astatine isotopes in the  ${}^7\text{Li}+{}^{\text{nat}}\text{Pb}$  were rather well reproduced with a statistical model calculation by the HIVAP code [7]; the calculation was independently carried out with the input parameters which systematically well reproduce a large number of experimental fusion-evaporation cross sections in the similar heavy-ion reactions without adjusting the input parameters to fit the present data [8]. Slightly large deviations of experimental data from the calculation are observed at higher incident energies, indicating the effect of breakup reaction of  ${}^7\text{Li}$ .

In the  $\alpha$ - and  $\gamma$ -spectrometry, only activities of astatine isotopes and their decaying daughters were observed in the samples prepared from the solution which obtained by the dry-distillation method. It shows that carrier free radioactive astatine isotopes were separated from lead targets with high radiochemical purity. Overall recovery yields of astatine in the dry-distillation method were approximately 65% for ethanol and water, and 25% for diisopropyl ether, implying chemical form of carrier free astatine. Using the ethanol solution of astatine, astatinated amino acid derivative was prepared in the high labeling yield, more than 97%, with electrophilic destannylation [9]. It indicates that the dry-distillation method provides carrier free astatine isotopes with high chemical purity.

- [1] S. Lindergren, T. Bäch, H. J. Jensen, *Appl. Radiat. Isot.*, 55 (2001) 157-160; S. Lindgren et al., *J. Nucl. Med.*, 49 (2008) 1537-1545.
- [2] H. Freiesleben et al., *Phys. Rev. C*, 10 (1974) 245-249.
- [3] M. Dasgupta et al., *Phys. Rev. C*, 66 (2002) 04602-1-4; M. Dasgupta et al., *Phys. Rev. C* 70 (2004) 024606-1-20.
- [4] Yu. E. Penionzhkevich et al., *J. Phys. G*, 36 (2009) 025104-1-12.
- [5] K. Roy and S. Lahiri, *Appl. Radiat. Isot.*, 55 (2008) 571-576; M. Maiti and S. Lahiri, *Phys. Rev. C*, 84 (2011) 067601-1-4.
- [6] I. Nishinaka et al., *JAEA-Review 2011-040* (2011) 50-51
- [7] W. Reisdorf and M. Schädel, *Z. Phys. A*, 343 (1992) 47.
- [8] K. Nishio, private communication.
- [9] S. Watanabe et al., 7<sup>th</sup> Int. Sym. On Radiohalogens (7ISR), Sep18th (2012), Whistler, BC

## Production of actinium-225 from natural thorium irradiated with protons

Aleksandr N. Vasiliev<sup>1</sup>, Valentina S. Ostapenko<sup>1</sup>, Ramiz A. Aliev<sup>1</sup>, Stepan N. Kalmykov<sup>1</sup>,  
 Elena V. Lapshina<sup>2</sup>, Stanislav V. Ermolaev<sup>2</sup> and Boris L. Zhuikov<sup>2</sup>

<sup>1</sup>Chemistry Department, Lomonosov Moscow State University, Leninskie Gory, Moscow 119991, Russia

<sup>2</sup>Institute for Nuclear Research of Russian Academy of Sciences, 60<sup>th</sup> October Anniversary Prospect, 7a, Moscow 117312, Russia

*New procedure for chemical separation and purification of <sup>225</sup>Ac from irradiated metallic Th targets for targeted radiotherapy of cancer is described.*

*Keywords – actinium-225, thorium, extraction chromatography*

As a result of irradiation of natural thorium with high-energy protons various fission and activation products of <sup>232</sup>Th are formed [1, 2]. Among them <sup>225</sup>Ac is formed, which has characteristics that enable to use it in radiotherapy of cancer. There is a growing demand for this radionuclide, while current methods for producing actinium have significant limitations and cannot satisfy it completely. Production of actinium from <sup>233</sup>U is limited by its inaccessibility. Actinium-225 may be used either directly for preparation of radioimmunoconjugates or as a mother radionuclide in <sup>213</sup>Bi isotope generator. In addition the formation of <sup>223</sup>Ra should be noted, which is also a promising  $\alpha$ -emitter for medicine.

The aim of this work is to develop the new method of chemical separation and purification of large quantities of <sup>225</sup>Ac from metallic Th irradiated with high-energy protons.

Radiochemical separation of Ac and Ra is a difficult task since a high activity of more than 80 other radionuclides have been observed in the gamma- and alpha-spectrum of Th-target after irradiation.

A developed method for chemical isolation of Ac is based on combination of liquid-liquid extraction and extraction chromatography.

Irradiated thorium is dissolved in a mixture of concentrated hydrochloric and nitric acids, or in concentrated nitric acid with the addition of catalytic amounts of hydrofluoric acid.

Tributylphosphate, trioktylphosphin oxide (TOPO) and di(2-ethylhexyl)orthophosphoric acid (HDEHP) are used in extraction experiments. The behavior of radionuclides, depending on the composition of the aqueous phase is studied.

For additional separation of remaining Th AG 1x8 (BioRad) anionite column and extraction chromatographic sorbent TEVA (Eichrom, mixture of trioctyl and tridecyl methyl ammonium chloride as extracting agent) are proposed. Sorption capacity of under experimental conditions (6 M HNO<sub>3</sub>) for those sorbents is investigated.

Sorbents DGA Resin (Eichrom), Ln Resin (Eichrom), TRU Resin (Eichrom), TDi-2 (Karpov Institute) are taken for

further chromatographic separations. The sorption behavior of radionuclides, depending on the parameters of the column and acidity of solution is given. It is shown that <sup>225</sup>Ac quantitatively adsorbed on Ln Resin and TDi-2 (di(2-ethylhexyl)orthophosphoric acid (HDEHP) as extracting agent) from dilute nitric acid (0.05 M HNO<sub>3</sub>). Desorption is carried out with acid of higher concentration (3 M). Significant difference in the sorption behavior of <sup>225</sup>Ac for Ln Resin and TDi-2 is not observed. In 0.05 M HNO<sub>3</sub> most of the fission products (Cs, Ra, Ba, Ag, Pb), are not retained on the column and are eluted in the first few milliliters. After switching to 3 M HNO<sub>3</sub>, actinium and rare earth elements (La, Nd and Ce) and ruthenium are eluted together in the fraction of 3 ml. On DGA Resin (N,N,N',N' tetroctyldiglicolamide as extracting agent) Ac absorbed from 6 M nitric acid solution and desorbed with dilute nitric acid (0.01 M HNO<sub>3</sub>). In this way it is possible to separate actinium fraction from ruthenium, this radionuclide makes some difficulties for the production of final preparation <sup>225</sup>Ac.

Actinium is eluted together with cerium and lanthanum. To separate Ac(III) from rare earth elements the eluted 3 ml fraction from Ln or DGA Resin (in 3 M HNO<sub>3</sub>) is loaded onto extraction-chromatographic columns filled with TRU Resin (octylphenyl-N,N-di-isobutyl carbomoylphosphine oxide dissolved in TBP as extracting agent).

The possible scheme of separation of <sup>225</sup>Ac from the isotopes produced in irradiated thorium target is includes two sequential solvent extractions using HDEHP. After sorption on DGA Resin, for further separation the 3 M nitric acid can be passed through the sorbent TRU Resin. The procedure provides obtaining a pure Ac fraction, containing less than 0.2% <sup>227</sup>Ac and no other radionuclides; the chemical yield is 90% or more [3].

- [1] S.V. Ermolaev, B.L. Zhuikov, V.M. Kokhanyuk, V.L. Matushko, S.N. Kalmykov, R.A. Aliev, I.G. Tananaev and B.F. Myasoedov. Production of actinium, thorium and radium isotopes from natural thorium irradiated with protons up to 141 MeV, Radiochim. Acta, 100, 1–7, 2012.
- [2] B.L. Zhuikov, S.N. Kalmykov, S.V. Ermolaev, R.A. Aliev, V.M. Kokhanyuk, Produce of <sup>225</sup>Ac and <sup>223</sup>Ra from thorium irradiated with protons, Radiochemistry, 2011, 53, 1, p. 66-72.
- [3] B.L. Zhuikov, S.N. Kalmykov, R.A. Aliev, S.V. Ermolaev, V.M. Kokhanyuk, V.M. Kokhanyuk, I.G. Tananaev and B.F. Myasoedov, A method of producing actinium-225 and radium isotopes and targets for its implementation (Options). Patent № 2373589, Russian Federation, 2009.

## Development of $^{99}\text{Mo}$ - $^{99\text{m}}\text{Tc}$ Domestic Production with High-Density $\text{MoO}_3$ Pellets by $(n, \gamma)$ Reaction

K. Tsuchiya<sup>\*1</sup>, M. Tanase<sup>\*2</sup>, T. Shiina<sup>\*2</sup>, A. Ohta<sup>\*2</sup>, M. Kobayashi<sup>\*3</sup>,  
A. Yamamoto<sup>\*3</sup>, Y. Morikawa<sup>\*3</sup>, M. Kaminaga<sup>\*1</sup>, H. Kawamura<sup>\*1</sup>

<sup>\*1</sup> : Japan Atomic Energy Agency, 4002 Narita, Oarai, Higashiibaraki, Ibaraki 311-1393, Japan

<sup>\*2</sup> : Chiyoda Technol Corporation, 3681 Narita, Oarai, Higashiibaraki, Ibaraki 311-1313, Japan

<sup>\*3</sup> : FUJIFILM RI Pharma Co. Ltd., 453-1 Shimo-okura, Matsuo, Sammu, Chiba 289-1592, Japan

*Keywords* –  $(n, \gamma)^{99}\text{Mo}$  production, high-density  $\text{MoO}_3$  pellets, solvent extraction,  $^{99\text{m}}\text{Tc}$  solution, JMT

demonstration tests will be carried out with the irradiated  $\text{MoO}_3$  pellets in JMTR.

The renewed JMTR will start rerunning from the later half of JFY2013, and it is expected to contribute to many fields not only developments for nuclear materials, but also the other fields such as medical diagnosis medicine, science and technology for fusion reactor, etc. As one of effective applications of the JMTR, JAEA has a plan to produce  $^{99}\text{Mo}$  by  $(n, \gamma)$  method ( $(n, \gamma)^{99}\text{Mo}$  production), a parent nuclide of  $^{99\text{m}}\text{Tc}$ .  $^{99\text{m}}\text{Tc}$  is most commonly used as a radiopharmaceutical in the field of nuclear medicine. In case of Japan up to now, the supplying of  $^{99}\text{Mo}$  depends only on imports from foreign countries. Thus, the  $(n, \gamma)^{99}\text{Mo}$  production was selected from viewpoints of safety, nuclear proliferation resistance and waste management and the R&D for domestic production were started in JMTR. The main R&D items for  $(n, \gamma)^{99}\text{Mo}$  production are as follows;

- (1) Fabrication development of irradiation target for the high-density  $\text{MoO}_3$  pellets,
- (2) Separation and concentration development of  $^{99\text{m}}\text{Tc}$  by the solvent extraction from  $^{99}\text{Mo}/^{99\text{m}}\text{Tc}$  solution, and
- (3) Examination of  $^{99\text{m}}\text{Tc}$  solution for a medicine.

In this study, the status of the R&D is presented for the  $(n, \gamma)^{99}\text{Mo}$  production. Molybdenum oxide ( $\text{MoO}_3$ ) is the most commonly used chemical form as irradiation target for the  $(n, \gamma)^{99}\text{Mo}$  production. The  $\text{MoO}_3$  pellet with high sintering density has been developed for large quantity  $(n, \gamma)^{99}\text{Mo}$  production, and the trial fabrication tests of  $\text{MoO}_3$  pellets were carried out by the plasma sintering method. The solvent extraction method employs MEK to extract  $^{99\text{m}}\text{Tc}$  from  $^{99}\text{Mo}/^{99\text{m}}\text{Tc}$  solution. The extracted  $^{99\text{m}}\text{Tc}$  content by the  $(n, \gamma)^{99}\text{Mo}$  production is less than that by the  $(n, f)$  methods and the concentration methods of  $^{99\text{m}}\text{Tc}$  solution were developed in the  $^{99\text{m}}\text{Tc}$  extraction devices. In the tests, rhenium (Re) was used instead of  $^{99\text{m}}\text{Tc}$  because Re and Tc were homologous elements. The R&D will be carried out with foreign organizations using  $^{99\text{m}}\text{Tc}$  based on the preliminary results with Re in the present work. It is important for medical use to determine detailed specifications of  $^{99\text{m}}\text{Tc}$  solution. In the preliminary tests with practice solution using Re, chemical purities such as Mo, Al and MEK were measured in the solution and the content of impurities will satisfy the requirement of radiopharmaceuticals. In future, the solvent extraction

## Preparation of $^{99}\text{Mo}$ - $^{99\text{m}}\text{Tc}$ by using Spallation Neutron

Y. Hayashi<sup>\*1</sup>, N. Takahashi<sup>1</sup>, K. Nakai<sup>1</sup>, H. Ikeda<sup>2</sup>, G. Horitsugi<sup>2</sup>, T. Watabe<sup>2</sup>, Y. Kanai<sup>2</sup>, H. Watabe<sup>2</sup>,  
E. Shimosegawa<sup>2</sup>, Y. Miyake<sup>2</sup>, J. Hatazawa<sup>2</sup>, M. Fukuda<sup>3</sup>, K. Hatanaka<sup>3</sup>, K. Takamiya<sup>4</sup>, S.  
Yamamoto<sup>5</sup>,  
Y. Kasamatsu<sup>1</sup> and A. Shinohara<sup>1</sup>

<sup>1</sup> Graduate School of Science, Osaka University

<sup>2</sup> Graduate School of Medicine, Osaka University

<sup>3</sup> Research Center for Nuclear Physics, Osaka University

<sup>4</sup> Kyoto University Research Reactor Institute

<sup>5</sup> Graduate School of Medicine, Nagoya University

*Abstract* – We developed the method for preparation of  $^{99\text{m}}\text{Tc}$  used for diagnostic radiopharmaceuticals. We produced  $^{99}\text{Mo}$ , the mother nuclide of  $^{99\text{m}}\text{Tc}$ , by the  $^{100}\text{Mo}(n,2n)^{99}\text{Mo}$  reaction using the spallation neutron which was produced by 400 MeV proton from a ring cyclotron. The  $^{99\text{m}}\text{Tc}$  was extracted with methyl ethyl ketone and purified with an aluminum column. Furthermore, we demonstrated the bone scintigraphy by injecting  $^{99\text{m}}\text{Tc}$ -MDP into the rats.

*Keywords* –  $^{99\text{m}}\text{Tc}$ ,  $^{99}\text{Mo}$ , Spallation neutron, Methyl ethyl ketone (MEK), Aluminum column

### I. INTRODUCTION

The  $^{99\text{m}}\text{Tc}$  is one of most important radioisotopes used for diagnostic radiopharmaceuticals today. The most of those are made with the several nuclear reactors in the world. However, all those reactors using highly enriched  $^{235}\text{U}$  fuel are aged more than 50 years, their deteriorations are anticipated and many alternative methods were explored for the production of  $^{99\text{m}}\text{Tc}$ , as the  $^{100}\text{Mo}(p, 2n)^{99\text{m}}\text{Tc}$  and  $^{100}\text{Mo}(p, d)^{99}\text{Mo}$  reactions. In our previous work, we tested to produce  $^{99\text{m}}\text{Tc}$  with spallation neutron by the  $^{100}\text{Mo}(n, 2n)^{99}\text{Mo}$  reaction which has larger cross section than the proton induced reactions. The radioactivity of  $^{99}\text{Mo}$  produced was 3MBq/( $\mu\text{A h g}$ ) and this result suggested that enough radioactivities of  $^{99}\text{Mo}$  for the medical use can be obtained with this method. However, the specific activity of  $^{99}\text{Mo}$  produced by an accelerator is very low,  $^{99\text{m}}\text{Tc}$  cannot be separated by the conventional alumina and PZC columns. In this work, we separated  $^{99\text{m}}\text{Tc}$  from macro amount of natural Mo by the solvent extraction with methyl ethyl ketone (MEK) and further purified it with the aluminum column. In addition we demonstrated the bone scintigraphy with the purified  $^{99\text{m}}\text{Tc}$  as a preclinical test.

### II. EXPERIMENTAL

We performed separation of  $^{99\text{m}}\text{Tc}$  by the previously mentioned method using commercial  $^{99\text{m}}\text{Tc}$  and macro amount of  $^{\text{nat}}\text{Mo}$  and examined the purity of the  $^{99\text{m}}\text{Tc}$  first. We prepared the Mo and  $^{99\text{m}}\text{Tc}$  mixture by dissolving 40 g of  $^{\text{nat}}\text{MoO}_3$  and 60 MBq of commercial  $^{99\text{m}}\text{Tc}$  solution with 120 mL of 4 M sodium hydroxide solution. The  $^{99\text{m}}\text{Tc}$  nuclide was extracted with 15 mL of MEK from macro amount of natural Mo. After the evaporation of the MEK solution under reduced pressure, the sample was dissolved

with a few ml of saline. The solution was passed through the neutral aluminum column to remove the Mo species by adsorbing them on the column. Amount of impurities in the  $^{99\text{m}}\text{Tc}$  solution were measured with ICP-MS and yield of  $^{99\text{m}}\text{Tc}$  was determined by gamma-ray measurement using a germanium semiconductor detector. Furthermore, the purified  $^{99\text{m}}\text{Tc}$  was labeled into MDP and injected into a rat. We determined the labeling efficiency of  $^{99\text{m}}\text{Tc}$ -MDP using a silica-gel-coated thin layer chromatography plate. We took the bone scintigraphy of the rat using a gamma camera [1].

### III. RESULTS & DISCUSSION

As the results of measurement with ICP-MS, we found that only less than 10 ppb of Mo and Al coexist in the purified  $^{99\text{m}}\text{Tc}$  solution. No other impurities were detected and this solution satisfied the demand of the United States Pharmacopeia (USP). The yield of  $^{99\text{m}}\text{Tc}$  was 75-90% and the volume was only 5 mL. The labeling efficiency of the  $^{99\text{m}}\text{Tc}$ -MDP was higher than 99%, well above the USP requirement (>90%). We obtained the bone scintigram which is not different from that obtained using commercial  $^{99\text{m}}\text{Tc}$  as shown in Fig.1. Thus, it is thought that this separation technique is available for preparation of  $^{99\text{m}}\text{Tc}$ . We have plan to separate  $^{99\text{m}}\text{Tc}$  from  $^{99}\text{Mo}$  produced by the  $^{100}\text{Mo}(n, 2n)^{99}\text{Mo}$  reaction and to demonstrate the bone scintigraphy. In this presentation, we will also report the results of these experiments.

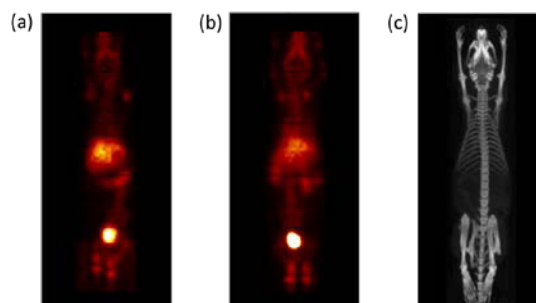


Fig.1 Bone scintigram by injecting with  $^{99\text{m}}\text{Tc}$ -MDP into the rat  
(a: purified  $^{99\text{m}}\text{Tc}$ , b: commercial  $^{99\text{m}}\text{Tc}$ , c:CT image)

[1] S Yamamoto et al., Med Phys. 39. 581. 8. (2012)

## Development of Automated Measurement System for Radioactive Intensities of Sealed Small Radiation Sources (Iodine-125 Seed Source) for Brachytherapy

M. Sakama,<sup>1,\*</sup> H. Ikushima,<sup>2</sup> T. Saze,<sup>3</sup> Y. Nagano,<sup>4</sup> T. Yamada,<sup>5</sup> T. Ichiraku,<sup>5</sup> H. Takai,<sup>5</sup> Y. Kuwahara,<sup>6</sup> and S. Nakayama<sup>7</sup>

<sup>1</sup>Department of Radiological Science (also Advanced Radio-Analytical Chemistry, Division of Biomedical Information Sciences, Institute of Health Biosciences, The University of Tokushima, Tokushima 770-8509, JAPAN

<sup>2</sup>Department of Radiation Therapy Technology, Division of Biomedical Information Sciences, Institute of Health Biosciences, The University of Tokushima, Tokushima 770-8509, JAPAN

<sup>3</sup>Otsuka Pharmaceutical Factory, Naruto, Tokushima 772-8601, JAPAN

<sup>4</sup>Department of Radiological Science, Division of Biomedical Information Sciences, Institute of Health Biosciences, The University of Tokushima, Tokushima 770-8509, JAPAN

<sup>5</sup>Dairyu Co. Ltd., Anan, Tokushima 774-0045, JAPAN

<sup>6</sup>Radioisotope Center, The University of Tokushima, Tokushima 770-8503, JAPAN

<sup>7</sup>Department of Nuclear Science, Institute of Socio-Arts and Sciences, The University of Tokushima, Tokushima 770-8502, JAPAN

We have developed full automated measurement system for radioactive intensities of sealed small radiation sources (iodine-125 seed source) for brachytherapy in this work. Today, quality assurance (QA) of I-125 seed radioactive sources for brachytherapy following AAPM (American Association of Physicists in Medicine) Society's guideline is one of important subjects for hospitals that operate on patients for prostate cancer and medical companies that manufacture and sell these radioactive sources. In order to survey defective seed products into all the number of I-125 seed sources (there are usually fifteen seeds, one seed of dimensions is 0.8 mm  $\phi$   $\times$  4.5 mm length) within a cartridge, we have applied the method of single slit collimator with moving a radiation detector to measure each radioactive intensity of these I-125 seeds. As a result, it was found that our developed system in the present work has good performance of surveying the defective products manufactured with radioactive intensities out of about  $\pm 15\%$  error ( $p < 0.05$ ).

### I. INTRODUCTION

Today, there is no doubt about increasing in the patient population of prostate cancer year after year. Since the authorization from the Ministry of Health, Labor and Welfare in 2003, a brachytherapy using I-125 seeds has been one of most effective therapies of primary and middle stages of prostate cancer in Japan, and all the number of annual clinical operations in Japan has been probably reached to about 3,500 in 2012. In terms of safety management on quality assurance (QA) for the brachytherapy, such kinds of the guidelines stated from AAPM Society [1] and JASTRO (Japanese Society for Therapeutic Radiology and Oncology) have recommended that each radioactive intensity of I-125 seed sources should be appropriately surveyed before the therapy of prostate cancer. However, in fact, there are only a few facilities such as surveying the radioactive intensity of I-125 seed source in Japan. It should be seemed that additional works such as QA make radiologic workers in hospital bothered due to time consuming and also exposed due to operations of these radioactive sources using a dose meter like an ionization chamber. The purpose of this work is to develop full automated measurement system for radioactive intensities of I-125 seed source to comply with the demands of medical workers.

### II. MATERIALS AND METHODS

The system has external dimensions of 600 mm width  $\times$  700 mm depth  $\times$  850 mm height and consists of a cartridge holder, NaI scintillation survey meter and drive mechanism, and a data analysis module. The survey meter is set behind a copper and stainless steel plate containing a slit (0.1 mm thick-

ness). Radioactivity of the seeds within a cartridge is measured by the survey meter that is moved slowly (0.1 mm/sec) in front of the cartridge by the drive mechanism. The survey meter detects gamma rays passing through the slit in the plate. By keeping the seeds inside the cartridge, their individual activities can be measured while maintaining a sterile state.



FIG. 1. Photograph view of our developed system (BSQAS-2).

### III. RESULTS

The system can automatically complete the activity measurement of all seeds contained inside 4 cartridges in less than 15 minutes, with about 15% of errors to detect miss-calibrated seed. This system enables us to survey the defective products manufactured with radioactive intensities out of about  $\pm 15\%$  error ( $p < 0.05$ ).

### IV. CONCLUSIONS

A full automatic measurement system of I-125 seed activity shows reliable precision and usability. Future development will include support for other source delivery methods parallel to efforts in reducing the size of the system.

[1] AAPM, MED. PHYS. **26**(10), 2054-2076 (1999).

\* Corresponding author, electronic address: sakama@medsci.tokushima-u.ac.jp, or; minorusakama@tokushima-u.ac.jp

## Extraction of astatine isotopes for development of radiopharmaceuticals

E. Maeda<sup>1</sup>, A. Yokoyama<sup>2</sup>, T. Taniguchi<sup>1</sup>, K. Washiyama<sup>3</sup>, I. Nishinaka<sup>4</sup>

<sup>1</sup>Grad. School Nat. Sci., Tech. Kanazawa Univ., <sup>2</sup>Inst. Sci. Eng., Kanazawa Univ.

<sup>3</sup>Sch. of Health Sci., College of Med., Pharma. Health Sci., Kanazawa Univ.

<sup>4</sup>ASRC, Japan Atomic Energy Agency

**Abstract**—The <sup>211</sup>At isotope has gathered attention as a promising  $\alpha$ -emitter for radionuclide therapy. We report the dependence of the distribution ratio of astatine on the concentration of HCl, and on the polarity of the organic solvent. The results will be useful for development of the <sup>211</sup>Rn-<sup>211</sup>At generator.

**Keywords**—Astatine / radiopharmaceutical / Distribution ratio / Organic solvent

### I. INTRODUCTION

Because of the short path length in tissues (<100  $\mu$  m) and the high linear energy transfer (~100 keV/ $\mu$  m),  $\alpha$ -particle therapy is expected to kill specific tumor cells efficiently with a low level of damage to surrounding tissues. There are approximately 100 radionuclides that decay with  $\alpha$ -particle emission. Among them, an <sup>211</sup>At isotope with a proper half-life (7.2 h), has gathered attention as a promising  $\alpha$ -emitter for radionuclide therapy. Because astatine isotopes are produced via a nuclear reaction, we have to separate astatine isotopes from irradiated targets with high purity. But, the chemical properties of astatine isotopes are not well known for that purpose. In order to research for preparation of astatine for a radiopharmaceuticals, we prepared for astatine isotopes by the reaction of <sup>nat</sup>Pb(<sup>7</sup>Li, xn)<sup>209-211</sup>At at the tandem accelerator of Japan Atomic Energy Agency–Tokai. We report dependence of the distribution ratio of astatine on the concentration of HCl, and on the polarity of the organic solvent as a part of the study.

### II. EXPERIMENTS

#### 1. Dependence of the concentration of HCl

A lead target (0.74 mg/cm<sup>2</sup>) was irradiated with 50MeV <sup>7</sup>Li beam with a current of 120~200 nA using the tandem accelerator of JAEA-Tokai, so that we prepared for astatine isotopes by the reaction of <sup>nat</sup>Pb(<sup>7</sup>Li, xn)<sup>209-211</sup>At. We put on irradiated target into a test tube and heated up at 650 °C for about 20 minutes in a electric furnace. Then carrier-free astatine was separated from the lead target by dry distillation. After the dry distillation, we trapped astatine isotopes in 4 M HCl solution. We adjusted the concentration of HCl (1~8 M) and then extracted astatine isotopes by shaking with an equal volume of DIPE for 5 minutes. The  $\gamma$ -activity of each phase was measured by a HPGe detector, and the distribution ratio of astatine isotopes was calculated by the measurements.

#### 2. Dependence of the polarity of organic solvent

Astatine isotopes are produced and distilled as in the previous section. Then astatine isotopes were trapped from test tube in 8 M HCl solution. They are extracted by shaking with equal volume of several different types of polarity of organic solvent for 5 minutes. The  $\gamma$ -activity of each two phase was measured by a HPGe detector and distribution ratio was calculated.

### III. RESULTS

Dependence of the distribution ratio on the concentration of HCl was observed for DIPE as show in Fig. 1. Tends to increase in concentration of HCl, the higher the distribution ratio was observed.

The astatine isotopes were well extracted into DIPE and MIBK, but no significant extraction was observed in toluene and decane as show in Fig. 2. It is assumed that the extraction process of astatine is related to polarity of the organic solvent. These results in this study will be useful for development of the <sup>211</sup>Rn-<sup>211</sup>At generator.

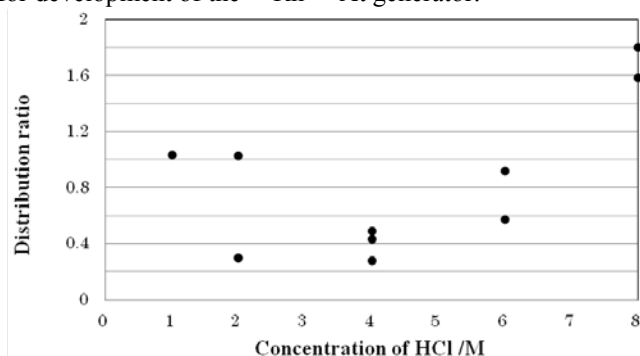


Fig. 1 Distribution ratios for several concentrations of HCl with DIPE.

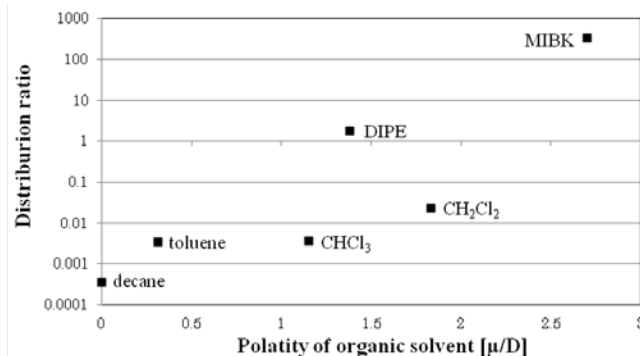


Fig. 2 Distribution ratio for different polarities of organic solvent with 8M HCl.

## Lutetium-177 Complexation of DOTA and DTPA in the Presence of Competing Metals

Satoshi Watanabe<sup>1</sup>, Kazuyuki Hashimoto<sup>2</sup>, Noriko S Ishioka<sup>1</sup>

<sup>1</sup>Medical Radioisotope Application Group, Quantum Beam Science Directorate, Japan Atomic Energy Agency, Takasaki, Gunma 370-1292, Japan

<sup>2</sup>Medical Radioisotope Application Group, Quantum Beam Science Directorate, Japan Atomic Energy Agency, Tokai-mura, Ibaraki 319-1195, Japan

*Abstract* – <sup>177</sup>Lu complexation of DOTA and DTPA is investigated by the addition of Ca(II), Fe(II) and Zn(II). The <sup>177</sup>Lu complexation yield of DTPA was higher than that of DOTA in the presence of Ca(II), Fe(II) and Zn(II). Therefore, it was found that the <sup>177</sup>Lu complexation of DTPA was more advantageous compared with DOTA in the presence of competing metals, Ca, Fe and Zn.

*Keywords* – Lutetium-177, Complexation, DOTA, DTPA, Competing metals

### I. INTRODUCTION

Lutetium-177 is considered to have potential for application in radioimmunotherapy, because it emits  $\beta$ -particles ( $E_{\beta, \max}=498$  keV) suitable to penetrate small tumors and its physical half-life of 6.734 days is long enough for <sup>177</sup>Lu-labeled antibodies to accumulate to tumor sites. In addition, real time imaging of biodistribution can be done by using the <sup>177</sup>Lu, because the energy of  $\gamma$ -rays ( $E_{\gamma}=113$  keV and 208 keV) emitted from <sup>177</sup>Lu is particularly suitable for imaging by single photon emission computed tomography.

We have succeeded in the production of high purity no-carrier-added <sup>177</sup>Lu of capable of labeling antibodies using reversed-phase ion-pair liquid chromatography [1]. Usually, as chelating agents of the labeling antibodies, DOTA (1,4,7,10-tetraazacyclododecan-N,N',N'',N'''-tetraacetic acid) and DTPA (diethylenetriamine-N,N,N',N'', N'''-pentaacetic acid) are mainly used. Therefore, we carried out the labeling experiment of <sup>177</sup>Lu-DOTA-antibody by using the <sup>177</sup>Lu produced in our method in that study. It was found that metallic impurities such as Ca, Fe and Zn inhibited the complexation between <sup>177</sup>Lu and DOTA. However, the details of the inhibition by the metallic impurities have not been understandable. Therefore, in the present paper, the <sup>177</sup>Lu complexation of DOTA and DTPA is investigated by the addition of competing metals, Ca, Fe and Zn.

### II. EXPERIMENTAL

The <sup>177</sup>Lu used in this experiment was produced by <sup>176</sup>Lu(n,  $\gamma$ )<sup>177</sup>Lu process. For the experiment of <sup>177</sup>Lu complexation of DOTA and DTPA, to the mixture of 5  $\mu$ L of the <sup>177</sup>Lu solution ( $5.0 \times 10^{-5}$  M as Lu) and 5  $\mu$ L solution of the competing metal (Ca(II), Fe(II) or Zn(II)) in a prescribed concentration, 0.875  $\mu$ L of acetate buffer (3 M, pH=6.0) was added. After that, a 10  $\mu$ L solution of DOTA or DTPA ( $5.0 \times 10^{-5}$  M) was added. After incubating for 1.5 hours at 40°C, the complexation yield,

which was defined as a percentage of the radioactivity of <sup>177</sup>Lu-DOTA or <sup>177</sup>Lu-DTPA to that of <sup>177</sup>Lu used for the complexation, was determined by thin layer chromatography on silica gel ITLC using aqueous ammonia : methanol : water (0.2 : 2 : 4) as a developing solvent. The unreactive <sup>177</sup>Lu remains at the origin point of a silica gel ITLC strip and the <sup>177</sup>Lu-DOTA or <sup>177</sup>Lu-DTPA moves to the solvent front.

### III. RESULTS AND DISCUSSION

Figure 1(a) shows the results of <sup>177</sup>Lu complexation of DOTA and DTPA by the addition of Ca(II). The <sup>177</sup>Lu complexation yield of DOTA decreases with increasing [Ca(II)]/[Lu], while that of DTPA is constant. This result indicates that <sup>177</sup>Lu complexation of DOTA is more inhibited by Ca(II) than that of DTPA.

The results of <sup>177</sup>Lu complexation by the addition of Fe(II) and Zn(II) are shown in Figs.1(b) and 1(c). The <sup>177</sup>Lu complexation yield of both DOTA and DTPA decreases with increasing [Fe(II)]/[Lu] and [Zn(II)]/[Lu]. From comparison between DOTA and DTPA, the decrease of the complexation yield of DOTA was rather high compared with that of DTPA in both cases of Fe(II) and Zn(II). Therefore, the inhibition for the <sup>177</sup>Lu complexation of DOTA is higher than that of DTPA.

Consequently, the <sup>177</sup>Lu complexation of DOTA was more inhibited by Ca(II), Fe(II) and Zn(II) than that of DTPA. Therefore, it was found that the <sup>177</sup>Lu complexation of DTPA was rather advantageous compared with DOTA in the presence of competing metals, Ca, Fe and Zn.

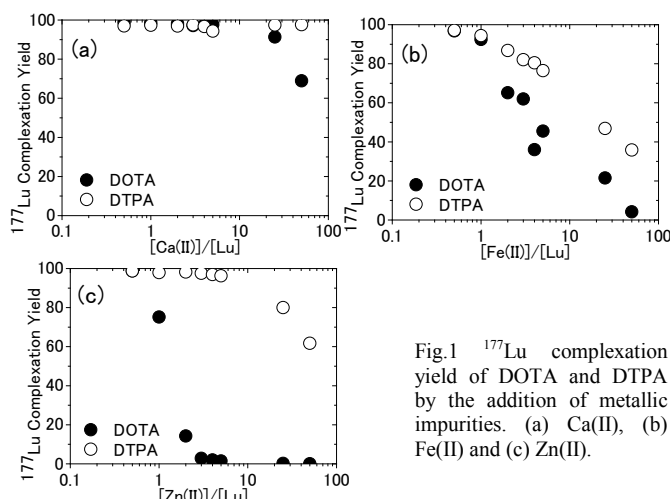


Fig.1 <sup>177</sup>Lu complexation yield of DOTA and DTPA by the addition of metallic impurities. (a) Ca(II), (b) Fe(II) and (c) Zn(II).

[1] Japanese patent application, 2010-223827.

## Hyperfine Fields at $^{140}\text{Ce}$ in He-Doped Fe

Y. Ohkubo<sup>1</sup>, A. Taniguchi<sup>1</sup>, Q. Xu<sup>1</sup>, M. Tanigaki<sup>1</sup>, K. Sato<sup>1</sup> and M. Tsuneyama<sup>2</sup>

<sup>1</sup>Research Reactor Institute, Kyoto University, Kumatori-cho, Sennan-gun, Osaka 590-0494, Japan

<sup>2</sup>Graduate School of Science, Kyoto University, Kitashirakawa, Sakyo-ku, Kyoto 606-8502, Japan

*Abstract* – Room-temperature TDPAC spectra of  $^{140}\text{Ce}$  in an Fe foil and two He-doped Fe foils, all annealed in vacuum at various temperatures were taken in order to see whether Ce and He form complexes in Fe as suggested in first-principles density functional theory calculations. The TDPAC results are presented.

*Keywords* – hyperfine fields,  $^{140}\text{Ce}$ , He-doped Fe, TDPAC, ion implantation, ISOL

### I. INTRODUCTION

The magnetic hyperfine fields at impurity elements in ferromagnetic metals are important quantities because they can be used to determine the magnetic moments of nuclear states having the same atomic number as the impurity elements and moreover, together with the electric field gradients, to test first principles calculations in condensed matter physics. Recently, we implanted  $^{140}\text{Cs}$  in an Fe foil at room temperature with the help of KUR-ISOL and successfully observed an oscillation pattern due to a unique magnetic hyperfine interaction at  $^{140}\text{Ce}$  arising from those  $^{140}\text{Cs}$  in a TDPAC (time-differential perturbed angular correlation) spectrum, which is identical to the one seen in Fig. 1(b). From the known magnetic hyperfine field at  $^{142}\text{Ce}$  in Fe, we have obtained the magnetic moment of the 2083-keV  $4^+$  state of  $^{140}\text{Ce}$  [1]. This time, we have taken room-temperature TDPAC spectra of  $^{140}\text{Ce}$  in an Fe foil (for short,  $^{140}\text{CeFe}$ ) and  $^{140}\text{Ce}$  in two He-doped Fe foils, all annealed in vacuum at various temperatures in order to see whether Ce and He form complexes in Fe as suggested in first-principles density functional theory calculations [2].

### II. EXPERIMENTAL PROCEDURES

Room-temperature implantations of 100-keV  $^{140}\text{Cs}$  ions were performed at KUR-ISOL. Each of three Fe foils was 0.1-mm thick and of 99.995% purity, which had been annealed in  $\text{H}_2$  atmosphere at 700°C for 2 h and then polished. 4-keV He irradiations were carried out at room temperature on two of the foils, one before  $^{140}\text{Cs}$  implantation ( $^{140}\text{CeHe}$ -doped Fe) and the other after  $^{140}\text{Cs}$  implantation ( $^{140}\text{CeFe}$  irradiated with He).

Before and after 0.5-h isochronous annealing in vacuum at various temperatures between 473-1073 K, the time dependences of the coincidence counts  $N(\theta, t)$  of the 329-487 keV cascade  $\gamma$  rays for the three Fe samples were taken at room temperature with two measurement systems, each consisting of standard fast-slow electronic modules and four  $\text{BaF}_2$  scintillation detectors. Here,  $\theta$  and  $t$  denote the angle and the time interval, respectively, between the cascade  $\gamma$  rays. The directional anisotropy  $A_{22}G_{22}(t)$  is obtained as follows:

$$A_{22}G_{22}(t) = 2 \frac{N(180^\circ, t) - N(90^\circ, t)}{N(180^\circ, t) + 2N(90^\circ, t)}. \quad (1)$$

### III. RESULTS

Figure 1 shows a part of the TDPAC spectra obtained for the three samples. Although the TDPAC spectra for the three samples before annealing are identical to the one shown in Fig. 1(b), there can be seen considerable differences among the samples, which may imply the existence of Ce and He complexes in He-doped Fe foils.

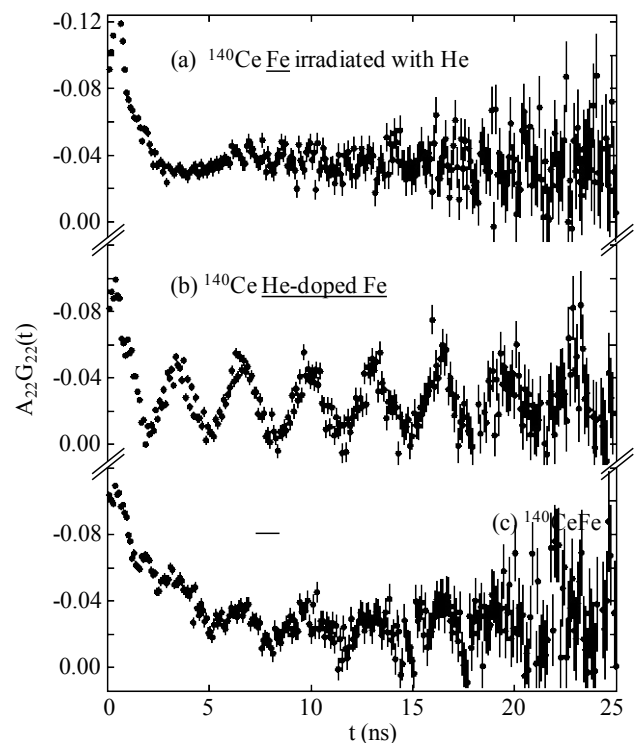


Fig. 1. Room-temperature TDPAC spectra of (a)  $^{140}\text{CeFe}$  irradiated with He, (b)  $^{140}\text{CeHe}$ -doped Fe, and (c)  $^{140}\text{CeFe}$ , all annealed at 673 K in vacuum.

### REFERENCES

- [1] Y. Ohkubo, A. Taniguchi, Q. Xu, M. Tanigaki, N. Shimizu and T. Otsuka, Phys. Rev. C. **87**, 044324 (2013).
- [2] W. Hao and W. T. Geng, Nucl. Instru. Meth. B **280**, 22 (2012).

## Mössbauer studies of lanthanum doped $\text{Ni}_{0.4}\text{Cu}_{0.2}\text{Zn}_{0.4}\text{Fe}_2\text{O}_4$ ferrites by Sol-Gel auto-combustion

Qing Lin<sup>1,2</sup>, Chenglong Lei<sup>1\*</sup>, Haifu Huang<sup>3</sup>, Hui Zhang<sup>1</sup>, Yun He<sup>1</sup>

<sup>1</sup>College of Physics and Technology, Guangxi Normal University, Guilin 541004, China

<sup>2</sup>Department of Information Technology, Hainan Medical College, Haikou 571101, China

<sup>3</sup>Nanjing National Laboratory of Microstructures and Jiangsu Provincial Laboratory for NanoTechnology, Department of Physics, Nanjing University, Nanjing 210093, China

e-mail:hy@gxnu.edu.cn

### Abstract:

In this literature,  $\text{La}^{3+}$  substituted  $\text{Ni}_{0.4}\text{Cu}_{0.2}\text{Zn}_{0.4}\text{Fe}_2\text{O}_4$   $x\text{La}_x\text{O}_4$  ( $0 \leq x \leq 0.15$ ) ferrites by using Sol-Gel auto-combustion route have been prepared. XRD of the powders calcined at  $800^\circ\text{C}/3\text{h}$  show only single phase cubic spinel ferrites and crystalline size decrease sharply, but at high temperature  $950^\circ\text{C}/3\text{h}$  that emerge extra phase  $\text{LaFeO}_3$  when  $x \geq 0.05$  and the crystalline sizes increase linearly. The Mössbauer spectrums at room temperature of samples at  $800^\circ\text{C}/3\text{h}$  vary from magnetic sextet to shrink magnetic sextet and collapse to relaxation doublet ( $x=0.1$ ). This variation of magnetic order state confirms the  $\text{Fe}^{3+}\text{-O}^{2-}\text{-Fe}^{3+}$  super exchange interaction decrease due to  $\text{La}^{3+}$  substitutions. However, when that processed at  $950^\circ\text{C}/3\text{h}$ , The hyperfine magnetic field distribution probability moves to high magnetic field region. The magnetic order for all samples exhibits relaxation sextet magnetic spectra and does not change obviously up to substitution  $x=0.15$ . A broadening line width observed in Mössbauer spectra is interpreted as originating from various cation distributions. The super exchange interaction should have been enhanced and the Curie temperature increases.

**Keywords:** Rare earth, Sol-Gel, XRD, Mössbauer, NiCuZn ferrite, Hyperfine magnetic field

### I. RESULTS AND DISCUSSION

We have successfully prepared ferrite system  $\text{La}^{3+}$  doped  $\text{Ni}_{0.4}\text{Cu}_{0.2}\text{Zn}_{0.4}\text{Fe}_{2-x}\text{La}_x\text{O}_4$  ( $0 \leq x \leq 0.15$ ) by Sol-Gel auto-combustion method. The XRD patterns of ferrite powders calcined at  $800^\circ\text{C}$  and  $950^\circ\text{C}$  are shown in Fig.1 and Fig.2, respectively.

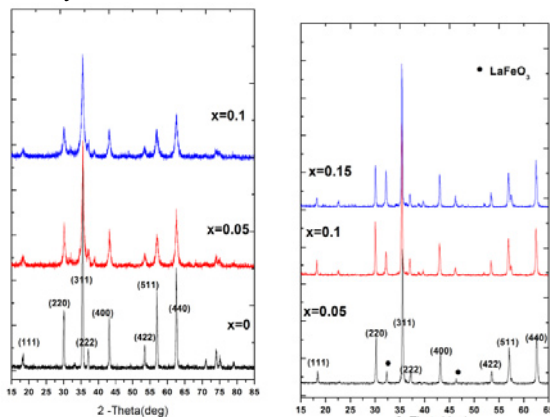


Fig.1 the XRD patterns of samples calcined at 80

Fig.2 the XRD patterns of samples calcined at 950°C

Fig.3 and Fig.4 show the Mössbauer spectra (RT) of  $\text{Ni}_{0.4}\text{Cu}_{0.2}\text{Zn}_{0.4}\text{La}_x\text{Fe}_{2-x}\text{O}_4$  nano-crystalline ferrite powders measured at room temperatures, respectively.

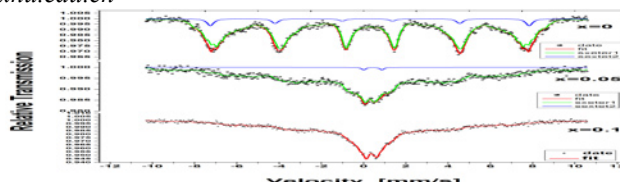


Fig.3 the mossbauer spectra at room temperature of  $\text{Ni}_{0.4}\text{Cu}_{0.2}\text{Zn}_{0.4}\text{La}_x\text{Fe}_{2-x}\text{O}_4$  ( $x=0,0.05,0.1$ ) calcined at  $800^\circ\text{C}$

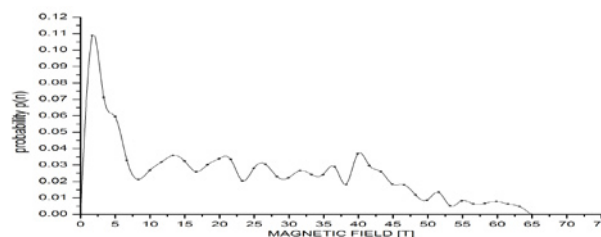


Fig.4 the distribution of super fine magnetic field with  $x=0.05$  calcined at  $800^\circ\text{C}$

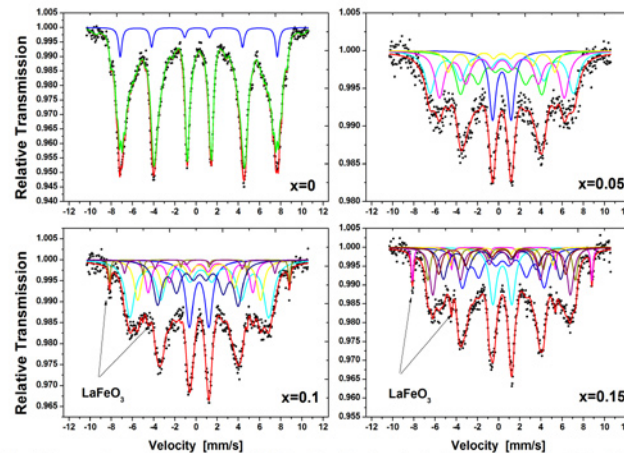


Fig.5 the mossbauer spectra (RT) of  $\text{Ni}_{0.4}\text{Cu}_{0.2}\text{Zn}_{0.4}\text{La}_x\text{Fe}_{2-x}\text{O}_4$  ( $x=0,0.05,0.1,0.15$ ) calcined at  $950^\circ\text{C}$

Fig.5 show the Mössbauer spectra of samples calcined at  $950^\circ\text{C}$ . The differences of Mössbauer spectra compared with the sample calcined at  $800^\circ\text{C}$  confirm that the substitution of  $\text{La}^{3+}$  ions need more bond energy and affect the  $(\text{Fe}^{3+})_A\text{-O}^{2-}\text{-(Fe}^{3+})_B$  super-exchange interaction so that the samples show ferromagnetism because of high sintering temperature.

- [1] Gabal, M.A., et al., *Structural, magnetic and electrical properties of Ga-substituted NiCuZn nanocrystalline ferrite*. Ceramics International, 2010. 36(4): p. 1339-1346.
- [2] Roy, P.K., B.B. Nayak, and J. Bera, *Study on electro-magnetic properties of La substituted Ni-Cu-Zn ferrite synthesized by auto-combustion method*. Journal of Magnetism and Magnetic Materials, 2008. 320(6): p. 1128-1132.
- [3] S.I.Moussa, R.R.Sheha, E.A.Saad, N.A.Tadros, Synthesis and characterization of magnetic nano-material for removal of  $\text{Eu}^{3+}$  ions from aqueous solutions, *Journal of Radioanalytical and Nuclear Chemistry*, 2013. 295: 929-935.

## Analysis of corrosion products formed on anti-weather steel

Matashige OYABU<sup>1</sup>, Ryo SATOH<sup>1</sup>, Kiyoshi NOMURA<sup>2</sup>

<sup>1</sup>Math & Science Division, Kanazawa Institute of Technology,  
 Ohigigaoka 7-1, Nonoichi, Ishikawa, Japan 921-8501

<sup>2</sup>The University of Tokyo,  
 Hongo 7-3-1, Bunkyo-ku, Tokyo, Japan 113-8656

### Abstract

Weathering steels (COR-TEN O) were corroded under the salty or acid rain condition in the laboratory. Corrosion products on weathering steel were analyzed by Mössbauer spectrometry and X-ray diffraction. The kind of products depended on the atmospheric condition.  $\beta$ -FeOOH, which disturbs the performance of weathering steel, was formed under the existence of chloride or fluoride ion. The formations of  $\beta$ -FeOOH,  $\alpha$ -FeOOH,  $\gamma$ -FeOOH and  $\gamma$ -Fe<sub>2</sub>O<sub>3</sub> were studied in various conditions.

### I. INTRODUCTION

In recent years, use of weathering steel is increasing, and it became to be used to about 30% as steel materials for a bridge. Weathering steel is designed to protect the internal corrosion of steel by generating stable rust on the surface without painting. The paint is not needed, and so the cost of painting and maintenance can be reduced. The life may exceed 100 years under good atmosphere condition. The life of weathering steel depends on the environments largely. Especially it is difficult to use the steel under salty environment like coastal area. The stable rust on the surface might be composed of fine  $\alpha$ -FeOOH,  $\gamma$ -FeOOH and magnetite. Those materials may form protection layer on the steel. However,  $\beta$ -FeOOH, which is not protective rust, may be generated under the existence of chloride ion. The formation on the surface and property of  $\beta$ -FeOOH should be studied to improve the performance of weathering steel. In this study, weathering steels were corroded under the different conditions and the corrosion products were analyzed by Mössbauer spectrometry and X-ray diffraction. With regard to  $\beta$ -FeOOH formation, pure material also was synthesized by hydrolysis of iron(III) solution and studied by X-ray diffraction.

### II. EXPERIMENT

**Corrosion test:** The steel plate of COR-TEN O with 1mm thickness was used. It was cut to 80 mm x 60 mm. Corrosion tests were carried out based on JIS H8502 method. Each piece was sprayed with test solutions and kept in dry condition followed by wet condition. One cycle took 12 hours. The cycle was repeated 20 times finally. Test solutions used are 5% NaCl, acid rain (NaCl, HNO<sub>3</sub>, H<sub>2</sub>SO<sub>4</sub>, pH3.5), acid rain "without NaCl", 5% NaF, and 5% (NaF+Na<sub>2</sub>SO<sub>4</sub>), respectively.

X-ray diffractions patterns were measured by Rigaku UltimaIV equipped with Cu target and monochromator, and were analyzed by Rietveld method to identify the crystalline products. Mössbauer spectra were measured at room temperature by using <sup>57</sup>Co(Cr) source and conventional instrument.

### III. RESULT AND DISCUSSION

Mössbauer spectra and the hyperfine distributions were shown in Fig.1. By spraying 5% NaCl solution, strong paramagnetic doublet was observed. It perhaps is due to the  $\beta$ -FeOOH and  $\gamma$ -FeOOH contained in the rust products. With respect to acid rain,  $\alpha$ -FeOOH,  $\gamma$ -FeOOH, and  $\gamma$ -Fe<sub>2</sub>O<sub>3</sub> were identified. The large amount of sextet with 49T due to  $\gamma$ -Fe<sub>2</sub>O<sub>3</sub> was produced under the condition of nitrate and sulfate solution.  $\alpha$ -FeOOH exhibits the broad and collapsed sextet with 34T at RT. The  $\alpha$ -FeOOH is considered to be poor crystalline or fine grains. Any corrosion product is composed from fine grains because the broadening sextets. Detailed discussion will be presented in the poster.

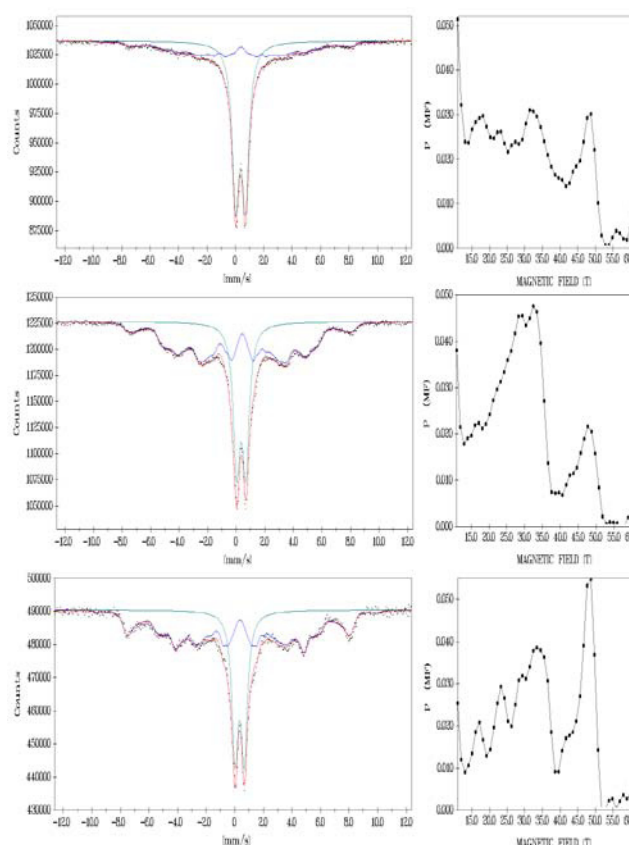


Figure 1 Mössbauer spectra of corrosion products using sprayed solution; (a) 5% NaCl (b) acid rain, and (c) nitrate and sulfate

### Reference

1. "COR-TEN Catalog" published by Nippon Steel
2. Shuichi HARA, Zairyo-to-kankyo, 57, 70-75(2008)

# Study of the Spin-Crossover Phenomena in 1D Coordination Polymers, $[\text{Fe}^{\text{II}}(\text{NH}_2\text{-triazole})_3](\text{C}_n\text{H}_{2n+1}\text{SO}_3)_2$ , by Fe-K edge XAFS and $^{57}\text{Fe}$ Mössbauer Spectroscopy

Hajime Kamebuchi<sup>1</sup>, Akio Nakamoto<sup>1</sup>, Masaya Enomoto<sup>2</sup>, Toshihiko Yokoyama<sup>3</sup>, Norimichi Kojima<sup>1</sup>

<sup>1</sup>Graduate School of Arts and Sciences, The University of Tokyo, Komaba 3-8-1, Meguro-ku, Tokyo 153-8902, Japan

<sup>2</sup>Department of Chemistry, Tokyo University of Science, Kagurazaka 1-3, Shinjuku-ku, Tokyo 162-8601, Japan

<sup>3</sup>Department of Materials Molecular Science, Institute for Molecular Science, Myodaiji-cho, Okazaki 444-8585, Japan

**Abstract** – The spin transition temperature of 1D spin-crossover system,  $[\text{Fe}^{\text{II}}(\text{NH}_2\text{-trz})_3](\text{C}_n\text{H}_{2n+1}\text{SO}_3)_2 \cdot x\text{H}_2\text{O}$  ( $\text{NH}_2\text{-trz}$  = 4-amino-1,2,4-triazole), was systematically controlled through the chemical pressure derived from the alkyl chain of counter-anion. We investigated the influence of the chemical pressure on the spin transition temperature and  $\pi$ -back donation from  $\text{Fe}^{\text{II}}$  ion to  $\text{NH}_2\text{-trz}$  ligand with increasing alkyl chain length by means of  $^{57}\text{Fe}$  Mössbauer and XANES spectra.

**Keywords** – Spin-Crossover,  $^{57}\text{Fe}$  Mössbauer, X-ray absorption

## I. INTRODUCTION

When a transition metal ion with an electron configuration of  $d^4\text{--}d^7$  is octahedrally coordinated by ligands, the ground state has a possibility to change the spin state between high-spin (HS) and low-spin (LS) states by external stimuli. Such the HS-LS transition is called spin-crossover phenomenon. In the past decades, one dimensional  $\text{Fe}^{\text{II}}$  coordination polymers bridged by 4-substituted-1,2,4-triazole (R-trz), whose general formula is  $[\text{Fe}^{\text{II}}(\text{R-trz})_3](\text{A})_2 \cdot x\text{H}_2\text{O}$  ( $\text{A}$  = monovalent anion), have attracted much attention because of their potential applications to molecular electronics or molecular devices [1, 2]. The primary reasons for this are that their spin transition behavior occurs around room temperature with wide thermal hysteresis. Furthermore, their spin transition temperature ( $T_{1/2}$ ) and hysteresis width ( $\Delta T_{1/2}$ ) are controllable by various chemical and physical approaches [1, 3, 4]. This research aims at the control of the spin transition behavior through chemical pressure effect and the analysis of the ligand field by X-ray absorption (XAFS) and  $^{57}\text{Fe}$  Mössbauer spectroscopy for  $[\text{Fe}^{\text{II}}(\text{NH}_2\text{-trz})_3](\text{C}_n\text{H}_{2n+1}\text{SO}_3)_2 \cdot x\text{H}_2\text{O}$  ( $n = 1 - 9$ ).

## II. RESULTS AND DISCUSSION

In  $[\text{Fe}^{\text{II}}(\text{NH}_2\text{-trz})_3](\text{C}_n\text{H}_{2n+1}\text{SO}_3)_2 \cdot x\text{H}_2\text{O}$ ,  $T_{1/2}$  increases in the heating and cooling processes with increasing the alkyl chain length ( $n$ ). In connection with this, there is a close relationship between  $T_{1/2}$  and the nearest neighbor Fe-Fe distance ( $R(\text{Fe-Fe})$ ) estimated from EXAFS (extended X-ray absorption fine structure), which is shown in Figure 1. These are highly suggestive of the increase of intra-chain interaction with the alkyl chain length being attributed to the uniaxial chemical pressure effect induced by self-assembly interaction between alkyl chains, so-called “fastener effect”.

In order to elucidate the effect of uniaxial chemical pressure on  $T_{1/2}$ , the ligand-field strength ( $Dq$ ) and Racah

parameter ( $B$ ) in the HS state were estimated by analysing the pre-edge region in Fe-K edge XANES (X-ray absorption near edge structure) spectra based on the ligand field theory. It is clear from Figure 2 that the increase of  $Dq$  and the decrease of  $B$  were found with increasing  $n$ , which are closely consistent with the relationship between  $T_{1/2}$  and the  $^{57}\text{Fe}$  Mössbauer isomer shift ( $IS$ ) at 200 K. Judging from these results, the following result is derived. The back donation from the 3d orbital of  $\text{Fe}^{\text{II}}$  ion to the  $\pi^*$  orbital of  $\text{NH}_2\text{-trz}$  ( $d_\pi\text{-}p_\pi$  back bonding) is enhanced by the uniaxial chemical pressure due to the fastener effect between the alkyl chains of counter-anion, which induces the expansion of the 3d orbital and the decrease of  $B$  of  $\text{Fe}^{\text{II}}$  ion. Thus  $Dq/B$  increases with the alkyl chain length, which is the key parameter determining  $T_{1/2}$  of spin crossover compounds.

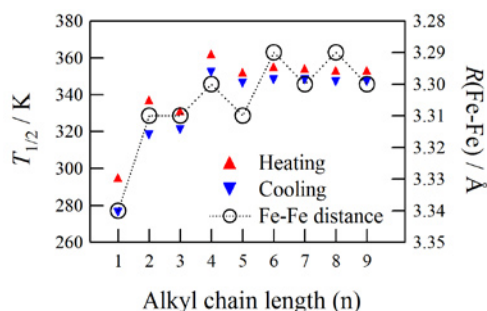


Figure 1. Correlation between spin transition temperature ( $T_{1/2}$ ) and the nearest neighbor Fe-Fe distance ( $R(\text{Fe-Fe})$ ).

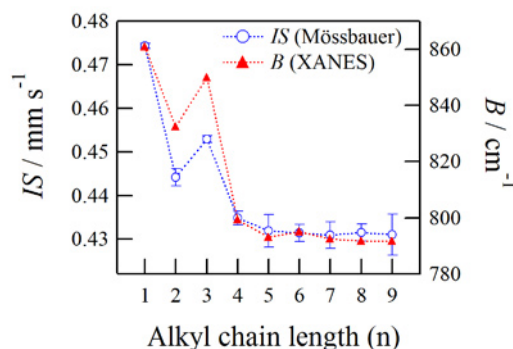


Figure 2. Correlation between  $^{57}\text{Fe}$  Mössbauer Isomer Shift ( $IS$ ) of the LS state and Racah parameter ( $B$ ).

## REFERENCES

- [1] O. Kahn, C. J. Martinez, *Science* 279 (1998) 44.
- [2] M. M. Dîrtu, F. Schmit, A. D. Naik, A. Rotaru, J. Marchand-Brynaert, Y. Garcia, *Int. J. Mol. Sci.* 12 (2011) 5339.
- [3] V. A. Varnek, L. G. Lavrenova, *J. Struct. Chem.* 36 (1995) 104.
- [4] P. Gütllich, V. Ksenofontov, A. B. Gaspar, *Coord. Chem. Rev.* 249 (2005) 1811.

# Mössbauer Spectroscopic and Powder X-ray Diffraction Studies on Incorporation of Gaseous Organic Molecules into Intermolecular Nano-voids of Mixed-valence Trinuclear Iron Pentafluorobenzoate Complex

Yoichi Sakai<sup>1</sup>, Satoru Onaka<sup>1</sup>, Ryo Ogiso<sup>1</sup>, Masashi Takahashi<sup>2</sup>,  
Tadahiro Nakamoto<sup>3</sup>, and Tsutomu Takayama<sup>1</sup>

<sup>1</sup>Daido University, Takiharuru-cho, Nagoya 457-8530, Japan

<sup>2</sup>Toho University, Miyama, Funabashi 274-8510, Japan

<sup>3</sup>Toray Research Center, Sonoyama, Otsu 520-8567, Japan

**Abstract** – Incorporation of gaseous organic molecules into polycrystalline mixed-valence trinuclear iron ( $Fe^{2+}, Fe^{3+}, Fe^{2.7+}$ ) pentafluorobenzoate complex  $Fe_3O(C_6F_5COO)_6(C_5H_5N)_3$  with intermolecular nano-voids was studied by  $^{57}Fe$ -Mössbauer spectroscopic and powder XRD measurements. Organic-molecule incorporation was mainly chased by using iron-valence fluctuation observed in a Mössbauer spectrum, and also researched supportively by a powder XRD technique.

**Keywords** – Intermolecular nano-void, Mixed-valence trinuclear iron complex, Valence fluctuation,  $^{57}Fe$ -Mössbauer spectroscopy, powder XRD

## I. INTRODUCTION

We have revealed that there is found a valence-detraped (averaged) state of three iron ions for  $Fe_3O(C_6F_5COO)_6(C_5H_5N)_3 \cdot CH_2Cl_2$  (**I**) at room temperature in our Mössbauer study, while a valence-trapped (localized) state for  $Fe_3O(C_6F_5COO)_6(C_5H_5N)_3$  (**2**) contrarily. In complex **I**, dichloromethane is contained as a crystalline solvated molecule. Complexes of **I** and **2** are synthesized in our work both of which are a novel compound; complex **2** was prepared by heating of **I** under a reduced pressure. It was revealed previously from our single-crystal X-ray structure analysis that solvated  $CH_2Cl_2$  molecules are arrayed in the intermolecular space of the complex **I** [2]. This finding led us into anticipating that gaseous organic molecules may be easily incorporated into such intermolecular nano-voids, since complex **2** was obtained by removing  $CH_2Cl_2$  molecules of the complex **I**. This expectation of ours was proved to be valid, which is reported elsewhere [2].

In the present work, the incorporation behaviors were examined by Mössbauer and powder X-ray Diffraction (XRD) techniques. Furthermore, the time constant of incorporation was also investigated.

## II. EXPERIMENTAL

Complexes of **I** and **2** were prepared according to the procedures reported in our previous papers [1,2]. Organic-vapor exposure experiments were carried out as described in Ref. [2]; polycrystalline powder of **2** was placed in a small-sized vial and then this vial was placed in a large vial. An adequate amount of organic liquid was poured in the large vial, which then was tightly capped.

All Mössbauer spectra and powder XRD patterns (Cu  $K\alpha$ ) were recorded at room temperature in ordinary ways.

## III. RESULTS AND DISCUSSION

Mössbauer spectra and powder XRD patterns at room temperature were shown in the left and right sides of Figure 1, respectively, where those for the following three samples are illustrated; a) polycrystalline powder of complex **2**, b) polycrystalline powder of complex **I**, and c) powder of **2** exposed to dichloromethane vapor at 20 °C for 21 h. Mössbauer spectrum c) for complex **2** exposed to  $CH_2Cl_2$  vapor shows that iron ions should be in the same valence-detraping state as that of complex **I**, implying a regain of solvated  $CH_2Cl_2$  molecules to return to complex **I** from complex **2**. Such regain and return were confirmed in the powder XRD patterns shown in Figure 1, where the patterns a) and c) could be ascribed to a hexagonal crystal form with  $a=1.35$  and  $c=2.10$  nm.

The re-absorption rate experiments suggested that benzene molecules were completely regained with a time constant of a few tens of seconds, surprisingly swift.

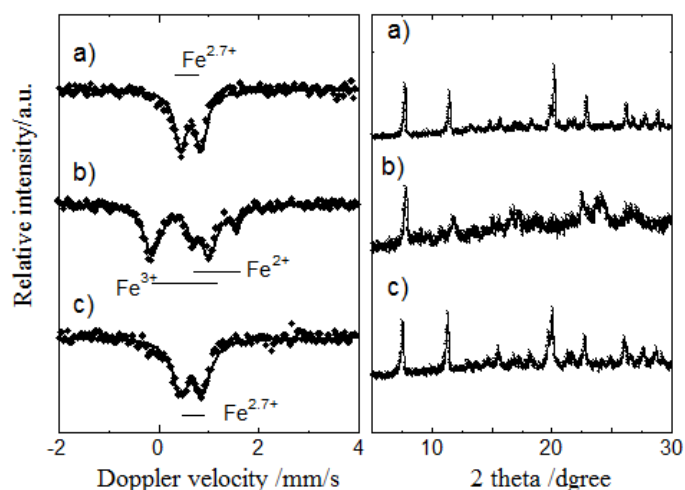


Figure 1.  $^{57}Fe$ -Mössbauer spectra (left) and powder XRD patterns (right) at room temperature: a)  $Fe_3O(C_6F_5COO)_6(C_5H_5N)_3 \cdot CH_2Cl_2$ , (**I**) b)  $Fe_3O(C_6F_5COO)_6(C_5H_5N)_3$ , (**2**) c)  $Fe_3O(C_6F_5COO)_6(C_5H_5N)_3$  (**2**) exposed to  $CH_2Cl_2$ -vapor at 20 °C for 21 h

[1] Y. Sakai et al., *Hyperfine Interactions*, **205** (2012) 1-5.

[2] S. Onaka et al., to be submitted to an international journal (2013).

## Dynamic Perturbation to $^{111}\text{Cd}(\leftarrow^{111}\text{Ag})$ Doped in AgI Nanoparticles

W. Sato<sup>1,2</sup>, R. Mizuuchi<sup>2</sup>, N. Irioka<sup>3</sup>, S. Komatsuda<sup>2</sup>, S. Kawata<sup>4</sup>, A. Taoka<sup>1,2</sup>, and Y. Ohkubo<sup>5</sup>

<sup>1</sup>Institute of Science and Engineering, Kanazawa University, Kanazawa, Ishikawa 920-1192, Japan

<sup>2</sup>Graduate School of Natural Science and Technology, Kanazawa University, Kanazawa, Ishikawa 920-1192, Japan

<sup>3</sup>School of Chemistry, Kanazawa University, Kanazawa, Ishikawa 920-1192, Japan

<sup>4</sup>Department of Chemistry, Faculty of Science, Fukuoka University, Fukuoka, Fukuoka 814-0180, Japan

<sup>5</sup>Research Reactor Institute, Kyoto University, Kumatori, Osaka 590-0494, Japan

*Abstract* – Dynamic behavior of the extranuclear field relative to the  $^{111}\text{Cd}(\leftarrow^{111}\text{Ag})$  probe doped in an ionic conductor silver iodide (AgI) was investigated by means of the time-differential perturbed angular correlation (TDPAC) technique. The room-temperature TDPAC spectrum for as-precipitated AgI powder shows no perturbation, reflecting the zinc blende crystal structure ( $\gamma$ -AgI); whereas in polymer-coated AgI nanoparticles, the  $^{111}\text{Cd}(\leftarrow^{111}\text{Ag})$  probe is dynamically perturbed. This result signifies that  $\text{Ag}^+$  ions in the latter sample can move around even at room temperature in the time scale of the present time window.

*Keywords* – Silver Iodide, Perturbed Angular Correlations, Dynamics, PVP, Nanoparticles, Superionic Conductivity

### I. INTRODUCTION

It is well known that silver iodide (AgI) offers superionic conductivity as in its high-temperature  $\alpha$  phase, and applications of this solid-state conductivity are desired in a wide field of industry. This conducting phenomenon, however, emerges at high temperature because of temperature-dependent crystal structures, which is indeed a barrier to the practical applications of this compound.

Recently, an epoch-making technique was reported to break through this situation: AgI powder coated by a poly-N-vinyl-2-pyrrolidone (PVP) can partially preserve the conducting  $\alpha$  phase even at room temperature, recording the conductivity of  $1.5 \times 10^{-2} \Omega^{-1} \text{cm}^{-1}$ [1]. The authors report that this achievement is due to successful control of the particle size as small as nanoscale. For a detailed understanding of ionic conductivity of this compound, it is of great importance to examine lattice-to-lattice hopping motion of  $\text{Ag}^+$  ions on an atomic scale. For that purpose, in the present work, dynamic behavior of  $\text{Ag}^+$  ions has been observed by means of the time-differential perturbed angular correlation (TDPAC) technique using the probe of  $^{111}\text{Cd}(\leftarrow^{111}\text{Ag})$  nuclei. Here, preliminary results of successful observation of room-temperature dynamic motion of  $\text{Ag}^+$  ions are reported.

### II. EXPERIMENTS

For the production of the TDPAC probe, Pd foil was irradiated by thermal neutrons in Kyoto University Reactor to produce  $^{111}\text{Pd}$ . After radioequilibrium was achieved between  $^{111}\text{Pd}$  and  $^{111}\text{Ag}$ , the Pd foil was dissolved in  $\text{HNO}_3$  aq. solution, and carrier-free  $^{111}\text{Ag}$  was isolated by an anion exchange chromatography. The separated  $^{111}\text{Ag}$  was incorporated together in AgI samples when the powder sample was synthesized by precipitation. In the present

work, two different samples were prepared: PVP-free and PVP-coated. We confirmed by transmission electron microscope that microscopic particles with sizes of 10-100 nm were expectedly synthesized for  $^{111}\text{Ag}$ -free PVP-coated AgI.

TDPAC measurements of the  $^{111}\text{Cd}(\leftarrow^{111}\text{Ag})$  probe were performed for both samples at various temperatures to observe temperature dependence of the spectra.

### III. RESULTS

For the PVP-free AgI polycrystals, time variation was not seen in the TDPAC spectrum at room temperature, which suggests that the  $^{111}\text{Cd}(\leftarrow^{111}\text{Ag})$  probe duly occupies tetrahedral lattice site of  $\text{Ag}^+$  in zinc blende crystal structure as in  $\gamma$  phase. At high-temperature ( $> 419 \text{ K}$ )  $\alpha$  phase, the TDPAC spectra showed an exponential relaxation, signifying dynamic motion of the extranuclear field relative to the probe nucleus.

As regards the PVP-coated AgI nanoparticles, on the other hand, typical dynamic perturbation was observed even at room temperature as shown in Fig. 1. The directional anisotropy of the spectrum shows a relaxation in the time scale of  $10^{-7} \text{ s}$ , which corresponds to nuclear relaxation time by the dynamic perturbation arising from fast fluctuation of the extranuclear charge distribution, namely, hopping motion of  $\text{Ag}^+$  ions. It is considered that PVP-coating has made it possible for the  $\alpha$  phase to survive at room temperature, realizing superionic conductivity.

For the hopping rate of  $\text{Ag}^+$  ions, it is essential to obtain the value of nuclear quadrupole frequency as they are still at their lattice site. Experiments for the data acquisition are now in progress.

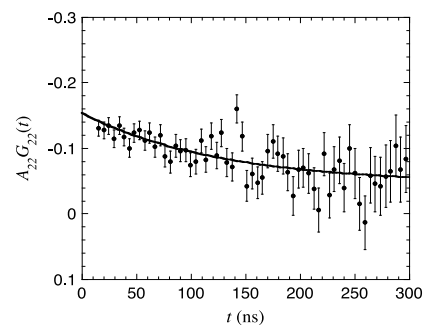


Fig. 1. TDPAC spectrum of  $^{111}\text{Cd}(\leftarrow^{111}\text{Ag})$  in PVP-coated AgI at room temperature, where  $A_{22}$  stands for the angular correlation coefficient and  $G_{22}(t)$  the time-differential perturbation factor as a function of the time interval of the cascade  $\gamma$ -ray emission,  $t$ .

[1] R. Makiura et al. Nature Mater. 8, 476 (2009).

## A prototype of a simple collection system for the determination of $^{14}\text{C}$

Tzu-Han Chuang, Tsuey-Lin Tsai, Hwa-Jou Wei, Lee-Chung Men

*Chemistry Division, Institute of Nuclear Energy Research, Longtan, Taoyuan 32546, Taiwan, R.O.C.*

### *Abstract*

*This study presents a simple and relatively cost-effective system for sampling  $^{14}\text{C}$  in biological samples or the radwaste from nuclear power plants. The proposed system uses a  $\text{CO}_2$  absorption technique to collect  $^{14}\text{C}$ . This technique involves placing a sample in a quartz tube inside a furnace in a flowing stream of oxygen, and then heating the tube to a minimum temperature of  $300^\circ\text{C}$  at heating rate of  $14^\circ\text{C}/\text{min}$ . In the combustion zone,  $\text{CuO}$  catalytic oxidation ensures that any  $\text{CO}$  produced from the incomplete combustion of the sample carbon present in the gas stream is oxidized to form  $\text{CO}_2$ . This process uses dilute sulfuric acid (5%) for steam absorption. The proposed collection technique also provides a simple procedure for subsequent sample preparation and activity measurement using a liquid scintillation counting. When combined with several counting vials, this trapping design can solve the overcapacity problem of carbon absorption for each collector. The following sample pretreatment also facilitates counting. This system achieves a minimum detectable activity level of  $20\text{ mBq/g}$  for an 1-g solid sample. This level of sensitivity is appropriate for the routine monitoring of radwaste at nuclear facilities.*

*Keywords:  $^{14}\text{C}$ ;  $\text{CO}_2$  absorption; liquid scintillation counting; radwaste*

## Elemental analysis of Korean adult toenail using of instrumental neutron activation analysis

Sun-Ha Kim<sup>1</sup>, Jong-Hwa Moon<sup>1</sup>, Yong-Sam Chung<sup>1</sup>, Ok-Hee Lee<sup>2</sup>

<sup>1</sup>Korea Atomic Energy Research Institute, Daedeok-daero 989-111, Yuseong-gu, Daejeon, 305-353, Korea

<sup>2</sup>Dept of Food Science and Nutrition, Yongin University, 470, Samga-dong, Cheoin-Gu, Yongin, 449-714, Korea

**Abstract** – The elemental contents in a toenail as a biological sample may depend on the dietary habit and health status. In this study, the inorganic elements in Korean adult toenail were determined by an instrumental neutron activation analysis (INAA). Toenail samples were collected from Korean adults, and the total number of samples was 50. The collected samples were pretreated and analyzed using INAA facilities at the HANARO research reactor. 15 elements, i.e., Al, As, Br, Ca, Cl, Co, Cr, Fe, Hg, K, Mn, Na, Se, V, and Zn in the toenail samples were determined and evaluated for the level of elemental concentration. Finally, correlation between 15 elements was examined. It is found that Mn-V, Na-Cl, Br-K, and Cr-Fe seem to be in close correlation.

**Keywords**–Instrumental Neutron Activation Analysis, Inorganic Elements, Toenail, Elemental Correlation

### I. INTRODUCTION

The organic elements in a human organism such as serum, hair, nail, and internal organs are able to provide valuable information to estimate the health status of the human body. The elemental contents in a toenail as a biological sample may depend on the dietary habit and health status. In this study, the inorganic elements in a Korean adult toenail were determined using instrumental neutron activation analysis (INAA). For this purpose, the analytical condition for INAA was established, and 15 elements were determined. Finally, correlation between the elements was examined.

### II. EXPERIMENTAL

The toenail samples were collected from Korean adults, and the total number of samples was 50. The collected samples were pretreated by cutting, cleaning, and homogenizing for INAA. The prepared samples were irradiated using NAA #1 or #2 irradiation holes at the HANARO research reactor. For the measurement of gamma-rays of the detectable nuclides, a HPGe detector coupled to a 16k-multichannel analyzer was used. The elemental concentration in the samples was determined by the absolute and/or relative method.

### III. RESULTS

15 elements, i.e., Al, As, Br, Ca, Cl, Co, Cr, Fe, Hg, K, Mn, Na, Se, V, and Zn in the toenail samples were determined by INAA. The mean elemental concentration is shown in Fig. 1.

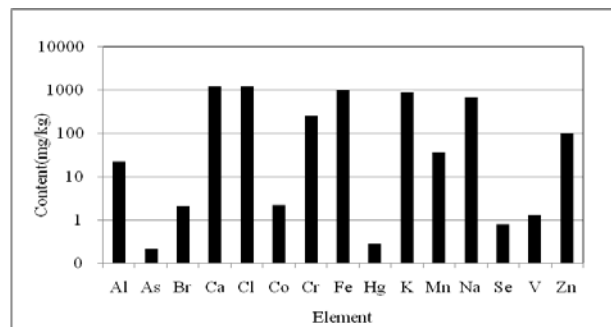


Fig. 1. Mean elemental concentrations in toenail samples

The correlation between the 15 elements was examined and Mn-V, Na-Cl, Br-K and Cr-Fe seem to be in close correlation. Fig. 2 shows the Cr-Fe correlation.

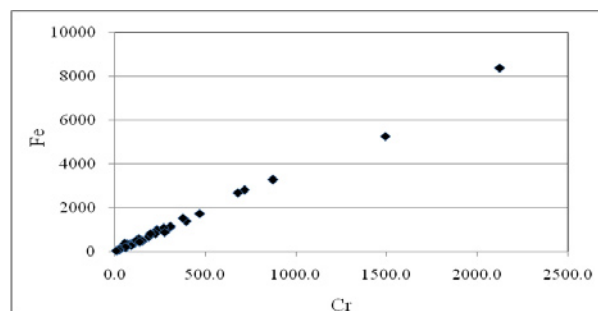


Fig. 2. Correlation between Cr and Fe in toenail samples

### ACKNOWLEDGEMENT

This work was carried out under the Nuclear Research and Development Program of the Korean Ministry of Education, Science, and Technology.

### REFERENCES

- [1] Rita Mehra, Meenu Juneja: Fingernails as biological indices of metal exposure, *Journal of Bioscience* 2005, 30(2):253-257.
- [2] World Health Organization (2006) Trace elements in human nutrition and health. Geneva, WHO, Belgium

# Determination of Vanadium at ppb Levels in Relatively High-Salt Biological Materials without Chemical Separation and using Neutron Activation coupled to Compton Suppression Gamma-Ray Spectrometry

W. Zhang and A. Chatt

Trace Analysis Research Centre, Department of Chemistry, Dalhousie University, Halifax, NS, B3H 4J3, Canada

Abstract – APSORC'13 Abstract

Keywords – vanadium, INAA, Compton suppression, biological materials

## I. INTRODUCTION

The toxicity of V has been known for some time. It is only recently that V has been recognized as an essential trace element. Its determination with high precision and accuracy in tissues, foods and other biological materials is needed. Techniques such as atomic absorption, X-ray fluorescence, and neutron activation analysis (NAA) can be used for this purpose. Vanadium can be determined by NAA through the interference-free 1434.2-keV gamma-ray of its short-lived (half-life of 3.74 min) nuclide  $^{52}\text{V}$  produced *via* the  $^{51}\text{V}(n,\gamma)^{52}\text{V}$  reaction. It has been reported that  $^{52}\text{V}$  has sufficient sensitivity for its measurement down to nanogram levels [1]. However, it is seldom assayed in practice by instrumental NAA (INAA) in conjunction with conventional gamma-ray spectrometry (INAA-CONV), in particular for low V content in relatively high-salt biological materials, due to the Compton background interference from nuclides such as  $^{28}\text{Al}$ ,  $^{38}\text{Cl}$ ,  $^{56}\text{Mn}$ , and  $^{24}\text{Na}$ . Preconcentration NAA (PNAA) and radiochemical NAA (RNAA) methods are commonly used to separate V from the major and interfering elements [2-3]. Compton suppression spectrometry (CSS) counting technique can be alternatively used under such situations [4]. One of the objectives of the present work was to fully explore the advantages of INAA coupled to CSS (INAA-CSS) for the determination of low levels of V without any chemical separation in biological materials in general, nutritional materials in particular, containing varying amounts of sodium chloride.

## II. EXPERIMENTAL

A total of 16 biological reference material (RM) and standard reference material (SRM) containing 1.4 to 1100 ppb V with low to high levels of sodium chloride were analyzed by INAA-CSS. Between 200 and 700 mg of these materials were irradiated in the Dalhousie University SLOWPOKE-2 Reactor facility at a neutron flux of  $5 \times 10^{11} \text{ cm}^{-2} \text{ s}^{-1}$  for 1 min, allowed to decay for 1 min, and counted for 10 min. The average sensitivity for V standard solutions under these conditions was  $5025 \text{ counts } \mu\text{g}^{-1}$  in the Compton suppression counting mode. The CSS used here consisted of a HPGe detector and a 10"x10" NaI(Tl) guard detector with a 3"x3" NaI(Tl) plug. The peak-to-Compton plateau ratio of this system was about 590:1.

## III. RESULTS AND DISCUSSION

The application of CSS can reduce the Compton background under the 1434.2-keV peak, improve the statistical accuracy of the peak and lower the detection limit, if Cl and Na levels are not too high [4]. For example, the V content of Wheat Flour (NIST SRM 1567a) was determined by INAA-CSS as  $9.0 \pm 2.9$  ppb compared to the Information value of 11 ppb; the detection limit was 1.8 ppb by INAA-CSS relative to 8.6 ppb by INAA-CONV. In the case of Peach Leaves (NIST SRM 1547) our measured value of  $355 \pm 17$  ppb agreed well with the certified value of  $370 \pm 30$  ppb; the detection limit of 13 ppb by INAA-CSS was about 3 times lower than that of 34 ppb by INAA-CONV.

The overall background around the 1434.2-keV region was reduced by a factor of 5 to 10 for several biological RMs and SRMs in the Compton suppression counting mode compared to conventional counting. Consequently, the detection limits were lowered by factors of 3 to 5 in INAA-CSS compared to INAA-CONV making rapid and reliable V determinations possible above 1.5 ppb levels without any chemical separation. The agreement between the certified (information) and measured values for the RM and SRM analyzed in this work was generally within  $\pm 10\%$ .

## References

- [1] A.J. Blotcky, F.G. Hamel, A. Stranik, A. Ebrahim, and R.B. Sharma, *J. Radioanal. Nucl. Chem.*, Articles, 131(1989)319-329.
- [2] A.J. Blotcky, W.C. Duckworth, and A. Ebrahim, *J. Radioanal. Nucl. Chem.*, Articles, 134(1989)151-160.
- [3] A.I. Kulathilake, A. Chatt, *Trans. Am. Nucl. Soc.*, 65(1992)172.
- [4] W. Zhang, Ph.D. Thesis, Dalhousie University, Halifax, NS, Canada, 1997.

## Radiochemical neutron activation analysis of halogens (Cl, Br and I) in geological and cosmochemical samples

Mitsuru Ebihara<sup>1</sup> and Shun Sekimoto<sup>2</sup>

<sup>1</sup>Tokyo Metropolitan University

<sup>2</sup>Kyoto University Research Reactor Institute

### I. INTRODUCTION

Accurate and reliable data of halogen abundance have been rarely reported for terrestrial samples, such as crustal rock and mantle material. Since halogens differ in volatility from element to element, their content and relative abundance are highly informative when discussing the petrogenesis of such samples. Among the halogens, iodine is the most informative element in discussion of the geochemical circulation of crustal materials (oceanic crust and continental crust) and mantle. Halogens are also important in meteorite samples, and in particular, iodine is of particular interest and of high importance in discussions of the cosmochemical behavior of its extinct nuclide <sup>129</sup>I (half-life of 15.7 million years) in the early solar system. However, the scarcity of halogen data for meteorite samples is more worrying.

There is a shortage of accurate and reliable data of halogens in meteorites, as well as in terrestrial rock samples, as can be witnessed in the data libraries, where only preferable, not certified values, and for some rocks, no values are listed. This deficit must be largely related to difficulties in determining trace amounts of halogens within these samples. To determine trace halogens in rock samples, either inductively coupled plasma mass spectrometry (ICP-MS) or neutron activation analysis (NAA) have commonly been utilized. Bromine and iodine are conventionally determined by ICP-MS after using pyrohydrolysis of rock powder, but neither fluorine nor chlorine can be reliably determined by this method. In principle, four halogens can be determined using NAA. However, only three halogens (chlorine, bromine, and iodine) have been routinely determined by NAA with radiochemical purification.<sup>1</sup>

In this study, trace three halogens (chlorine, bromine, and iodine) were determined by radiochemical NAA (RNAA) for geological and cosmochemical powder samples. Similar studies have been conducted for many years by a senior author of this paper and his colleagues with use of different types of reactors. Now that the Kyoto University reactor (KUR) is currently the only research reactor running in Japan, we initiated to perform RNAA of three halogens by using KUR. Our first goal was to present a modified radiochemical procedure for RNAA of three heavy halogens, which was to be more effective and convenient compared with the previous one. A part of our outcomes will be published soon.<sup>2</sup> In this paper, we demonstrated that RNAA data for bromine and iodine are more reliable and accurate than the data obtained by ICP-MS coupled with pyrohydrolysis preconcentration. Another goal was to apply our RNAA procedure to geological and

cosmochemical samples for discussing geochemical and cosmochemical implications based on the analytical data for such samples. A part of the progress related to this goal is presented here.

### II. EXPERIMENTAL

Both geological rocks (mantle xenoliths) and cosmochemical samples (Antarctic meteorites) were analyzed, along with several geological reference rock powders. Approximately 100 mg of each powder sample was weighed, inserted into a clean, small plastic vial. Chemical standard solutions of the three halogens were prepared for their quantifications. An appropriate amount of each solution was dropped onto a paper disk (17 mm  $\phi$ ), weighed, dried under a heat lamp and doubly sealed into polyethylene bags. Two rock samples, together with a set of three reference halogen samples, were irradiated for 10 min with a thermal neutron flux of  $3.3 \times 10^{12}$  n/cm<sup>2</sup>/s at Kyoto University Research Reactor Institute. After irradiation, the rock samples were cooled for a few minutes to enable the decay of <sup>28</sup>Al, and were then subjected to radiochemical separation of neutron-induced radionuclides of <sup>38</sup>Cl, <sup>82</sup>Br, and <sup>128</sup>I. We basically followed the radiochemical procedure for RNAA of three heavy halogens, as described by Ozaki and Ebihara,<sup>3</sup> and others cited within this paper. Chemical yields were determined by reactivation method.

### III. RESULTS AND DISCUSSION

Our RNAA procedure was applied to several rock samples in powder. In addition, the Smithsonian Institution Allende meteorite powder sample, which has been repeatedly analyzed for many years, was also analyzed as a control sample. Our present data are consistent with the precious results. RNAA results of halogens for the Antarctic meteorite recovered from the Ice were compared with those for meteorites recovered from the bare ice field and a similar enrichment was observed for both of them, suggesting that halogens were added during the storage in Antarctic ice.

Reference: [1] Ebihara M. et al. (1997) JRNC, 216, 107-112. [2] Sekimoto S. and Ebihara M. (2013) Anal. Chem., in press. [3] Ozaki H. and Ebihara M. (2007) Ana. Chim. Acta, 583, 384.

## Multielement analysis of KIGAM reference samples by INAA, ICP-AES and ICP-MS

Naoki Shirai<sup>1</sup>, Meiramkhan Toktaganov<sup>2</sup>, Hiroki Takahashi<sup>1</sup>, Yuta Yokozuka<sup>1</sup>, Shun Sekimoto<sup>3</sup>,  
 Mitsuru Ebihara<sup>1</sup>

<sup>1</sup>Tokyo Metropolitan University

<sup>2</sup>National Nuclear Center Republic of Kazakhstan Institute of Atomic Energy

<sup>3</sup>Kyoto University Research Reactor Institute

### I. INTRODUCTION

Bulk chemical compositions of geochemical and cosmochemical materials provide us the information of evolution processes and magmatism of planetary bodies. Instrumental neutron activation analysis (INAA), inductively coupled plasma mass spectrometry (ICP-MS) and X-ray fluorescence (XRF) have been used for the determination of bulk chemical compositions of these samples. For these analytical methods, reference materials are used as standard samples. Therefore, the quality of analytical data depends on accuracy and precision of such reference materials. Many kinds of reference materials having a wide range of chemical compositions were prepared and distributed by different institutions. Korean Institute of Geology, Mining and Materials (KIGAM) issued geological reference materials. However, the number of published values is very limited [1] and recommended values are not established. In this study, we aimed to determine chemical compositions for KIGAM reference materials by using three analytical methods.

### II. EXPERIMENTAL

Eleven KIGAM reference materials (KB-1, KGB-1, KD-1, KT-1, KF-1, KF-2, KP-1, KP-2, KP-3, KG-1 and KG-2) were analyzed. In addition, JB-2 published by GSJ was analyzed as control sample. In INAA, samples were irradiated two times with different irradiation periods which are adjusted for half lives of nuclides usable for determining elements. Samples weighing about 0.04 g were irradiated for 10s at a neutron flux of  $4.6 \times 10^{12} \text{ cm}^{-2}\text{s}^{-1}$  at Kyoto University Research Reactor Institute (KURRI) and were immediately measured for their emitting gamma ray. The samples were reirradiated for 4 hrs at a neutron flux of  $5.6 \times 10^{12} \text{ cm}^{-2}\text{s}^{-1}$  at KURRI. After irradiation, samples were measured for gamma rays several times with different cooling intervals at KURRI and the RI Research Center of Tokyo Metropolitan University. ICP-AES and ICP-MS were used for determination of major and minor elements, and rare earth elements (REEs), Th and U, respectively. Samples were digested with HF, HNO<sub>3</sub> and HClO<sub>4</sub>. Dissolved samples were dried and redissolved in HNO<sub>3</sub>. By using a 10 % aliquot sample solution, REEs, Th and U abundances were determined by ICP-MS. Remaining sample solutions were used for determination of major and minor elements by using ICP-AES.

### III. RESULTS AND DISCUSSION

About 40 elements were determined by INAA, ICP-MS and ICP-AES for each reference sample. Figure 1 shows CI-chondrite normalized REE abundance patterns for KB-1 and KGB-1. INAA and ICP-MS data are in good agreement with each other for comparable elements. REE abundances patterns for KB-1 and KGB-1 obtained by Sakamoto et al. [1] show small zigzag patterns in middle REEs, while our abundances patterns are smooth. CI-normalized REEs abundances patterns for KB-1 and KGB-1 are very close to each other and similar to those for continental crustal materials.

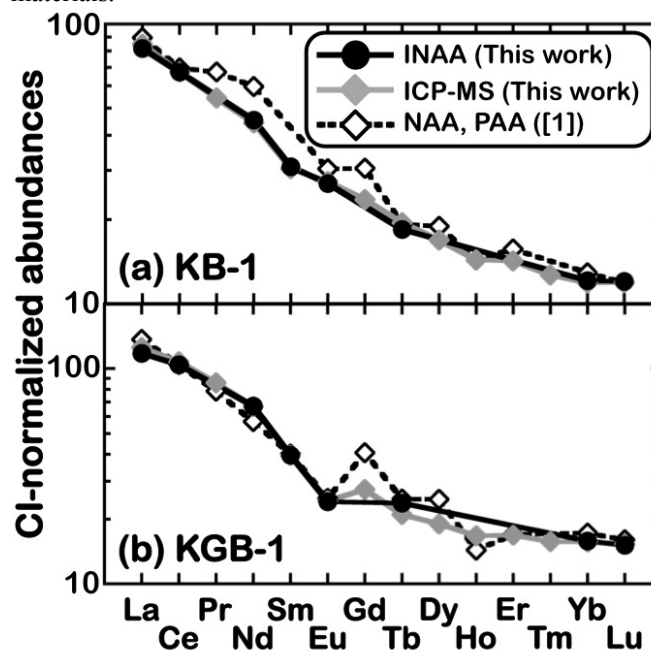


Fig. 1. CI-normalized REE abundances for KB-1 (a) and KGB-1 (b).

Reference: [1] Sakamoto K. et al. (1997) J. Radioanal. Nucl. Chem., 215 (1), 69-76.

## Comparison of Calculated Results with NTD Measured Data for Establishment of Burned Core Model for Monte Carlo Simulation of HANARO Reactor

Dong-Keun Cho and Myong-Seop Kim

Korea Atomic Energy Research Institute, Dukjin-dong 150, Yuseong, Daejeon 305-353, Republic of Korea

*Keywords – Monte Carlo Simulation, MCNP, Research Reactor*

HANARO is a multipurpose research reactor operated for material testing, production of key radioisotopes, neutron activation analysis of nuclear-grade materials, and neutron radiography. To support various researches, HANARO has a very heterogeneous configuration with 25 vertical irradiation thimbles and seven horizontal beam tubes. Although the reactor core is predicted by HANARO core management system, called HANAFMS, equipped with WIMS and VENTURE, heterogeneity of the core and newly installed device for specific experiment makes the neutronic analysis difficult and sometimes doubtful. To resolve these limitations, MCNP has been utilized for neutron transport calculation in the HANARO reactor.

For HANARO, MCNP core model filled with fresh fuels has been used to support the experiments in addition to HANAFMS. And, the model has supplied acceptable analysis results for a design of experimental devices and facilities. However, it is definite that burned core model can provide better result than that obtained from the core model with fresh fuels. In this study, MCNP burned core model was established and then its viability was investigated through comparison of calculated result from the burned core model and measurement data from neutron transmutation doping (NTD) for producing silicon semiconductor.

Burned full-core model for MCNP simulation was established by using the data generated by WIMS and VENTURE codes. Burnup-dependent number density was calculated for each rod for each fuel assembly by WIMS to assign appropriate isotopic number density to each region of irradiated fuel of the core. The power and burnup of each region of fuel region were calculated by VENTURE for the equilibrium core of HANARO. Based on the burnup-dependent number density library calculated by WIMS, the number densities of major nuclides corresponding to the

burnup of each region were assigned to each region of the irradiated fuel of MCNP model.

HANARO has two vertical holes in the heavy water reflector tank for the NTD- NTD1 and NTD2 holes having diameters of 22 and 18cm respectively. Because these two holes showed excellent conditions for NTD in the aspects of high thermal neutron flux and large hole size, and low fast neutron flux and gamma heating, commercial service for a 5 in., silicon ingot has been provided to produce silicon semiconductor at NTD hole. And measurement was also performed to check radial and axial uniformity of neutron irradiation in silicon ingots.

The actual irradiation geometry for silicon ingots as were used for the experiment were described almost exactly in the MCNP burned core model. Absolute and relative neutron flux distributions along radial and axial direction of the ingots for NTD were calculated by using MCNP burned core model. The neutron flux was averaged over each ring radially divided with the same thickness from the center of ingots. The reason why the calculated neutron fluxes were averaged azimuthally is to consider the rotation of the ingot during irradiation to obtain low RRG (radial resistivity gradient). Three axial positions of a silicon ingot - the top, bottom, and middle planes – were obtained as well. The longitudinal length of each plane was 2 cm.

Finally, these calculated data were compared with those from the measured data for silicon ingots for neutron transmutation doping carried out at NTD-1 and NTD-2 irradiation holes of HANARO research reactor.

1. M.S. Kim, et al., "Radial Uniformity of Neutron Irradiation in Silicon Ingots for Neutron Transmutation Doping at HANARO," *Nuclear Engineering and Technology*, **38**(1). 2006.

## Neutron Activation Analysis of JCFA-1, JCu-1 and JZn-1

Shun Sekimoto<sup>1</sup>, Yuta Homura<sup>1</sup>, Ryo Okumura<sup>1</sup>, Naoki Shirai<sup>2</sup>

<sup>1</sup>Kyoto University Research Reactor Institute

<sup>2</sup>Tokyo Metropolitan University

*Abstract* – We present NAA results of JCFA-1, JCu-1 and JZn-1 reference samples prepared by GSJ. Through NAA of those three reference samples, appropriate reference samples for quantification by INAA are discussed. We also report fundamental property of each irradiation port, such as neutron fluence rate, at Kyoto University Reactor after renewal of the reactor fuel.

*Keywords* – JCFA-1; JCu-1; JZn-1; Neutron activation analysis; Kyoto University Reactor; GSJ reference sample

### I. INTRODUCTION

Geological Survey of Japan (GSJ) has prepared various kinds of geochemical reference materials [1]. In the most of igneous rock samples and sedimentary rock samples, their chemical compositions are presented as the certified values through compilation of a lot of data [2, 3]. In several reference samples, however, certified values have not been given yet, and provisional, recommended, or information values are given, and then multielement analysis by neutron activation analysis (NAA) has never been performed. In this work, the first NAA results of a coal fly ash reference sample (JCFA-1) and ore reference samples (JCu-1 and JZn-1), where certified values have never been given, are reported and compared to the literature data obtained by atomic absorption spectrometry (AAS), inductively coupled plasma-atomic emission spectrometry (ICP-AES), etc. [4, 5] Through NAA of the above three reference samples, we investigate appropriate reference monitor samples for quantification by INAA. The characteristics of the NAA systems using Kyoto University Reactor (KUR) after the fuel conversion to low-enriched uranium intend to be presented.

### II. EXPERIMENTAL

#### A. Sample preparation

Three reference samples analyzed in this work are JCFA-1 as coal fly ash, JCu-1 as copper ore, and JZn-1 as zinc ore, which were prepared by GSJ and were commercially distributed [4-5]. As reference monitor samples for quantifications by NAA, JA-1 (andesite), JB-1b (basalt), JG-1 (granite), and JP-1 (peridotite) are also prepared [2]. All the samples were in powder, and were not subjected to any additional treatment such as drying. Approximately 100 mg of each powder sample was weighed, doubly sealed into clean polyethylene bags.

#### B. Neutron irradiation

First, each sample was irradiated one by one for 10 s at pneumatic transport system No. 3 (Pn-3). After the 10 s

irradiation, the outer bag of the sample was replaced by a new one and then the sample was immediately subjected to gamma-ray spectrometry for measurement of short half-life nuclides: <sup>28</sup>Al, <sup>52</sup>V, <sup>49</sup>Ca, <sup>27</sup>Mg, etc. Next the three reference samples together with all reference monitor samples were placed in one capsule and irradiated for 4 h at Pn-2. After 4 h irradiation, samples whose outer bags were also replaced in a similar manner as 10 s irradiation were subjected to gamma-ray spectrometry for measurements of long half-life nuclides: <sup>59</sup>Fe, <sup>60</sup>Co, etc.

#### C. Kyoto University Reactor

Kyoto University Reactor (KUR), a 5 MW research reactor in Japan, has worked as the central place to support the university researchers using NAA for their analytical studies. After four-year shutdown period for fuel conversion to low-enriched uranium fuel, KUR restarted in May 2010, and thereby a new inter-university research project using NAA system at KUR also restarted. During this renewal of the reactor fuel, the control system of the pneumatic irradiation system was refurbished to digital-control type. This improvement has been introduced elsewhere [6] and operated well after KUR restarted. To promote this inter-university research project successfully, fundamental properties of the irradiation sites, such as neutron fluence rate, cadmium ratio of gold, and temperature inner capsules during neutron irradiation at each pneumatic irradiation system used for NAA are shown in the presentation.

### III. RESULTS AND DISCUSSION

Elemental contents of the three reference samples measured by NAA are reported. Among four reference monitor samples (JA-1, JB-1b, JG-1 and JP-1), inconsistencies in the activities of radionuclides produced by (n,γ) reaction per amounts of their corresponding elements was found in several elements determined. Through NAA of the three reference samples, we also investigate which reference sample is suitable or not for each element determined.

### REFERENCES

- [1] <http://riodb02.ibase.aist.go.jp/geostand/welcome.html>
- [2] N. Imai et al., *Geochem. J.* **1995**, 29, 91-95
- [3] N. Imai et al., *Geostand. Newslett.* **1996**, 20, 165-216.
- [4] S. Terashima et al., *Geostand. Newslett.* **1998**, 22, 113-117.
- [5] S. Terashima et al., *Geostand. Newslett.* **2003**, 27, 259-271.
- [6] K. Takamiya et al., *J. Radioanal. Nucl. Chem.* **2008**, 278, 719-721.

## Prompt Gamma-ray Analysis of Chloride Concentration in Blended Cement Concretes

A. A. Naqvi<sup>1\*</sup>, M. Maslehuddin<sup>2</sup>, O.S.B. Al-Amoudi<sup>3</sup>, Khateeb-ur-Rehman<sup>1</sup> and M. Raashid<sup>1</sup>

<sup>1</sup>Department of Physics, <sup>2</sup>Center for Engineering Research, and <sup>3</sup>Department of Civil and Environmental Engineering  
King Fahd University of Petroleum and Minerals, Dhahran, Saudi Arabia

*Abstract – The chloride concentration in plain and blast furnace slag cement concrete has been measured using a D-D portable neutron generator. The setup has been used to measure chloride concentration in specimens using chlorine prompt gamma-rays with different energies*

*. Out of several chlorine gamma ray data, an optimum and a unique chlorine gamma-ray line has been chosen for the detection of chloride in all the blended cement concretes specimen including fly ash, blast furnace slag and superpozz cement concrete utilizing the portable neutron generator-based PGNA setup*

*Keywords – Chloride detection, blended concrete specimen, BGO detector, Portable D-D neutron generator based PGNA setup, Monte Carlo simulations,*

### I. INTRODUCTION

Industrial by-products, such as fly ash, silica fume and blast furnace slag, are added to concrete, as partial replacement of cement, to increase its denseness and impermeability. The increased impermeability of blended cement concretes decreases the rate of diffusion of chloride ions to the steel surface. Since reinforcement corrosion is predominantly attributed to the presence of chloride ions at the steel surface, a non-destructive technique is required to assess the level of chloride concentration in concrete. A portable neutron generator-based prompt Gamma-ray Neutron Activation setup has been designed by the authors to measure the chloride concentration in plain and blended concretes using a cylindrical 100 mm x 100 mm (diameter x height) BGO detector.

The setup has been used to measure chloride concentration in fly ash and blast furnace slag cement concrete specimens using chlorine prompt gamma-rays with different energies. An excellent agreement has been observed between the chlorine prompt gamma-ray experimental yield and the calculated values obtained through Monte Carlo simulations. The optimum choice of unique chlorine gamma-ray line for the detection of chloride in the blended cement concretes utilizing the portable neutron generator-based PGNA setup data taken in present study and earlier [1,2] is presented.

- [1] Naqvi, A. A., Zameer Kalakada, Faris A. Al-Matouq, M. Maslehuddin and O.S.B. Al-Amoudi. Prompt Gamma-Ray Analysis of Chlorine in Superpozz Cement Concrete. Nuclear Inst. and Methods in Physics Research, A Vol. 693 (November 2012), pp. 67-73
- [2] Naqvi, A. A., Zameer Kalakada, Faris A. Al-Matouq, M. Maslehuddin and O.S.B. Al-Amoudi. Chlorine Detection in Fly Ash Concrete using a Portable Neutron Generator. Applied Radiation and Isotopes Vol70(2012) pp.1671-4.

## Cold Neutron and Thermal Neutron PGAA facilities at The HANARO Research Reactor

G.M. Sun<sup>1</sup>, E.J. Lee<sup>1</sup>, B.G. Park<sup>1</sup>, J.H. Moon<sup>1</sup>

<sup>1</sup>Neutron Utilization Technology Division, Korea Atomic Energy Research Institute, 305-353, Korea

*A new cold neutron prompt gamma activation analysis facility has been developed at a cold neutron source of the HANARO research reactor and be prepared to open to users until the end of 2013. The performance tests were carried out and compared with an old thermal neutron facility. The neutron beam characteristics such as neutron flux, spatial distribution and energy spectrum were investigated and a background was also studied in detail. The measurements for the standard reference material provide the performance of the new facility and comparison with the old thermal neutron facility*

*Keywords –cold neutron, thermal neutron, prompt gamma activation analysis, HANARO*

### I. INTRODUCTION

Prompt gamma-ray activation analysis (PGAA) is based on the radiative neutron capture, which has been considered to be a complementary method to the conventional instrumental neutron activation analysis though in principle it can analyze almost elements in the elemental table. If a guided cold neutron beam with a relatively low background can provide a possibility that a PGAA itself becomes a complete elemental analysis tools. We operated a thermal neutron PGAA (SNU-KAERI PGAA) [1] on the horizontal ST1 beam line of the HANARO research reactor and newly developed a cold neutron PGAA (CN-PGAA) on the CG2B cold neutron guide from a cold neutron source. Figure 1 shows a SNU-KAERI PGAA facility, which was developed by a group from Seoul National University, has a neutron flux of  $1 \times 10^8$  n/cm<sup>2</sup>s and detection limit for boron elemental of about 60 ng. Figure 2 shows a new CN-PGAA facility. Neutron guide after the end of the guide to a sample position is normally made of aluminum but Teflon chopper and The Teflon tube has a length of 100 cm and a double-layer structure and the space between double layers



Figure 1. Thermal neutron PGAA (SNU-KAERI) facility at the ST1 horizontal beam line of the HANARO research reactor.

is introduced as material for the flight tube between disk chopper and is filled with 95% enriched <sup>6</sup>Li<sub>2</sub>CO<sub>3</sub> powder, whose thickness is 1 cm. Lithium layer catches neutrons scattered out from the path. Neutron beam is shaped with a <sup>6</sup>LiF beam cutter to have a rectangular shape of 2 cm x 2 cm. We investigated neutron characteristics such a neutron flux and its spatial distribution by using a gold foil activation method and neutron energy spectrum by using a time-of flight method. True integrated neutron flux at the sample position is about  $5 \times 10^8$  n/cm<sup>2</sup>s. The total beam characteristics of the CN-PGAA were compared with that of the SNU-KAERI PGAA and background was investigated in detail.



Figure 2. Cold Neutron Activation Station, where a cold neutron PGAA (CN-PGAA) was installed.

- [1] S.H. Byun, G.M. Sun and H.D. Choi, "Development of a Prompt Gamma Activation Analysis Facility Using Diffracted Polychromatic Neutron Beam", Nuclear Instruments and Methods in Physics Research A, Vol. 487, (2002), pp. 521 ~ 529.
- [2] G.M. Sun, "Development of HANARO Cold Neutron Activation Station", 2012 Asia-Pacific Winter Conference on plasma spectrochemistry, Jeju, Aug. 2012.

## Exposing dogs to uranium contained in commercial diets

Camila Elias,<sup>1</sup> Elisabete A. De Nadai Fernandes,<sup>1</sup> Márcio A. Bacchi,<sup>1</sup> Peter Bode<sup>2</sup>

1. University of São Paulo, Nuclear Energy Center for Agriculture, P.O. Box 96, 13400-970 Piracicaba, SP, Brazil

2. Reactor Institute Delft, Delft University of Technology, Mekelweg 15, 2629 JB, Delft, The Netherlands

### Abstract

The presence of uranium in dry dog food samples was investigated by instrumental neutron activation analysis (INAA). Some commercial brands showed uranium concentration as high as 4 mg kg<sup>-1</sup>, which may lead to chronic exposure of dogs to a level about a thousand higher than the normal ingestion level for humans according to the US-EPA.

Keywords – Food safety, dog food, INAA

### I. INTRODUCTION

Dry dog food is intended to be a complete and balanced diet and may be the unique source feeding the animal in all stages of life. Therefore, it is extremely important to choose a product capable of providing optimal nutrition, with all necessary substances at adequate levels and free of contaminants, for promoting long-term health.

The safety of dog diets has recently received increasing attention since the contamination with melamine caused the death of several animals and a major recall of pet food in the United States. In fact, the use of low quality ingredients in the pet food composition can introduce residues of pesticides, mycotoxins, hazard chemical elements and other toxic substances. Products derived from phosphate rocks, as dicalcium phosphate (DCP), normally used as feed additives to supplement phosphorus may have high concentrations of uranium [1].

Experiments with dogs, rabbits and rats have demonstrated that the animals are sensitive to both inhalation and oral exposure to uranium compounds. Uranium accumulates mainly in the bones, kidneys and liver, and presents both chemical and radiological toxicity.

The overexposure to uranium may cause pathological alterations to the kidneys, leading in extreme cases to renal failure. In this context, this work investigated the presence of uranium in several commercial brands of dry dog foods produced in Brazil.

### II. EXPERIMENTAL

For this work, 61 dry dog food samples of 37 different commercial brands, including food for puppies and adults, were purchased in the local market of Piracicaba, SP, Brazil. After homogenization, a 300 g subsample of each dog food package of 1 kg was reduced in a knife mill for analysis by INAA. For analytical quality control, certified reference materials were used. Test portions of 200 mg were inserted in polyethylene vials and irradiated in the nuclear research reactor IEA-R1 of IPEN/CNEN at a thermal neutron flux of  $7 \times 10^{12} \text{ cm}^{-2} \text{ s}^{-1}$  for 4 h. Element concentrations and expanded uncertainties were calculated by the  $k_0$ -method, using the software package Quantu [2].

### III. RESULTS AND DISCUSSION

A total of 14 samples out of 61 showed uranium concentrations above the detection limit of 0.2 mg kg<sup>-1</sup>, with values ranging from 0.24 mg kg<sup>-1</sup> to 3.61 mg kg<sup>-1</sup>. Nine samples were for adult dogs and five for puppies. Two special foods, for intestinal and hypoallergenic treatments, respectively had uranium values of 1.05 mg kg<sup>-1</sup> and 2.30 mg kg<sup>-1</sup>. Some commercial brands from the same producers consistently presented higher uranium content.

Data were compared to values obtained in a previous study [3] as seen in Table 1. Two commercial brands were analyzed in both occasions. For one brand, uranium content was reduced from 3.15 mg kg<sup>-1</sup> to 0.83 mg kg<sup>-1</sup>, while for the other the content was similar, with 3.99 mg kg<sup>-1</sup> in the first study and 3.61 mg kg<sup>-1</sup> in the second.

Table 1. Uranium concentration (mg kg<sup>-1</sup>) in dry dog foods compared with results published in previous work [3].

	This study	Previous work
Min	0.24	0.46
Max	3.61	3.99
Median	0.91	0.70
Average	1.49	1.36
Stdev (%)	81	85
N	14	13

No maximum regulatory limit was found for uranium in dog food, despite its nephrotoxic effects known already for a long time, causing renal diseases. According to US Environmental Protection Agency (EPA) [4], the average daily intake of uranium from food ranges from 0.07 µg to 1.1 µg for humans. The intake for a dog of 40 kg that consumes about 500 g of dry food per day would be as high as 2 mg of uranium, which can be considered a very high value compared to the range published by EPA.

### REFERENCES

- [1] Casacuberta N, Masquéa P, Garcia-Orellana J, Bruach J M, Anguita M, Gasa J, Villa M, Hurtado S, Garcia-Tenorio R (2009) J. Hazard. Mater. 170: 814-823.
- [2] Bacchi M A, Fernandes E A N (2003) J. Radioanal. Nucl. Chem. 257: 577-582.
- [3] Elias C, Fernandes E A N, Bacchi M A (2012) J. Radioanal. Nucl. Chem. 291: 245-250.
- [4] United States Environmental Protection Agency (2010) Understanding radiation in your life, your world. <http://www.epa.gov/radiation/radionuclides/uranium.html>.